ASSESSMENT OF DROUGHT INDICES FOR THE METEOROLOGICAL SUBDIVISIONS OF INDIA USING MACHINE LEARNING TECHNIQUES

Thesis

Submitted in partial fulfilment of the requirements for the degree of

DOCTOR OF PHILOSOPHY

by

AYILOBENI KIKON

DEPARTMENT OF WATER RESOURCES AND OCEAN ENGINEERING

NATIONAL INSTITUTE OF TECHNOLOGY KARNATAKA,

SURATHKAL, MANGALURU - 575 025

January 2024

ASSESSMENT OF DROUGHT INDICES FOR THE METEOROLOGICAL SUBDIVISIONS OF INDIA USING MACHINE LEARNING TECHNIQUES

Thesis

Submitted in partial fulfilment of the requirements for the degree of

DOCTOR OF PHILOSOPHY

by

AYILOBENI KIKON

(187001AM003)

Under the Guidance of

Prof. B M DODAMANI

DEPARTMENT OF WATER RESOURCES AND OCEAN ENGINEERING

NATIONAL INSTITUTE OF TECHNOLOGY KARNATAKA,

SURATHKAL, MANGALURU - 575 025

January 2024

DECLARATION

By the Ph.D. Research Scholar

I hereby *declare* that the Research Thesis entitled "**Assessment of Drought Indices for the Meteorological subdivisions of India using Machine Learning Techniques**" which is being submitted to the **National Institute of Technology Karnataka, Surathkal** in partial fulfilment of the requirements for the award of the Degree of **Doctor of Philosophy** in **Department of Water Resources and Ocean Engineering** is a *bonafide report of the research work* carried out by me. The material contained in this Research Thesis has not been submitted to any University or Institution for the award of any degree.

187001AM003, AYILOBENI KIKON

(Register Number, Name & Signature of the Research Scholar)

Department of Water Resources and Ocean Engineering

Place: NITK-Surathkal

Date: 10/01/2024

CERTIFICATE

This is to *certify* that the Research Thesis entitled "**Assessment of Drought Indices for the Meteorological subdivisions of India using Machine Learning Techniques**" submitted by **Ayilobeni Kikon** (Register Number: 187001AM003) as the record of the research work carried out by her, is *accepted as the Research Thesis submission* in partial fulfilment of the requirements for the award of degree of **Doctor of Philosophy**.

Prof. B M DODAMANI
(Research Supervisor)

Varija. K
15.1.24

(Chairman – DRPC)

Chairman (DRPC)
Dept. of Water Resources & Ocean Engineering

DEPARTMENT OF WATER RESOURCES AND OCEAN ENGINEERING
NATIONAL INSTITUTE OF TECHNOLOGY KARNATAKA,
SURATHKAL, MANGALURU - 575 025

ACKNOWLEDGMENT

At the outset, I offer my sincere gratitude to my Research Guide**, Late Prof. Paresh Chandra Deka**, Department of Water Resources and Ocean Engineering, NITK, Surathkal. His untimely demise was a great loss, and I will always cherish the valuable guidance, support and mentorship he has provided during the initial stages of my research work. His expertise and encouragement played a significant role in shaping and directing the study, I will forever be grateful for the knowledge and inspiration he imparted to me.

In the midst of the unfortunate circumstances, I would express my gratitude to **Prof. B. M. Dodamani** (former Head of the Department), who graciously stepped in as my new Research supervisor. I am thankful for his willingness to take on this role. His support and guidance for the rest of my research journey. His expertise and encouragement are invaluable in steering this study to its completion.

I extend my heartfelt thanks to the members of the RPAC committee, **Prof. B. B. Das**, Department of Civil Engineering and **Prof. Varija K** (Head of the Department), for their meticulous evaluation and valuable recommendations during the progress of my research. I am also grateful to Prof. Amba Shetty, former Head of the Department, for granting me access to the laboratory and departmental facilities for the completion of this work. I thank all the faculty members of the Department of Water Resources and Ocean Engineering for their support.

I express my sincere gratitude to Prof. B. Ravi (Director), Prof. Prasad Krishna, Prof. Karanam Uma Maheshwar Rao and Prof. Udaykumar R. Yaragatti, former Director, NITK Surathkal humbly for providing me necessary facilities, funding and support during the phase of this project work.

I also express my thanks to **Dr. Debabrata Karmakar**, i/c Computational Hydrodynamics Laboratory, for providing the computational facilities in carrying out my research work.

My sincere appreciation goes out to my former and current **Research Scholars** in the Department of Water Resources & Ocean Engineering, NITK, Surthakal for their support and encouragement during this research journey.

A special and heartfelt thanks to the Department staff both **teaching and non-teaching** for their support and assistance.

Last but not least, I am deeply grateful to each and every of my family members, **Late Eyingo Kikon (Father), Mrs. Khodano Kikon (Mother), my brothers and sisters** for their unwavering faith in me, unconditional love, sacrifices, and constant encouragement in every aspect of my life. Finally, I humbly acknowledge the Almighty for making this thesis a reality and for providing me with the strength and guidance throughout this journey.

Ayilobeni Kikon

ABSTRACT

Drought is a highly damaging natural event having a significant impact on the environment, agriculture, economy and public health resulting in a cascade of vulnerabilities across several sectors. Drought occurs in all climatic zones mainly because of deficit in precipitation for a prolonged period. Every year significant areas and population around the globe are affected by drought which can last anywhere between weeks to years. Understanding the numerous climatic parameters affecting the variability of rainfall and outbreaks of drought is a major scientific challenge. Due to changes in the climate and activities by people, there is a need to understand the various catastrophe causing due to drought and adopt measures to overcome and prevent the drought consequences. Drought prediction emerges as one of the crucial tools that can provide helpful information and may be used to mitigate drought impacts. Meteorological drought is a type of drought that results from inadequate amounts of rainfall in any region. The study has been conducted in the Indian region consisting of thirty-four meteorological subdivisions. The study aims to analyse the rainfall and drought indices trend using the monthly precipitation data from 1958-2017. The Mann-Kendall test has been applied to determine the trends in rainfall and drought indices. The Effective Drought Index (EDI) and Standardized Precipitation Index with 9-month and 12-month timescale are the meteorological drought indices that are assessed using monthly rainfall data. These meteorological drought indices are predicted using machine learning algorithms such as the Genetic Algorithm-Adaptive Neural Fuzzy Inference System (GA-ANFIS), Particle Swarm Optimization-Adaptive Neural Fuzzy Inference System (PSO-ANFIS), and Generalized Regression Neural Network (GRNN), and the obtained results are compared.

The Mann-Kendall test results showed a clear indication that rainfall has been consistently decreasing during the study period, leading to water shortages and dry conditions. Understanding both rainfall patterns and drought trends is therefore essential for efficient planning and control of the numerous impacts of drought. The

machine learning algorithms employed in this work show they are capable of predicting meteorological drought indices under various climatic situations. Based on performance measures such as coefficient of determination (R^2), Nash-Sutcliffe Efficiency (NSE) and Normalized root mean square error (NRMSE), comparative study of the models shows that hybrid machine learning models (GA-ANFIS and PSO-ANFIS) perform better than the non-hybrid model (GRNN). Notably, it has been observed that, as the timescale for the drought index increases, it shows a better performance with more accuracy of the performance metrics. Based on the study findings, it emphasizes in assessing the rainfall and drought trend could be beneficial in understanding the drought behaviour and identify drought prone locations and develop mitigation strategies to overcome the drought impacts. Overall, this study plays a significant role in understanding the rainfall pattern and its distribution for water management and planning for future water use. Adopting hybrid machine learning algorithms for predicting of meteorological drought indices may provide a better outcome for drought assessment. Also, assessing the historical droughts provides a better understanding and management of past drought occurrences. Future research attempts could be focused on improving drought vulnerability mapping by modelling and probabilistic climate data analysis. Additionally, understanding the dynamics of drought may also be improved by investigating at how drought occurrences begin and terminate. The exploration of alternative hybrid machine learning approaches and the incorporation of additional drought indices could contribute to more robust evaluations in assessing drought conditions.

Keywords: Drought, Effective drought index, Standardized precipitation index, Mann-Kendall test, Drought prediction, Machine learning algorithms.

CONTENTS

LIST OF FIGURES

LIST OF TABLES

CHAPTER 1

INTRODUCTION

1.1 BACKGROUND

Drought is a natural disaster characterized by a prolonged period of deficient rainfall, and its impacts can be far-reaching, affecting various aspects of human life and the environment. There are four main types of droughts: meteorological, hydrological, agricultural, and socioeconomic drought, each focusing on different aspects of the phenomenon. Meteorological drought refers to a deficiency in precipitation and is primarily concerned with the atmospheric conditions and lack of rainfall. Hydrological drought involves reduced water availability in various water systems, addressing impacts on water resources and the overall water cycle. Agricultural drought occurs when soil moisture reduction significantly affects crop growth, livestock, and agricultural productivity. Socioeconomic drought considers economic and social impacts, encompassing water scarcity, food security, and economic consequences for various sectors.

Drought consequences are severe and multifaceted, leading to water shortages, crop failures, increased food prices, conflicts over water resources, and reduced hydropower allocation. Addressing drought involves adopting drought-resistant agricultural practices, establishing early warning systems, implementing contingency planning, and building resilience in affected communities and ecosystems. Climate change exacerbates drought conditions with changing precipitation patterns and weather systems, necessitating climate change mitigation and adaptation strategies to manage associated risks.

Under the changing climate, drought is projected to become more prevalent and devastating in many regions of the world (Spinoni et al. 2018). Detecting the onset and termination of droughts can be challenging, as it may take weeks, months, or even years before their occurrence is realized. Even short and intense droughts can cause substantial damage to local economies and livelihoods. Drought mitigation and

management solutions can be developed by understanding the causes and consequences of drought. Droughts in certain parts of the globe have resulted in reduced food production and increased food prices. Thus, the socio-economic and environmental consequences of drought mitigation and management framework should be considered (Hassan et al. 2019). Globally drought has a considerable impact on agriculture, migration, human settlement, etc. Considering the different studies conducted by the researchers, initiation of drought planning, drought preparedness, drought alert and drought mitigation plans are necessary to set up in all the regions.

1.2 CAUSES OF DROUGHT

Droughts can arise from a complex interaction of natural and human factors, leading to significant water scarcity in affected regions. One of the primary contributors to drought is the insufficient precipitation over prolonged periods, resulting in below-average rainfall. However, human activities also play a pivotal role in exacerbating drought conditions through both direct and indirect means.

Factors such as excessive water consumption, unsustainable irrigation practices, over extraction of ground water, deforestation and urbanization can deplete water resources and exacerbate drought vulnerability. Additionally, excessive irrigation promotes desertification leading to drought at a certain period. Deforestation is another significant human-induced cause of drought, as it reduces water storage capacity in the soil, leaving the entire region more susceptible to drought conditions. Moreover, the imbalance between water demand and supply can contribute to drought situations. With a growing global population and extensive agricultural practices, the need for water escalates, potentially leading to more frequent and severe drought events.

Global climate change is yet another factor that influences the frequency and intensity of droughts. Altered temperature and precipitation patterns, shifts in weather systems, and increased climate variability can all impact the likelihood and severity of drought occurrences. Rising temperatures contribute to increased evaporation of water from various water bodies, reducing rainfall and exacerbating water scarcity, thus amplifying drought situations. It is crucial to acknowledge that the causes and characteristics of

drought can vary significantly from one region to another. A comprehensive understanding of the specific causes of drought in a particular area necessitates detailed analysis of local climate conditions, water availability, and human activities. Additionally, the combined influence of natural climate variations and human-caused climate change can further complicate the causes and trends of drought events worldwide. Therefore, developing effective strategies to mitigate and adapt to drought conditions requires a multidimensional approach that considers both natural factors and human influences on water resources.

1.3 IMPORTANCE OF RAINFALL AND DROUGHT STUDY

The study of rainfall holds immense significance in climatology and has been a subject of extensive research over time. Analysing rainfall data is a crucial prerequisite as it serves multiple important purposes, including monitoring flood and drought conditions, facilitating agricultural planning and management, forecasting tropical cyclones, evaluating soil moisture conditions, and assessing freshwater availability. Rainfall stands as the most pivotal factor in comprehending the distribution of precipitation across different seasons and spatial scales. Understanding the distribution of rainfall across different seasons and spatial scales aids in assessing water availability, planning water infrastructure, and implementing conservation measures. Accurate information about rainfall and drought conditions is vital for ensuring preparedness and mitigating the impacts of drought events on various sectors. Rainfall patterns are influenced by climate change, and studying rainfall helps in assessing climate change impacts. Moreover, studying rainfall patterns using long term data provides insights in evaluating climate change impacts, enabling researchers to model future scenarios and develop adaptation strategies.

Drought, characterized by prolonged inadequate precipitation leading to water deficits, has far-reaching impacts on flora, fauna, and human populations. Investigating drought allows us to comprehend its effects on individuals and communities and explore collaborative efforts to minimize its societal repercussions. As one of the most harmful natural hazards, drought's consequences are widespread, affecting multiple sectors of

the economy and people simultaneously. Their consequences are broad and prevalent, affecting multiple sectors of the economy and people at the same time. The impacts of drought are extensively varied and dependent on the socioeconomic environment of the affected community. Consequently, choosing appropriate drought indicators for monitoring and early warning strategies becomes critical to address varied impacts based on the socioeconomic context of the affected community. Drought early warning systems plays a pivotal role in assessing the availability of water, climate and hydrology. Drought study entails measuring changes in precipitation, temperature, surface and groundwater supplies. Ideally, they involve both prediction and monitoring components intending to provide information before and during the onset of drought and trigger actions that can reduce potential damages.

Rainfall and drought investigations play a crucial role in identifying flood and drought-prone areas, enabling the development of disaster preparedness plans, early warning systems, and risk mitigation strategies. These studies offer indispensable insights for water resource management, agriculture, disaster risk reduction, climate change assessment, and ecosystem preservation. By understanding and mitigating the impacts of drought, sustainable water availability can be ensured, supporting the well-being of both human and natural systems. The continuous analysis of rainfall and drought data remains essential in the face of changing climate patterns, safeguarding communities and ecosystems from the adverse effects of extreme weather events.

1.4 INSIGHTS INTO DROUGHT TREND AND DROUGHT PREDICTION

Drought trends and drought prediction offers valuable information for understanding and managing water resources during drought events. By studying historical rainfall data, researchers can identify long-term patterns and changes in precipitation, providing crucial insights into climate variability and potential climate change impacts.

Rainfall trend analysis helps in assessing the distribution of rainfall across different regions and seasons, enabling better flood and drought monitoring and agricultural

planning. It also aids in predicting tropical cyclones and understanding soil moisture conditions and freshwater availability. On the other hand, drought prediction plays a vital role in drought management and preparedness. Early warning systems based on drought predicting allow for timely detection and preparation for approaching drought conditions. This enables water managers to implement proactive measures to mitigate water shortages, such as water conservation, groundwater management, and demand control strategies. Moreover, drought prediction is essential for climate change adaptation efforts. As climate change influences precipitation patterns and exacerbates drought frequency and intensity, understanding drought trends becomes critical for assessing changing climate conditions and developing adaptation strategies to enhance resilience to future drought events.

In summary, insights from rainfall trend analysis and drought prediction contribute to effective water resource management, disaster preparedness, and climate change adaptation, ultimately ensuring sustainable water availability and minimizing the impacts of drought on various sectors of society.

1.5 DROUGHT INDICES

Drought indices are quantitative measures used to assess the severity of a drought in a specific area over defined periods. They provide a standardized way to evaluate and compare drought severity, duration and spatial extent across regions based on various factors like precipitation, temperature, streamflow, groundwater, reservoir levels, soil moisture, and snowpack. Several widely employed drought indices are utilized in drought prone areas to identify vulnerable regions and make informed decisions regarding water allocation, irrigation and drought mitigation efforts. The Standardized Precipitation Index (SPI) is one of the extensively utilized drought index in research for the drought study (Mckee et al. 1993) quantifies the deviation of precipitation from normal, providing valuable insights into meteorological drought conditions. Overall, SPI is a valuable tool for assessing and monitoring the state of drought since it provides a standardized measure of precipitation anomalies that aids in understanding and managing the impacts of drought. The Effective Drought Index (EDI) developed by

(Byun and Wilhite 1999) is another a valuable index used to assess the severity and impact of drought conditions, providing early warning systems to various sectors such as agriculture, water management and disaster preparedness. By understanding drought conditions through the EDI, informed decisions can be made regarding drought response and mitigation strategies.

In summary, drought indices play a crucial role in assessing drought severity, monitoring drought conditions, and providing early warning systems. The SPI and EDI are two widely used drought indices that aid in understanding and managing drought impacts, making informed decisions for water resources, and implementing effective drought response and mitigation strategies.

1.6 ORGANISATION OF THE THESIS

The introduction to the thesis and background of the drought, causes of drought, importance of rainfall and drought study, insights of drought trend and drought prediction, drought indices and scope regarding the present research work are discussed in Chapter 1.

In Chapter 2, an overview of the relevant literature is provided on trend studies of rainfall, meteorological drought indices, and drought studies utilizing various machine-learning approaches. The review of the literature is followed by a summary of the chapter. Based on the knowledge gap identified, the research problem and objectives of the present work are formulated.

The method adopted and the data required for the present study are described in Chapter 3. This chapter also presents the description of the study area along with the thirty-four meteorological subdivisions for India.

Chapter 4 discusses the descriptive and statistical results of the present works that has been carried out. Further, assessment of the machine learning models for meteorological drought indices are presented in this chapter. The present research work is summarised and the important conclusions obtained are presented in Chapter 5.

CHAPTER 2

LITERATURE REVIEW AND PROBLEM IDENTIFICATION

2.1 BACKGROUND

Drought is a catastrophic event with widespread impacts on agriculture, water resources, ecosystems and socio-economic systems. It is caused by both natural activities and human intervention, necessitating a comprehensive understanding of its causes, manifestations and consequences. To develop effective drought management, planning, and mitigation strategies, researchers globally have dedicated significant efforts to investigate the intricacies of drought, including its origins, monitoring techniques, prediction models, and the development of drought indices. This literature review aims to provide a comprehensive overview of the trends of rainfall and drought studies, highlighting key findings, methodologies and gaps in understanding.

The literature review encompasses a wide array of sources from various disciplines, including climatology, hydrology and agriculture covering diverse aspects of drought study. Key areas of focus include rainfall and drought trend analysis, drought indices, development of drought prediction models, the impacts of drought on ecosystems and water resources, adaptation strategies, and policy frameworks for drought management. This study aims to provide a comprehensive understanding of the current state of knowledge in the field of drought research. It seeks to identify gaps in our understanding of drought dynamics and recommend potential avenues for further exploration. Through a thorough analysis of existing literature, this review intends to contribute valuable insights into rainfall and drought studies and support the development of informed policies and practices for drought resilience and disaster preparedness.

2.2 RAINFALL AND DROUGHT TREND STUDIES

A changing trend in the occurrence of drought has been observed across various regions. Rainfall is one of the essential parameters for assessing drought conditions in a region. Various studies on rainfall and drought are being studied at diverse spatial and

temporal scales. For efficient water resources management, particularly in areas with significant spatiotemporal variability in rainfall, a more detailed understanding of rainfall trends, distribution and characteristics is of utmost importance (Mathew et al. 2021). Investigation of precipitation distribution and its trends using the Mann-Kendall approach in regions with a humid to subtropical monsoon climate holds great importance (Zamani et al. 2018). A study conducted for long-term rainfall reveals that during the rainy season there is an increase in rainfall showing a positive significant trend and during the non-rainy season there is a downward trend (Rustum et al. 2017).

As drought is one of the complex threats to measure, it is very challenging to evaluate and understand the drought trend. Precipitation is unquestionably the variable that most influences the prevalence and severity of droughts (Vicente-Serrano et al. 2022). Meteorological drought indices such as EDI and SPI are widely used to assess drought trends using precipitation data, aiding in planning and mitigation efforts in drought - affected regions under changing climate scenario (Svoboda and Fuchs 2017).

Rainfall analysis, including the decadal analysis, is important because it identifies the significantly monotonic monthly and seasonal trends that are extremely valuable for improving the aspect of changing rainfall patterns and global warming impacts (Saini et al. 2020). Investigating seasonal and yearly precipitation trends aids in preparedness and response actions and promotes effective water resource utilization (Datta and Das 2019). Understanding rainfall trends and drought features will aid in developing water resource management, agricultural productivity, climate change projections, and rainfall pattern prediction (Deng et al. 2018; Malik and Kumar 2020; Marumbwa et al. 2019; Sanikhani et al. 2018).

The use of historical records of drought disasters to study drought's spatial and temporal properties could be a useful tool for detecting and characterizing drought progression (Cheng et al. 2020). Investigation of rainfall variability using standardized indices offers insights into distinct spatial patterns, enabling assessment at different timescales (Guntu et al. 2020). Drought trend studies based on the precipitation data in drought vulnerability regions may differ depending on their rainfall distribution (Kalisa et al.

2020). Drought trends are not only related to rainfall trends but also to the daily rainfall concentration variations as well as the monthly rainfall heterogeneity and rainfall seasonality (Deng et al. 2018). Drought hazard mapping and associated trend analysis are important amidst rising drought impact due to climate change and posing challenges in effective monitoring of drought-related trend analysis (Pandey et al. 2021). The impact of long-term changes and fluctuations in rainfall plays a significant role in agricultural growth and climate change alterations (Panda and Sahu 2019). An immediate and long-term drought evolution is also affected by the changes in the seasonality of rainfall. Drought impacts the population, agriculture, direct economic losses and total crop failure (Shi et al. 2020). The duration, severity, and intensity of the drought on a monthly, seasonal and yearly time frame have been all crucial because they show how intense, persistent, and severe the occurrence of the drought was in different places (Musonda et al. 2020).

Drought characteristics and temporal trends are essential for decision-making and climate variability adaptation measures (Byakatonda et al. 2018). The severity of drought is being measured due to global warming which has a higher impact on semi-arid areas. Drought monitoring relies on climate variables and provides techniques for reducing climatic variability. Historical rainfall trend data is useful in various fields, including hydrology, ecosystems, agriculture, climate change mitigation, and drought hotspot identification (Marumbwa et al. 2019). Understanding regional drought frequency, severity, and duration may prove greatly beneficial in developing efficient drought mitigation strategies in those areas having chaotic and inter-annual rainfall variability (Amrit et al. 2018). Meteorological drought indices demonstrate gradual responses to drought onset, advancement, and termination (Wambua et al. 2014).

Drought frequency varies throughout time and the findings on drought prediction assist decision-makers in addressing water-related challenges (Achour et al. 2020). Understanding the precipitation trends as well as the drought scenario reveals the rainfall distribution and drought severity, contributing to future disaster mitigation (Thomas and Prasannakumar 2016). The climate model scenario projects the increasing

and decreasing trend of rainfall and investigates the potential effects of climate change on water resources and reflects on the future climate scenario (Chanapathi et al. 2018). To better understand how rainfall changes relate to climatic diversity, maps that show patterns of rainfall trends utilising geographical description, statistical analysis, and interpretive data are designed to serve a purpose (Ghosh 2018). The spatiotemporal rainfall change scenario study has enormous potential for developing thorough adaptation and mitigation plans to deal with the climate change scenario in the drought-stricken area, and other regions with a similar climate (Jana et al. 2017).

In recent years, increasing temperatures have resulted in an upsurge in the severity and frequency of droughts during different seasons and climatic zones, where a continuous temperature rise will result in severe drought events in the future owing to global warming (Shiru et al. 2019). The spatial association between yearly rainfall variability and meteorological droughts in agro-ecological zones with common orographic rainfall in lowlands highlights the importance of studying rainfall variabilities and trends (Tesfamariam et al. 2019). Precipitation trend studies in semi-arid developing country such as Mauritania in Northwest Africa is crucial for assessing the precipitation deficit and drought situations (Yacoub and Tayfur 2020). Global climate change is driving extreme rainfall trends and understanding the phenomena necessitates a most extended time series rainfall data which is crucial in addressing water-related issues (Malik et al. 2020). Understanding the detailed rainfall variability across the agro-climatic zones could help to comprehend the trend of rainfall which could be important for developing robust water resources management and water stress planning (Singh et al. 2020).

2.3 DROUGHT STUDIES USING VARIOUS DROUGHT INDICES

Drought studies often employ various drought indices for predicting and monitoring drought conditions. Each index requires different input variables, such as rainfall, streamflow, temperature, humidity, evapotranspiration and potential evapotranspiration. One of the widely used drought index is the Standardized Precipitation Index (SPI) which can represent both short-term and long-term water deficits, providing valuable information about meteorological and hydrological drought

propagation (Li et al. 2020). SPI and Standardized Precipitation Evapotranspiration Index (SPEI) are studied for current and future climate projects have significant changes that will anticipate future drought events (Ahmadalipour et al. 2017). Another index, Standardized Precipitation Evapotranspiration Runoff indicator (SPERI) is a multi-scalar drought index that has been established to assess the state of drought in various places, and also to determine the effects of climate change on drought (Wang et al. 2019).

SPI and EDI combined with the Statistical Downscaling Method (SDSM) helps in framing the drought event outlook by monitoring the evolution of drought events and assessing their severity, duration and extent (Huang et al. 2016). SPI is also used to assess the spatiotemporal patterns and severity of drought events (Tesfamariam et al. 2019), wherein the computation is carried out utilizing satellite-gauge rainfall grid data that helps to better comprehend the spatial distribution and quantify environmental and socioeconomic drought events. The Reconnaissance Drought Index (RDI) and SPI analysis drought severity in semi-arid regions and also monitor and assess to distinguish drought concerns (Haied et al. 2017). SPI and SPEI identify temporal variability of droughts (Tirivarombo et al. 2018), where SPI identifies extreme category droughts and SPEI identifies moderate droughts. SPEI and SPI assess spatiotemporal drought variations in drought frequency, duration, intensity, and events, that are essential for future drought mitigation measures (Haile et al. 2019).

Palmer Drought Severity Index (PDSI), RDI, SPEI and Standardized Palmer Drought Index (SPDI) indicate sensitivity to precipitation as well as evapotranspiration, making them relevant choices of drought indices for different applications (Vicente-Serrano et al. 2015). Understanding and comparing the various drought indices, which include Percent of Normal (PN), SPI, statistical Z-score, and EDI are crucial for monitoring and providing valuable information for water resources management (Li et al. 2019). Satellite-derived Vegetation Condition Index is essential for assessing drought and improving agricultural production, while remote sensing data and various drought indices enhance the identification and prediction of drought (Baniya et al. 2019). PDSI and SPI of different time scales in evaluating and verifying the drought utility have

considerable potential for drought monitoring (Karamouz et al. 2004; Zhong et al. 2019).

The standardized Streamflow index (SSI) is useful for depicting hydrological aspects of droughts providing vital details for water resources management and assessment of hydrological droughts in a changing environment (Zou et al. 2018). Drought assessment based on SSI provides valuable references for drought monitoring and forecasting systems (Liu et al. 2016). Characterizing the spatial and temporal pattern of meteorological drought using SPI helps in understanding and taking necessary actions for effective planning and management strategies related to drought (Mondol et al. 2017). It also helps in the development plans and water allocation schemes affected by drought. A Hybrid Drought Index (HDI) developed by combining SPI, water surface supply index and PDSI (Karamouz et al. 2009) presents a probable drought severity and mitigating strategies. For agricultural drought assessment, the SPEI serves as a suitable index (Ebrahimpour et al. 2015). Overall, these various drought indices contribute to better understanding and management of drought events in different regions and climatic conditions.

2.4 DROUGHT STUDIES USING MACHINE LEARNING TECHNIQUES

Drought prediction is a critical aspect of drought modelling that involves analysing and understanding the current meteorological and hydrological conditions of ongoing droughts while also predicting future drought events. Various methods and tools have been adopted for drought prediction, and machine learning algorithms have gained popularity in this domain due to their effectiveness in different fields, including engineering, agriculture, medicine, and marketing. Applying machine learning to drought modelling and forecasting provides relevant information that can significantly improve drought disaster management and mitigation strategies (Prodhan et al. 2022). The gradual changes in drought indices facilitate the importance of understanding and forecasting drought, emphasizing its negative impacts on the environment (Alawsi et al. 2022).

Researchers have employed a statistical model and a machine learning approach were used to forecast SPEI, providing an applicable approach for predicting droughts and benefiting the development of mitigation measures, as well as the management of water supply systems and sustainable water schemes (Zhang et al. 2019; Alawsi et al. 2022). Additionally, an algorithm known as extreme machine learning (ELM) efficiently used in many applications (Huang et al. 2006), demonstrates a rapid learning rate as well as good generalization efficacy when it comes to drought prediction and response capability. In drought prediction studies, an ANN-based approach using time series of nonlinear aggregated drought index (NADI) considering hydrometeorological variables has been performed. Moreover, Linear stochastic models (ARIMA/SARIMA), recursive multistep neural network (RMSNN) and direct multi-step neural network (DMSNN) models applied using SPI series exhibit the capability to forecast drought over times series making them useful for sustainable development and prevent environmental degradation of the ecosystem (Mishra and Desai 2006). Furthermore, a preliminary investigation employing a number of statistical, dynamic, and hybrid models with SPI assists in improving drought prediction and early drought warning as the probabilities of drought onset depends on the site and models (Xu et al. 2018). Another study, based on the time series of the Vegetation Temperature Condition index (VTCI), highlights that ARIMA/SARIMA models provides a better drought forecasting model when compared with the monitoring ones (Tian et al. 2016).

Machine learning algorithms such as wavelet pre-processing incorporated into models have shown improved computation and forecasting of drought events (Belayneh and Adamowski 2013; Deo et al. 2017). Additionally, other wavelet models like (WA-SVR, WA-ANN) evaluated long-term SPI with other stochastic models like (ARIMA/SARIMA) have demonstrated that different characteristics and climatology have no distinct effect on forecast accuracy (Belayneh et al. 2014). Incorporating hybrid meteorological and remotely sensed data with wavelet transform analysis is critical for agricultural strategy, reservoir management and water resource distribution, offering a viable option for effective drought assessment and categorizing (Barua et al. 2012; Tan and Perkowski 2015; Sadiq et al. 2023).

Multi-stage committee-based ELM model forecasting SPI ascertains the accuracy of the data-intelligent model for forecasting future drought and mitigating strategies for better crop management (Ali et al. 2018). The impact of the drought is eventually decreased by a high-resolution meteorological drought forecasting model based on SPI and SPEI for hydrologic regions (Rhee and Im 2017). To overcome the limits of drought forecasting in an unmeasured area, machine learning algorithms have been used. ELM and data-driven models (MLR, ANN, and LSSVR) predict SPEI in places that are prone to drought, demonstrating their potential utility for drought mitigation measures and the development of sustainable water supply networks (Mouatadid et al. 2018). Machine learning algorithms, when combined with deep learning techniques and multi-source spatial data, have strong applicability in monitoring meteorological and agricultural droughts, providing valuable insights for drought forecasting and mitigation measures (Shen et al. 2019).

In the realm of machine learning algorithms for drought prediction, the evolutionarily neuro-fuzzy approaches like ANFIS combined with PSO, GA, ACO, and BOA, have proven beneficial for drought prediction and planning in arid and semi-arid environments (Kisi et al. 2019). Hybrid machine-learning models utilizing monthly precipitation data to predict meteorological droughts have been proven to be more effective and produce better predictions (Citakoglu and Coşkun 2022; Mishra et al. 2007). Notably, drought study using hybrid machine learning algorithms has shown better predictions in arid, semi-arid and Mediterranean climates surpassing the performance of conventional machine learning algorithms (Aghelpour et al. 2020; Nabipour et al. 2020).

Meteorological drought parameters such as precipitation, temperature and humidity are more efficient in enhancing the forecast performance (Mokhtarzad et al. 2017). However, long-term drought forecasting becomes challenging due to changes in trend of teleconnections across various spatial and temporal scales. To improve vulnerability reduction and enhance long-range prediction, further investigation is needed to identify the factors connected to climatological, marine, meteorological and hydrological parameters. Drought forecasting models have been developed to assist with agricultural

planning and the effective management of irrigation systems in drought-prone areas, providing certainty related to long-term drought situations (Achite et al. 2022; Ganguli and Reddy 2014). In arid regions, various remotely sensed drought variables have been effectively used to monitor agricultural drought, providing thorough spatial information on drought extent and severity (Feng et al. 2019). Machine learning techniques applied to meteorological drought prediction based on SPI have presented appropriate details for various timeline SPI under drought situations in the semi-arid region, offering a less time-consuming and less sophisticated approach (Elbeltagi et al. 2023). The predictive accuracy of the machine learning model such as SVM may vary with different timescales and this information is essential for understanding the model's performance under different hydrological conditions (Achite et al. 2022).

Drought prediction is a crucial component of early warning systems offering planners time to prepare for threat responses and reduces the impact of drought risk (Khan et al. 2020). Traditional models assume that there is a linear relationship between the variables which might make them inappropriate for addressing problems in real-world applications in drought prediction (Agana and Homaifar 2018). As a result, algorithms that can simulate the complexity of the dataset are needed for drought forecasting. Machine learning algorithms, particularly artificial intelligence (AI) techniques, have gained significant focus, outperforming traditional methods and providing valuable insights for drought prediction and mitigation measures (Belayneh et al. 2016; Docheshmeh Gorgij et al. 2022; Nabipour et al. 2020; Zhang et al. 2017). AI is being used to forecast droughts using a variety of algorithms that take into account the statistical parameters of the models, which are crucial for water management applications (Rozos et al. 2022). Hybrid model which is developed by blending different algorithms have demonstrated superiority over standalone and their utilization is recommended to improve prediction accuracy (Adnan et al. 2021; Hajirahimi and Khashei 2022). In recent times, hybrid machine learning models are becoming more popular and offers promising opportunities for drought prediction providing more accurate outcomes and enabling better decision-making for effective drought response and mitigation strategies in various regions and climate conditions.

2.5 SUMMARY

The review offers a comprehensive overview of rainfall patterns, drought variability, and the use of machine learning techniques in predicting meteorological drought indices. Numerous literature studies on the rainfall trend provide information on the rainfall pattern both in the Indian context and globally, revealing significant declines in certain regions associated with drought conditions. Researchers have employed the Mann-Kendall test to analyse and understand the changing rainfall trends that has occurred in diverse climate conditions. The spatial and temporal characteristics of rainfall and drought further complicate the distribution of rainfall and the drought occurrence across different climate zones.

In addressing the prediction of meteorological drought indices, machine learning approaches have proven to be highly effective. Machine learning algorithms serves as valuable tools for drought prediction, facilitating the formulation of mitigation strategies and sustainable water management practices. Furthermore, the advancement in technology have led to the development of hybrid machine learning models specifically designed for drought prediction. Based on the review of the literature, it indicates that hybrid machine learning models have emerged as reliable and effective tools for assessing drought events. By exploiting the effectiveness of machine learning techniques, these models offer promising prospects for improved drought prediction, ultimately contributing to better preparedness and response strategies for managing drought impacts.

2.6 RESEARCH GAP

The geographical diversity of India, encompassing landscapes from the snow-clad Himalayas to arid regions, plains, mountains, and plateaus, poses a challenge in specifying its climate. This diverse topography gives rise to various water-related challenges affecting agriculture, the economy, and the environment in different regions of the country. To tackle these challenges effectively, a comprehensive understanding of rainfall patterns and an investigation into meteorological drought indices become imperative. Despite the significance of this research need, a thorough review of existing

literature reveals a noticeable dearth of studies utilizing machine learning algorithms to predict meteorological drought indices in the specified study area.

This research gap emphasises the limited exploration of the potential of machine learning algorithms in addressing meteorological drought prediction challenges in the diverse climatic zones of India. To bridge this gap, the current study attempts to meticulously examine rainfall trends and meteorological drought patterns. Additionally, the research aims to assess the efficacy of machine learning algorithms in predicting meteorological drought indices. By undertaking these investigations, the study aspires to provide valuable insights into drought prediction and mitigation strategies. These insights are crucial for fostering sustainable water management practices and optimizing resource allocation in the region, thus contributing significantly to addressing the pressing water-related challenges faced by different areas in India.

In summary, the identified research gaps encompass a range of areas, including the understanding of climatic parameters, measures to address drought consequences, challenges in drought prediction, variability in machine learning model performance, improvements in drought vulnerability mapping, dynamics of drought occurrences, and exploration of alternative methods and indices for drought assessment. These gaps highlight opportunities for future research and the advancement of knowledge in the field of drought studies.

2.7 PROBLEM FORMULATION

Drought has emerged as a widespread global calamity, posing a significant threat to development and becoming a recurring phenomenon in many regions. Addressing this issue is of utmost importance, especially as it adversely impacts various sectors, including agriculture, water availability, and overall development. To mitigate the impact of droughts, early warning systems play a vital role, and accurate drought prediction tools offer policymakers the opportunity to respond proactively. Given the critical implications of drought prediction for agricultural production and water security, it becomes imperative to develop effective methods that can provide sufficient

lead time to implement strategies like water storage, identification of alternative freshwater sources, and adoption of water-saving farming practices. Emphasizing the need for practical measures, drought mitigation becomes an essential consideration.

In recent times, machine learning techniques have gained significant interest from researchers in the field of drought assessment, holding promise for more accurate and efficient predictions. By evaluating different drought indices, the study seeks to precisely identify and understand the prevailing drought conditions in the study region. Ultimately, the research aims to contribute to the development of reliable and helpful drought prediction tools, aiding in effective drought mitigation strategies and safeguarding food and water security in the area.

2.8 OBJECTIVES

Based on the literature gaps identified, the objectives of the study are:

1. (a) To examine the trend analysis of rainfall (Annual, Monthly and Seasonal) using Mann-Kendall test

   (b) To compute Meteorological drought indices: Effective Drought Index (EDI) and Standardized Precipitation Index (SPI) and examine the trend analysis.

2. To assess the meteorological drought indices using the following machine learning techniques.

   (a) Generalized Regression Neural Network (GRNN)

   (b) Genetic Algorithm-Adaptive Neuro-Fuzzy Inference System (GA-ANFIS)

   (c) Particle Swarm Optimization-Adaptive Neuro-Fuzzy Inference System (PSO-ANFIS)

3 (a) To examine the best predicting model for the meteorological drought indices by a comparative examination of machine learning algorithms

(b) To evaluate the effectiveness of the meteorological drought indices in detecting the historical droughts.

2.9 SCOPE OF THE STUDY

The primary focus is on employing the Mann-Kendall test to discern trends in both rainfall and meteorological drought indices, particularly the Effective Drought Index (EDI) and Standardized Precipitation Index with 9-month and 12-month timescales.

Machines learning algorithms, namely the Genetic Algorithm-Adaptive Neural Fuzzy Inference System (GA-ANFIS), Particle Swarm Optimization-Adaptive Neural Fuzzy Inference System (PSO-ANFIS), and Generalized Regression Neural Network (GRNN), are utilized to predict meteorological drought indices. The study critically evaluates these simulations, comparing their performance through metrics such as coefficient of determination (R2), Nash-Sutcliffe Efficiency (NSE), and Normalized root mean square error (NRMSE).

The Mann-Kendall test results reveal a consistent decrease in rainfall over the study period, leading to water shortages and dry conditions. Understanding the interplay between rainfall patterns and drought trends is identified as crucial for effective planning and control of drought impacts. The study underscores the capability of hybrid machine learning models (GA-ANFIS and PSO-ANFIS) in outperforming the non-hybrid model (GRNN), particularly as the timescale for the drought index increases.

The findings emphasize the benefits of assessing rainfall and drought trends for understanding drought behavior, identifying prone locations, and formulating mitigation strategies. The study also highlights the significance of historical drought assessment for a better understanding and management of past occurrences. Future research suggestions include enhancing drought vulnerability mapping through modeling and probabilistic climate data analysis, investigating the initiation and termination dynamics of drought occurrences, and exploring additional hybrid machine learning methods and drought indices for more reliable assessments. Overall, this research contributes significantly to comprehending rainfall patterns, their distribution for water management, and future water use planning, advocating for the adoption of hybrid machine learning algorithms for improved meteorological drought prediction.

CHAPTER 3

MATERIALS AND METHODS

3.1 DESCRIPTION OF THE STUDY AREA

India is situated between 8°04' and 37°06' North latitude and 68°07' and 97°25' East longitude. With a total land area of 32,87,590 Sq.km, India is the world's seventh-largest country. It is surrounded by the Arabian Sea in the southwest and the Bay of Bengal in the Southeast and has a total shoreline of 7,516 Kilometres. The country's geographical features encompass the majestic Himalayas in the north, northeast, and northwest, while the southernmost point is Kanyakumari, where the Indian Peninsula narrows towards the Indian Ocean. Additionally, India includes the Andaman and Nicobar Islands in the Bay of Bengal and Lakshadweep in the Arabian sea as parts of its territory.

The climate in India exhibits a remarkable diversity, ranging from tropical in the south to temperate in the north, with some regions experiencing polar climates. Meteorologists classify the year into four main seasons: pre-monsoon, monsoon, post-monsoon and winter. Due to the varying climatic zones, rainfall patterns also differ across regions. Based on the Koppen climate system, India is classified into six major climatic subtypes encompassing arid deserts, semi-arid, alpine tundra, glaciers, humid tropical regions and subtropical zones. The tropical wet climates, which cover the Malabar Coast, the Western Ghats, and southern Assam, typically receive above 2,000 mm of rainfall per annum (Chouhan 1992). The tropical wet and dry climate, prevalent in inland Peninsular regions except for the semi-arid rain shadow east of the Western Ghats, experiences an annual average rainfall ranging between 750 to 1,500 mm (Farooq 2002). The Ganges Delta is largely situated in a tropical wet climate zone witnessing annual rainfall ranging from 1,500 to 2,000 mm in the western part and 2,000 to 3,000 mm in the eastern part (Healy 2011). Moving towards the hot semi-arid climate, which includes Karnataka, inland Tamil Nadu, western Andhra Pradesh, and central Maharashtra, receive between 400 to750 mm annually (Caviedes 2001). The

arid-climatic region receives about 300 mm of annual rainfall while the tropical and sub-tropical steppe climate receives 300 to 650 mm of annual rainfall. In the North-Eastern region, the climate predominantly humid subtropical with annual rainfall ranging from 1,000 mm to 2,500 mm (Kimmel 2000). Notably, the village of Mawsynram in the state of Meghalaya holds the record for the highest annual rainfall about 11,872 mm. The monsoon precipitation is becoming extreme and regionally varied and droughts are becoming more regional in the study area (Mallya et al. 2015).

In the recent years, India has faced extensive drought conditions since 2015 and around 600 million people are experiencing the country's worst-ever water crisis as reported by the government. With India being the largest user of groundwater globally, there are concerns that many cities may face water shortages by 2030, impacting approximately 40% of the country's population in terms of access to drinking water. As climate change worsens, water scarcity is becoming a significant economic challenge for the nation. Figure 3.1 represents the study area with Thirty-four meteorological subdivisions.

Table 3.1 Meteorological subdivisions of India used in the study (IMD)

Homogenous Monsoon Regions	Central Northeast	North-East	North-West	Peninsular	West Central
Meteorological sub-divisions	Bihar (BI)	Arunachal Pradesh (AR)	East Rajasthan (ER)	Coastal Andhra Pradesh (CAP)	Chhattisgarh (CH)
	East Uttar Pradesh (EUP)	Assam-Meghalaya (AM)	Gujarat (GJ)	Coastal Karnataka (CK)	East Madhya Pradesh (EMP)
	Jharkhand (JH)	Gangetic West Bengal (GWB)	Haryana Chandigarh Delhi (HCD)	Kerala (KL)	Konkan-Goa (KG)
	Orissa (OR)	Nagaland Manipur Mizoram Tripura (NMMT)	Himachal Pradesh (HP)	Rayalaseema (RA)	Madhya Maharashtra (MM)
	Uttarakhand (UK)	Sub-Himalayan West Bengal Sikkim (SHWBS)	Jammu Kashmir (JK)	South Interior Karnataka (SIK)	Marathwada (MA)
	West Uttar Pradesh (WUP)		Punjab (PN)	Tamil Nadu-Pondicherry (TN-P)	North Interior Karnataka (NIK)
			Saurashtra Kutch Diu (SKD)		Telangana (TE)
			West Rajasthan (WR)		Vidarbha (VI)
					West Madhya Pradesh (WMP)

Figure 3.1 Index map of India with thirty-four meteorological subdivisions

3.2 DATA

According to India Meteorological Department (IMD), India has been classified into five Homogenous Regions namely Central Northeast, North-East, North-west, Peninsular and West central India based on monsoon distribution. A total of thirty-six meteorological sub-division have been categorized according to IMD. Monthly rainfall data for 60 years period (1958-2017) is obtained from IMD. In this study, thirty-four meteorological sub-divisions in the Indian region are considered in the computation of

drought indices, EDI and SPI values for different times scales. Due to the non-availability of proper rainfall data for two islands, Andaman & Nicobar and Lakshadweep has been excluded from the study.

3.3 MANN-KENDALL TEST

In the present study, Mann-Kendall test is employed to analyse collected data overtime to identify consistently increasing or decreasing trends. The Mann-Kendall test was proposed by Mann (1945), Kendall (1975) and Gilbert (1987) which is widely used for detecting the trend in hydro-climatic data series. The Mann-Kendall test is evaluated as:

$$S = \sum_{j=i+1}^{n} \sum_{i=1}^{n-1} sign\,(x_j - x_i) \tag{3.1}$$

where n is the number of data points, x_i and x_j are the data points in the time series i^{th} and j^{th} $(j > i)$.

The variance is evaluated as:

$$var(S) = \frac{n(n-1)(2n+5) - \sum_{i=1}^{m} t_i(i-1)(2i+5)}{18} \tag{3.2}$$

t_i represents the number of data values in i^{th} and m^{th} groups.

The standard test statistic Z is computed as follows:

$$Z = \begin{cases} \frac{S-1}{\sqrt{var(S)}}, if\ S > 0 \\ 0 \quad , if\ S = 0 \\ \frac{S+1}{\sqrt{var(S)}}, if\ S < 0 \end{cases} \tag{3.3}$$

The positive value of Z signifies an increasing trend and the negative value of Z signifies a decreasing trend. The Z-value is used to determine if a statistically significant trend exists. The significance level is used to test if a monotonic upward or downward trend exists. For this study, a significance threshold of α=0.05 is adopted, indicating a 95% confidence level, to assess the rainfall and drought trend in the study area. If the *p* -value is lower than the significance level, it provides statistically significant evidence of a trend in the time series data.

3.4 DROUGHT INDICES

3.4.1 Standardized Precipitation Index (SPI)

SPI is a statistical tool used to quantify and represent the precipitation deficit or surplus for a specific timescale at a given location. It is designed to assess and monitor meteorological droughts or wet periods. SPI is one of the most widely used drought indices developed by (McKee et al., 1993). It primarily based on the precipitation data for computation. To calculate the SPI a probability distribution is fitted to the aggregated monthly precipitation series. The SPI is calculated to build a frequency distribution from the historical precipitation data for a specific period at a given location. The choice of the gamma distribution for fitting the empirical distribution of precipitation frequency for specific time scales, such SPI-9 and SPI-12 depends on factors. The gamma distribution is versatile and can accommodate a wide range of shapes, making it flexible for modeling precipitation data. The decision to use the gamma distribution is often supported by statistical fit assessments and goodness-of-fit. If the fitted gamma distribution provides a good match to the empirical data, it suggests that the chosen distribution is a suitable representation of the observed precipitation frequency. It is important to note that the selection of a distribution for modeling precipitation frequency is often based on the characteristics of the data and the objectives of the study. It is important to note that while the gamma distribution is commonly used, other distributions may also be considered based on the characteristics of the precipitation data and the specific requirements of the analysis. The appropriateness of the chosen distribution should be assessed through goodness-of-fit tests and a thorough understanding of the underlying physical processes influencing precipitation at the chosen time scale. Then, a theoretical probability density function of the gamma distribution is fitted to the empirical distribution of precipitation frequency for the selected time scale. The probability density function of gamma distribution is given as follows,

$$g(x) = \frac{1}{\beta^{\alpha}\Gamma(\alpha)} x^{\alpha-1} e^{-\left(\frac{x}{\beta}\right)}, \quad (3.4)$$

Where, $\alpha > 0$ is the shape factor, $\beta > 0$ is the scale parameter and $x > 0$ is the amount of precipitation. Γ (α) is the value taken by the standard mathematical function known as the Gamma function, which is defined by the integral,

$$\Gamma(\alpha) = \int_0^{\infty} y^{\alpha-1} e^{-y} dy \quad (3.5)$$

For estimating the parameters of α and β, different methods have been suggested,

$$\alpha = \frac{1}{4A}\left(1 + \sqrt{1 + \frac{4A}{3}}\right) \quad (3.6)$$

$$\beta = \frac{x}{\alpha}$$

where for "n" observations, $A = ln(x) - \frac{\sum ln(x)}{n}$

After finding α and β, the cumulative probability G(x) corresponding to observed precipitation is given by,

$$G(x) = \int_0^x g(x)dx = \frac{1}{\beta\Gamma(\alpha)} \int_0^x x^{\alpha-1} e^{-\left(\frac{x}{\beta}\right)} dx \quad (3.7)$$

Since the gamma function is undefined for x=0 and a precipitation distribution may contain zeros, therefore cumulative probability,

$$P(x) = q + (1 - q)G(x) \quad (3.8)$$

Where, q is the probability of monthly rainfall equal to zero, P(x) is the cumulative probability of precipitation observed.

Edwards and Mckee (1997) transform this P(x) to the standard normal random variable Z having mean zero and variance as one to get the value of SPI as,

$$Z = SPI = -\left[t - \frac{c_0 + c_1 t + c_2 t}{t + d_1 t + d_2 t^2 + d_3 t^3}\right] \quad (3.9)$$

where $t = \sqrt{ln\left(\frac{1}{H(x)^2}\right)}$ when $0 < H(x) \leq 0.5$

$$Z = SPI = +\left[t - \frac{c_0 + c_1 t + c_2 t}{t + d_1 t + d_2 t^2 + d_3 t^3}\right] \quad (3.10)$$

where $t = \sqrt{ln\left(\frac{1}{(1-H(x))^2}\right)}$ when $0.5 < H(x) \leq 1.0$

The negative and positive SPI values are computed by equation (3.9) and (3.10) respectively. On computing the SPI values as mentioned above, the drought is classified as shows in the Table 3.2.

Table 3.2 Categorization of SPI and EDI values for drought severity

Drought Category	SPI range	EDI range
Extreme dry	≤ -2.0	≤ -2.0
Severe dry	-1.5 to -1.99	-1.5 to -1.99
Moderate dry	-1.0 to -1.49	-1.0 to -1.49
Normal	-0.99 to 0.99	-0.99 to 0.99
Moderate wet	1.0 to 1.49	1.0 to 1.49
Severe wet	1.5 to 1.99	1.5 to 1.99
Extreme wet	≥ 2	≥ 2

3.4.2 Effective Drought Index (EDI)

EDI is a meteorological drought index that quantifies the severity of drought conditions based on precipitation deficits over a specified time scale. It is designed to assess the impact of precipitation anomalies on water availability and, by extension, on agriculture, water resources, and ecosystems. The EDI is particularly useful in evaluating the cumulative effects of precipitation deficits over longer durations.

EDI drought index has been developed by (Byun and Wilhite 1999). It utilizes precipitation data as input to assess drought conditions. For calculating the Effective Drought Index various parameters like Effective Precipitation (EP), Mean Effective Precipitation (MEP), Deviation of Effective Precipitation (DEP) and the standardized value of DEP is required to be evaluated using the precipitation data. The calculation of EDI is performed using the following equations,

i. Calculate the monthly Effective Precipitation (EP),

$$EP_i = P_1 + \frac{P_1+P_2}{2} + \frac{P_1+P_2+P_3}{3} + \cdots + \frac{P_1+P_2+\cdots+P_{12}}{12} \quad (3.11)$$

where i denotes the ith month of precipitation P.

ii. Calculation of the DEP, the difference between the EP and MEP,

$$DEP = EP - MEP \quad (3.12)$$

iii. Calculate precipitation needed for return to normal DEP_i, which is expressed as,

$$DEP_i = \frac{DEP_j}{\sum_{n=1}^{j} \frac{1}{n}} \quad (3.13)$$

where j is the total duration (i.e., the number of days over which precipitation deficit is accumulated). The summation term is the sum of all the months' reciprocals in the duration n (1, 2, 3, 4, …, j).

iv. Calculate EDI as,

$$EDI = \frac{DEP_i}{SD(DEP_i)} \quad (3.14)$$

Where, $SD(DEP_i)$ is the standard deviation of DEP for the jth month throughout the record, MEP is the mean effective precipitation.

The limits of EDI ranges from less than -2 to more than +2 where negative values represent dryness and positive values represents wetness which is presented in Table 3.2.

3.5 MACHINE LEARNING ALGORITHMS

Machine learning is a branch of artificial intelligence (AI) that focuses on the development of algorithms and models that allow computers to learn from data and make predictions or decisions based on it. A machine learning system, rather than being explicitly programmed to do a task, employs statistical patterns and inference to improve its performance overtime. Machine learning algorithms are used in a wide range of sectors, including natural language processing, computer vision, speech recognition, medical diagnosis, finance, and more. The qualities of the data, the nature of the work, and the unique requirements of the problem at hand all influence the choice of an appropriate algorithm.

Using machine learning techniques for the determination of drought indices offers a several advantage over conventional techniques. Drought assessment often involves complex variables and hence using conventional methods may struggle to capture the intricate relationships while machine learning excels in solving the complex relationships. Machine learning algorithms can automatically identify and select relevant features from a large set of variables. This feature selection process helps in

focusing on the most influential factors contributing to drought conditions, improving the efficiency and interpretability of the model.

Drought conditions are influenced by a multitude of variables, and machine learning allows for a data-driven approach to identify relevant features and optimize model performance. This adaptability is particularly valuable in the context of drought, where multiple factors contribute to the overall assessment. Machine learning models, when properly trained and validated, can offer superior predictive accuracy compared to conventional methods. In drought studies, where precise predictions are crucial for effective water resource management and risk mitigation, this heightened accuracy is a significant advantage. Machine learning methods are well-suited for integrating diverse data sources, such as satellite imagery, meteorological data, and ground-based observations. This integrated approach allows for a more holistic assessment of drought conditions.

Machine learning models can automatically adapt to changing conditions without manual recalibration. This is especially valuable in drought studies where conditions may evolve, and the ability to automatically learn and adapt ensures the model's ongoing relevance. Machine learning models have demonstrated superior predictive capabilities in various environmental studies (Karbasi et al. 2023; Khan et al. 2020). By leveraging these techniques, we aim to enhance the accuracy and reliability of drought predictions, contributing to a more robust and effective assessment. Conventional methods may still be appropriate in certain situations, and the choice between machine learning and conventional techniques should be driven by a thoughtful consideration of the study's goals and characteristics.

3.5.1 Adaptive Neuro-Fuzzy Inference System (ANFIS)

The Adaptive Neuro-Fuzzy Inference System (ANFIS) is an approach introduced by Jang (Jang 1993), which combines human knowledge and reasoning processes through fuzzy logic and interconnected neural networks (Mehrabi et al. 2012). The schematic structure of ANFIS is shown in Figure 3.2 having a five-layer architecture where each

layer serves a specific purpose. In layer 1, each node represents the membership of input variable, while layer 2 is the rule-based layer which uses multiplication operator. In layer 3, it computes and normalizes the previous layer, layer 4 moves towards the output model and the layer 5 gives the final output model. The combination of fuzzy logic and neural networks in ANFIS makes it a robust artificial intelligence algorithm capable of performing inference and modelling tasks effectively. The selection of membership functions significantly influences ANFIS performance, often determined through trial and error. ANFIS is widely used in various applications such as pattern recognition, system modelling, prediction, and control, providing the interpretability of fuzzy logic and the learning capabilities of neural networks. To optimize the parameters of ANFIS, Genetic Algorithm (GA) and Particle Swarm Optimization (PSO) were employed. These optimization techniques fine-tune the ANFIS structure and enhance its performance in various applications.

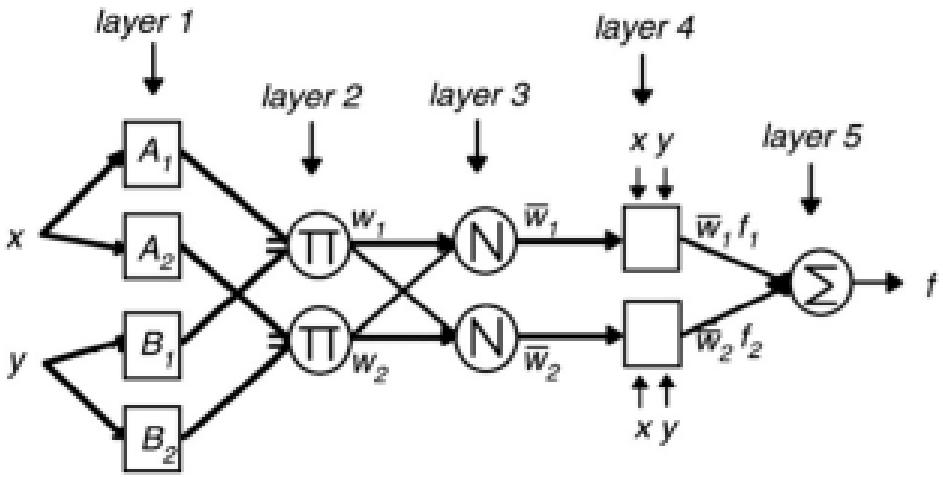

Figure 3.2 Representation of ANFIS (Zounemat-Kermani and Teshnehlab, 2008)

3.5.2 Generalized Regression Neural Networks (GRNN)

GRNN was proposed by Donald F. Specht in 1991 and it is categorized as a probabilistic neural network (Specht 1991). It represents an improved technique based on non-parametric regression within the realm of neural networks. GRNN serves versatile purposes, including regression, prediction, and classification tasks. One of its

significant advantages is that it requires only a fraction of the training samples needed by backpropagation neural networks. In scenarios where data availability is limited for an operating system or measurements, the probabilistic neural network of GRNN becomes highly beneficial. It efficiently converges the underlying function of the data with a small number of training samples, making it an ideal choice when data is scarce. Additionally, GRNN exhibits ease of use, as it demands relatively little prior knowledge from the user for fitting, and no additional input is required during the process.

The Gaussian function employed by GRNN for estimation contributes to its ability to provide highly accurate results. As a result, GRNN finds application in various fields, such as the modeling of dynamic plants (Seng et al. 2002), predicting aerodynamic forces (Song and Ren 2005; Yao et al. 2012), forecasting solar photovoltaic power (Alhakeem et al. 2015), and modeling non-linear systems (Yibin and Ying 2005). For additional information regarding GRNN, its applications and model building networks, one may refer to DF Specht (1991).

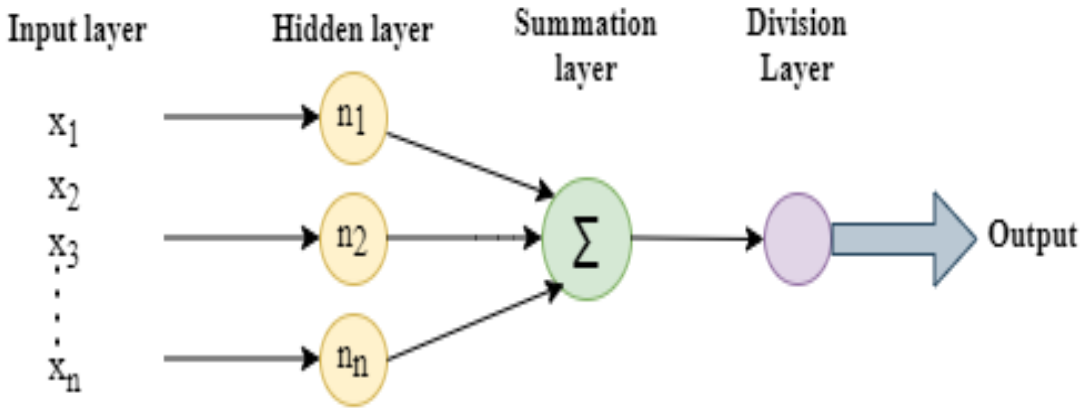

Figure 3.3 General structure of GRNN

3.5.3 Genetic Algorithm (GA)

The Genetic Algorithm (GA) is a computational process employing stochastic search principles grounded in the evolutionary theories of natural selection and genetics. This approach yields advantageous or nearly optimal solutions for combinatorial optimization problems. Examples of such problems include the traveling salesman problem, scheduling problems, heuristic search, and process planning problems

(Goldberg 1989). The basic concept of Genetic Algorithm is to implement genetic operators like crossover, mutation, selection for up-gradation and search for the best population by imitating the natural evolution process artificially. GA is a well-known metaheuristic algorithm that draws inspiration from the biological evolution process (Michalewicz 1996).

The advantages of GA include (1) fast convergence to near-global optimum, (2) superior global searching capability in the space which has a complex searching surface and (3) applicability to the searching space where one cannot use gradient information of the space. Hence, the present study aims to search for the meta-parameters of ANFIS using a genetic algorithm. The use of GA as an optimising technique is advantageous over other optimising techniques. It also supports multi-objective optimisation, proves to be useful for noisy data, gets better with time, is inherently parallel and quickly distributed. GA also has an easy and flexible solution for hybrid applications.

3.5.4 Particle Swarm Optimizer (PSO)

Particle Swarm Optimiser (PSO) technique was developed by Kennedy and Eberhart (1995). PSO, a population-based stochastic optimisation method, is a very straightforward algorithm that seems to work well for optimising a variety of functions. PSO shares some similarities with the Genetic Algorithm technique. PSO is an evolutionary algorithm and follows a societal animal's activities that do not have a particular group leader. Like many evolutionary computation frameworks, it utilised the idea of fitness. A computational method optimises some problem constraints to enhance any feasible sets regarding quality measurements using iterations. The PSO consists of a swarm of particles represented by a potential solution (Omran et al. 2005) and is influenced by the velocity. By comparing with the other computational technique, there are only a few parameters to adjust in PSO. Hence, it is easy to implement. PSO has been widely used in function optimisation, artificial neural network training, fuzzy system control and GA areas.

3.6 HYBRID MACHINE LEARNING MODELS

3.6.1 Genetic Algorithm-Adaptive Neuro Fuzzy Inference System (GA-ANFIS)

The methodology employed in this study involves the integration of a Genetic Algorithm (GA) with an Adaptive Neuro-Fuzzy Inference System (ANFIS), creating a hybrid approach known as GA-ANFIS. This hybridization is designed to harness the strengths of both techniques for efficient problem-solving. ANFIS uses a structure of fuzzy inference systems with parameters adapted through a learning process. For integration, GA is applied to optimize the parameters of the ANFIS model. GA determines the optimal set of parameters for the fuzzy inference system enhancing the overall performance. The formulation of the model firstly the rule base is carried out which is typically organised in a fuzzy rule base that map input variables to output variables. Secondly, the fuzzy sets and membership functions define the linguistic terms and their degrees of membership. And thirdly, GA optimizes the parameters of the ANFIS model adjusting the fuzzy rule base and membership functions. The model is implemented through a stepwise approach. The GA iteratively refines the fuzzy rules and membership functions to optimize the model. Then the hybrid model underdoes training and testing using a dataset where the GA adjusts parameters based on the fitness od individuals in the population. The model can be implemented using programming language either Python or MATLAB. For Table 3.4 describes the parameter settings of GA-ANFIS considered for the requirement of the model.

Table 3.3 Parameters settings of GA-ANFIS

Parameters	GA-ANFIS
Maximum iteration	1000
Population size	25
Cross over percentage	0.4
Mutation percentage	0.7
Mutation rate	0.15
Selection pressure, β	8

3.6.2 Particle Swarm Optimization-Adaptive Neuro Fuzzy Inference System (PSO-ANFIS)

PSO-ANFIS combines Particle Swarm Optimization (PSO) with the Adaptive Neuro-Fuzzy Inference System. PSO is a population-based optimization algorithm inspired by the social behaviour of bird flocking or fish schooling. In PSO-ANFIS, the particles in the swarm represent potential ANFIS configurations, and their positions are updated based on their own best-known positions and the global best position in the swarm. Similar to GA-ANFIS, ANFIS is the underlying fuzzy logic system with adaptive learning capabilities. This process allows the particles to search for an optimal ANFIS model configuration that minimizes the objective function. Table 3.4 shows the input parameters adopted for the model.

Table 3.4 Parameters settings of PSO-ANFIS

Parameters	PSO-ANFIS
Maximum iteration	1000
Population size	25
Damping ratio	0.99
Inertia weight	1

Both GA-ANFIS and PSO-ANFIS can be implemented using languages like Python or MATLAB. In this study, the models are implemented through a systematic approach and their performance is evaluated using evaluation metrics. The hybrid models like GA-ANFIS and PSO-ANFIS offer advantages in terms of adaptability and optimization while GRNN may excel in scenarios where memory-based learning and robustness to noise are critical. In summary, both GA-ANFIS and PSO-ANFIS hybrid models offers advantages in terms of overcoming overfitting, effective optimization for predicting and improved predictive accuracy (Li et al. 2022; Mokhtar et al. 2021; Adnan et al. 2020; Ahmed et al. 2017).

3.7 DEVELOPMENT OF MACHINE LEARNING MODELS

In the present study, GA-ANFIS, PSO-ANFIS and GRNN models are adopted for meteorological drought indices prediction. The input variable used is the monthly

precipitation data from 1958-2017. The development process involves problem formulation, data collection and pre-processing, feature selection, model selection, dataset training, evaluation, hyperparameter tuning and deployment. The development of machine learning algorithms is an iterative and dynamic process, constantly learning, adapting and refining to achieve accurate and reliable predictions in real world applications. For training purposes, 80% of the dataset is utilized, while the remaining 20% is reserved for testing, ensuring a robust evaluation of the machine learning algorithms. The developed models are trained using the optimal values obtained from the process. Once the models are optimized, the performance of the various models for meteorological drought indices, EDI, SPI-9 and SPI-12 simulations are evaluated using evaluation metrics such as R^2, RRMSE, and NSE. By comparing the results obtained from the evaluation metrics, aim of the study to determine the best predicting model using machine learning algorithms. This comparison enables us to select the most suitable model that provides accurate and reliable predictions for meteorological drought indices.

3.8 PERFORMANCE EVALUATION METRICS

Performance evaluation metrics play a crucial role in assessing the effectiveness and accuracy of machine learning models. They provide valuable insights into how well the models perform in making predictions and allow for comparisons among different models, algorithms, or approaches. The selection of appropriate evaluation metrics depends on the specific task, problem domain and the significance of various types of errors. In this study, the selection of appropriate evaluation metrics depends on the accuracy and precision of the models, model interpretability and their performance, temporal consistency and robustness to variability. However, researchers typically aim to select metrics that align with the goals of the study and provide a comprehensive assessment of model performance. Table 3.5 shows the list of the statistical metrics adopted in the study.

Table 3.5 List of statistical metrics with their description

Statistical criteria	Values/Ranges	Inference
Coefficient of determination (R^2)	0 to 1	0 = The model does not predict the outcome Between 0 and 1: The models partially predict the outcome 1 = The model perfectly predicts the outcome
Nash-Sutcliffe Efficiency, $NSE = 1 - \frac{\sum_{i=1}^{N}(P_i - O_i)^2}{\sum_{i=1}^{N}(O_i - \bar{O})^2}$	0.75 < NSE < 1.0 0.65 < NSE ≤ 0.75 0.50 < NSE ≤ 0.65 0.4 < NSE ≤ 0.50 NSE ≤ 0.40	Very good Good Satisfactory Acceptable Unsatisfactory
Relative Root Mean Square Error $RRMSE = \sqrt{\frac{\frac{\sum_{i=1}^{n}(O_i - P_i)^2}{N}}{\sigma_{obs}}}$	0 ≤ RRMSE ≤ 0.10 0.10 ≤ RRMSE≤0.30 0.30≤RRMSE≤0.50 RRMSE > 0.70	Very good Good Satisfactory Poor

where O_i is the observed value, P_i is the predicted value, N is the total number of observations, $\bar{O}$ is the mean of the observed value and σ_{obs} is the standard deviation of the observed value.

By utilizing these evaluation metrics, we aim to gain a comprehensive understanding of the capabilities of each machine learning algorithm and identify the best-performing model for predicting meteorological drought indices. The evaluation process enables us to make informed decisions and ensures the reliability and accuracy of our predictions.

Figure 3.4 illustrates the schematic representation of the methodology adopted for the study. The workflow overview for the methodology adopted in the study can be summarized as follows:

Objective 1: Trend Analysis of Rainfall and Drought Indices

Data Collection: Accumulation of monthly rainfall data for the specified study period.

Mann-Kendall Test: Application of the Mann-Kendall test for trend analysis of both rainfall and drought indices. Identification of trends in precipitation and drought indices over time.

Meteorological Drought Indices: Computation of meteorological drought indices using the collected monthly rainfall data.

Objective 2 and Objective 3: Machine Learning Models for Meteorological Drought Indices Predictions

Machine Learning Model Development: Implementation of machine learning models for predicting meteorological drought indices. The models employed are GA-ANFIS, PSO-ANFIS and GRNN.

Performance Evaluation Metrics:

Application of performance evaluation metrics to assess the effectiveness of the developed machine learning models. Metrics including, Coefficient of determination (R^2), Nash-Sutcliffe Efficiency (NSE) and Normalized root mean square error (NRMSE).

Identification of Best Models:

Selection of the best-performing machine learning models based on the outcomes of the evaluation metrics. Recognition of models demonstrating superior performance in predicting meteorological drought indices.

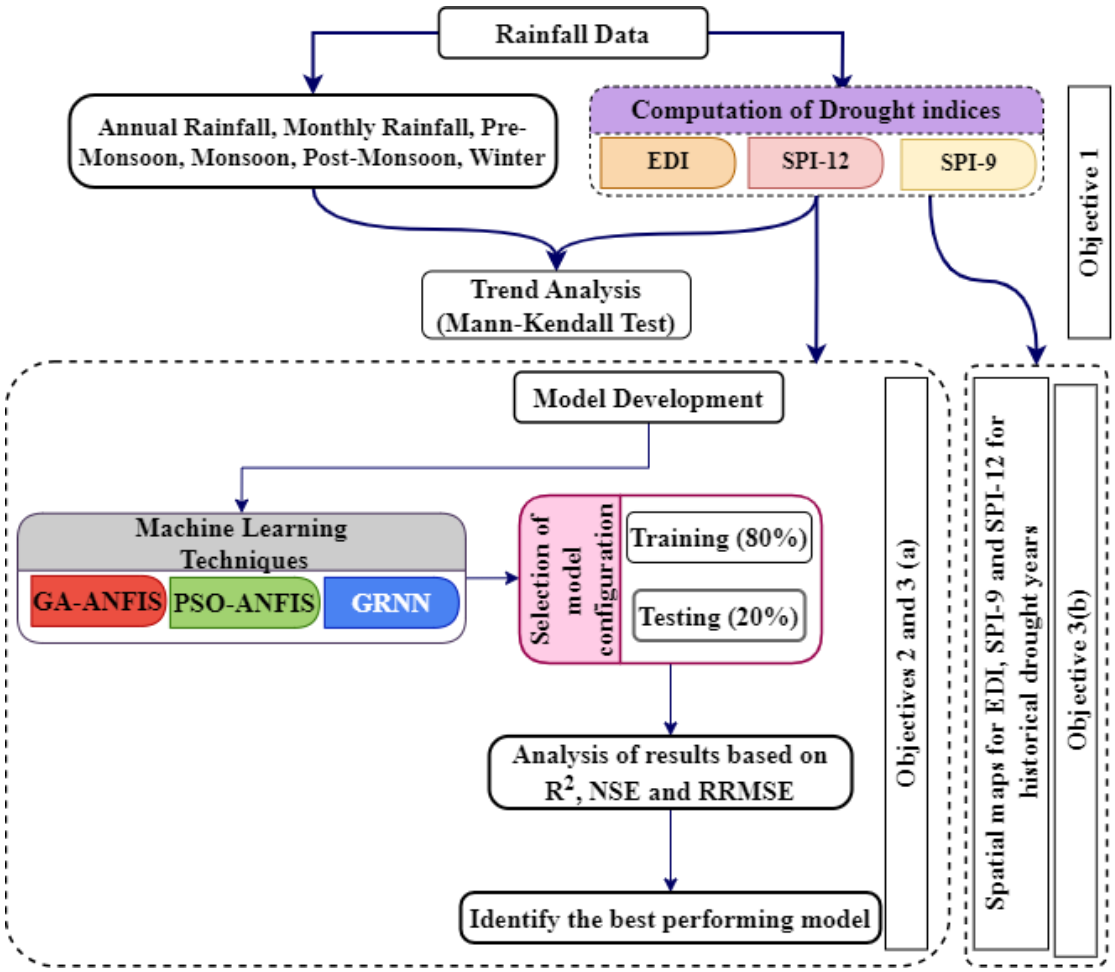

Figure 3.4 Flowchart of the methodology

CHAPTER 4

RESULTS AND DISCUSSION

4.1 TREND ANALYSIS OF ANNUAL RAINFALL, MONTHLY RAINFALL AND SEASONAL RAINFALL

This section represents the descriptive results of the trend analysis of rainfall and meteorological drought indices, which is crucial for understanding the impact of climate change on ecosystems and its implications for human activities. To achieve this, the study utilizes data from thirty-four meteorological subdivisions of India, spanning 60 years of monthly rainfall data from 1958 to 2017. The primary aim of the trend analysis is to identify patterns, variations, and potential changes in precipitation levels over time. The analysis involves assessing statistical parameters using the Mann-Kendall test to evaluate trends in annual, monthly and seasonal rainfall, including pre-monsoon, monsoon, post-monsoon, and winter rainfall. Similarly, meteorological drought indices, such as EDI, SPI-9, and SPI-12, are also subjected to trend analysis. Additionally, the average distribution of rainfall is computed for annual, monthly and seasonal periods, enabling a visual understanding of rainfall patterns throughout the study region.

India is a vast country with diverse climatic zones resulting in a wide range of rainfall patterns across different regions, influenced by various factors such as the monsoon season, topography and proximity to water bodies. The southwest monsoon is the primary rainy season in most parts of India contributing to a significant portion of the country's annual rainfall. It originates from the Arabian sea and Bay of Bengal and brings moisture-laden winds that lead to widespread rainfall. The southwest monsoon affects the western ghats including the western coastal regions including Kerala, Karnataka and Maharashtra.

The spatial distribution maps depicting the annual average, average monthly, average pre-monsoon, average monsoon, average post-monsoon and average winter rainfall are illustrated in Figure 4.1 (a-f). The illustrations reveal that rainfall patterns can vary

significantly across different regions within a country and helps in identifying the regions with high rainfall and low rainfall enabling a better understanding of regional variations and local climate characteristics. Overall, the spatial distribution maps of rainfall provide a valuable insight into the variability of precipitation across different regions, helping with various aspects of planning, resource management, disaster preparedness and environmental conservation initiatives.

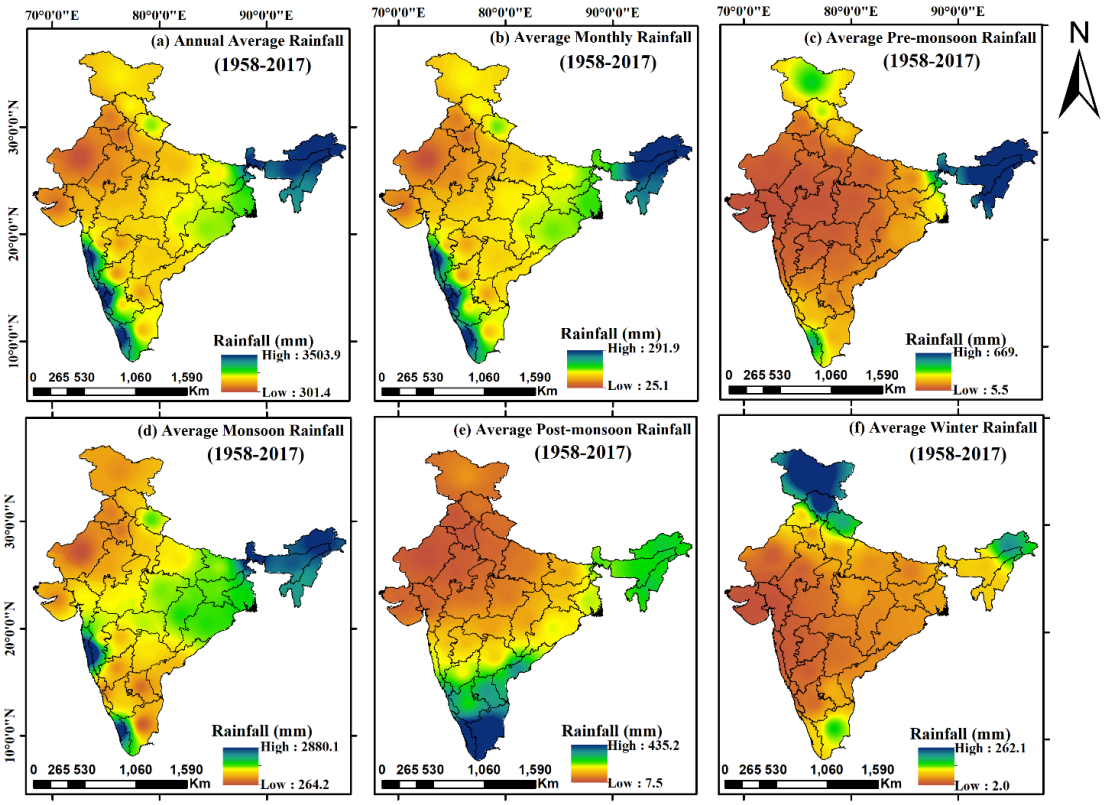

Figure 4.1 (a-f). Spatial distribution map for Annual average, average Monthly and average Seasonal Rainfall (1958-2017)

4.1.1 Annual Rainfall

The average annual rainfall for different meteorological subdivisions has been calculated, revealing Coastal Karnataka as the region with the highest average annual rainfall at 3500 mm as depicted in Figure 4.1 (a). The coastal region of Karnataka experiences high rainfall during the monsoon season since it is situated on the windward side of the Western Ghats. Moreover, it also receives more moisture from the sea

compared with other regions of India. Other meteorological subdivisions like Konkan-Goa, Kerala, Arunachal Pradesh, Sub-Himalayan West Bengal Sikkim and Assam-Meghalaya experience an average annual rainfall of more than 2500 mm during the study period. Due to the mountainous landscape, the North-East region experiences high amount of rainfall in some locations. In contrast, the meteorological subdivision of west Rajasthan receives the lowest average annual rainfall of around 300 mm. Rainfall in Rajasthan is mainly brought by the Bay of Bengal which is geographically far from the region so it results in less rainfall. Due to its location in the shadow effect and arid climate with high temperature and little humidity, west Rajasthan receives less rainfall throughout the year.

The meteorological subdivisions such as Saurashtra-Kutch-Diu, Haryana-Chandigarh-Delhi, and Punjab receive less than 600 mm of annual rainfall on average as the Himalayan Mountains act as a barrier restricting moisture from the Arabian Sea and the Bay of Bengal to enter these regions. Furthermore, these regions have arid or semi-arid climatic conditions with high temperatures and low humidity, resulting in less precipitation. The remaining meteorological subdivisions experience an average annual rainfall of 600 to 2500 mm depending on their geography, orographic rainfall, monsoon winds and topography of the region. Overall, the maximum annual average rainfall has been observed in North-East India and some parts of Peninsular India.

The annual rainfall trend analysis is presented in Figure 4.2 (a). The observed decreasing or increasing trends in different regions can be attributed to various factors, including topography, temperature, and other climate-related aspects. Gangetic West Bengal, west Rajasthan, Saurashtra-Kutch-Diu, Rayalaseema, and Tamil Nadu-Pondicherry subdivisions display an increasing trend, though not statistically significant (p -value > 0.05). On the other hand, the remaining meteorological subdivisions show a non-statistically significant decreasing annual trend. Statistically significant decreasing annual trends, at a 95% confidence level, have been observed in meteorological subdivisions such as Assam-Meghalaya, Nagaland-Manipur-Mizoram-Tripura, Sub-Himalayan West Bengal Sikkim, East and West Uttar Pradesh, Himachal

Pradesh, Punjab, Haryana-Chandigarh-Delhi, and West Madhya Pradesh. These trends suggest possible changes in rainfall patterns, raising concerns about climate change's potential impact on India's rainfall distribution. Some studies have highlighted the likelihood of increased severe rainfall events in the future, but the exact nature and significance of these changes remain uncertain (Mukherjee et al. 2018; Shahi et al. 2023; Yaduvanshi et al. 2019).

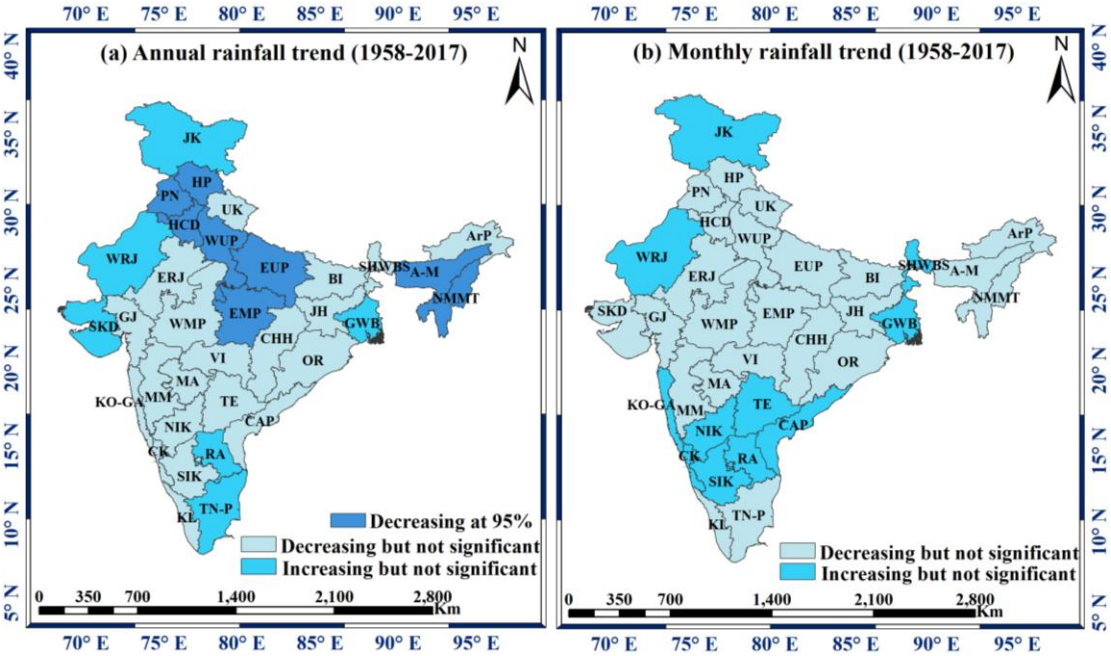

Figure 4.2 (a & b) Meteorological subdivision wise for Annual and Monthly Rainfall trend for the period (1958-2017)

4.1.2 Monthly rainfall

For the average monthly rainfall, represented in Figure 4.1 (b), regions like Coastal Karnataka, Konkan-Goa, Arunachal Pradesh, Kerala, and Assam-Meghalaya experience an average monthly rainfall of 292.09 mm, 255.18 mm, 239.23 mm, 235.29 mm and 220.67 mm of rainfall respectively. While regions like west Rajasthan, Saurashtra-Kutch-Diu, Haryana-Chandigarh-Delhi and Punjab experienced 25.08 mm, 43.93 mm, 44.52 mm and 49.18 mm of rainfall respectively because of its arid and semi-arid conditions. The remaining regions generally receive between 50 to 200 mm of average monthly rainfall. This information is crucial for understanding the

distribution of rainfall across the country and its impact on various regions' ecosystems, agriculture, and water resources.

As depicted in Figure 4.2 (b), the trend analysis for monthly rainfall indicates that certain regions such as Gangetic West Bengal, Sub-Himalayan West Bengal Sikkim, Jammu-Kashmir, west Rajasthan, Coastal Andhra Pradesh, Telangana, Rayalaseema, Coastal Karnataka, Konkan Goa, South Interior Karnataka and North Interior Karnataka have shown an increasing trend in rainfall which is not statistically significant. However, the lack of statistical significance in these trends suggests that they might be driven by natural variability rather than long-term climate changes. On the contrary, the remaining meteorological subdivisions exhibit a decreasing trend in monthly rainfall, which is also not statistically significant. These findings emphasize the complexity of rainfall patterns and the influence of multiple factors on regional climate variations.

The rainfall pattern in the study region exhibits significant spatial and temporal variations. Table 4.1 shows the p -values and Table 4.2 shows Kendall's tau evaluated from the Mann-Kendall test for Annual, Monthly and Seasonal Rainfall. The p -value is crucial in determining the statistical significance of the results obtained from the test. If the p -value is less than the predetermined significance level, it suggests that the observed trend is statistically significant. On the other hand, if the p -value is greater than the significance level, it indicates that the observed trend is not statistically significant. The p -value is crucial in interpreting the results of the Mann-Kendall test and determining the presence or absence of a trend in the dataset. Kendall's tau quantifies the strength and direction of the trends in the data. Kendall's tau ranges from positive to negative values where the positive value indicates an increasing trend in the data and the negative value indicates a decreasing trend in the data. The statistical significance is calculated at 95%, where $p < 0.05$ represents that a statistically significant trend exists in the dataset.

Table 4.1 *p* -values for Annual, Monthly and Seasonal Rainfall

Meteorological subdivisions	*p* -values					
	Annual	**Monthly**	**Pre-Monsoon**	**Monsoon**	**Post-Monsoon**	**Winter**
BI	0.264	0.633	**0.021**	0.443	0.096	0.574
EUP	**0.0002**	0.101	1	**0.001**	**0.031**	0.431
JH	0.475	0.446	0.64	0.569	0.427	0.069
OR	0.914	0.551	0.711	0.386	0.251	0.286
UK	0.101	0.075	0.6	0.504	**0.001**	**0.041**
WUP	**0.0003**	0.238	0.666	**0.004**	**0.032**	1
AP	0.115	0.381	0.694	0.245	0.212	**0.021**
AM	**0.037**	0..244	0.253	0.862	0.198	0.209
GWB	0.287	0.533	0.059	0.414	0.752	0.837
NMMT	**0.008**	0.116	0.896	**0.007**	0.161	**0.017**
SHWBS	0.433	0.693	0.103	0.36	0.89	0.896
ER	0.678	0.843	0.421	0.902	0.216	0.512
GJ	0.873	0.222	0.055	0.98	0.87	0.651
HCD	**0.017**	0.795	0.139	**0.011**	**0.026**	0.736
HP	**0.011**	0.196	0.399	0.255	**0.027**	0.421
JK	0.241	0.498	0.536	0.287	0.158	**0.034**
PN	**0.007**	0.694	0.536	**0.005**	0.127	0.694
SKD	0.418	0.304	0.07	0.207	0.811	0.315
WR	0.142	0.302	0.107	0.174	0.686	0.488
CAP	0.853	0.545	0.066	0.902	0.295	0.41
CK	0.597	0.492	0.985	0.443	0.231	0.261
KL	0.614	0.847	0.339	0.36	0.147	0.379
RAY	0.382	0.278	**0.045**	0.504	0.93	0.339
SIK	0.745	0.588	0.379	0.225	0.791	0.269
TNP	0.904	0.396	0.536	0.198	0.91	0.64
CHH	0.115	0.423	0.389	0.266	0.87	0.269
EMP	**0.034**	0.37	0.359	0.245	0.96	0.303
KG	0.985	0.662	0.881	0.98	0.472	0.97
MM	0.697	0.506	**0.023**	0.748	1	0.587
MA	0.121	0.607	0.223	0.414	0.96	0.476
NIK	0.23	0.751	0.5	0.335	0.623	0.388
TE	0.553	0.486	0.12	0.443	0.696	0.736
VI	0.495	0.162	**0.045**	0.785	0.83	0.261
WMP	0.311	0.53	0.64	0.674	0.161	0.808

Bold values indicate significant trend at 95% confidence level.

Table 4.2 Kendall's Tau for Annual, Monthly and Seasonal Rainfall

Meteorological Subdivisions	Kendall's Tau					
	Annual	Monthly	Pre-Monsoon	Monsoon	Post-Monsoon	Winter
BI	-0.10	-0.012	0.22	-0.08	-0.15	-0.05
EUP	-0.34	-0.041	0.00	-0.33	-0.20	-0.08
JH	-0.06	-0.019	0.05	-0.06	-0.07	-0.17
OR	-0.01	-0.015	0.03	-0.09	-0.11	-0.10
UK	-0.15	-0.044	0.05	-0.07	-0.30	-0.19
WUP	-0.32	-0.029	0.04	-0.28	-0.20	0.00
AP	-0.14	-0.022	-0.04	-0.11	-0.12	-0.22
AM	-0.19	-0.029	-0.11	0.02	-0.12	-0.12
GWB	0.10	0.016	0.18	0.08	-0.03	0.02
NMMT	-0.23	-0.039	-0.01	-0.26	-0.13	-0.23
SHWBS	-0.07	0.01	0.15	-0.09	-0.01	0.01
ER	-0.04	-0.005	0.08	0.01	-0.11	0.06
GJ	-0.02	-0.032	-0.18	0.01	-0.02	-0.05
HCD	-0.21	-0.007	0.14	-0.25	-0.20	0.03
HP	-0.23	-0.032	-0.08	-0.11	-0.20	-0.08
JK	0.11	0.017	-0.06	0.11	-0.13	0.20
PN	-0.24	-0.01	0.06	-0.27	-0.14	-0.04
SKD	0.07	-0.027	-0.17	0.12	-0.02	-0.10
WR	0.13	0.026	0.15	0.13	-0.04	0.07
CAP	-0.02	0.015	0.17	0.01	-0.10	0.08
CK	-0.05	0.017	0.00	-0.08	0.11	0.11
KL	-0.05	-0.005	-0.09	-0.09	0.13	-0.08
RAY	0.08	0.027	0.19	0.07	-0.01	0.09
SIK	-0.03	0.014	0.08	-0.12	0.03	-0.11
TNP	0.01	-0.021	-0.06	-0.13	0.01	-0.05
CHH	-0.14	-0.02	-0.08	-0.11	-0.02	-0.11
EMP	-0.19	-0.022	-0.09	-0.11	-0.01	-0.10
KG	0.00	0.011	-0.02	0.01	0.07	0.01
MM	-0.04	-0.017	-0.21	-0.03	0.00	-0.05
MA	-0.14	-0.013	-0.12	-0.08	-0.01	-0.07
NIK	-0.11	0.008	-0.07	-0.10	-0.05	0.08
TE	-0.05	0.017	0.15	-0.08	-0.04	0.03
VI	-0.06	-0.035	-0.19	-0.03	-0.02	-0.11
WMP	-0.09	-0.016	-0.05	-0.04	-0.13	-0.03

4.1.3 Pre-monsoon rainfall

During the pre-monsoon season, which typically spans from March to May, the distribution of average rainfall across different regions of India varies significantly. The meteorological subdivisions of Arunachal Pradesh and Assam-Meghalaya in the North-East experience the highest average pre-monsoon rainfall, recording 669.18 mm and 607.03 mm of rainfall, respectively. Conversely, Saurashtra-Kutch-Diu and Gujarat receive the least average pre-monsoon rainfall, with values of 5.48 mm and 5.71 mm, respectively. The remaining regions generally fall within the range of 10 mm to 500 mm of pre-monsoon rainfall.

An insightful analysis of the pre-monsoon rainfall trend is represented in Figure 4.3 (a). The meteorological subdivisions of East Uttar Pradesh show neither an increasing nor decreasing trend. On the other hand, Bihar and Rayalaseema exhibit an increasing trend, while Vidarbha and Madhya Maharashtra display a decreasing pre-monsoon rainfall trend that is statistically significant at a 95% confidence level. In contrast, the Central Northeast region, Gangetic West Bengal, Sub-Himalayan West Bengal Sikkim, East and West Rajasthan, Haryana-Chandigarh-Delhi, Punjab, Coastal Andhra Pradesh, Telangana, South Interior Karnataka, and Uttarakhand show an increasing trend in pre-monsoon rainfall, but the trends are not statistically significant. The remaining meteorological subdivisions exhibit a decreasing trend in pre-monsoon rainfall, but like the previous group, the trends are not statistically significant.

Understanding the trends in pre-monsoon rainfall is of vital importance for India's water balance, as it can significantly impact groundwater recharge and reservoir levels. Regions experiencing decreasing pre-monsoon rainfall trends may face challenges in water availability and agricultural productivity. However, regions with increasing trends may experience changes in local ecosystems and hydrological patterns. However, it is important to note that the non-significance of some observed trends indicates that they are likely driven by natural climate variability rather than long-term changes. Hence, further research and monitoring are necessary to comprehensively

assess the impact of pre-monsoon rainfall trends and their implications for water resources and agricultural practices.

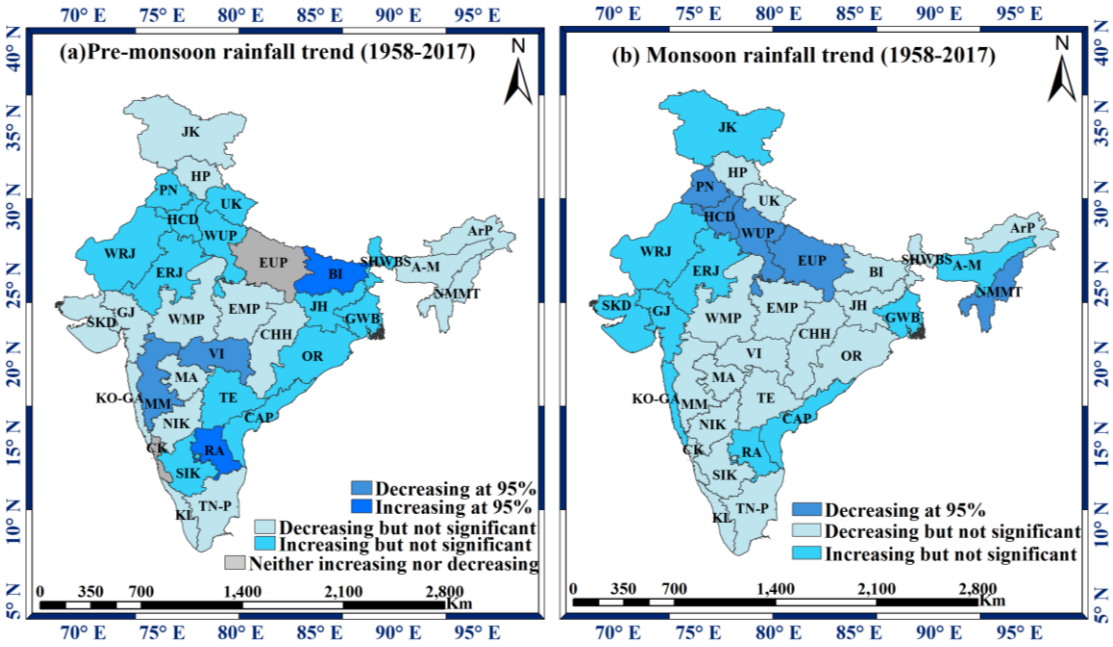

Figure 4.3(a & b) Meteorological subdivisions wise for pre-monsoon and monsoon rainfall trend for the period (1958-2017)

4.1.4 Monsoon rainfall

During the monsoon period, which typically spans from June to September, the spatial distribution of average monsoon rainfall across India shows considerable variation. Regions such as Konkan-Goa, Sub-Himalayan West Bengal, Kerala, Arunachal Pradesh, and Assam-Meghalaya experience the highest average monsoon rainfall, with precipitation levels exceeding 2500 mm. On the contrary, the region of West Rajasthan receives the least average monsoon rain, with rainfall measuring less than 300 mm. Figure 4.1(b) provides a spatial distribution map illustrating the average monsoon rainfall trend across the country.

To ascertain the significance of the observed trends, a trend analysis is conducted using the Mann-Kendall test. The results indicate that the subdivisions of Nagaland-Manipur-Mizoram-Tripura, East and West Uttar Pradesh, Haryana-Chandigarh-Delhi, and Punjab exhibit a statistically significant decreasing trend in monsoon rainfall. On the

other hand, the subdivisions of Assam-Meghalaya, Gangetic West Bengal, Jammu-Kashmir, East and West Rajasthan, Gujarat, Saurashtra-Kutch-Diu, Coastal Andhra Pradesh, Rayalaseema, and Konkan Goa show an increasing trend, but these trends are not statistically significant. The remaining regions display decreasing trends that are also not statistically significant.

The monsoon rainfall holds paramount importance for India's agriculture, water resources, and overall economy. It is a critical factor in determining agricultural productivity and plays a crucial role in replenishing water bodies and reservoirs. Hence, monitoring and understanding the trends in monsoon rainfall are essential for effective water resource management and disaster preparedness.

Figure 4.2 (b) provides a graphical representation of the monsoon rainfall trend, allowing for a clear visualization of the observed patterns across different meteorological subdivisions. Identifying significant trends in monsoon rainfall helps policymakers and stakeholders in formulating adaptive strategies to mitigate the impacts of climate variability on agriculture, water availability, and livelihoods. However, it is important to interpret the non-significant trends with caution, as they may result from natural climate variability rather than long-term climate changes. Continued monitoring and analysis of monsoon patterns are necessary to comprehend the dynamics of this critical climatic phenomenon and prepare for potential challenges posed by climate change.

4.1.5 Post-monsoon rainfall

The post-monsoon season in India spans October and November, and the distribution of average post-monsoon rainfall exhibits considerable regional variability. The meteorological subdivisions of Kerala and Tamil Nadu-Pondicherry experience the highest average post-monsoon rainfall, with precipitation levels exceeding 350 mm as depicted in Figure 4.1 (e). In contrast, the region of West Rajasthan, Haryana-Chandigarh-Delhi, and Punjab receive the lowest average post-monsoon rainfall, with less than 15 mm of rainfall. The remaining regions typically experience post-monsoon rainfall ranging from 20 mm to 260 mm.

As illustrated in Figure 4.3 (a), the trend analysis of post-monsoon rainfall reveals that India's post-monsoon rainfall has been variable over the years, with some years experiencing above-normal rainfall and others experiencing below-normal rainfall. The Mann-Kendall test, employed for trend analysis, identifies significant trends in certain meteorological subdivisions. The subdivisions of East and West Uttar Pradesh, Uttarakhand, Haryana-Chandigarh-Delhi, and Himachal Pradesh show a statistically significant decreasing trend in post-monsoon rainfall. On the other hand, the meteorological subdivisions of Coastal Karnataka, Kerala, Konkan-Goa, South Interior Karnataka, and Tamil Nadu-Pondicherry exhibit an increasing trend, but the trend is not statistically significant during the post-monsoon period. The remaining meteorological subdivisions experience a decreasing trend, though not statistically significant. The spatial distribution map for the Mann-Kendall test can be seen in Figure 4.3(a), while the statistical details of the Mann-Kendall test are provided in Tables 4.1 and 4.2.

Understanding post-monsoon rainfall trends is vital for assessing the region's water availability, especially during the dry season. Regions experiencing a decreasing trend in post-monsoon rainfall may face water scarcity and challenges in water resource management. On the contrary, regions with an increasing trend in post-monsoon rainfall may need to consider potential impacts on flooding, agriculture, and infrastructure.

4.1.6 Winter rainfall

During the winter season, spanning from December to February, the distribution of average winter rainfall across different regions of India exhibits considerable variation. Jammu-Kashmir and Himachal Pradesh experience the highest average winter rainfall, with precipitation levels reaching 262.35 mm and 218.64 mm, respectively (Figure 4.1(f)). Conversely, regions like Saurashtra-Kutch-Diu, Gujarat, Konkan-Goa, Madhya Maharashtra, and West Rajasthan receive the least average winter rainfall, with precipitation levels falling below 10 mm. The Mann-Kendall (M-K) test provides insights into the trends of winter rainfall in different regions. Results from the test show that Jammu-Kashmir exhibits an increasing trend, while Arunachal Pradesh, Nagaland-Manipur-Mizoram-Tripura, and Uttarakhand have a statistically significant decreasing

trend in winter rainfall. The trend analysis for winter rainfall further reveals that certain regions, including Gangetic West Bengal, Coastal Andhra Pradesh, Coastal Karnataka, Rayalaseema, South Interior Karnataka, Konkan-Goa, North Interior Karnataka, East and West Rajasthan, Haryana-Chandigarh-Delhi, and Jammu-Kashmir, indicate an increasing trend in winter rainfall. However, this increasing trend is not statistically significant. On the other hand, the remaining meteorological subdivisions display a decreasing trend in winter rainfall, also not statistically significant. West Uttar Pradesh, as depicted in Figure 4.3(b), shows neither an increasing nor decreasing trend in winter rainfall.

It is essential for agriculture and maintaining the water balance to understand the patterns of winter rainfall in different regions. Adequate winter rainfall is vital for replenishing groundwater and reservoirs, supporting agricultural activities during the dry season, and ensuring water availability for various human needs. In regions experiencing a decreasing trend in winter rainfall, there might be concerns regarding water shortages and potential impacts on agriculture and water resources.

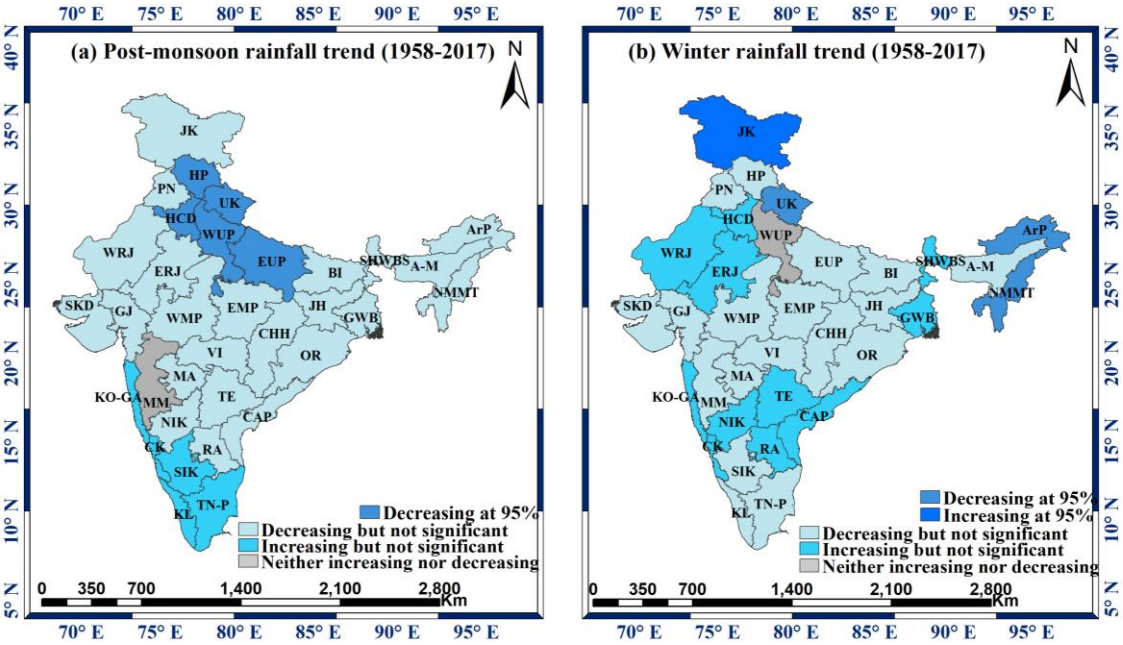

Figure 4.4 (a & b) Meteorological subdivisions wise for post-monsoon and Winter Rainfall trend for the period (1958-2017)

4.1.7 Trend analysis of meteorological drought indices

The trend analysis of meteorological drought indicators is a crucial aspect that requires an extensive assessment of patterns and variations in these indices over time. It aims to identify any systematic trends in drought conditions which can provide insights into the dynamics or drought occurrence and severity. To achieve this, the Mann-Kendall test is employed, which is a robust statistical method used to detect temporal trends in drought indices, specifically the Effective Drought Index (EDI) and Standardized Precipitation Index (SPI) with various timescales. The Mann-Kendall test is an ideal choice for this analysis due to its non-parametric nature, making it suitable for datasets that may not follow a normal distribution. By evaluating the data over a specific period, the test can determine if there are significant trends in drought conditions, whether they may be increasing or decreasing in severity over time.

Identifying trends in drought indices is crucial for effective water resource management and disaster preparedness. A consistent increase or decrease in drought severity could indicate the need for targeted mitigation strategies, such as implementing water conservation measures or drought-resistant agricultural practices. On the other hand, a lack of significant trends might suggest natural variability in drought occurrence, which is equally important for understanding regional climate patterns and planning appropriate responses.

Overall, conducting trend analysis using Mann-Kendall test on meteorological drought indices is a valuable step in enhancing our understanding of drought dynamics in the study region.

4.1.7.1 Effective Drought Index (EDI)

EDI is a widely recognized drought index which plays a crucial role in assessing drought severity by considering precipitation data. Conducting a trend analysis Mann-Kendall test for EDI during the period 1958-2017 in the meteorological subdivisions of India provides valuable insights into the temporal patterns of drought events during this study period. The trend analysis of EDI reveals a generally decreasing trend over the

specified period, although not statistically significant. This observation suggests that while there might be fluctuations in drought severity, there is no clear overall increasing or decreasing trend across the entire country.

The visual representation of the EDI trend during 1958-2017 is shown in Figure 4.5, illustrating the fluctuating nature of drought severity across different regions of India. Understanding such trends aids in formulating evidence-based policies for drought mitigation, resource planning, and climate resilience efforts.

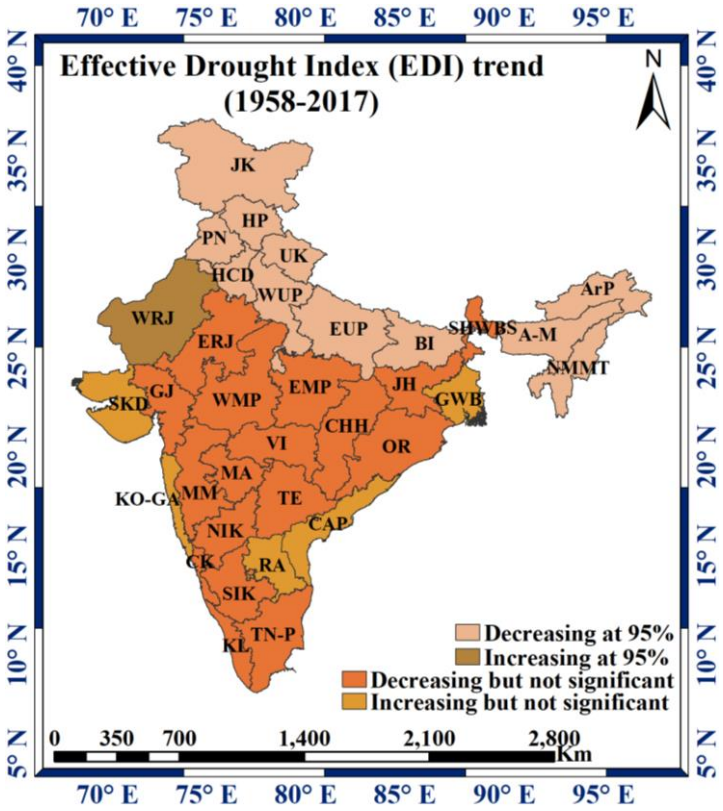

Figure 4.5 Meteorological subdivision wise for Effective Drought Index trend for the period (1958-2017)

However, when examining specific meteorological subdivisions, interesting patterns emerge. Regions like Bihar, East Uttar Pradesh, Uttarakhand, West Uttar Pradesh, Arunachal Pradesh, Assam-Meghalaya, Nagaland-Manipur-Mizoram-Tripura, Haryana-Chandigarh-Delhi, Himachal Pradesh, and Punjab display statistically significant decreasing trends in EDI. This indicates a potential worsening of drought

conditions in these areas during the study period. On the other hand, Jammu-Kashmir and West Rajasthan experience an increasing trend in EDI, indicating a potential improvement in drought conditions in these regions over the years. For the remaining meteorological subdivisions, the EDI trend is not statistically significant, suggesting that drought severity has remained relatively stable in those areas during the study period.

The findings of the EDI trend analysis emphasize the importance of effective drought management strategies in India. Proactive water management and conservation practices are crucial to mitigate the impacts of droughts on agriculture, water resources, and socio-economic activities. Additionally, regions which experiences statistically significant decreasing trends in EDI may require targeted interventions to tackle worsening drought conditions and ensure sustainable water availability.

In this study, the Mann-Kendall test was conducted with a significance level set at 95%, ensuring that the obtained results are reliable and robust. The p -values derived from the test are essential indicators of the statistical significance of the trends observed in the EDI data. Table 4.3 provides a comprehensive overview of the Mann-Kendall test results, including the test statistics, p -values, and Kendall's tau, specifically for the Effective Drought Index (EDI). The Mann-Kendall test is a vital statistical tool utilized to identify trends and assess their significance in time series data.

The analysis reveals that not all meteorological subdivisions demonstrated statistically significant trends for EDI. This finding implies that while some regions may have experienced notable changes in drought severity over time, these changes may not be considered statistically significant within the scope of this study. The non-significant trends can result from a variety of factors, including natural variability, data limitations, or the influence of multiple drivers impacting drought conditions. It is crucial to understand that these non-significant trends provide valuable insights into the complexity of drought changing aspects in different regions.

Table 4.3 Mann-Kendall statistical properties of 34 Meteorological subdivisions for EDI

Meteorological subdivisions	Kendall's tau	*p* -value	Min
BI	-0.02	**0.03**	-1.49
EUP	-0.11	**<0.0001**	-1.42
JH	-0.03	0.28	-1.46
OR	0.00	0.89	-1.54
UK	-0.07	**0.00**	-1.64
WUP	-0.12	**<0.0001**	-1.45
AP	-0.08	**0.00**	-1.60
AM	-0.07	**0.01**	-1.71
GWB	0.05	0.06	-1.53
NMMT	-0.12	**<0.0001**	-1.45
SHWBS	-0.01	0.79	-1.58
ER	-0.01	0.57	-1.35
GJ	0.00	0.88	-1.32
HCD	-0.08	**0.00**	-1.38
HP	-0.10	**<0.0001**	-1.79
JK	0.08	**0.00**	-2.05
PN	-0.11	**<0.0001**	-1.50
SKD	0.04	0.12	-1.26
WR	0.06	**0.01**	-1.34
CAP	0.01	0.69	-1.64
CK	0.00	0.86	-1.46
KL	-0.02	0.38	-1.73
RAY	0.04	0.14	-1.66
SIK	-0.01	0.84	-1.66
TNP	-0.05	0.05	-2.02
CHH	-0.03	0.30	-1.45
EMP	-0.04	0.14	-1.45
KG	0.01	0.73	-1.53
MM	0.00	0.96	-1.57
MA	-0.03	0.17	-1.62
NIK	-0.03	0.25	-1.56
TE	0.00	0.94	-1.52
VI	-0.01	0.59	-1.49
WMP	-0.01	0.63	-1.40

4.1.7.2 Standardized Precipitation Index (SPI-9 and SPI-12)

SPI is a widely use meteorological drought index which quantifies anomalies. SPI is often used to assess and monitor drought conditions and can be computed over different timescales. SPI-9 and SPI-12 refers to the 9-month and 12-month timescale and assesses precipitation anomalies and drought conditions over 9 months and 12 months. Figure 4.6 (a & b) illustrates the trends of the SPI-9 and SPI-12, which are essential drought indices used to assess meteorological drought conditions. The analysis of these trends provides valuable insights into the changing patterns of drought occurrence and severity over time.

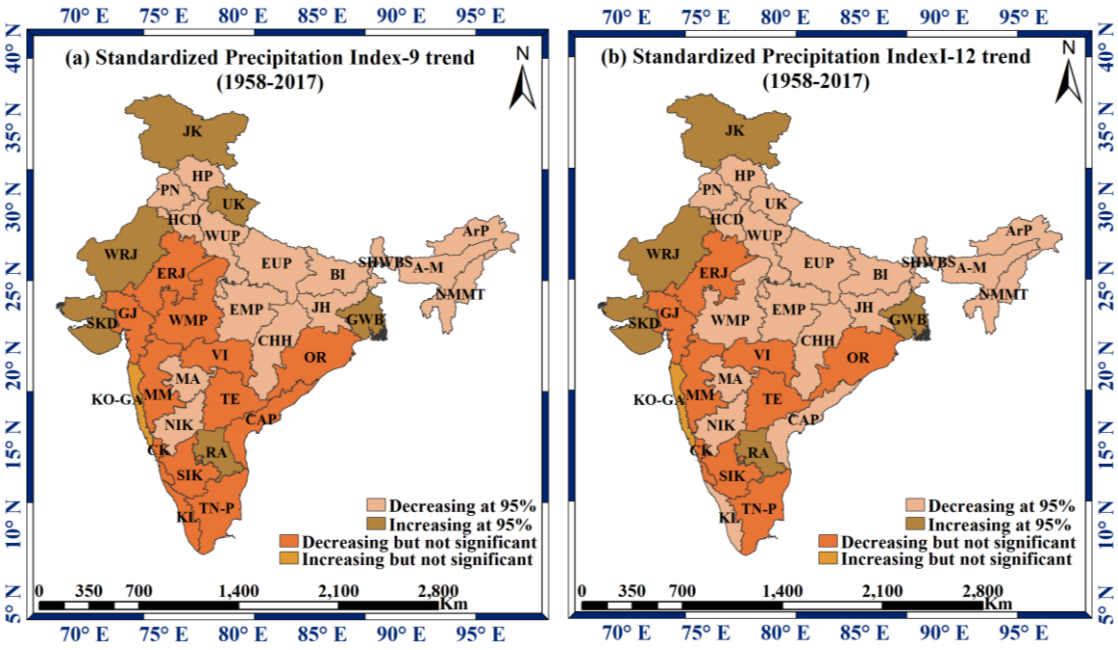

Figure 4.6 (a & b). Meteorological subdivision wise for SPI-9 and SPI-12 trend for the period (1958-2017)

In Figure 4.6 (a), a statistically significant increasing trend in drought severity is observed for certain regions. Notably, Gangetic West Bengal, Uttarakhand, Jammu-Kashmir, West Rajasthan, Saurashtra-Kutch-Diu, and Rayalaseema exhibit a clear and statistically significant upward trend in drought severity based on the SPI-9. In Figure 4.6 (b), a statistically significant trend is observed in Coastal Andhra Pradesh, Kerala, Rayalaseema, Uttarakhand and West Madhya Pradesh based on SPI-12. These findings

suggest that these regions have experienced a consistent increase in the severity and frequency of meteorological drought events, posing challenges to water resources and agricultural activities. In contrast, the Konkan-Goa region displays an increasing trend in drought severity as well; however, it is not statistically significant. This finding implies that while there is an observable increase in drought severity in this region, further analysis is required to determine whether this trend is significant or simply a result of natural variability. For several other regions, including Arunachal Pradesh, Assam-Meghalaya, Sub-Himalayan West Bengal Sikkim, Bihar Jharkhand, East and West Uttar Pradesh, Haryana-Chandigarh-Delhi, Himachal Pradesh, East and West Madhya Pradesh, Chhattisgarh, Marathwada, North Interior Karnataka, and Kerala, a statistically significant decreasing trend in drought severity is identified at a 95% confidence level. This indicates that these regions have experienced a reduction in drought severity over time. Such trends can have implications for water resource management and agriculture in these areas.

The data suggests an overall increasing trend in SPI-9 and SPI-12 values, implying that drought events have become more frequent and severe in recent years. This observation is a matter of concern as it highlights the escalating impact of drought on water resources, agriculture, and ecosystems in the study region. The increasing trend in drought severity aligns with climate change projections, which also indicate a rise in the frequency and intensity of extreme events, including droughts, in many regions across the globe.

The statistical parameters of the Mann-Kendall test for SPI-9 and SPI-12 are listed in Table 4.4, providing essential insights into the strength and direction of the trends observed. These parameters help establish the statistical significance of the trends and determine their impact on drought conditions. The statistical significance of the SPI-9 and SPI-12 trends is crucial for decision-making and policy formulation to address the growing challenges posed by drought events. It emphasizes the urgency of adopting sustainable practices and adaptive measures to effectively manage and cope with the increasing frequency and severity of drought events driven by climatic changes.

Table 4.4 Mann-Kendall statistical properties of 34 Meteorological subdivisions for SPI-9 and SPI-12

Meteorological Subdivisions	SPI-9			SPI-12		
	Kendall' s tau	*p* -value	Min	Kendall' s tau	*p* -value	Min
BI	-0.080	**0.001**	-3.154	-0.085	**0.001**	-3.223
EUP	-0.282	**<0.0001**	-3.604	-0.322	**<0.0001**	-3.086
JH	-0.065	**0.009**	-3.314	-0.079	**0.002**	-3.227
OR	-0.026	0.292	-3.847	-0.020	0.434	-2.498
UK	0.147	**<0.0001**	-3.643	-0.164	**<0.0001**	-2.997
WUP	-0.254	**<0.0001**	-3.155	-0.307	**<0.0001**	-3.432
AP	-0.136	**<0.0001**	-2.122	-0.139	**<0.0001**	-1.836
AM	-0.167	**<0.0001**	-2.523	-0.190	**<0.0001**	-2.326
GWB	0.129	**<0.0001**	-2.343	0.123	**<0.0001**	-2.309
NMMT	-0.229	**<0.0001**	-2.131	-0.254	**<0.0001**	-2.001
SHWBS	-0.061	**0.015**	-3.044	-0.074	**0.003**	-2.833
ER	-0.029	0.248	-3.321	-0.035	0.164	-3.594
GJ	-0.012	0.632	-2.746	-0.011	0.663	-2.713
HCD	-0.165	**<0.0001**	-2.824	-0.220	**<0.0001**	-2.740
HP	-0.182	**<0.0001**	-2.561	-0.201	**<0.0001**	-2.380
JK	0.091	**0.0003**	-2.476	0.113	**<0.0001**	-2.548
PN	-0.208	**<0.0001**	-3.575	-0.248	**<0.0001**	-3.569
SKD	0.061	**0.016**	-3.124	0.075	**0.003**	-3.468
WR	0.113	**<0.0001**	-3.233	0.123	**<0.0001**	-3.496
CAP	-0.006	0.808	-2.215	-0.001	0.965	-2.408
CK	-0.012	0.633	-2.333	-0.027	0.277	-2.076
KL	-0.047	0.059	-3.334	-0.062	**0.013**	-2.691
RAY	0.064	**0.011**	-3.043	0.075	**0.003**	-2.981
SIK	-0.024	0.345	-3.538	-0.036	0.148	-3.416
TNP	-0.023	0.365	-4.605	-0.017	0.502	-4.895
CHH	-0.105	**<0.0001**	-4.123	-0.113	**<0.0001**	-2.453
EMP	-0.131	**<0.0001**	-3.039	-0.153	**<0.0001**	-3.078
KG	0.011	0.663	-2.924	0.001	0.964	-3.206
MM	-0.027	0.278	-3.085	-0.030	0.236	-3.199
MA	-0.103	**<0.0001**	-3.654	-0.117	**<0.0001**	-3.099
NIK	-0.082	**0.001**	-3.114	-0.104	**<0.0001**	-2.361
TE	-0.027	0.277	-3.361	-0.037	0.145	-2.209
VI	-0.043	0.084	-3.436	-0.041	0.101	-2.210
WMP	-0.048	0.053	-3.514	-0.059	**0.020**	-2.885

Overall, the trend analysis of SPI-9 and SPI-12 in Figure 4.5(a & b) provides a comprehensive understanding of the spatial and temporal variations in drought severity across different regions of India. The inclusion of statistical significance helps distinguish meaningful trends from random variations, offering a reliable basis for decision-making and policy formulation related to drought management and adaptation.

4.1.7.3 Drought frequency

Drought frequency is a crucial aspect of drought analysis, providing insights into the occurrence and patterns of drought events over a specific period in different regions. It quantifies how frequently droughts happen in each meteorological subdivision, offering valuable information for drought management and planning. Understanding drought frequency is crucial for assessing the climatic patterns and often uses historical climate data and statistical analysis to identify patterns and trends. To assess drought frequency, historical records of drought events are analysed, and their occurrence and duration are determined. In this study, three drought indices, namely EDI, SPI-9, and SPI-12, are utilized to quantify and characterize the frequency of droughts in each of the thirty-four meteorological subdivisions. Drought frequency can is calculated using the following formula,

$$\text{Drought frequency} = \frac{Number\ of\ drought\ events}{Total\ number\ of\ years} \times 100$$

The drought frequency figures are presented with the help of 3-D bar charts showing the three axes (x, y and z). The 3-D visualization. Shows a quantitative information making it easier to compare the data. Figure 4.7 (a-e), Figure 4.8 (a-e) and Figure 4.9 (a-e) represent the results of the drought frequency analysis for EDI, SPI-9, and SPI-12, respectively using bar charts. The bar charts visually depict the occurrence and patterns of drought events for each region over the study period. The drought frequency analysis using these indices provides a comprehensive understanding of the variation in drought occurrence and duration across the study region. It enables the identification of regions that experience frequent and prolonged droughts, as well as areas that are relatively less affected by drought events. This information is essential for

policymakers, water resource managers, and other stakeholders to develop targeted drought mitigation strategies, improve water allocation, and implement effective drought preparedness measures. The use of multiple drought indices (EDI, SPI-9, and SPI-12) for the frequency analysis allows for a robust assessment of drought patterns, considering various timescales and drought severity levels. This comprehensive approach ensures a more accurate representation of the actual drought scenario in each meteorological subdivision.

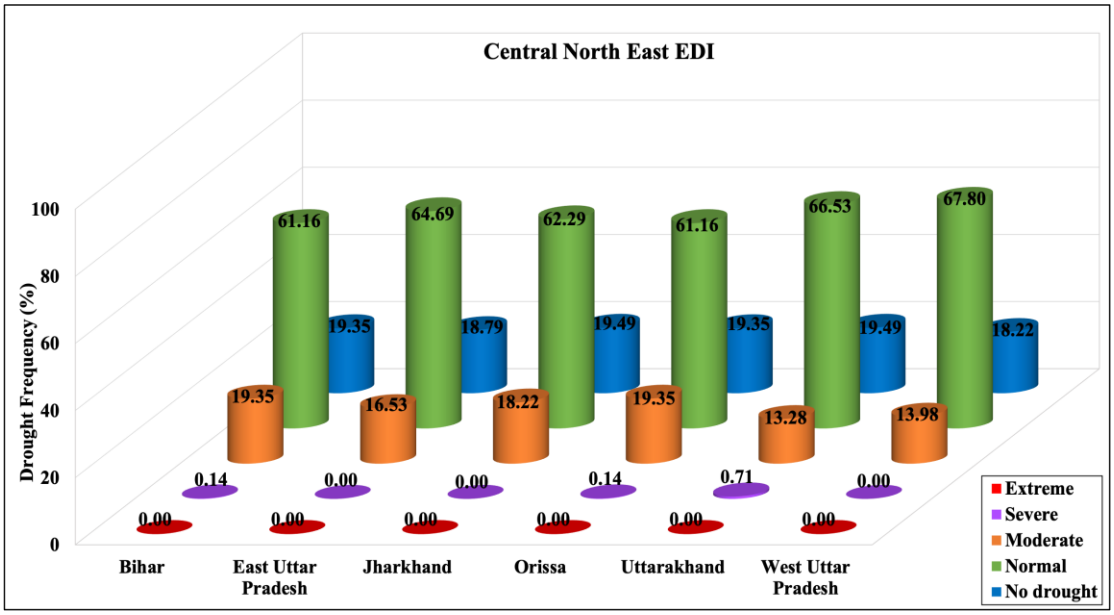

Figure 4.7 (a) Bar charts of drought frequency for Central Northeast along with numerical percentage using EDI

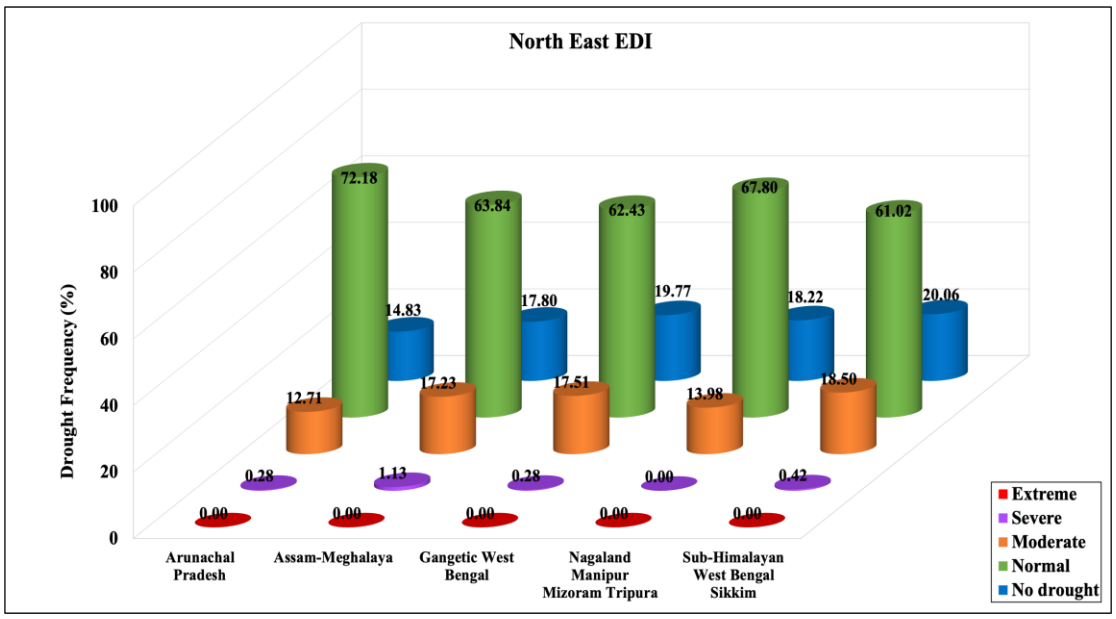

Figure 4.7 (b) Bar charts of drought frequency for North-East along with numerical percentage using EDI

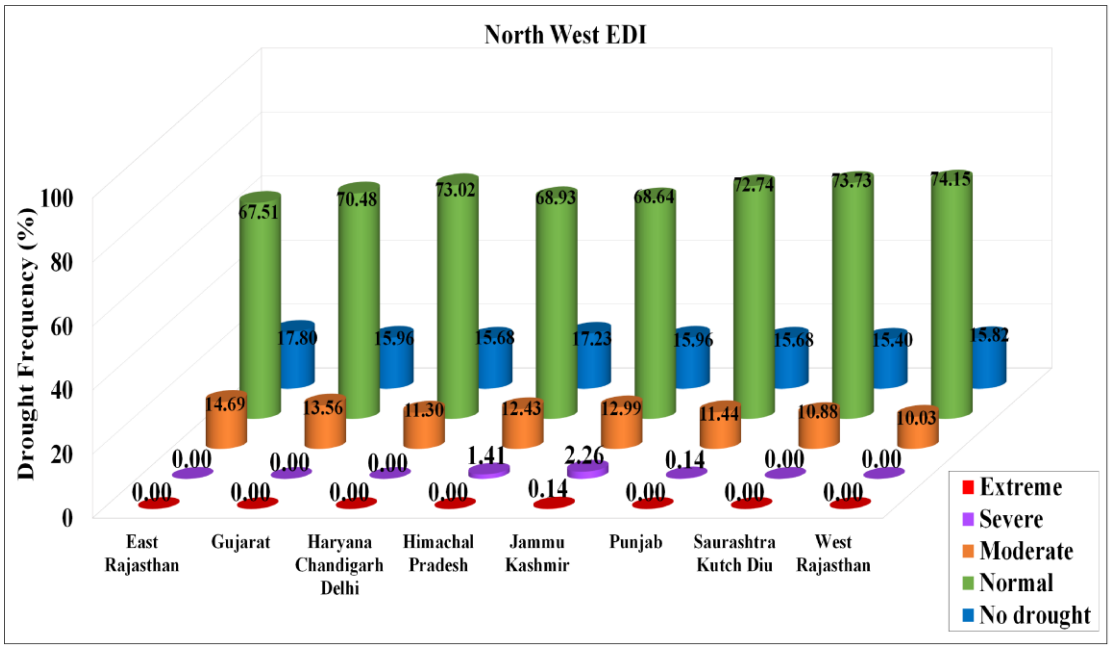

Figure 4.7 (c) Bar charts of drought frequency for North-West along with numerical percentage using EDI

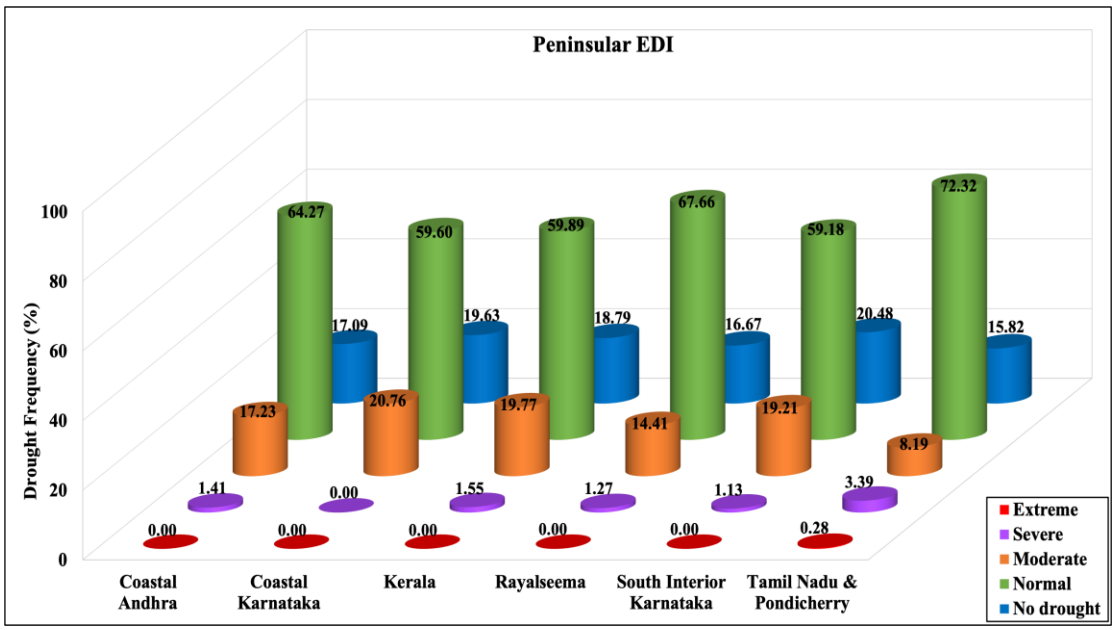

Figure 4.7 (d) Bar charts of drought frequency for Peninsular along with numerical percentage using EDI

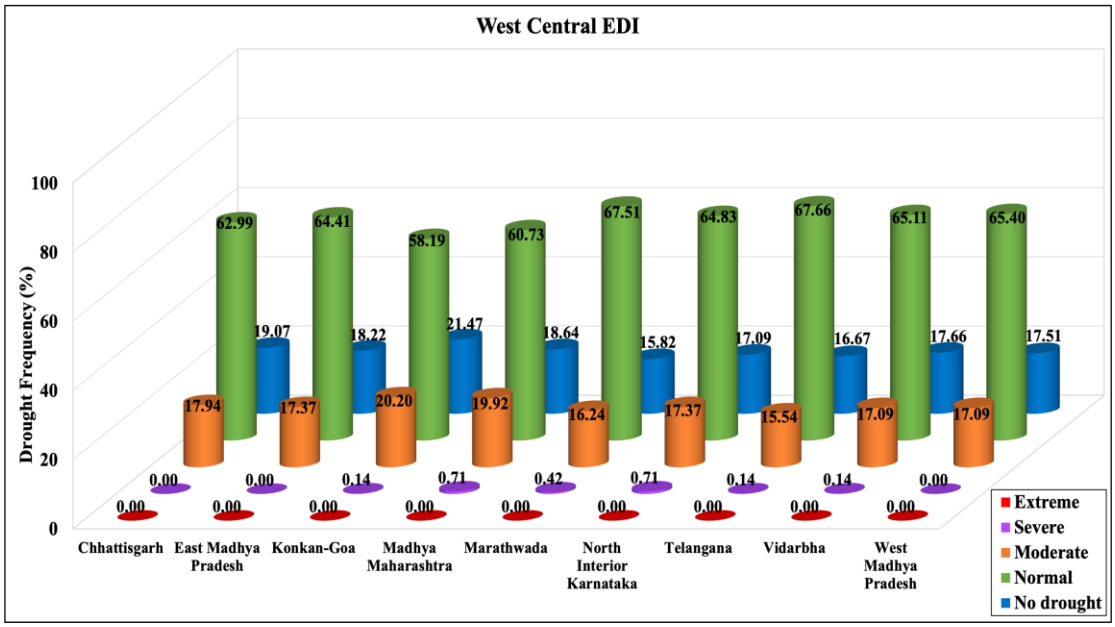

Figure 4.7 (e) Bar charts of drought frequency for West Central along with numerical percentage using EDI

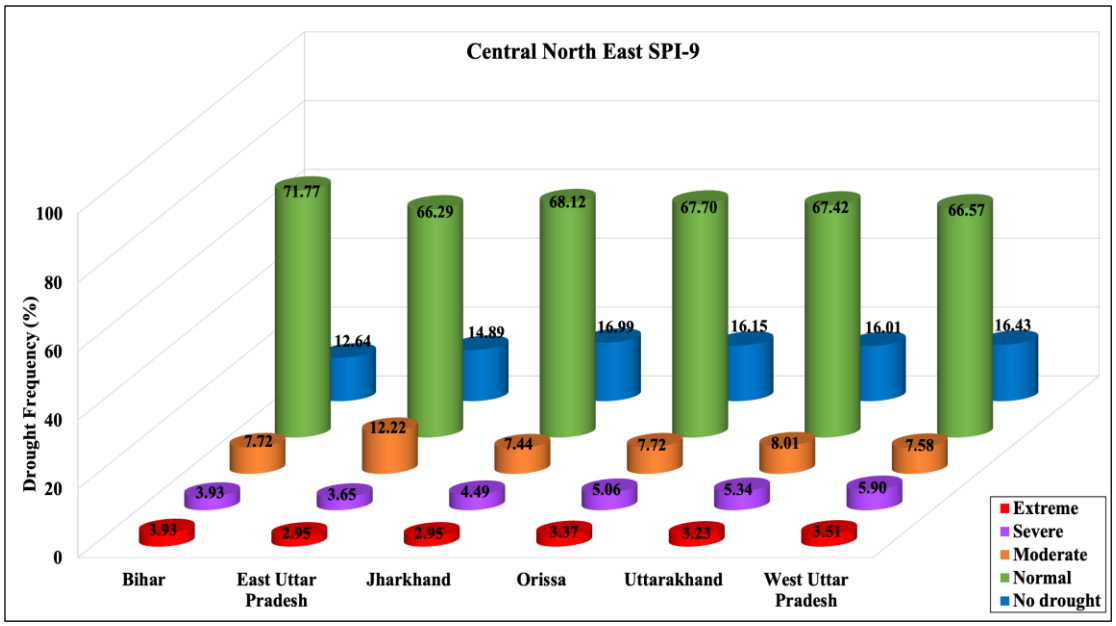

Figure 4.8 (a) Bar charts of drought frequency for Central Northeast along with numerical percentage using SPI-9

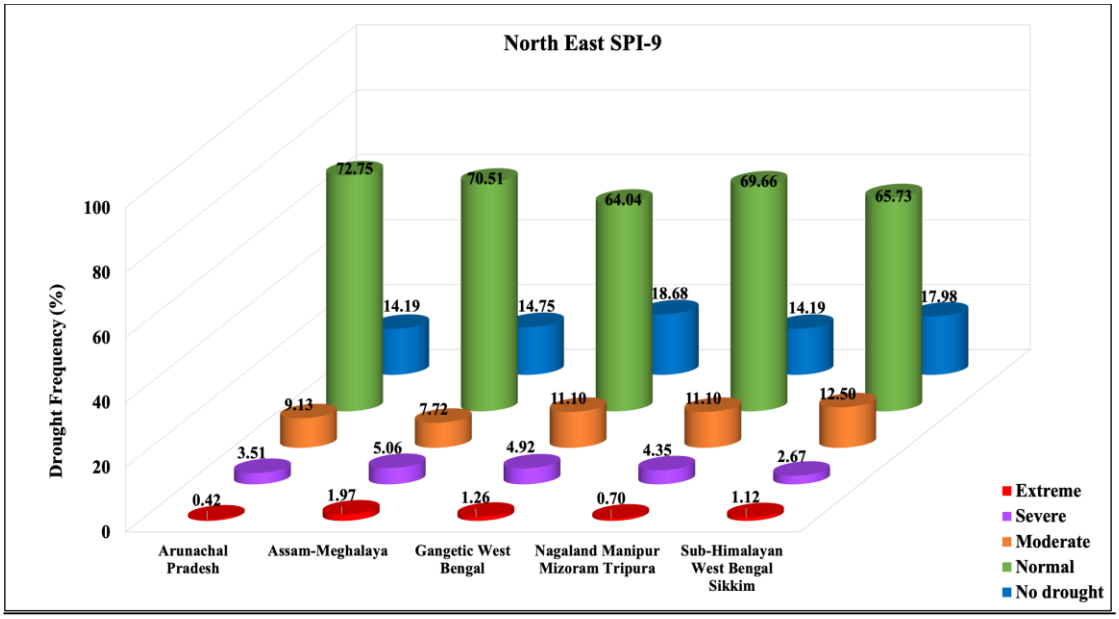

Figure 4.8 (b) Bar charts of drought frequency for North-East along with numerical percentage using SPI-9

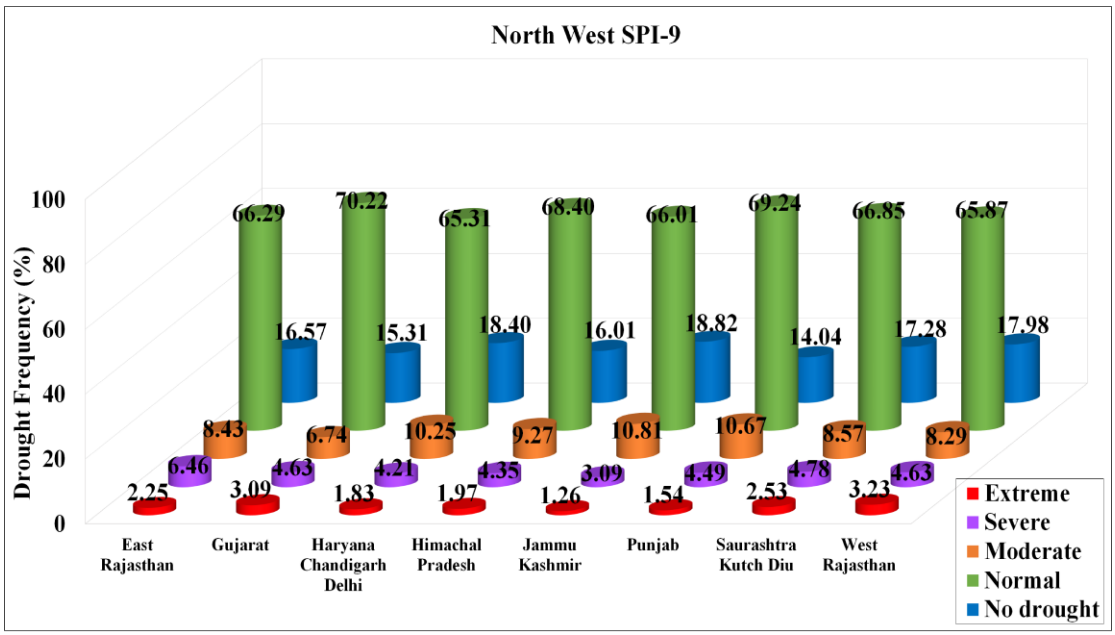

Figure 4.8 (c) Bar charts of drought frequency for North-West along with numerical percentage using SPI-9

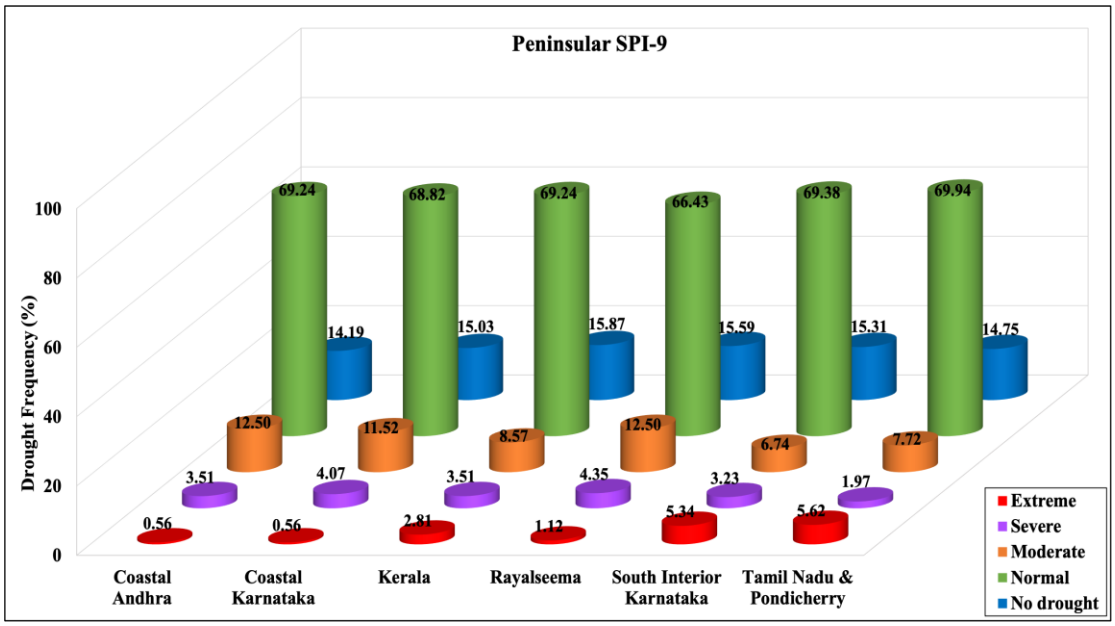

Figure 4.8 (d) Bar charts of drought frequency for Peninsular along with numerical percentage using SPI-9

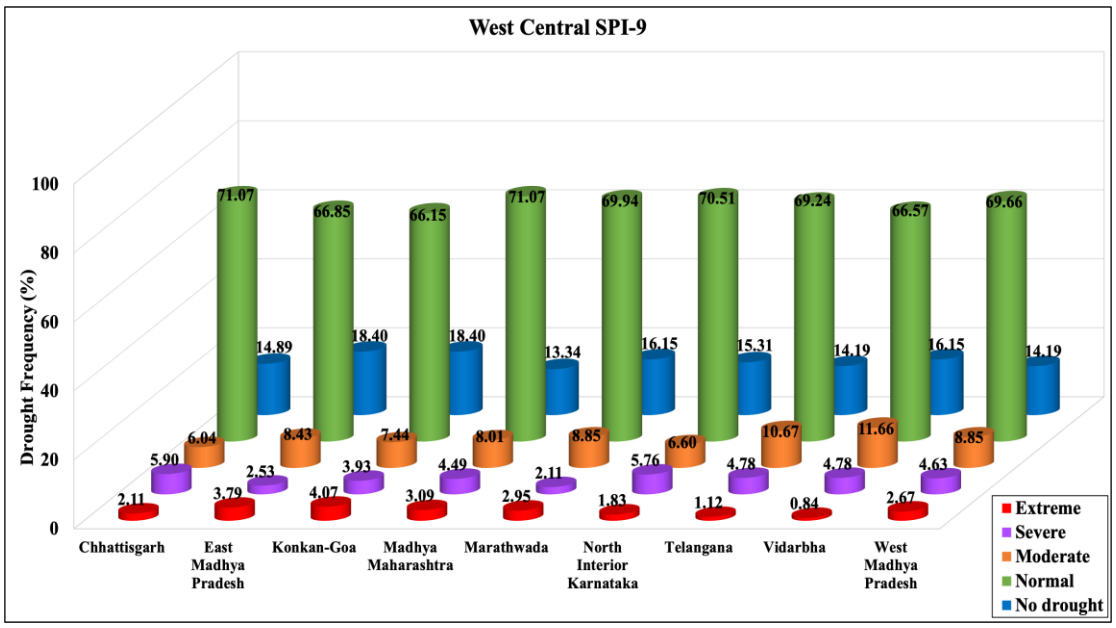

Figure 4.8 (e) Bar charts of drought frequency for west Central along with numerical percentage using SPI-9

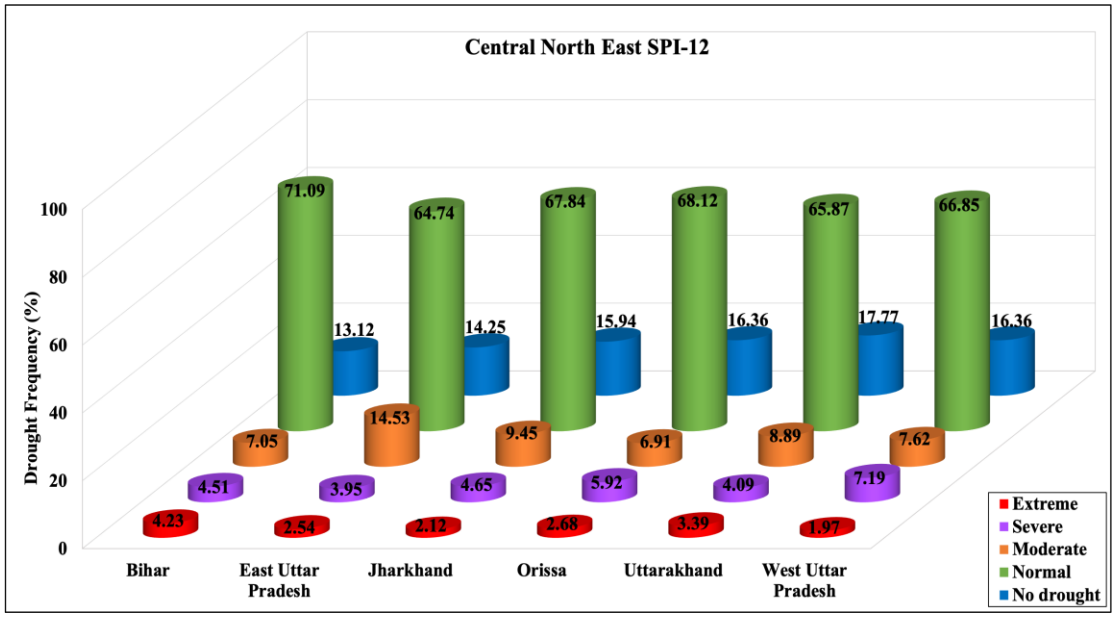

Figure 4.9 (a) Bar charts of drought frequency for Central Northeast along with numerical percentage using SPI-12

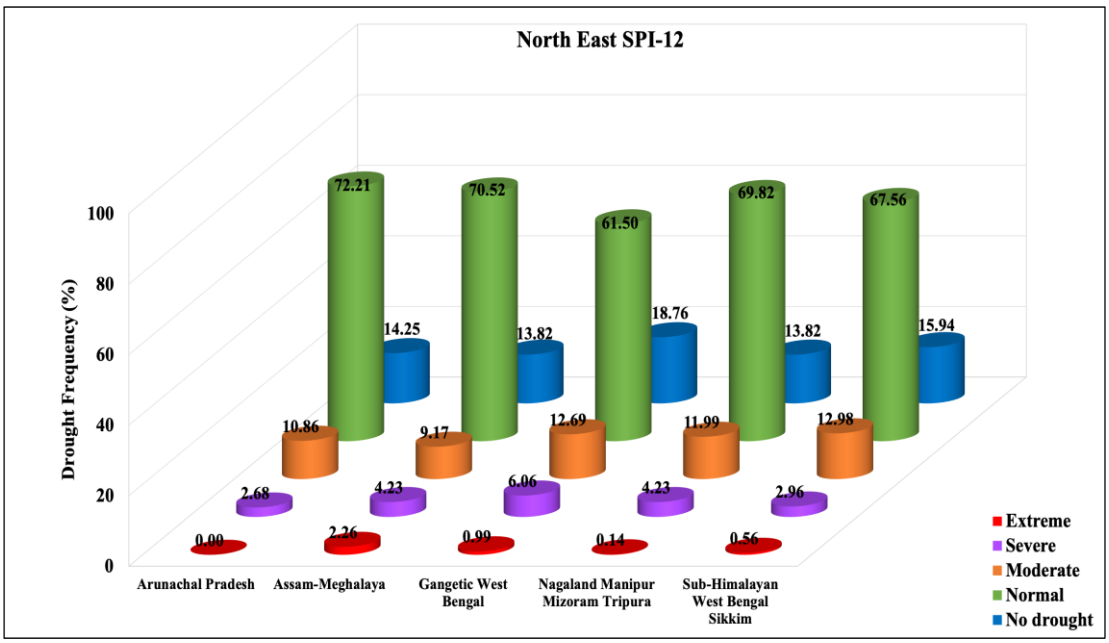

Figure 4.9 (b) Bar charts of drought frequency for North-East along with numerical percentage using SPI-12

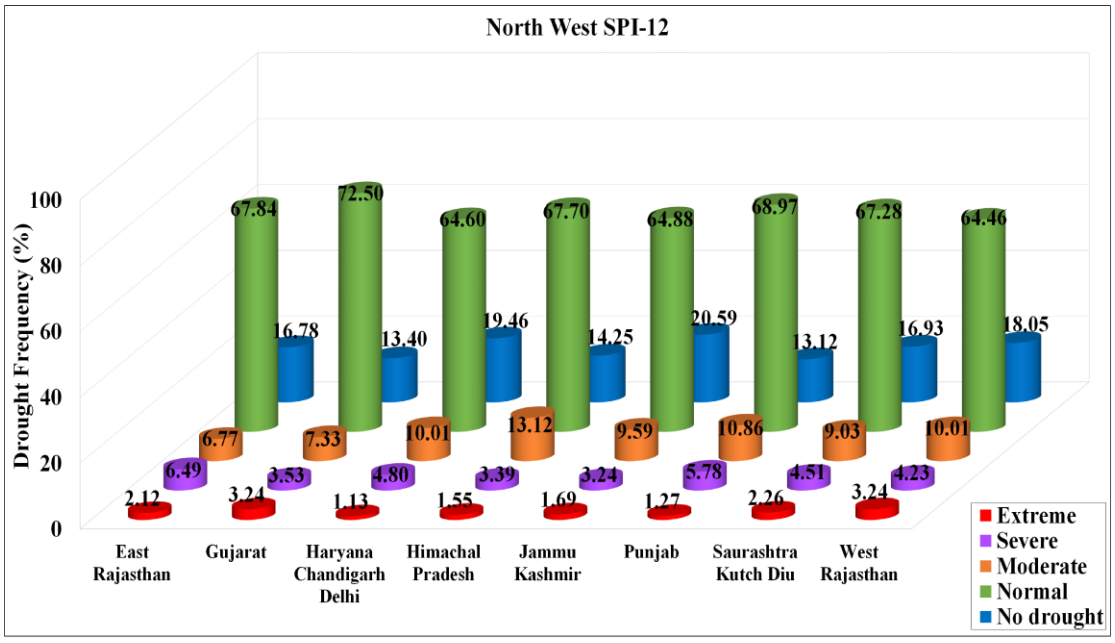

Figure 4.9 (c) Bar charts of drought frequency for North-west along with numerical percentage using SPI-12

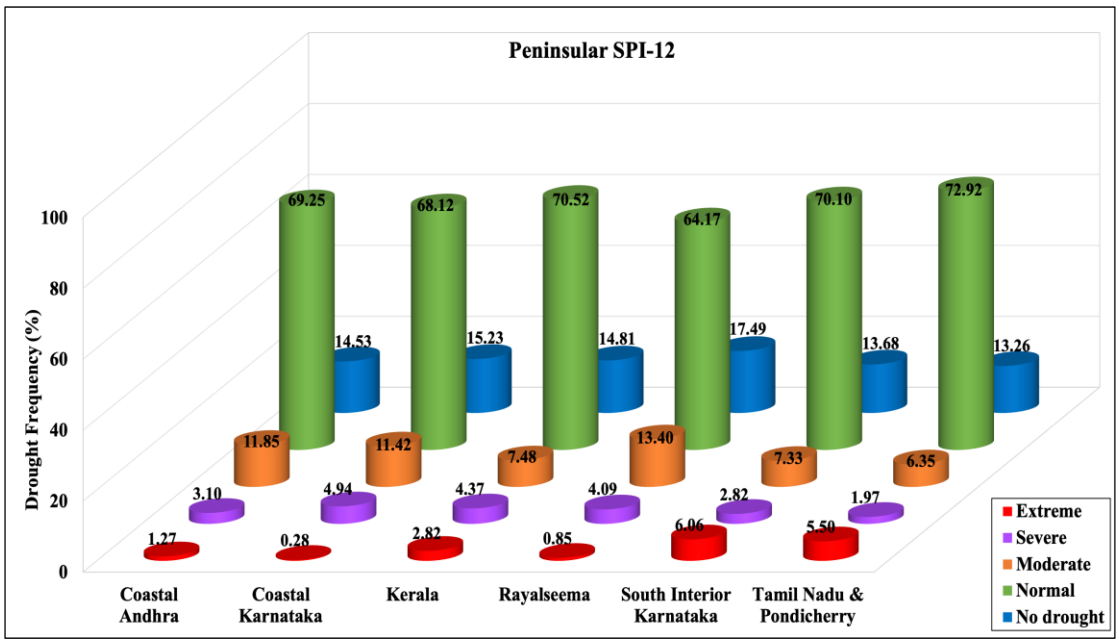

Figure 4.9 (d) Bar charts of drought frequency for Peninsular along with numerical percentage using SPI-12

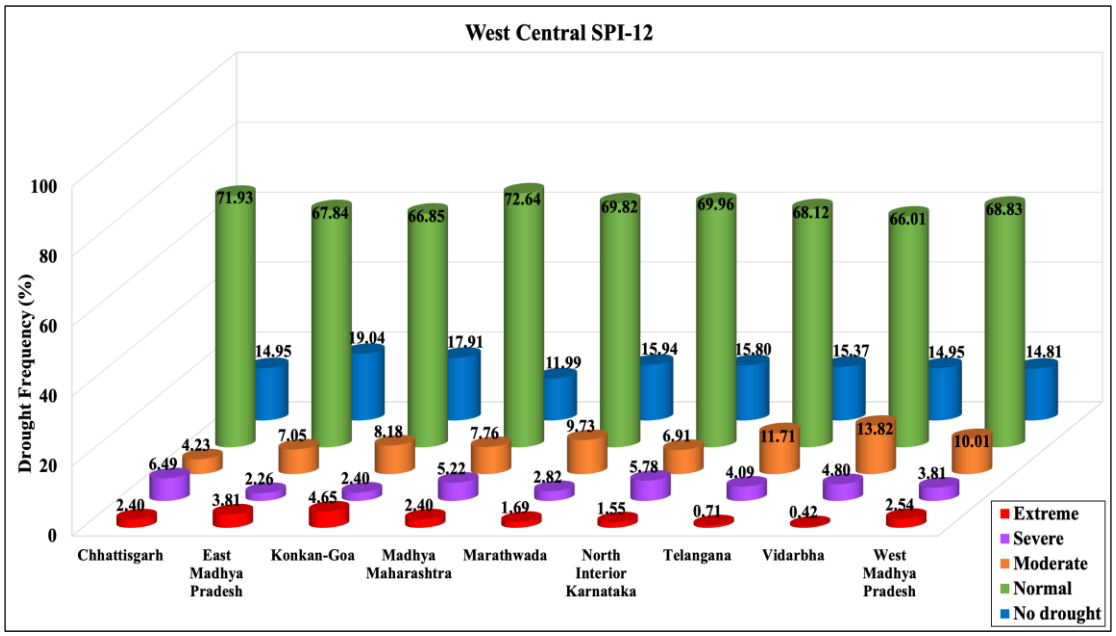

Figure 4.9 (e) Bar charts of drought frequency for West Central along with numerical percentage using SPI-12

From the bar charts, it has been observed that the occurrence of extreme drought condition is of very less frequency as compared to other conditions of drought. Certain locations may experience drought frequently, whereas other areas might go for years without one, depending on the geography, climate, and other climatic factors. The frequency of normal drought occurrence was in the range of 60-75%, moderate drought has 6-20%, severe drought has 0-7% and extreme drought has 0-6%. However, for EDI, extreme drought conditions are seen in Jammu and Kashmir of the North-West region and Tamil Nadu-Pondicherry of the Peninsular region during the study period. The climate of Jammu and Kashmir is categorized as subtropical, and rainfall amounts and distribution change significantly over time. Because of this, there will be a prolonged period of no rain, which will cause extreme drought conditions. On the other side, Tamil Nadu-Pondicherry is also experiencing severe drought conditions as a result of several weak or delayed monsoon events over the years.

Overall, the analysis of drought frequency using the EDI, SPI-9, and SPI-12 indices provides valuable insights into the historical occurrence and characteristics of drought events. These findings contribute to a better understanding of drought vulnerability and resilience in different regions, facilitating informed decision-making and adaptive strategies to mitigate the impacts of drought on various sectors, including agriculture, water resources, and the environment.

From the drought frequency analysis, it is seen that extreme drought conditions for SPI-9 and SPI-12 timescale occur in the study region except that for SPI-12 in the Arunachal Pradesh subdivisions of the North-East region. From Table 4.5, 4.7 and 4.8, it is observed that in most of the subdivisions, severe drought is dominant for EDI whereas for SPI-9 and SPI-12 extreme dry condition is the most dominant. The most intense drought was observed at Jammu-Kashmir with EDI value of -2.05. For SPI-9, the most intense drought is observed in Tamil Nadu-Pondicherry with -4.895. SPI-12 shows the most intense drought in Tamil Nadu-Pondicherry. The variations in the rainfall pattern play an important role in drought conditions. Over the years, the amount of rainfall has also been decreasing leading to a shortage in water supply in most of the regions. Hence,

understanding drought frequency may help develop strategies to mitigate and adapt to the impacts of droughts.

Table 4.5 Most severe drought for EDI, drought category, Year and Rainfall

Homogenous Monsoon Regions	Meteorological Subdivision	EDI	Category	Month-Year	Rainfall (mm)
Central Northeast	BI	-1.49	Moderate	Jun-1975	143.2
	EUP	-1.42	Moderate	Jul-2012	234.2
	JH	-1.46	Moderate	May-1989	66.4
	OR	-1.54	Severe	Jun-1975	193.3
	UK	-1.64	Severe	May-1999	50.5
	WUP	-1.45	Moderate	Jul-2012	145.1
North-East	AP	-1.60	Severe	Apr-1969	127
	AM	-1.71	Severe	Apr-2012	209.6
	GWB	-1.53	Severe	May-1966	43.4
	NMMT	-1.45	Moderate	Jul-2012	249.1
	SHWBS	-1.58	Severe	May-1960	293.2
North-west	ER	-1.35	Moderate	Jun-2010	27.3
	GJ	-1.32	Moderate	Jun-1987	69.6
	HCD	-1.38	Moderate	Jul-2012	68.1
	HP	-1.79	Severe	Jul-2012	241.5
	JK	-2.05	Extreme	May-1970	37.5
	PN	-1.50	Severe	Jun-2010	41.8
	SKD	-1.26	Moderate	Jun-1988	12.7
	WR	-1.34	Moderate	Jul-1969	3
Peninsular	CAP	-1.64	Severe	Jun-1985	105.1
	CK	-1.46	Moderate	Jun-1986	976.5
	KL	-1.73	Severe	Jun-1983	322.8
	RAY	-1.66	Severe	May-2017	39.9
	SIK	-1.66	Severe	May-1966	90.9
	TNP	-2.02	Extreme	May-2004	101.1
West Central	CHH	-1.45	Moderate	Jun-2009	45.3
	EMP	-1.45	Moderate	Jun-2008	307.6
	KG	-1.53	Severe	Jun-1973	455.9
	MM	-1.57	Severe	Jun-1973	124.7
	MA	-1.62	Severe	Jun-1973	112.3
	NIK	-1.56	Severe	May-1973	29.7
	TE	-1.52	Severe	Jun-1973	110.5
	VI	-1.49	Moderate	Jun-1992	167.9
	WMP	-1.40	Moderate	Jun-1966	69.2

Table 4.6 Most severe drought for SPI-9, drought category, Year and Rainfall

Homogenous Monsoon Regions	Meteorological Subdivision	SPI9	Category	Month-Year	Rainfall (mm)
Central Northeast	BI	-3.154	Extreme	Aug-1972	154.9
	EUP	-3.604	Extreme	Apr-1998	6.6
	JH	-3.314	Extreme	Sep-2010	160.5
	OR	-3.847	Extreme	Jun-2009	87.3
	UK	-3.643	Extreme	Jul-2009	157.5
	WUP	-3.155	Extreme	Jul-2012	145.1
North-East	AP	-2.122	Extreme	Apr-1969	127
	AM	-2.523	Extreme	Jun-2009	295.7
	GWB	-2.343	Extreme	Jan-1983	9.1
	NMMT	-2.131	Extreme	Jan-1973	16.5
	SHWBS	-3.044	Extreme	Jun-1966	287.5
North-west	ER	-3.321	Extreme	Mar-2003	0.5
	GJ	-2.746	Extreme	May-1987	0.3
	HCD	-2.824	Extreme	Jul-2012	68.1
	HP	-2.561	Extreme	Jun-2012	31.1
	JK	-2.476	Extreme	Aug-1970	99.8
	PN	-3.575	Extreme	Jul-2002	50.4
	SKD	-3.124	Extreme	Oct-1987	0.1
	WR	-3.233	Extreme	Aug-2002	17.2
Peninsular	CAP	-2.215	Extreme	Jan-2003	6.3
	CK	-2.333	Extreme	Jun-2009	450.3
	KL	-3.334	Extreme	Jun-1983	322.8
	RAY	-3.043	Extreme	Apr-2017	8.8
	SIK	-3.538	Extreme	Apr-2017	34.1
	TNP	-4.605	Extreme	Nov-2002	47.2
West Central	CHH	-4.123	Extreme	Jun-2009	45.3
	EMP	-3.039	Extreme	Jul-2002	84.7
	KG	-2.924	Extreme	May-1992	6.2
	MM	-3.085	Extreme	Oct-1972	7.3
	MA	-3.654	Extreme	Apr-1992	3.5
	NIK	-3.114	Extreme	Jul-2001	62.1
	TE	-3.361	Extreme	Jun-1966	67.2
	VI	-3.436	Extreme	May-1992	5.7
	WMP	-3.514	Extreme	Apr-2001	6.0

Table 4.7 Most severe drought for SPI-12, drought category, Year and Rainfall

Homogenous Monsoon Region	Meteorological Sub-station	SPI-12	Category	Month-Year	Rainfall (mm)
Central Northeast	BI	-3.223	Extreme	Dec-2010	2.1
	EUP	-3.086	Extreme	Jul-1998	218.3
	JH	-3.227	Extreme	Nov-2010	4.7
	OR	-2.498	Extreme	May-1975	18.4
	UK	-2.997	Extreme	Aug-2009	202.6
	WUP	-3.432	Extreme	Jul-2002	29.6
North-East	AP	-1.836	Severe	Nov-1967	10
	AM	-2.326	Extreme	Mar-2012	19.4
	GWB	-2.309	Extreme	Jun-1967	131.6
	NMMT	-2.001	Extreme	Dec-1972	4.5
	SHWBS	-2.833	Extreme	Jun-1979	271.3
North-west	ER	-3.594	Extreme	Aug-2002	130.6
	GJ	-2.713	Extreme	Aug-1987	180.6
	HCD	-2.74	Extreme	Aug-2002	78.2
	HP	-2.38	Extreme	Nov-1974	2.4
	JK	-2.548	Extreme	Mar-1971	10.4
	PN	-3.569	Extreme	Jul-2002	50.4
	SKD	-3.468	Extreme	Aug-1987	33.5
	WR	-3.496	Extreme	Aug-2002	17.2
Peninsular	CAP	-2.408	Extreme	Aug-1968	45.5
	CK	-2.076	Extreme	Jul-2002	545.7
	KL	-2.691	Extreme	Jul-2017	378.5
	RAY	-2.981	Extreme	Jul-2017	52.2
	SIK	-3.416	Extreme	Jul-2017	125.9
	TNP	-4.895	Extreme	Sep-2002	32.2
West Central	CHH	-2.453	Extreme	Sep-2009	104.7
	EMP	-3.078	Extreme	Aug-2007	491.8
	KG	-3.206	Extreme	Jun-1973	455.9
	MM	-3.199	Extreme	Oct-1972	7.3
	MA	-3.099	Extreme	Oct-1972	4.2
	NIK	-2.361	Extreme	Jun-2003	66.9
	TE	-2.209	Extreme	Jun-1973	110.5
	VI	-2.21	Extreme	Jul-1992	241.3
	WMP	-2.885	Extreme	Jul-2002	46.9

4.2 PREDICTION OF METROLOGICAL DROUGHT INDICES USING MACHINE LEARNING ALGORITHMS

In this section, the descriptive and statistical results reasoning of hybrid machine learning models adopted for meteorological drought study is presented. The obtained statistical measures are thoroughly discussed and comparatively evaluated to comprehend the best possible machine learning models for the meteorological drought indices. The study employs three machine learning algorithms:

(a) Generalized Regression Neural Network (GRNN)
(b) Genetic Algorithm-Adaptive Neuro-Fuzzy Inference System (GA-ANFIS)
(c) Particle Swarm Optimization-Adaptive Neuro-Fuzzy Inference System (PSO-ANFIS).

To ensure comprehensive and accurate predictions, two hybrid ANFIS models, namely GA-ANFIS and PSO-ANFIS, along with the GRNN algorithm, are applied for predicting the meteorological drought indices in thirty-four meteorological sub-divisions of India. The dataset used for training and testing the models consists of monthly rainfall data from 1958 to 2017. From this data, EDI, SPI-9 and SPI-12 are calculated for each meteorological subdivision. To evaluate the performance of the machine learning models, various performance metrics, including R^2, NSE and RRMSE are utilized to assess the performance of each model in predicting the meteorological drought indices. These metrics provide a comprehensive understanding of the accuracy and reliability of the models' predictions (Reihanifear et al. 2023). By comparing the results obtained from the three machine learning models, it is aimed to identify the model that demonstrates the highest accuracy and best prediction capability. The use of hybrid ANFIS models (GA-ANFIS and PSO-ANFIS) alongside the GRNN algorithm allows for a robust and adaptive approach to model the complex relationships between meteorological variables and drought indices. This combination of algorithms enhances the predictive capabilities of the models, ensuring accurate and reliable prediction.

Overall, this section provides a detail examination of the machine learning models performance, allowing us to make informed decisions about the most suitable model

for predicting meteorological drought indices. The results obtained from this analysis can significantly contribute to better drought preparedness, water resource management, and sustainable planning in the studied regions.

4.2.1 Performance evaluation of Effective drought index (EDI) prediction

In this study, EDI prediction has been conducted for all thirty-four meteorological subdivisions (MSDs) in India. In this section, we present a detailed analysis of the performance evaluation of three hybrid machine learning models: GA-ANFIS, PSO-ANFIS, and GRNN, for prediction of EDI. The accuracy of the models is assessed based on three key metrics: R^2, RRMSE, and NSE. The comparative evaluation across MSDs provides valuable insights into the efficacy of the prediction models for EDI and helps identify the most suitable model for specific regions. These findings are crucial for guiding effective decision-making and resource management strategies to mitigate the impacts of drought conditions.

To determine the effectiveness of the machine learning models GA-ANFIS, PSO-ANFIS, and GRNN performance at predicting the EDI, emphasis has been given to the Central Northeast region, which has six meteorological subdivisions. The results are depicted in Figure 4.10, which showcases the scatterplot of observed and predicted EDI values. Remarkably, the GA-ANFIS model exhibits a remarkable agreement with the observed EDI, emphasizing the robustness and consistency of this hybrid model in capturing the variations in drought conditions. The close alignment between the observed and predicted EDI points to the model's capability to provide reliable predictions. The high R^2 value indicates a strong correlation between the observed and predicted EDI values, while the low RRMSE and NSE values signify the model's accuracy in minimizing the error and capturing the variability in the observed data, respectively. Each model's performance results for the respective MSDs within each Homogenous monsoon regions (HMR) are presented in Table 4.8 for EDI. Moreover, a detail comparative analysis of the models reveals that the GA-ANFIS model stands out as the best-performing model in the Central Northeast region. It yields impressive performance with R^2, RRMSE, and NSE values of 0.884, 0.407, and 0.833, respectively.

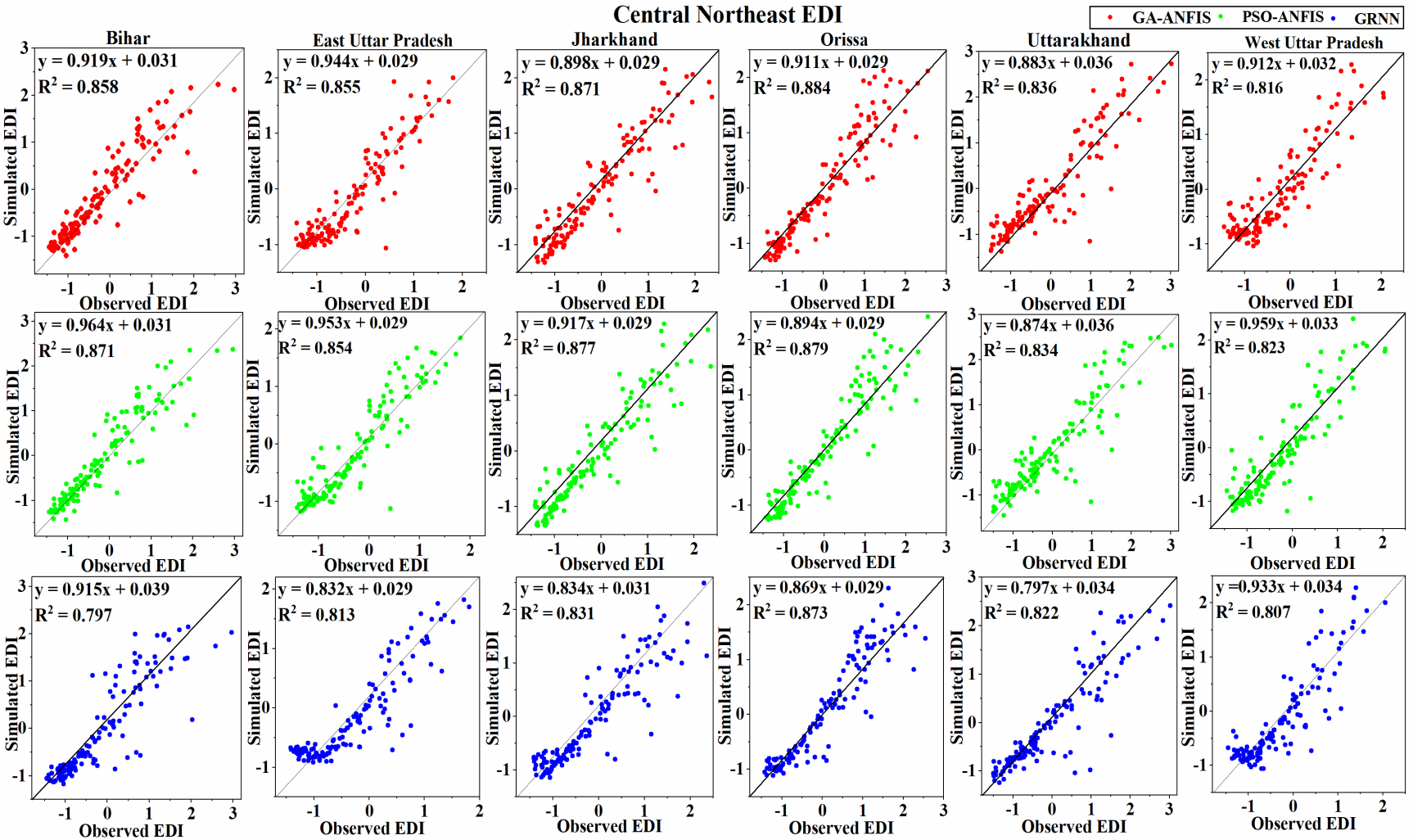

Figure 4.10 Scatterplot of observed and predicted EDI of GA-ANFIS, PSO-ANFIS and GRNN models for Central Northeast

Table 4.8 Performance metrics of GA-ANFIS, PSO-ANFIS and GRNN for EDI

MSD	R^2			RRMSE			NSE		
	GA-ANFIS	PSO-ANFIS	GRNN	GA-ANFIS	PSO-ANFIS	GRNN	GA-ANFIS	PSO-ANFIS	GRNN
BI	0.858	**0.871**	0.797	0.387	**0.380**	0.478	0.849	**0.855**	0.770
EUP	**0.855**	0.854	0.813	**0.426**	0.434	0.458	**0.818**	0.811	0.788
JH	0.871	**0.877**	0.831	0.366	**0.357**	0.414	0.865	**0.872**	0.827
OR	**0.884**	0.879	0.873	**0.342**	0.347	0.356	**0.882**	0.879	0.873
UK	**0.836**	0.834	0.822	**0.407**	0.409	0.421	**0.833**	0.832	0.822
WUP	0.816	**0.823**	0.807	0.495	**0.476**	0.483	0.753	**0.772**	0.765
AP	0.834	**0.841**	0.825	0.415	**0.407**	0.423	0.826	**0.833**	0.820
AM	**0.898**	0.896	0.838	**0.355**	0.370	0.423	**0.873**	0.862	0.814
GWB	0.846	**0.852**	0.813	0.392	**0.385**	0.433	0.845	**0.850**	0.811
NMMT	0.882	**0.917**	0.871	0.404	**0.348**	0.483	0.836	**0.878**	0.765
SHWBS	0.911	**0.919**	0.888	0.311	**0.291**	0.343	0.903	**0.915**	0.882
ER	0.876	**0.877**	0.855	0.388	**0.352**	0.393	0.849	**0.875**	0.844
GJ	0.825	**0.844**	0.759	0.418	**0.394**	0.499	0.824	**0.844**	0.749
HCD	**0.773**	0.729	0.671	**0.498**	0.533	0.576	**0.750**	0.714	0.666
HP	**0.685**	**0.685**	0.613	**0.577**	0.585	0.631	**0.664**	0.655	0.599
JK	0.556	**0.570**	0.496	0.671	**0.665**	0.712	0.546	**0.555**	0.489
PN	**0.733**	0.729	0.693	**0.535**	0.537	0.553	**0.712**	0.710	0.691
SKD	0.719	**0.753**	0.583	0.538	**0.509**	0.662	0.709	**0.739**	0.558
WR	**0.774**	0.773	0.700	**0.480**	0.481	0.567	**0.768**	0.767	0.676
CAP	0.788	**0.795**	0.705	0.460	**0.456**	0.543	0.787	**0.791**	0.703
CK	**0.898**	0.893	0.894	**0.321**	0.330	0.333	**0.896**	0.890	0.888
KL	0.842	**0.847**	0.795	0.397	**0.391**	0.458	0.842	**0.846**	0.789
RAY	0.743	**0.762**	0.731	0.530	**0.519**	0.547	0.717	**0.729**	0.707
SIK	0.857	**0.867**	0.845	0.378	**0.366**	0.401	0.856	**0.865**	0.838
TNP	0.706	**0.711**	0.698	0.542	**0.538**	0.553	0.704	**0.709**	0.692
CHH	0.914	**0.921**	0.911	0.299	**0.284**	0.305	0.910	**0.919**	0.906
EMP	0.859	**0.869**	0.841	0.378	**0.373**	0.404	0.856	**0.860**	0.836
KG	0.901	**0.919**	0.885	0.324	**0.291**	0.361	0.894	**0.915**	0.868
MM	0.869	**0.887**	0.866	0.384	**0.374**	0.438	0.851	**0.859**	0.807
MA	0.809	**0.815**	0.760	0.439	**0.430**	0.488	0.806	**0.813**	0.760
NIK	0.828	**0.835**	0.819	0.418	**0.414**	0.424	0.819	**0.824**	0.798
TE	0.844	**0.856**	0.802	0.394	**0.379**	0.440	0.844	**0.856**	0.805
VI	0.878	**0.889**	0.865	0.352	**0.350**	0.385	0.875	**0.877**	0.850
WMP	**0.882**	0.871	0.852	**0.343**	0.360	0.387	**0.881**	0.869	0.849

*****Bold values indicate the best prediction result for the model***

The Northeast region, comprising five meteorological subdivisions, was subjected to a comprehensive evaluation of three hybrid machine learning models: GA-ANFIS, PSO, and GRNN, to assess their predicting capabilities for the EDI. The results are depicted in Figure 4.11, which presents the scatterplot of observed and predicted EDI values for each model. Among the three models, it is evident that the GA-ANFIS model demonstrates superior prediction accuracy in the Northeast region. This is highlighted by the impressive values of the evaluation metrics with R^2 value of 0.898 indicates a strong correlation between the observed and predicted EDI values. A high R^2 value signifies the model's ability to capture the variation in the data and produce accurate prediction. The NSE value of 0.875 and RRMSE value of 0.355 further confirms the GA-ANFIS model's predictive capabilities defines that the model has better accuracy between the observed and predicted EDI values in the North-East region. A low RRMSE indicates that the model's prediction is close to the actual values, signifying its reliability and precision.

The superior performance of the GA-ANFIS model in the Northeast region suggests its potential as a valuable tool for drought prediction in this region. The model's ability to provide accurate and consistent predictions can aid regional authorities, policymakers, and stakeholders in making informed decisions to mitigate the impacts of drought, manage water resources effectively, and implement appropriate drought relief measures. The reliable predictions generated by the GA-ANFIS model can contribute to better planning and preparedness for drought events, thus enhancing resilience and adaptive capacity in the Northeast region.

In analysis of the North-West region, consisting of eight meteorological subdivisions, it has been explored that the performance of the PSO-ANFIS model shows a better prediction for EDI. Among the subdivisions, the East Rajasthan subdivision have demonstrated remarkable predictive accuracy with R^2 value of 0.877, RRMSE = 0.352 and NSE = 0.875. Additionally, Figure 4.12 provides a graphical comparison of the PSO-ANFIS, GA-ANFIS and GRNN models in the Northwest region between the predicted and observed EDI. The graphs clearly illustrate that PSO-ANFIS models

holds good significant potential as a valuable tool for drought prediction in the Northwest region, particularly in the East Rajasthan region. The PSO-ANFIS model's reliability can boost resilience and preparedness against drought impacts, supporting sustainable water management and agricultural practices in the North-West region.

In the Peninsular region, comparison among the six meteorological subdivisions has been conducted. Notably, the Coastal Karnataka subdivision shows an R^2 of 0.898, RRMSE of 0.321 and NSE of 0.896 for the GA-ANFIS model. Furthermore, the scatterplot in Figure 4.13 illustrates the EDI results for the Peninsular region, particularly focusing on the Coastal Karnataka subdivisions. The graph demonstrates the GA-ANFIS model's strong performance, particularly when comparing the R^2 values. The model's ability to yield similar R^2 values to the PSO-ANFIS model in the Coastal Karnataka and Kerala subdivisions reinforces the consistency and reliability of the GA-ANFIS model's predictions. These results indicate that the GA-ANFIS model is highly effective in predicting the EDI values in the Coastal Karnataka subdivision of the Peninsular region. Its robust correlation, low error, and skillful predictions empower stakeholders and decision-makers in the region to make informed choices in managing water resources, implementing drought mitigation strategies, and planning for potential drought events.

In the West Central region, the GA-ANFIS model shows a higher performance accuracy having R^2, RRMSE and NSE of 0.921, 0.284 and 0.919 respectively in Chhattisgarh subdivisions. Figure 4.14 provides a graphical representation of the EDI results in the West Central region, highlighting the GA-ANFIS model's excellence in Chhattisgarh subdivisions. The scatterplot shows a strong agreement between the predicted and observed EDI values, further corroborating the model's accuracy and consistency.

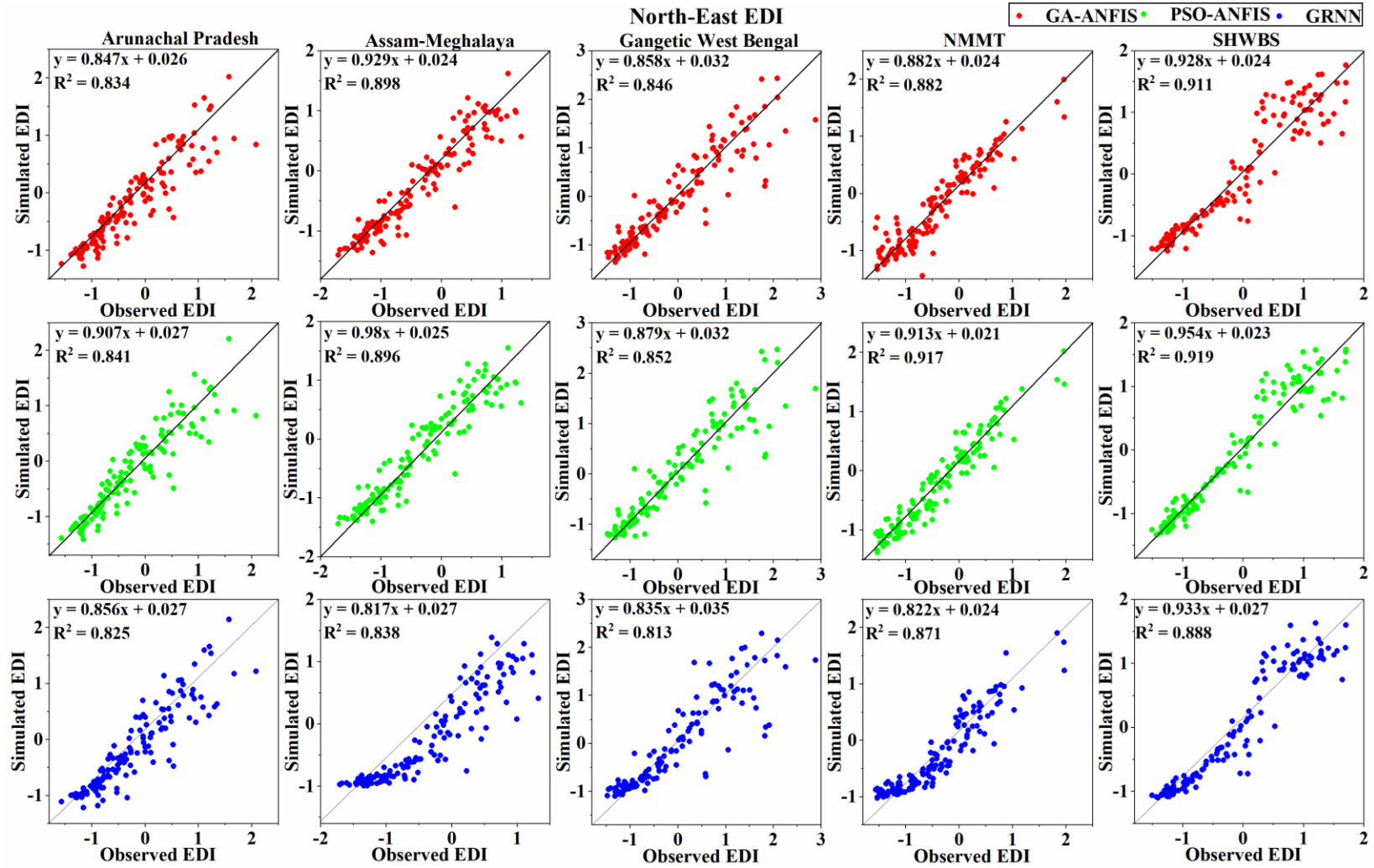

Figure 4.11 Scatterplot of observed and predicted EDI of GA-ANFIS, PSO-ANFIS and GRNN models for North-East

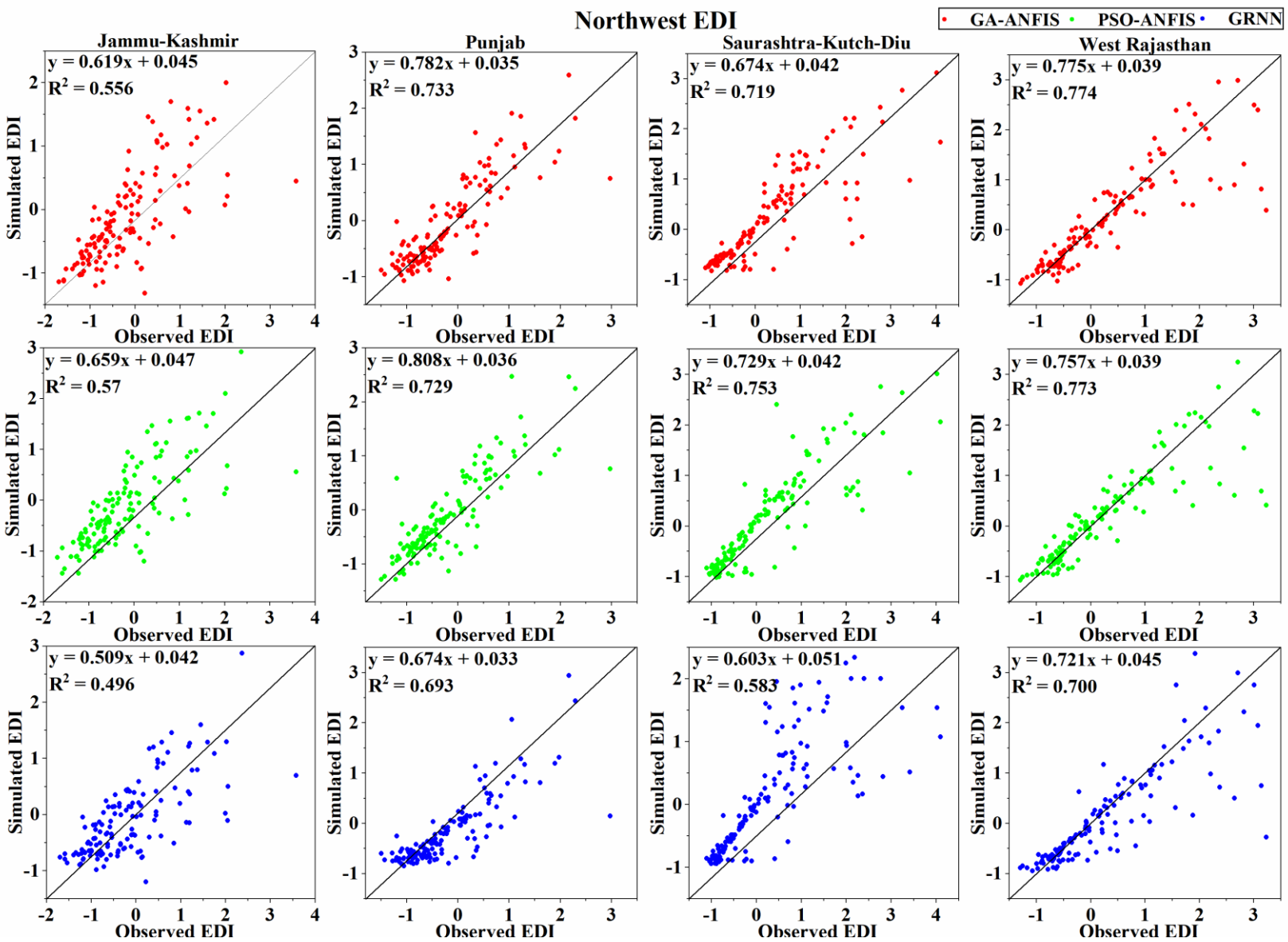
Northwest EDI
GA-ANFIS
PSO-ANFIS
GRNN
Jammu-Kashmir
Punjab
Saurashtra-Kutch-Diu
West Rajasthan
y = 0.619x + 0.045
R² = 0.556
y = 0.782x + 0.035
R² = 0.733
y = 0.674x + 0.042
R² = 0.719
y = 0.775x + 0.039
R² = 0.774
y = 0.659x + 0.047
R² = 0.57
y = 0.808x + 0.036
R² = 0.729
y = 0.729x + 0.042
R² = 0.753
y = 0.757x + 0.039
R² = 0.773
y = 0.509x + 0.042
R² = 0.496
y = 0.674x + 0.033
R² = 0.693
y = 0.603x + 0.051
R² = 0.583
y = 0.721x + 0.045
R² = 0.700
Simulated EDI
Observed EDI

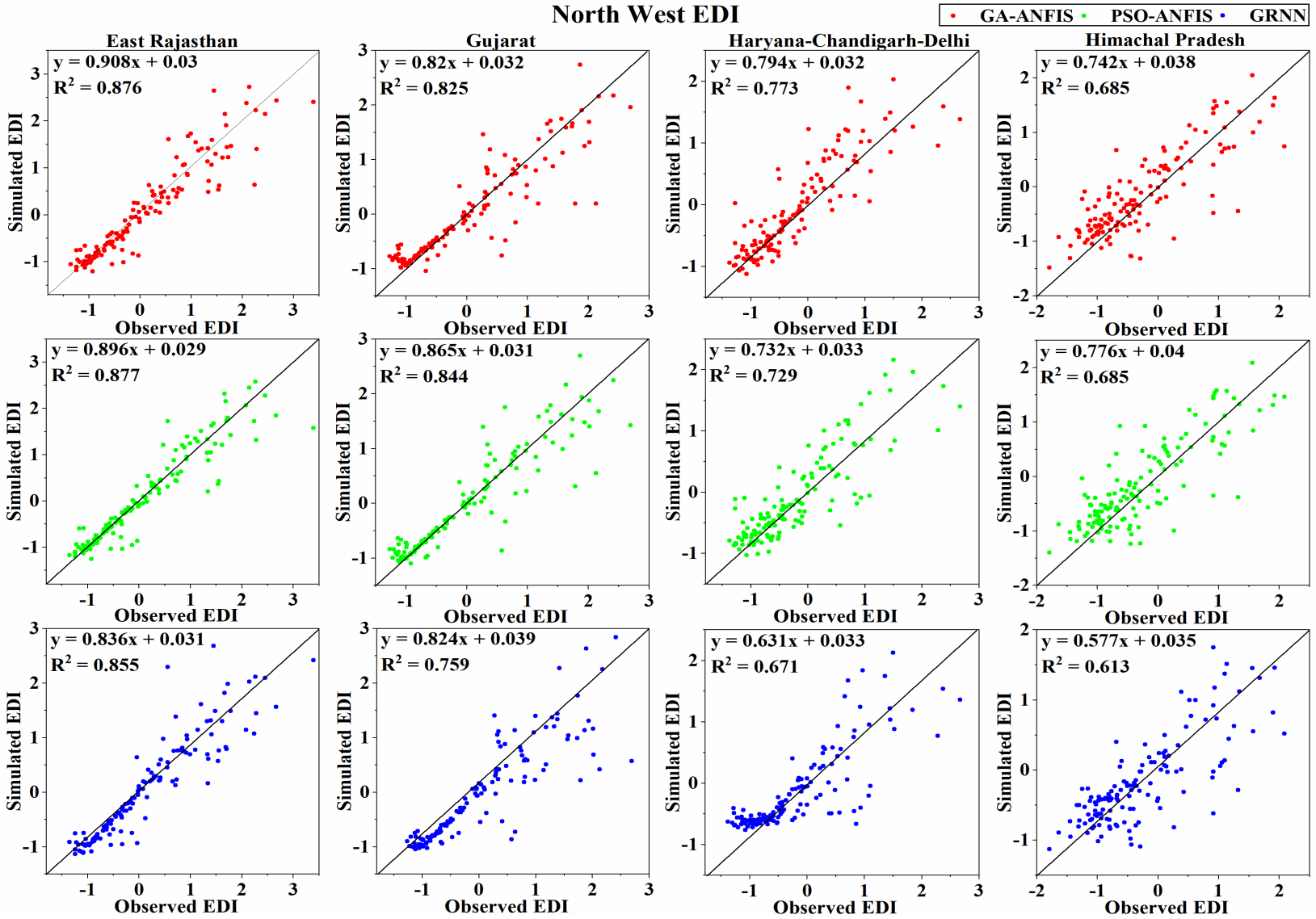

Figure 4.12 Scatterplot of observed and predicted EDI of GA-ANFIS, PSO-ANFIS and GRNN models for North-West

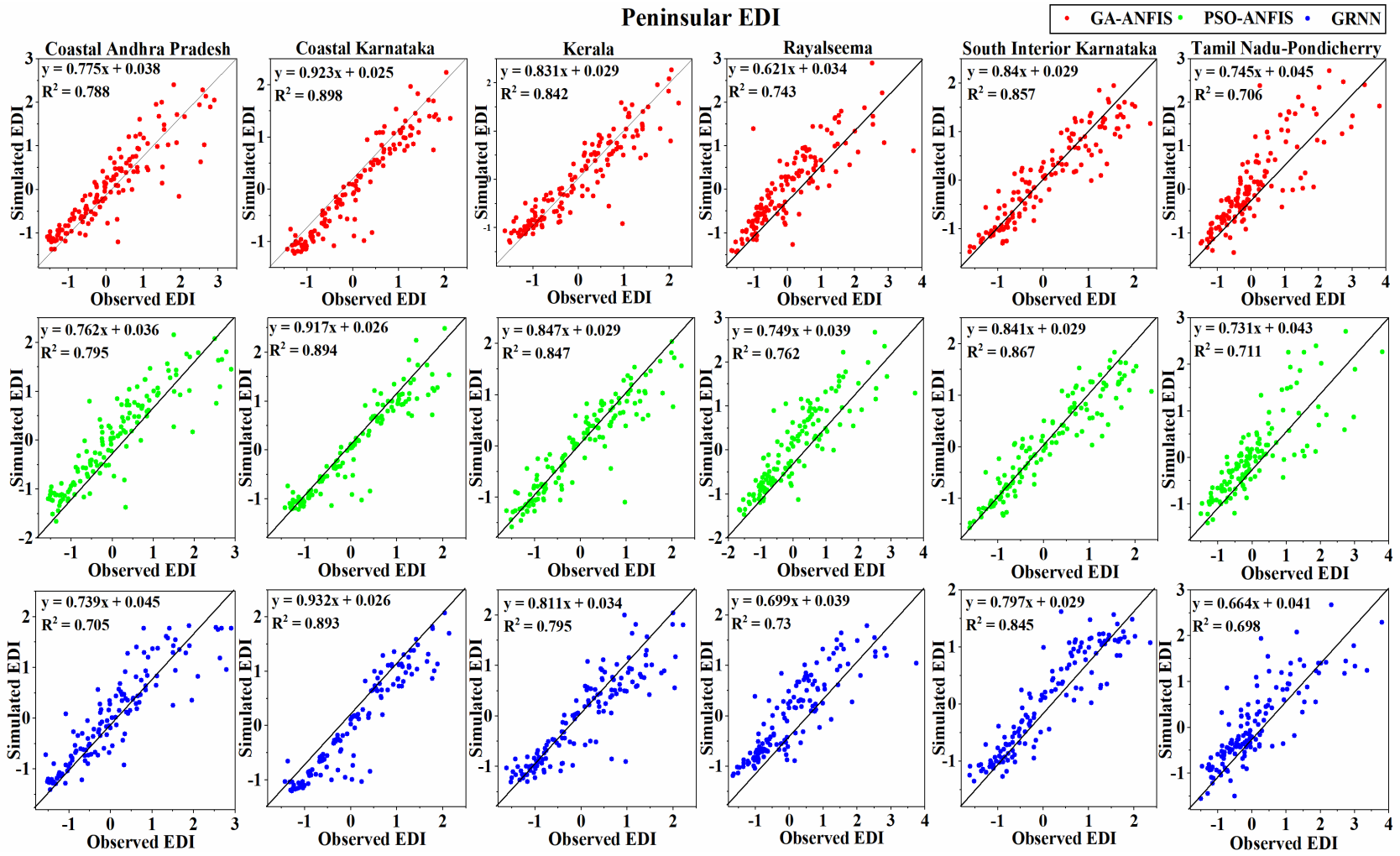

Figure 4.13 Scatterplot of observed and predicted EDI of GA-ANFIS, PSO-ANFIS and GRNN models for Peninsular

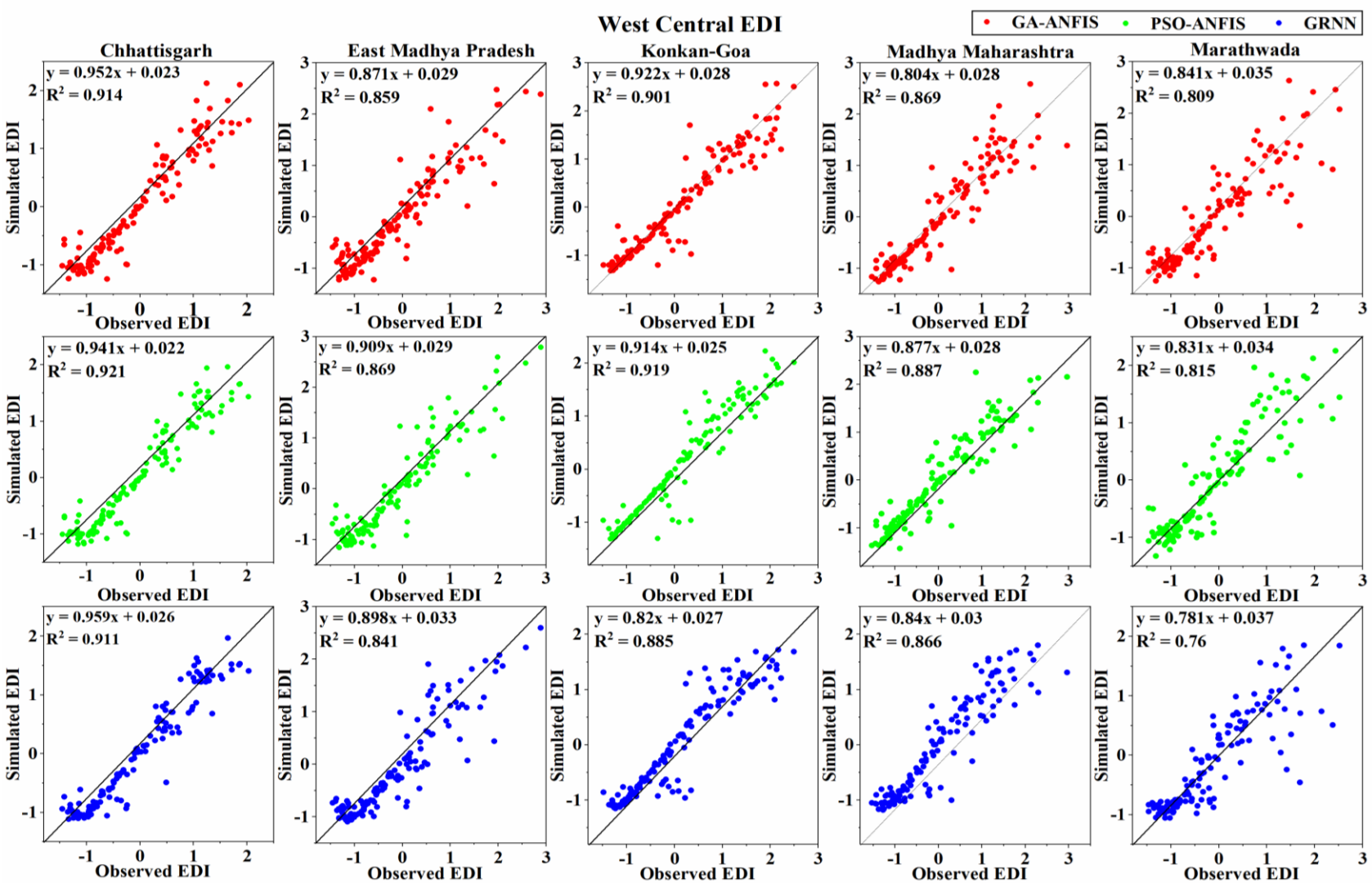
West Central EDI
GA-ANFIS
PSO-ANFIS
GRNN
Chhattisgarh
East Madhya Pradesh
Konkan-Goa
Madhya Maharashtra
Marathwada
y = 0.952x + 0.023
R² = 0.914
y = 0.871x + 0.029
R² = 0.859
y = 0.922x + 0.028
R² = 0.901
y = 0.804x + 0.028
R² = 0.869
y = 0.841x + 0.035
R² = 0.809
y = 0.941x + 0.022
R² = 0.921
y = 0.909x + 0.029
R² = 0.869
y = 0.914x + 0.025
R² = 0.919
y = 0.877x + 0.028
R² = 0.887
y = 0.831x + 0.034
R² = 0.815
y = 0.959x + 0.026
R² = 0.911
y = 0.898x + 0.033
R² = 0.841
y = 0.82x + 0.027
R² = 0.885
y = 0.84x + 0.03
R² = 0.866
y = 0.781x + 0.037
R² = 0.76
Simulated EDI
Observed EDI

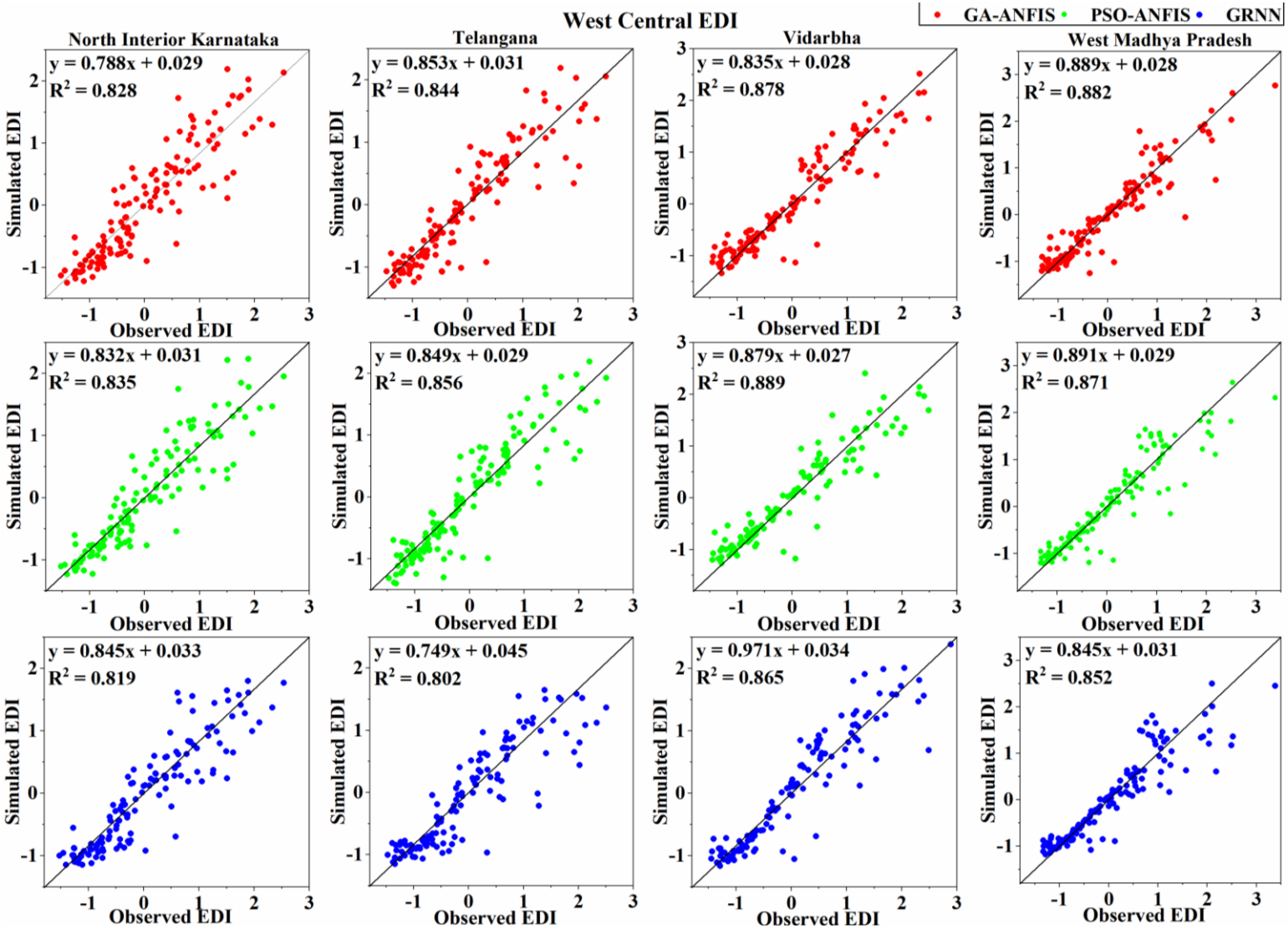

Figure 4.14 Scatterplot of observed and predicted EDI of GA-ANFIS, PSO-ANFIS and GRNN for West Central

Comparing the results of different performance metrics, it is evident that the hybrid machine learning models, particularly GA-ANFIS, exhibit a better agreement with the GRNN model in terms of R^2, RRMSE, and NSE. This suggests that the GA-ANFIS model not only outperforms the GRNN model but also provides more reliable and accurate prediction for the Chhattisgarh subdivisions within the West Central region. These findings indicate that the GA-ANFIS model is a promising tool for EDI prediction in the West Central region, particularly for Chhattisgarh subdivisions.

Figures 4.10 to 4.14 illustrate the scatterplot for observed and predicted EDI using GA-ANFIS, PSO-ANFIS and GRNN for all the meteorological subdivisions which are again segregated concerning homogenous monsoon regions. The entire analysis demonstrates the superior performance of GA-ANFIS and PSO-ANFIS models compared to the GRNN model across all meteorological subdivisions. The scatterplots visibly depict the close agreement between the observed and predicted EDI values for most of the meteorological subdivisions using GA-ANFIS and PSO-ANFIS models. This consistency demonstrates the robustness of these hybrid models in capturing the complex patterns of EDI and providing reliable prediction throughout the study area. The models' ability to closely align with the observed data indicates their effectiveness in predicting drought events accurately.

The statistical indices for EDI in terms of RRMSE showcase the accuracy of the models' predictions. The RRMSE values for GA-ANFIS, PSO-ANFIS, and GRNN models fall within the range of 0.299 to 0.671, 0.283 to 0.665, and 0.305 to 0.712, respectively. Lower RRMSE values signify better accuracy in capturing the variations between observed and predicted EDI values. Here, it is observed that both GA-ANFIS and PSO-ANFIS models consistently yield lower RRMSE values, indicating their proficiency in generating more accurate predictions compared to the GRNN model. Most subdivisions show RRMSE values between 0.3 and 0.5, which are considered relatively poor. However, it is worth noting that some subdivisions exhibit excellent RRMSE values below 0.3, indicating high accuracy in the models' predictions for those specific regions. The overall performance of GA-ANFIS and PSO-ANFIS models highlights

their superiority in delivering precise prediction, especially in subdivisions with lower RRMSE values.

The findings suggest that the hybrid machine learning models, particularly GA-ANFIS and PSO-ANFIS, are well-suited for EDI prediction in the study area. Their consistent performance, as depicted in the scatterplots, demonstrates their potential in aiding drought preparedness, water resource management, and climate adaptation strategies. The higher accuracy measures of GA-ANFIS and PSO-ANFIS models underscore their significance in generating reliable predictions, which can be invaluable for decision-makers, agricultural planners, and stakeholders in mitigating the impacts of droughts and ensuring sustainable resource management.

4.2.2 Performance evaluation of SPI-9 prediction

The performance evaluation of SPI-9 is a crucial aspect of the study as it assesses the accuracy and reliability of the predicted drought index value compared to the observed data. This evaluation helps in understanding the effectiveness of the machine learning models used for predicting SPI-9 and provides insights into their prediction capabilities for different meteorological subdivisions. The performance evaluation is typically based on several statistical measures. Each of these metrics serves a specific purpose in assessing the quality of the predictions and their agreement with the observed data.

Among the meteorological subdivisions in the Central Northeast region, Uttarakhand stands out with exceptional prediction results using the PSO-ANFIS model. Notably, it achieved R^2, RRMSE, and NSE values of 0.823, 0.416, and 0.823, respectively. These high-performance metrics indicate the model's superior ability to capture the SPI-9 variations accurately, making it the most effective among the three models tested. The findings suggest that for SPI-9 predicting in the Central Northeast region, the PSO-ANFIS model is the most reliable and accurate among the three machine learning models. The selection of an appropriate prediction model is critical for decision-making and policy formulation to address drought-related challenges effectively. Based on the results presented in Table 4.6, the PSO-ANFIS model emerges as the most suitable choice for SPI-9 prediction in the Central Northeast India, offering improved accuracy and reliability compared to the other models.

For SPI-9, in the North-East region, GA-ANFIS has the best prediction results with 0.859, 0.395 and 0.843 in terms of R^2, RRMSE and NSE, respectively which are obtained in Nagaland-Manipur-Mizoram-Tripura subdivision. The R^2 value of 0.859 is particularly noteworthy as it indicates a strong and positive correlation between the observed and the predicted SPI-9 as illustrated in Figure 4.15. This suggests that the GA-ANFIS model has effectively captured the underlying patterns and drought occurrence in this subdivision. The findings indicate that the GA-ANFIS model is well-suited for SPI-9 prediction in the North-East region, with the Nagaland-Manipur-Mizoram-Tripura subdivision benefiting from its robust predictions. The high R^2 value confirms the model's proficiency in explaining the variations in SPI-9 data, while the low RRMSE and high NSE values further validate its accuracy and capability.

In the Northwest region, the performance of three machine learning models, namely GA-ANFIS, PSO-ANFIS, and GRNN, has been evaluated by comparing the predicted SPI with the observed SPI values in the eight meteorological subdivisions for SPI-9 (Figure 4.17). The statistical analysis was conducted to assess the accuracy and reliability of each model's predictions in capturing the variability of SPI for this specific region. Based on the analysis, it was found that the GA-ANFIS model outperformed the other models in terms of prediction accuracy for the North-West region. Notably, the Jammu-Kashmir subdivision stood out as it exhibited the best prediction results for the GA-ANFIS model, achieving R^2, RRMSE, and NSE values of 0.803, 0.447, and 0.799, respectively.

In the Peninsular region, which consists of six meteorological subdivisions, the performance of three machine learning models, namely GA-ANFIS, PSO-ANFIS, and GRNN, was evaluated in terms of their prediction accuracy for SPI-9. Among these models, the PSO-ANFIS model emerged as the best performer for SPI-9 in Kerala subdivisions (Figure 4.18). It generated the best predicted results of 0.818, 0.464 and 0.784 in terms of R^2, RRMSE and NSE for the PSO-ANFIS model which outperformed the GA-ANFIS and GRNN models. The superior performance of the PSO-ANFIS model in the Peninsular region, particularly for the Kerala subdivisions, suggests that this model is well-suited for predicting drought conditions in this area.

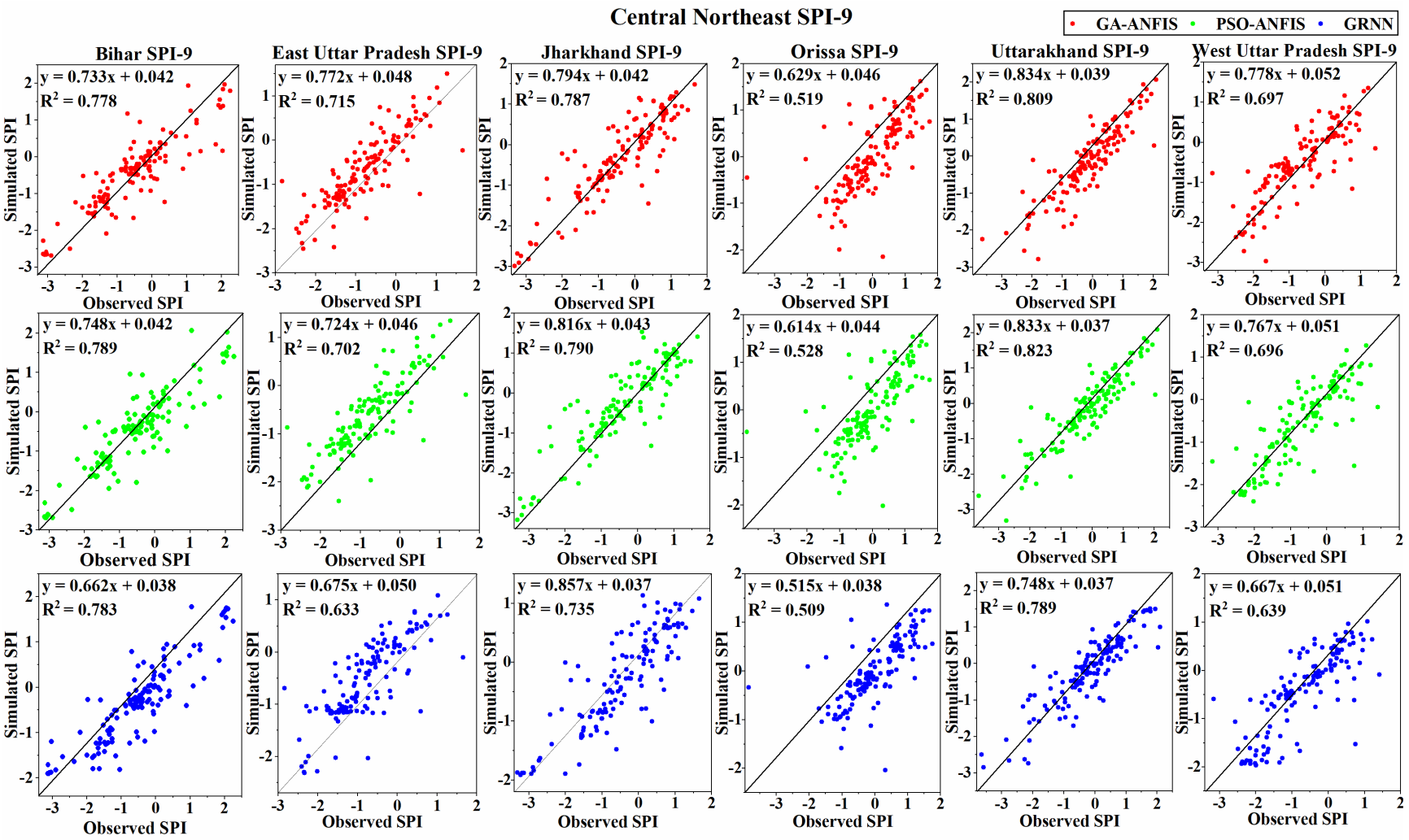

Figure 4.15 Scatterplot of observed and predicted SPI-9 of GA-ANFIS, PSO-ANFIS and GRNN models for Central North East

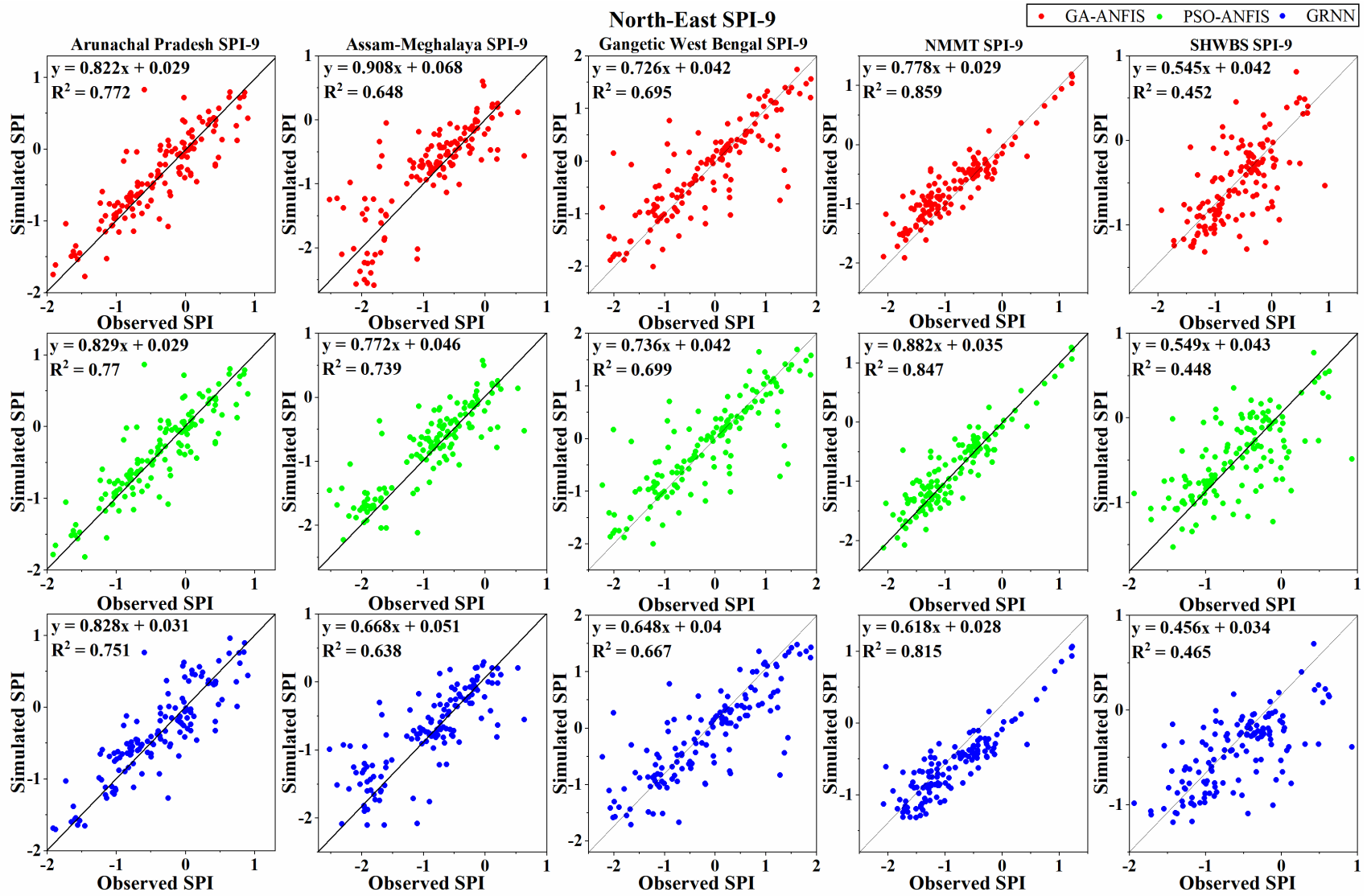

Figure 4.16 Scatterplot of observed and predicted SPI-9 of GA-ANFIS, PSO-ANFIS and GRNN models for North-East

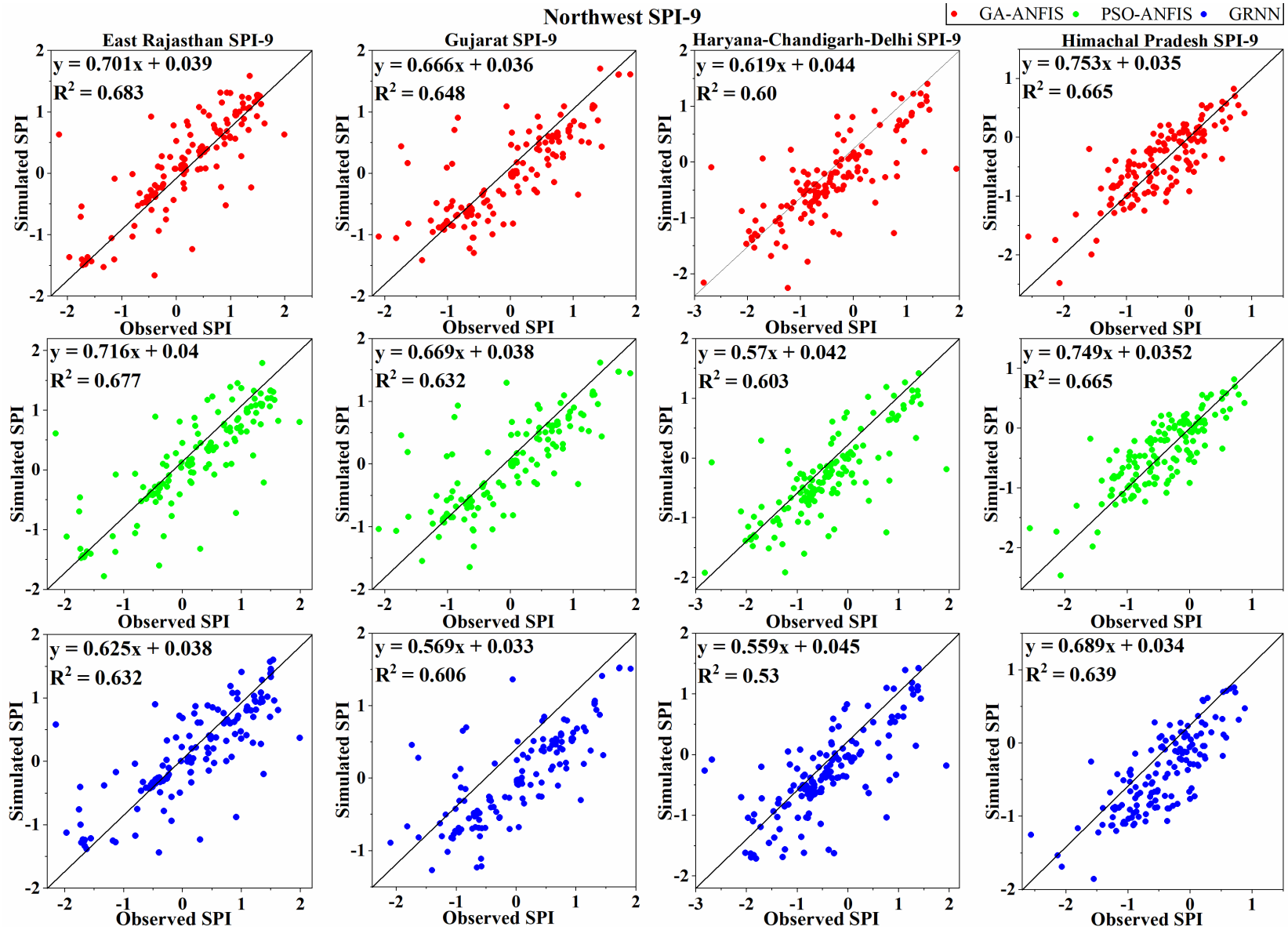
Northwest SPI-9
GA-ANFIS
PSO-ANFIS
GRNN
East Rajasthan SPI-9
y = 0.701x + 0.039
R2 = 0.683
Gujarat SPI-9
y = 0.666x + 0.036
R2 = 0.648
Haryana-Chandigarh-Delhi SPI-9
y = 0.619x + 0.044
R2 = 0.60
Himachal Pradesh SPI-9
y = 0.753x + 0.035
R2 = 0.665
y = 0.716x + 0.04
R2 = 0.677
y = 0.669x + 0.038
R2 = 0.632
y = 0.57x + 0.042
R2 = 0.603
y = 0.749x + 0.0352
R2 = 0.665
y = 0.625x + 0.038
R2 = 0.632
y = 0.569x + 0.033
R2 = 0.606
y = 0.559x + 0.045
R2 = 0.53
y = 0.689x + 0.034
R2 = 0.639
Simulated SPI
Observed SPI

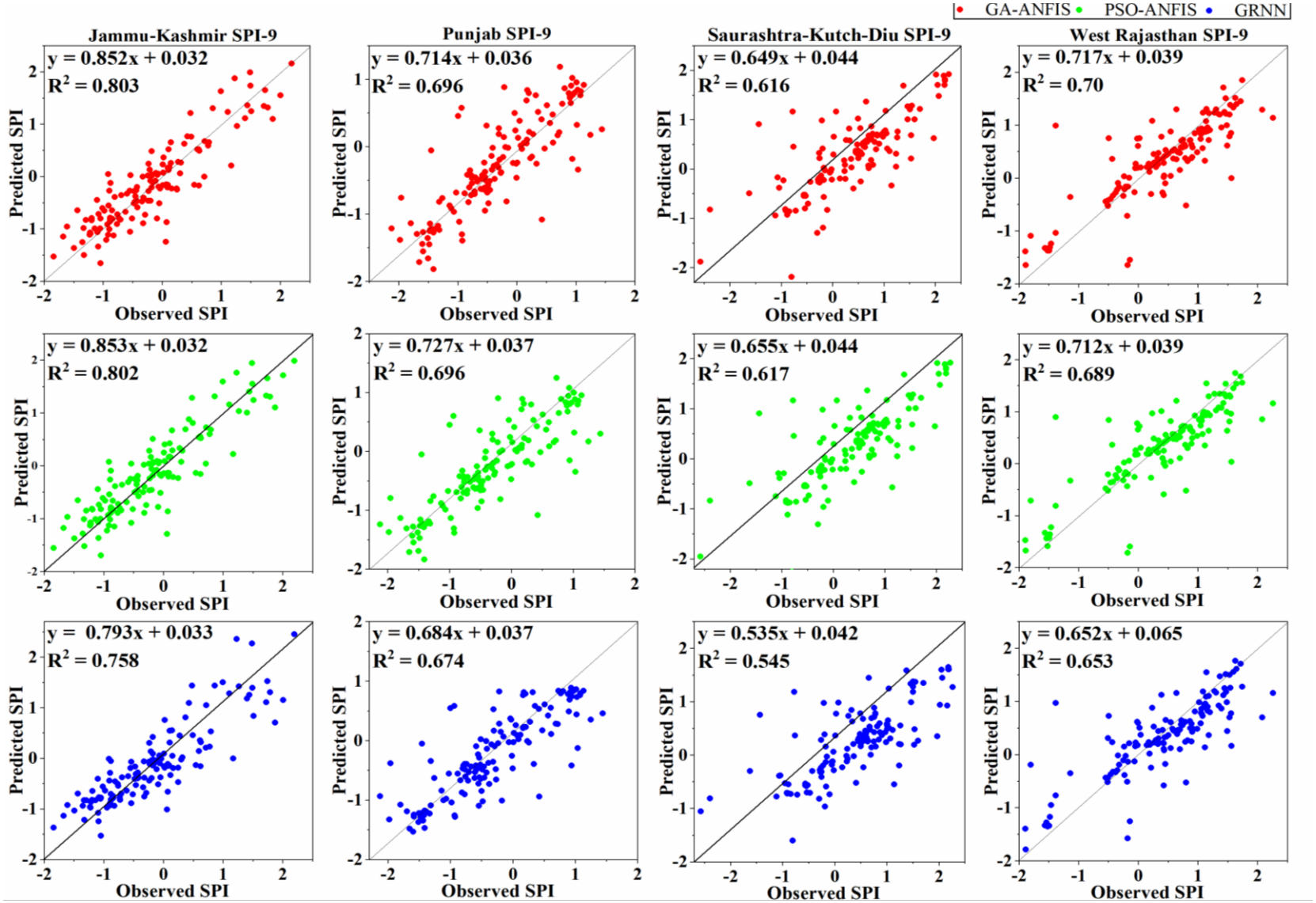

Figure 4.17 Scatterplot of observed and predicted SPI-9 of GA-ANFIS, PSO-ANFIS and GRNN models for North-West

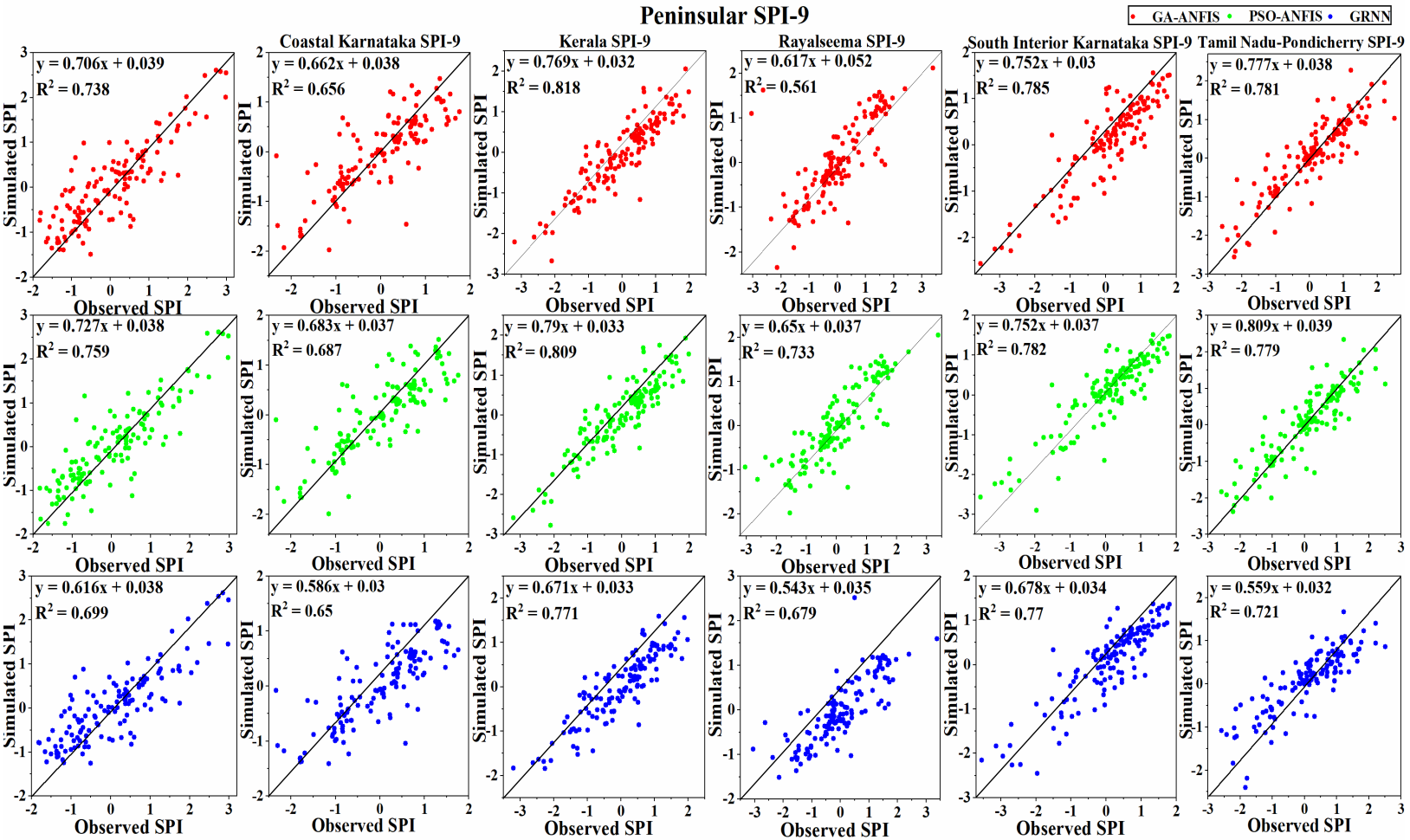

Figure 4.18 Scatterplot of observed and predicted SPI-9 of GA-ANFIS, PSO-ANFIS and GRNN models for Peninsular

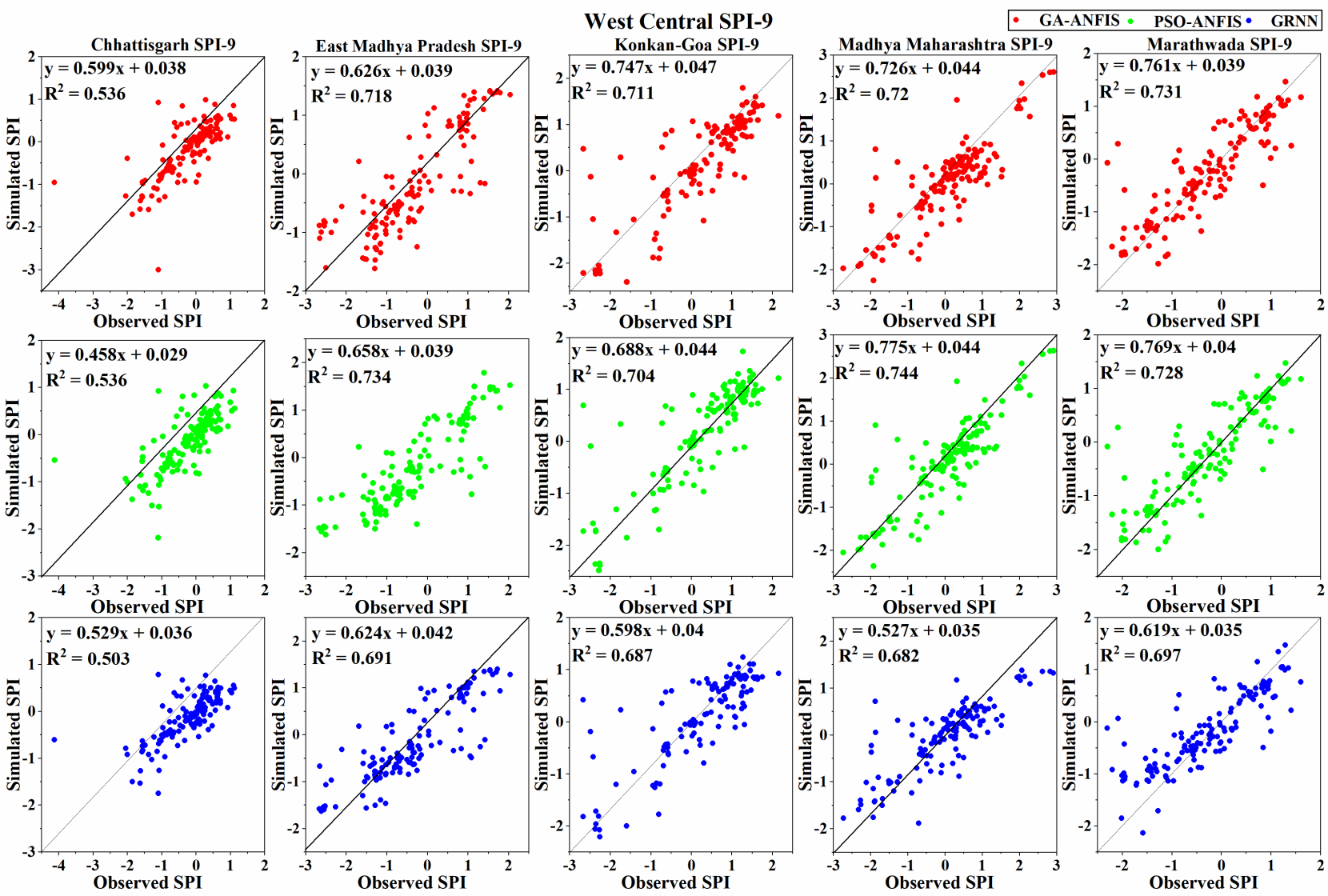
West Central SPI-9
GA-ANFIS
PSO-ANFIS
GRNN
Chhattisgarh SPI-9
y = 0.599x + 0.038
R2 = 0.536
East Madhya Pradesh SPI-9
y = 0.626x + 0.039
R2 = 0.718
Konkan-Goa SPI-9
y = 0.747x + 0.047
R2 = 0.711
Madhya Maharashtra SPI-9
y = 0.726x + 0.044
R2 = 0.72
Marathwada SPI-9
y = 0.761x + 0.039
R2 = 0.731
y = 0.458x + 0.029
R2 = 0.536
y = 0.658x + 0.039
R2 = 0.734
y = 0.688x + 0.044
R2 = 0.704
y = 0.775x + 0.044
R2 = 0.744
y = 0.769x + 0.04
R2 = 0.728
y = 0.529x + 0.036
R2 = 0.503
y = 0.624x + 0.042
R2 = 0.691
y = 0.598x + 0.04
R2 = 0.687
y = 0.527x + 0.035
R2 = 0.682
y = 0.619x + 0.035
R2 = 0.697
Simulated SPI
Observed SPI

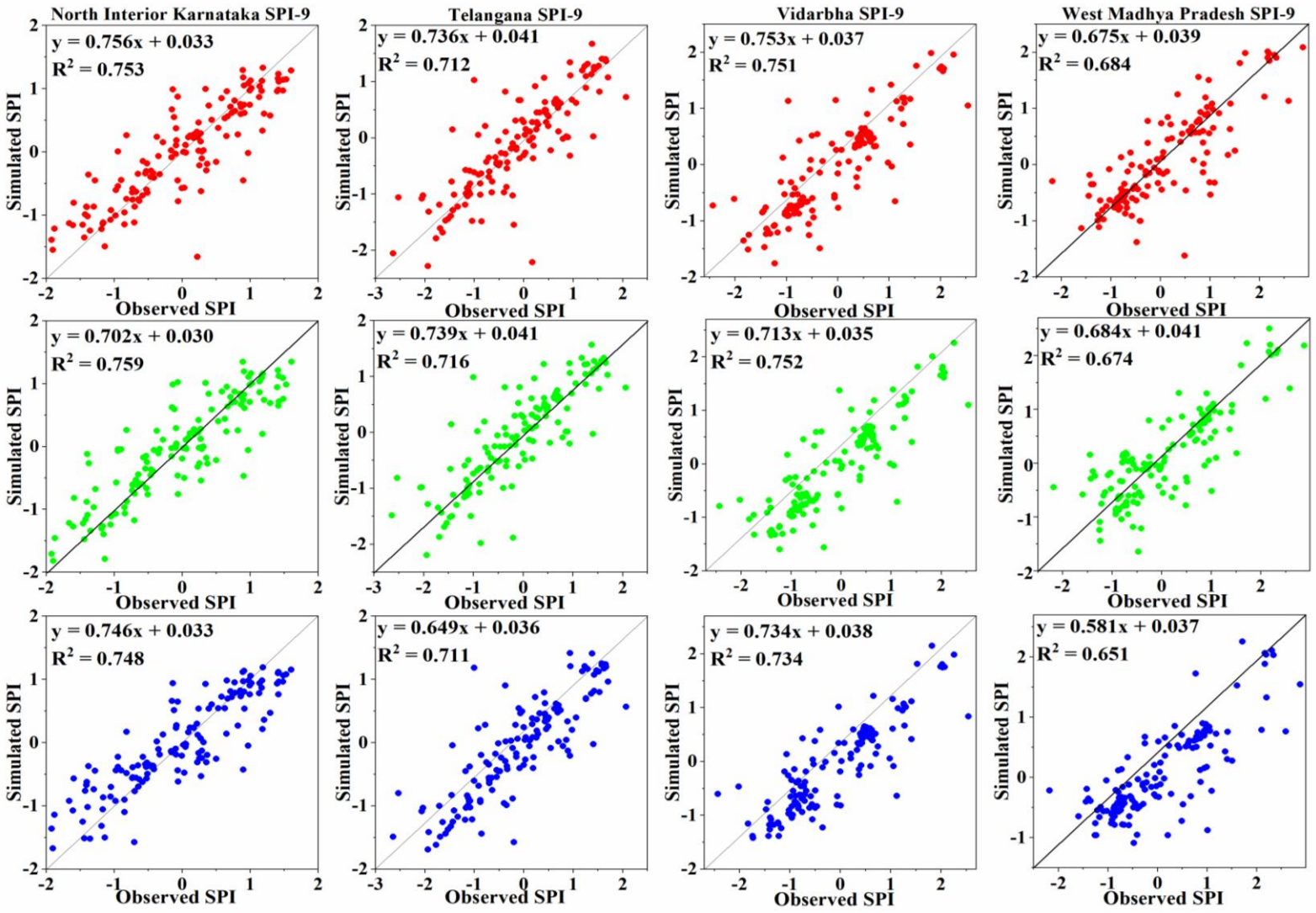

Figure 4.19 Scatterplot of observed and simulated SPI-9 of GA-ANFIS, PSO-ANFIS and GRNN models for West Central

In the West Central region, which comprises of nine meteorological subdivisions, the performance of different machine learning models was evaluated for predicting the SPI. Among these models, the PSO-ANFIS model demonstrated the best predicting performance for the North Interior Karnataka subdivision (Figure 4.19). The PSO-ANFIS model exhibited has the best performance in North Interior Karnataka as compared with the other meteorological subdivisions with 0.859, 0.493 and 0.729 in terms of R^2, RRMSE and NSE. By outperforming other models, such as GA-ANFIS and GRNN, the PSO-ANFIS model proves its superiority as a valuable tool for drought prediction and monitoring in the North Interior Karnataka subdivision and, more broadly, the West Central region of India.

In Figures (4.15 - 4.19), the scatterplots of the observed and predicted SPI-9 of the GA-ANFIS, PSO and GRNN models are presented. These figures provide a visual representation of the model performance and demonstrate the robustness and consistency of the generated hybrid models, particularly the GA-ANFIS and PSO-ANFIS models, in accurately predicting SPI-9 values. The close agreement between the observed and predicted SPI-9 values across multiple meteorological subdivisions and regions demonstrates the effectiveness of the GA-ANFIS and PSO-ANFIS models in predicting drought conditions. These hybrid machine learning models are useful in understanding and making effective decision in water sector domain. Their ability to capture regional drought patterns and the observed data reaffirms their potential to aid in drought monitoring and mitigation efforts. Overall, the scatterplots presented in Figures (4.15 to 4.19) provide visual evidence of the robustness and consistency of the GA-ANFIS and PSO-ANFIS models in predicting SPI-9 values across different regions in India.

Table 4.9 presents the performance statistics for the predicted results of the SPI-9 in thirty-four meteorological subdivisions. This evaluation offers valuable insights into the accuracy and effectiveness of the models in predicting SPI-9.

Table 4.9 Performance metrics of GA-ANFIS, PSO-ANFIS and GRNN for SPI-9

MSD	R^2			RRMSE			NSE		
	GA-ANFIS	PSO-ANFIS	GRNN	GA-ANFIS	PSO-ANFIS	GRNN	GA-ANFIS	PSO-ANFIS	GRNN
BI	0.783	**0.789**	0.778	0.548	**0.508**	0.546	0.7	**0.740**	0.698
EUP	**0.715**	0.702	0.633	**0.552**	0.572	0.663	**0.693**	0.671	0.558
JH	0.787	**0.790**	0.735	0.470	**0.467**	0.551	0.777	**0.781**	0.694
OR	0.519	**0.528**	0.509	0.709	**0.696**	0.698	0.509	**0.513**	0.494
UK	0.809	**0.823**	0.789	0.436	**0.419**	0.460	0.809	**0.823**	0.787
WUP	**0.697**	0.696	0.639	**0.570**	0.573	0.656	**0.673**	0.669	0.566
AP	**0.772**	0.770	0.751	**0.481**	0.483	0.509	**0.767**	0.765	0.739
AM	0.648	**0.739**	0.638	0.677	**0.532**	0.652	0.572	**0.715**	0.538
GWB	0.695	**0.699**	0.667	0.552	**0.549**	0.577	0.693	**0.696**	0.665
NMMT	**0.859**	0.847	0.815	**0.395**	0.425	0.605	**0.843**	0.818	0.631
SHWBS	0.452	**0.465**	0.448	0.784	**0.767**	0.774	0.397	**0.408**	0.381
ER	**0.683**	0.677	0.632	**0.563**	0.569	0.607	**0.681**	0.675	0.630
GJ	**0.648**	0.632	0.606	**0.592**	0.606	0.627	**0.648**	0.630	0.604
HCD	0.600	**0.603**	0.530	0.638	**0.637**	0.692	0.591	**0.598**	0.517
HP	**0.665**	**0.665**	0.639	**0.588**	**0.589**	0.605	**0.652**	**0.650**	0.631
JK	**0.803**	0.802	0.758	**0.447**	0.448	0.496	**0.799**	0.798	0.752
PN	**0.696**	**0.696**	0.674	**0.553**	**0.555**	0.578	**0.692**	0.689	0.663
SKD	0.616	**0.617**	0.545	0.63	**0.628**	0.693	0.600	**0.603**	0.517
WR	**0.700**	0.689	0.653	**0.555**	0.563	0.595	**0.690**	0.681	0.644
CAP	0.738	**0.759**	0.699	0.511	**0.493**	0.557	0.737	**0.756**	0.688
CK	0.656	**0.687**	0.650	0.585	**0.558**	0.595	0.656	**0.687**	0.644
KL	**0.818**	0.809	0.771	**0.464**	0.479	0.490	**0.784**	0.770	0.758
RAY	0.561	**0.733**	0.679	0.665	**0.524**	0.589	0.651	**0.723**	0.555
SIK	**0.785**	0.782	0.770	**0.464**	0.466	0.489	**0.783**	0.781	0.759
TNP	**0.781**	0.779	0.721	**0.467**	0.470	0.560	**0.781**	0.778	0.685
CHH	**0.536**	0.536	0.503	**0.688**	0.702	0.717	**0.524**	0.504	0.482
EUP	0.718	**0.734**	0.691	0.568	**0.558**	0.58	0.662	**0.687**	0.675
KG	**0.711**	0.704	0.687	**0.538**	0.552	0.584	**0.708**	0.694	0.656
MM	0.720	**0.744**	0.682	0.527	**0.506**	0.595	0.720	**0.743**	0.644
MA	**0.731**	0.728	0.697	**0.518**	0.524	0.566	**0.729**	0.724	0.678
NIK	0.753	**0.759**	0.748	0.496	**0.493**	0.500	0.752	**0.755**	0.748
TE	0.712	**0.716**	0.711	0.536	**0.532**	0.541	0.711	**0.715**	0.705
VI	0.751	**0.752**	0.734	0.515	**0.499**	0.599	0.733	**0.749**	0.709
WMP	**0.684**	0.674	0.651	**0.560**	0.573	0.595	**0.684**	0.669	0.643

The evaluation of these models based on multiple performance metrics helps in identifying the most accurate and reliable model for each region, facilitating effective drought monitoring and management strategies. It offers valuable insights into the strengths and weaknesses of each model and aids in making informed decisions for various applications related to climate and water resource management.

4.2.3 Performance evaluation of SPI-12 prediction

The performance evaluation of the 12-month timescale Standardized Precipitation Index (SPI-12) is a crucial aspect of drought monitoring and prediction. It involves assessing the accuracy and effectiveness of predicting models, such as GRNN, GA-ANFIS, and PSO-ANFIS, in predicting SPI-12 values for different meteorological subdivisions. The evaluation aims to determine the most accurate and reliable prediction model for SPI-12. The evaluation results contribute to climate studies by providing insights into long-term drought trends and variations across different regions. In summary, the performance evaluation of the SPI-12 for predicting the models is essential for understanding the accuracy of drought predictions in different meteorological subdivisions.

From figure 4.20, both GA-ANFIS and PSO-ANFIS models demonstrate remarkable prediction results in the Central North-East region, specifically in the Uttarakhand subdivision. The scatterplot for this region reveals a close alignment between the observed and predicted SPI-12 values by both models. The high R^2 value of 0.881 indicates a strong correlation between the observed and predicted values, while the low RRMSE value of 0.344 and high NSE value of 0.881 highlight the models' accuracy and ability to capture the variability in SPI-12. This close agreement in the scatterplot confirms the robustness and reliability of both models in capturing the precipitation patterns that lead to drought conditions in the Uttarakhand subdivision of Central Northeast region.

In the North-East region, the PSO-ANFIS model stands out with the best predicted results, specifically in the Nagaland-Manipur-Mizoram-Tripura subdivision. The scatterplot for this subdivision indicates a strong alignment between the observed SPI-

12 values and the SPI-12 values predicted by the PSO-ANFIS model as illustrated in Figure 4.21. The high R^2 value of 0.907 further reinforces the strong correlation between the observed and predicted values, while the low RRMSE value of 0.315 and high NSE value of 0.9 demonstrate the model's accuracy in capturing long-term precipitation patterns and drought conditions in this region. The visually close grouping of data points in the scatterplot confirms the reliability and effectiveness of the PSO-ANFIS model in predicting SPI-12 for the Nagaland-Manipur-Mizoram-Tripura subdivision.

The PSO-ANFIS model also exhibits the best prediction results in the Northwest region, specifically in the Jammu-Kashmir subdivision (Figure 4.22). The scatterplot for this subdivision shows a strong alignment between the observed and the predicted SPI-12 values by the PSO-ANFIS model. The high R^2 value of 0.878 reflects the strong correlation between the observed and predicted values, while the low RRMSE value of 0.348 and high NSE value of 0.891 emphasize the model's accuracy in capturing the variability in SPI-12 over a 12-month period in the Jammu-Kashmir subdivision. The scatterplot's clustering of data points around the regression line reinforces the model's reliability and effectiveness in predicting the SPI-12 for this region.

In the Peninsular region, the GA-ANFIS model stands out with the best prediction results, specifically in the Kerala subdivision (Figure 4.23). The scatterplot for this subdivision reveals a close alignment between the observed SPI-12 values and the SPI-12 values predicted by the GA-ANFIS model. The high R^2 value of 0.884 indicates a strong correlation between the observed and predicted values, while the low RRMSE value of 0.339 and high NSE value of 0.884 highlight the model's accuracy in capturing the long-term precipitation patterns and drought conditions in Kerala. The tight clustering of data points around the regression line in the scatterplot confirms the model's reliability and effectiveness in predicting SPI-12 for this region.

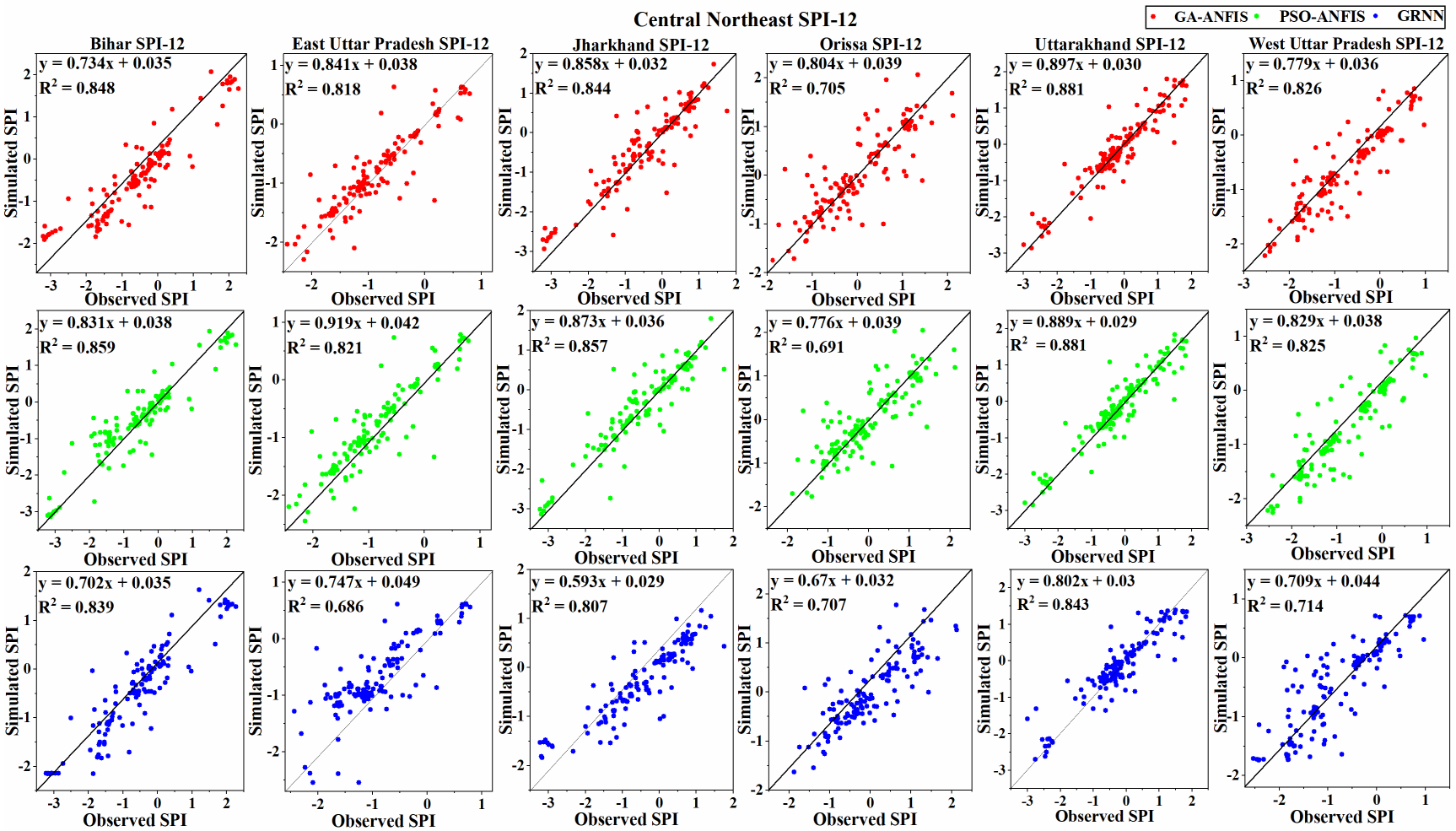

Figure 4.20 Scatterplot of observed and simulated SPI-12 of GA-ANFIS,PSO-ANFIS and GRNN models for Central Northeast

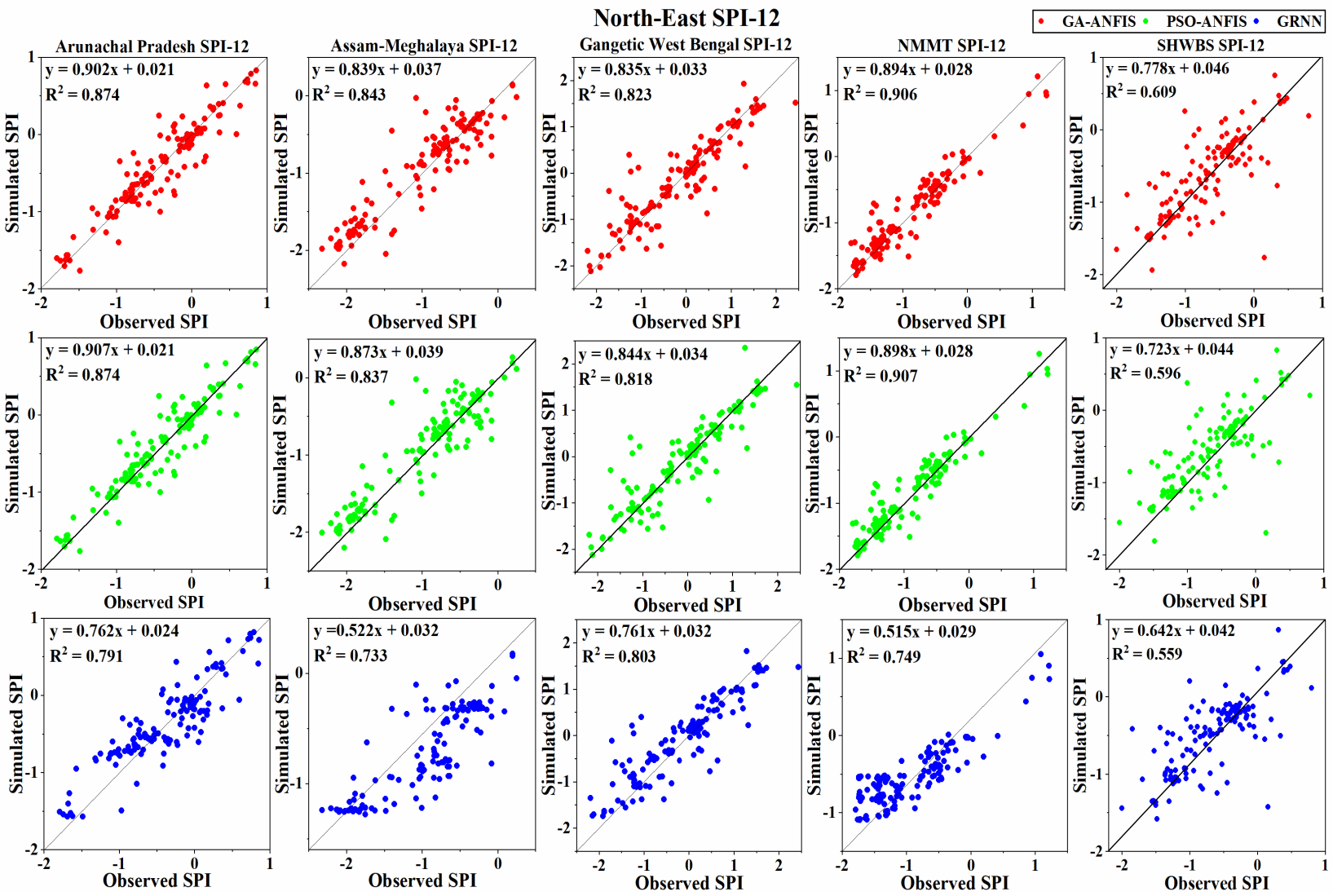

Figure 4.21 Scatterplot of observed and simulated SPI-12 of GA-ANFIS,PSO-ANFIS and GRNN models for North-East

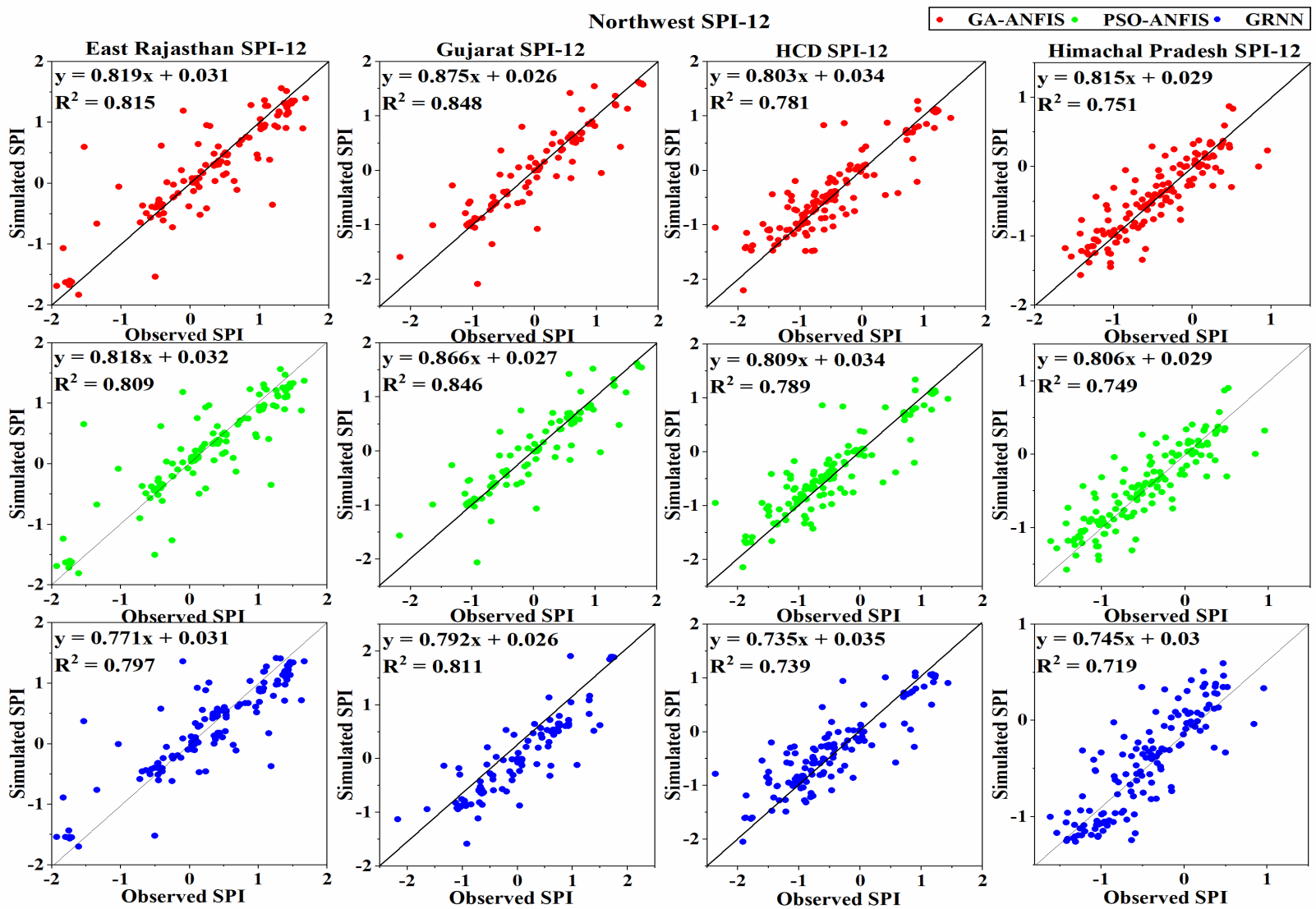
Northwest SPI-12
GA-ANFIS
PSO-ANFIS
GRNN
East Rajasthan SPI-12
y = 0.819x + 0.031
R² = 0.815
Gujarat SPI-12
y = 0.875x + 0.026
R² = 0.848
HCD SPI-12
y = 0.803x + 0.034
R² = 0.781
Himachal Pradesh SPI-12
y = 0.815x + 0.029
R² = 0.751
y = 0.818x + 0.032
R² = 0.809
y = 0.866x + 0.027
R² = 0.846
y = 0.809x + 0.034
R² = 0.789
y = 0.806x + 0.029
R² = 0.749
y = 0.771x + 0.031
R² = 0.797
y = 0.792x + 0.026
R² = 0.811
y = 0.735x + 0.035
R² = 0.739
y = 0.745x + 0.03
R² = 0.719
Simulated SPI
Observed SPI

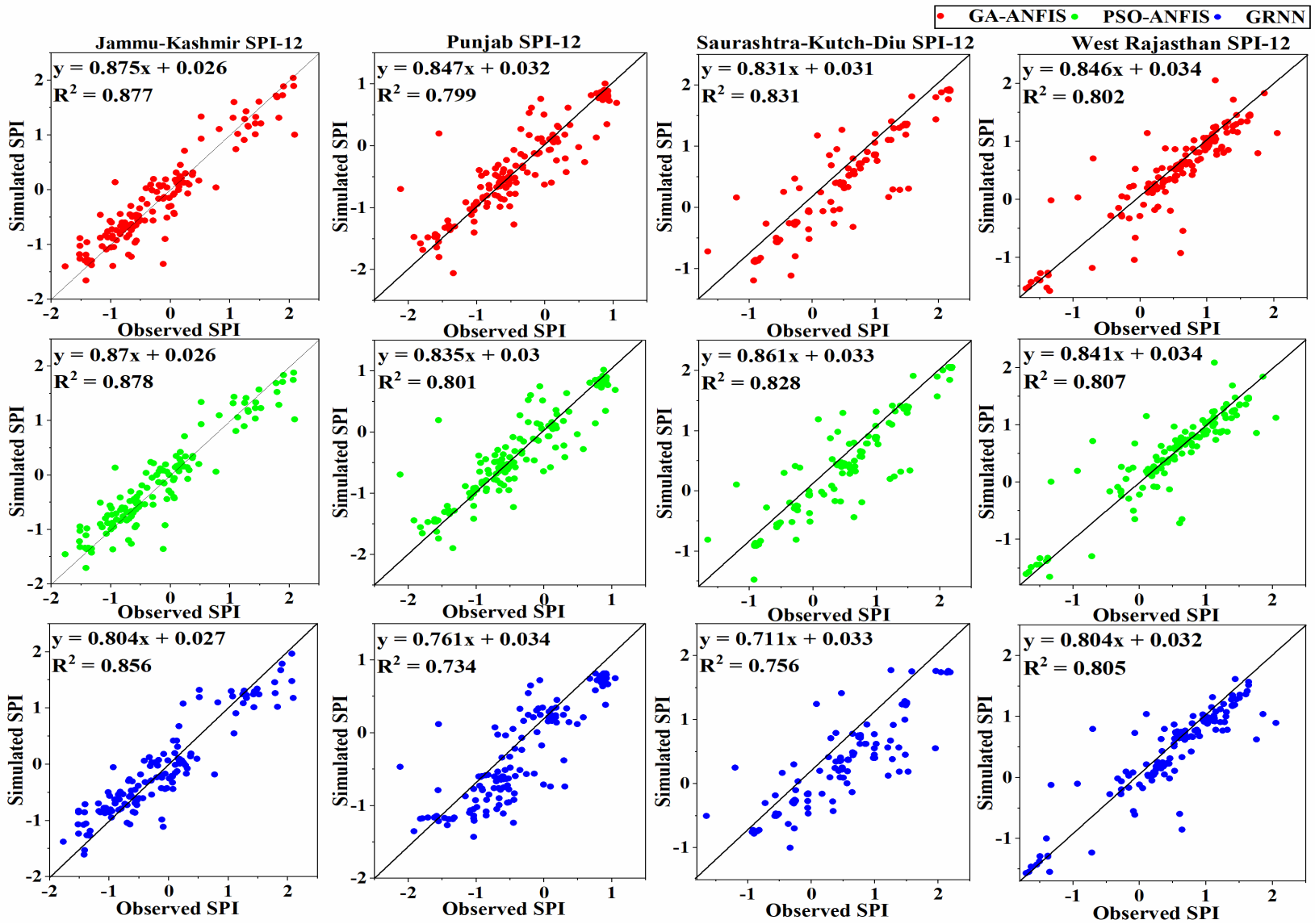

Figure 4.22 Scatterplot of observed and simulated SPI-12 of GA-ANFIS, PSO-ANFIS and GRNN models for North-West

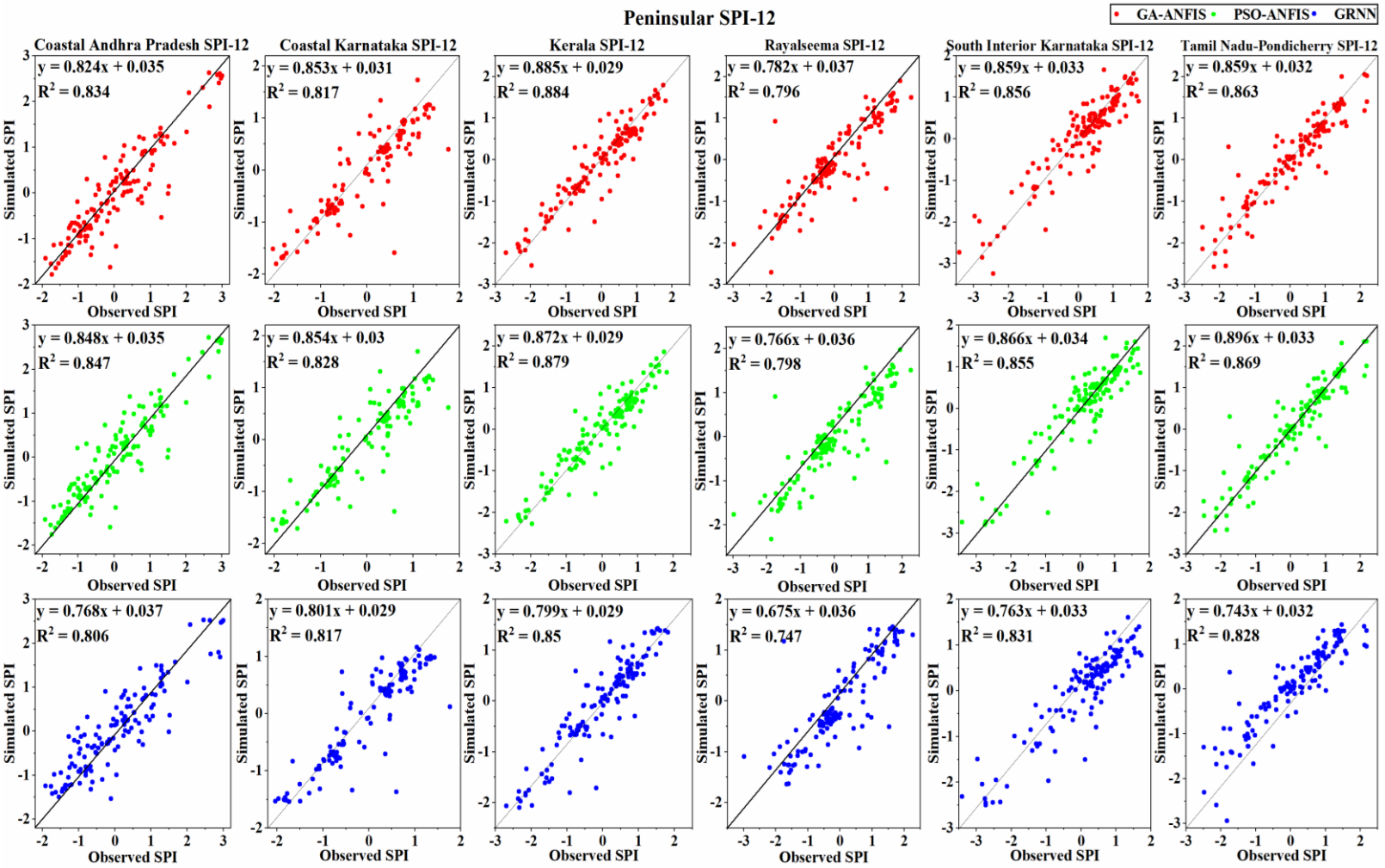

Figure 4.23 Scatterplot of observed and simulated SPI-12 of GA-ANFIS, PSO-ANFIS and GRNN models for Peninsular

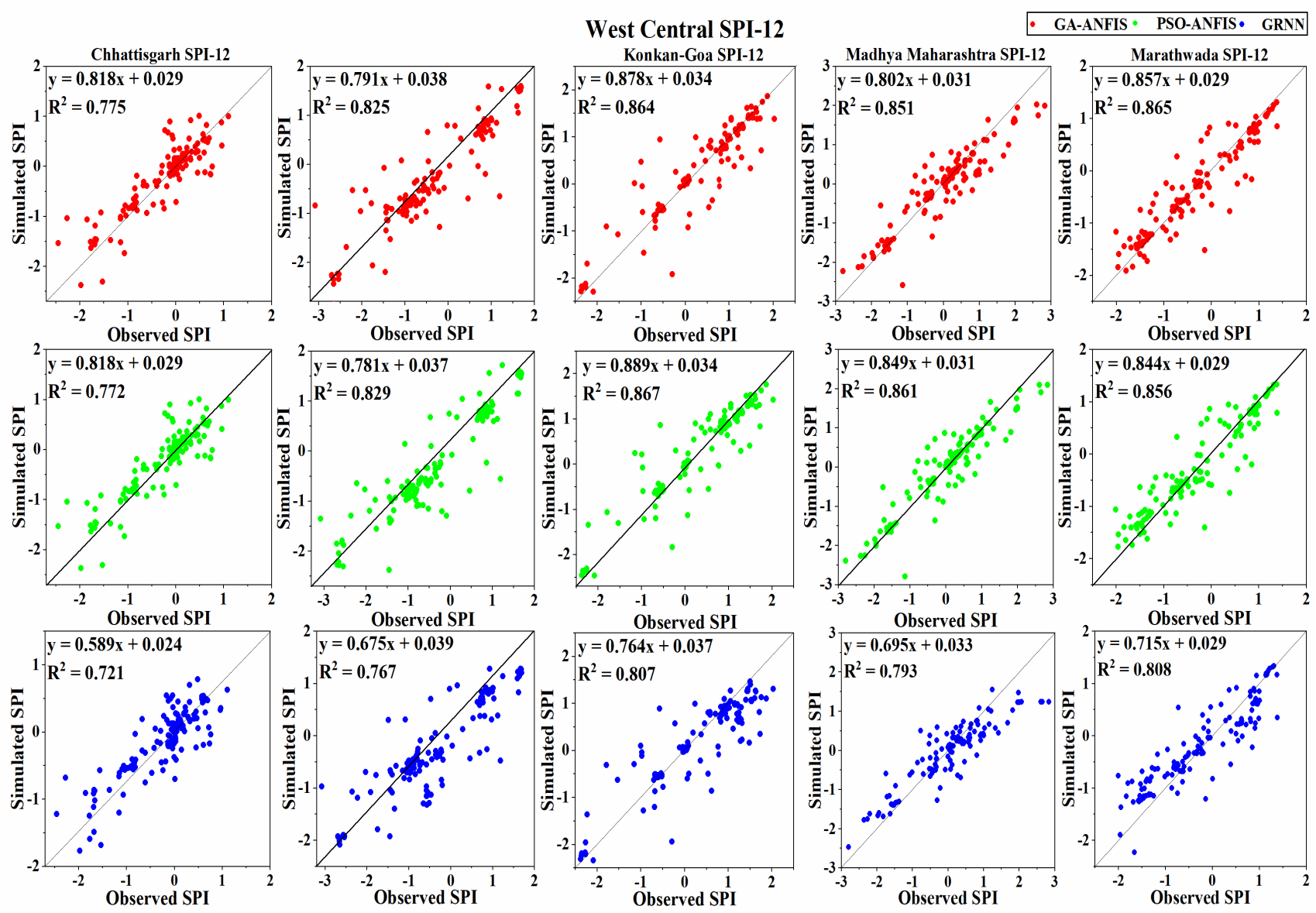
West Central SPI-12
GA-ANFIS
PSO-ANFIS
GRNN
Chhattisgarh SPI-12
y = 0.818x + 0.029
R² = 0.775
y = 0.818x + 0.029
R² = 0.772
y = 0.589x + 0.024
R² = 0.721
Konkan-Goa SPI-12
y = 0.878x + 0.034
R² = 0.864
y = 0.889x + 0.034
R² = 0.867
y = 0.764x + 0.037
R² = 0.807
Madhya Maharashtra SPI-12
y = 0.802x + 0.031
R² = 0.851
y = 0.849x + 0.031
R² = 0.861
y = 0.695x + 0.033
R² = 0.793
Marathwada SPI-12
y = 0.857x + 0.029
R² = 0.865
y = 0.844x + 0.029
R² = 0.856
y = 0.715x + 0.029
R² = 0.808
Simulated SPI
Observed SPI

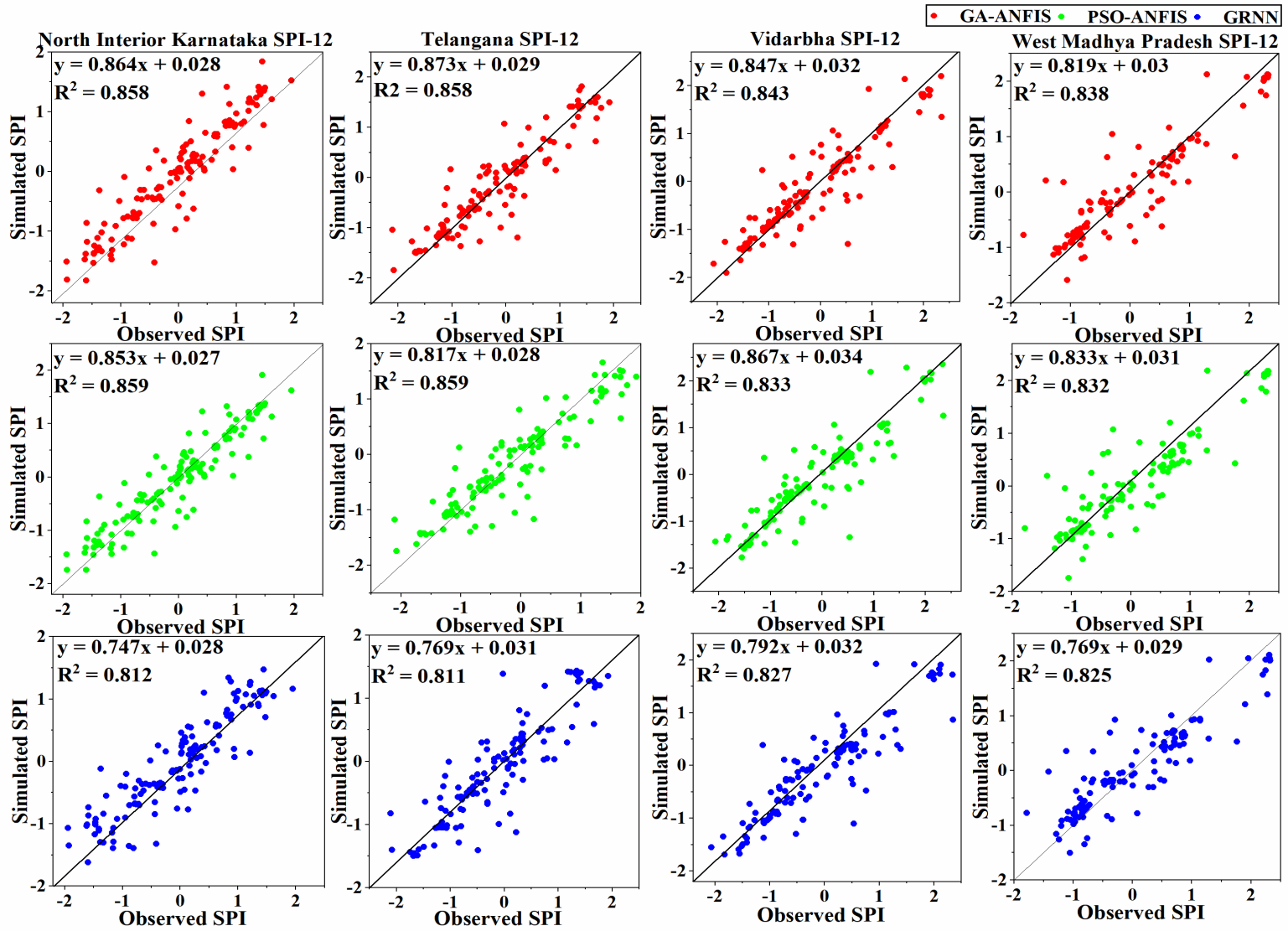

Figure 4.24 Scatterplot of observed and simulated SPI-12 of GA-ANFIS, PSO-ANFIS and GRNN models for West Central

The PSO-ANFIS model exhibits the best performance in the West Central region, particularly in the Konkan-Goa subdivision. The scatterplot for this subdivision demonstrates a strong alignment between the observed and predicted SPI-12 by the PSO-ANFIS model (Figure 4.24). The high R^2 value of 0.867 indicates a strong correlation between the observed and predicted values, while the low RRMSE value of 0.367 and high NSE value of 0.863 underscore the model's accuracy in capturing the variability in SPI-12 in Konkan-Goa. The close grouping of data points around the regression line in the scatterplot further verifies the model's reliability and effectiveness in predicting SPI-12 for this region compared to the other meteorological subdivisions.

Figures 4.20 to 4.24 display the scatterplots, which visually illustrate the relationship between the observed and the predicted SPI-12 values by these machine learning models. The scatterplots cover the Central Northeast, North-East, Northwest, Peninsular, and West Central regions, encompassing thirty-four meteorological subdivisions (MSDs). The scatterplots allow for a direct visual comparison between the observed and predicted SPI-12 values, enabling the evaluation of the models' performance in capturing the variability and patterns of precipitation that lead to drought conditions in each meteorological subdivision. The robustness and consistency of the hybrid GA-ANFIS and PSO-ANFIS models are apparent from their ability to closely approximate the observed SPI-12 values in a large number of MSDs, providing valuable insights into the effectiveness of these models in capturing long-term precipitation patterns. In addition, the prediction of SPI-9 and SPI-12 can be noted that as the timescale increases, the model performance also improved.

Table 4.10 presents the predicted results for the SPI-12, exhibiting a similar pattern of results to SPI-9. The evaluation compares the performance of three machine learning models: GA-ANFIS, PSO-ANFIS, and GRNN, in predicting SPI-12 values across different meteorological subdivisions. Similar to the analysis for SPI-9, it offers a comprehensive evaluation of the predictive capabilities of the three models for SPI-12 on three key performance metrics, R^2, RRMSE and NSE providing a quantitative assessment of the accuracy and reliability of each model's predictions.

Table 4.10 Performance metrics of GA-ANFIS, PSO-ANFIS and GRNN for SPI-12

MSD	R^2			RRMSE			NSE		
	GA-ANFIS	PSO-ANFIS	GRNN	GA-ANFIS	PSO-ANFIS	GRNN	GA-ANFIS	PSO-ANFIS	GRNN
BI	0.848	**0.859**	0.839	0.429	**0.386**	0.443	0.814	**0.850**	0.802
EUP	**0.818**	0.821	0.686	**0.430**	0.440	0.597	**0.813**	0.805	0.633
JH	0.844	**0.857**	0.807	0.397	**0.380**	0.529	0.841	**0.855**	0.718
OR	0.705	**0.707**	0.691	0.554	**0.541**	0.564	0.691	**0.705**	0.680
UK	**0.881**	**0.881**	0.843	**0.344**	**0.344**	0.398	**0.881**	**0.881**	0.841
WUP	**0.826**	0.825	0.714	**0.435**	0.452	0.581	**0.810**	0.794	0.645
AP	**0.873**	**0.874**	0.791	**0.356**	**0.356**	0.461	**0.873**	**0.873**	0.786
AM	**0.843**	0.837	0.733	**0.409**	0.414	0.537	**0.831**	0.828	0.710
GWB	**0.823**	0.818	0.803	**0.419**	0.426	0.453	**0.823**	0.817	0.793
NMMT	0.906	**0.907**	0.749	0.316	**0.315**	0.521	0.900	**0.901**	0.727
SHWBS	**0.609**	0.596	0.559	**0.371**	0.376	0.410	**0.552**	0.542	0.455
ER	**0.815**	0.809	0.797	**0.429**	0.436	0.451	**0.814**	0.809	0.795
GJ	**0.848**	0.846	0.811	**0.390**	0.392	0.435	**0.847**	0.846	0.810
HCD	0.781	**0.789**	0.739	0.471	**0.466**	0.522	0.776	**0.781**	0.726
HP	**0.751**	0.749	0.719	**0.504**	0.505	0.530	**0.744**	0.743	0.717
JK	0.877	**0.878**	0.856	0.350	**0.348**	0.382	0.890	**0.891**	0.872
PN	0.799	**0.801**	0.734	0.452	**0.448**	0.523	0.795	**0.797**	0.725
SKD	0.831	**0.828**	0.756	0.422	**0.417**	0.533	0.825	**0.821**	0.714
WR	0.805	**0.807**	0.802	0.448	**0.440**	0.449	0.798	**0.805**	0.797
CAP	0.834	**0.847**	0.806	0.410	**0.391**	0.441	0.831	**0.846**	0.804
CK	0.819	**0.828**	0.817	0.426	**0.414**	0.429	0.817	**0.828**	0.816
KL	**0.884**	0.879	0.850	**0.339**	0.345	0.390	**0.884**	0.880	0.847
RAY	0.796	**0.798**	0.747	0.453	**0.450**	0.510	0.794	**0.796**	0.738
SIK	**0.856**	0.855	0.831	**0.379**	0.380	0.419	**0.856**	0.855	0.824
TNP	0.863	**0.869**	0.828	0.370	**0.362**	0.424	0.862	**0.868**	0.819
CHH	**0.775**	0.772	0.721	**0.479**	0.481	0.570	**0.769**	0.767	0.673
EUP	0.825	**0.829**	0.767	0.425	**0.422**	0.502	0.818	**0.821**	0.746
KG	0.864	**0.867**	0.807	0.369	**0.367**	0.455	0.863	**0.863**	0.792
MM	0.851	**0.861**	0.793	0.394	**0.373**	0.477	0.844	**0.860**	0.771
MA	**0.865**	0.856	0.808	**0.366**	0.380	0.453	**0.865**	0.855	0.793
NIK	0.858	**0.859**	0.812	0.376	**0.375**	0.438	0.857	**0.858**	0.806
TE	0.858	**0.860**	0.811	0.376	**0.377**	0.436	0.857	**0.858**	0.809
VI	**0.843**	0.833	0.827	**0.395**	0.409	0.418	**0.843**	0.832	0.824
WMP	**0.838**	0.832	0.825	**0.402**	0.408	0.422	**0.837**	0.832	0.821

Overall, the study presents a thorough evaluation of the performance of machine learning models in predicting the drought indices, specifically the EDI, SPI-9 and SPI-12. Three machine learning models, namely GA-ANFIS, PSO-ANFIS and GRNN were employed and their predictions were assessed based on various statistical metrics. Visual representation through scatterplots demonstrated the effectiveness of GA-ANFIS and PSO-ANFIS models in predicting EDI, SPI-9 and SPI-12. The hybrid models GA-ANFIS and PSO-ANFIS were found to give consistent superior performance across different regions and timescales. Comparing with GRNN model consistently favoured GA-ANFIS and PSO-ANFIS models in terms of accuracy and reliability. The comprehensive evaluation and visualization presented valuable insights into the effectiveness of machine learning models for predicting drought indices in different regions, providing a basis for informed decision-making in the face of changing climatic conditions.

4.2.4 Comparative analysis of Machine Learning Algorithms

In this study, a comprehensive comparative analysis of machine learning algorithms for predicting and evaluating drought indices, namely EDI, SPI-9, and SPI-12, has been conducted. The machine learning models utilized for this assessment include GA-ANFIS, PSO-ANFIS, and GRNN. The evaluation of these models is based on the R^2 metric, and the results have been visually represented through spatial maps for EDI, SPI-9, and SPI-12 in Figures 4.25, 4.26, and 4.27, respectively. The spatial maps demonstrate the potential of the GA-ANFIS, PSO-ANFIS, and GRNN models to predict the drought indices accurately under varying climatic and meteorological conditions in the study area. Remarkably, the hybrid machine learning models, GA-ANFIS and PSO-ANFIS, have exhibited superior performance compared to the non-hybrid GRNN model across all regions. The R^2 results validate the effectiveness of machine learning algorithms in predicting the drought indices, with GA-ANFIS and PSO-ANFIS models consistently yielding higher accuracy results in comparison to the GRNN model. The success of the GA-ANFIS and PSO-ANFIS models can be attributed to their ability to fine-tune parameters using metaheuristic algorithms like

GA and PSO, which significantly enhance prediction accuracy as compared to conventional approaches. The findings of this comparative analysis affirm the reliability and robustness of the machine learning models, particularly the GA-ANFIS and PSO-ANFIS models, in predicting drought indices in diverse climatic and geographic conditions. These outcomes hold significant implications for drought monitoring, early warning systems, and water resource management, as the accurate prediction of drought indices can aid in mitigating the impacts of drought events and optimizing resource allocation.

Overall, the spatial analysis and R^2 evaluation demonstrate the potential of machine learning algorithms, particularly the hybrid GA-ANFIS and PSO-ANFIS models, as valuable tools for drought prediction in the study area and beyond. The utilization of these advanced predictive models can lead to improved decision-making processes and better preparedness in the face of changing climatic conditions and potential drought events.

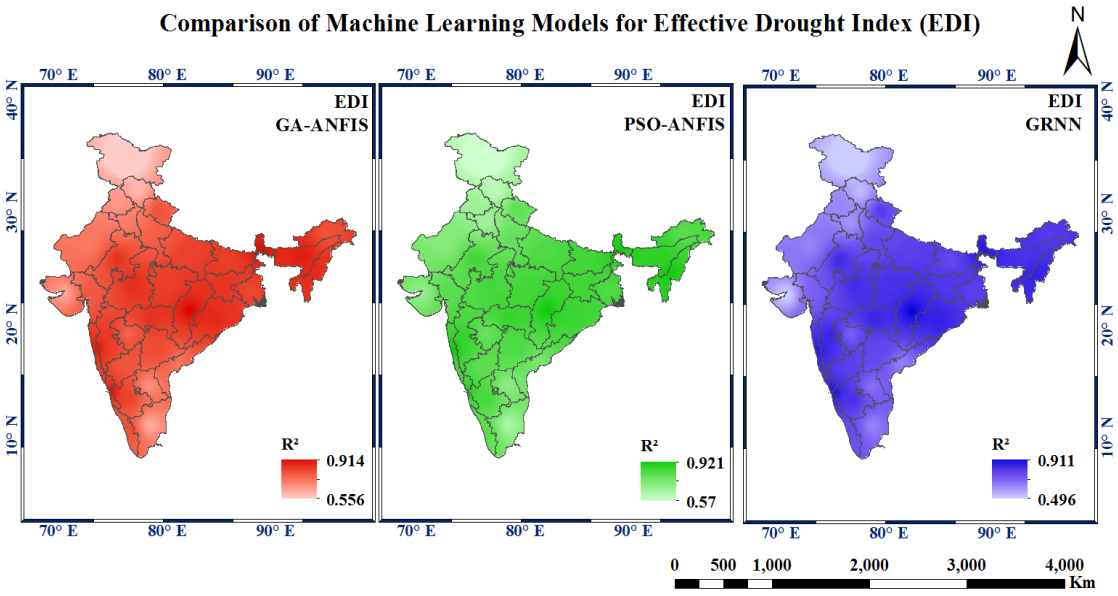

Figure 4.25 Spatial map representation for EDI using GA-ANFIS, PSO-ANFIS and GRNN (R^2)

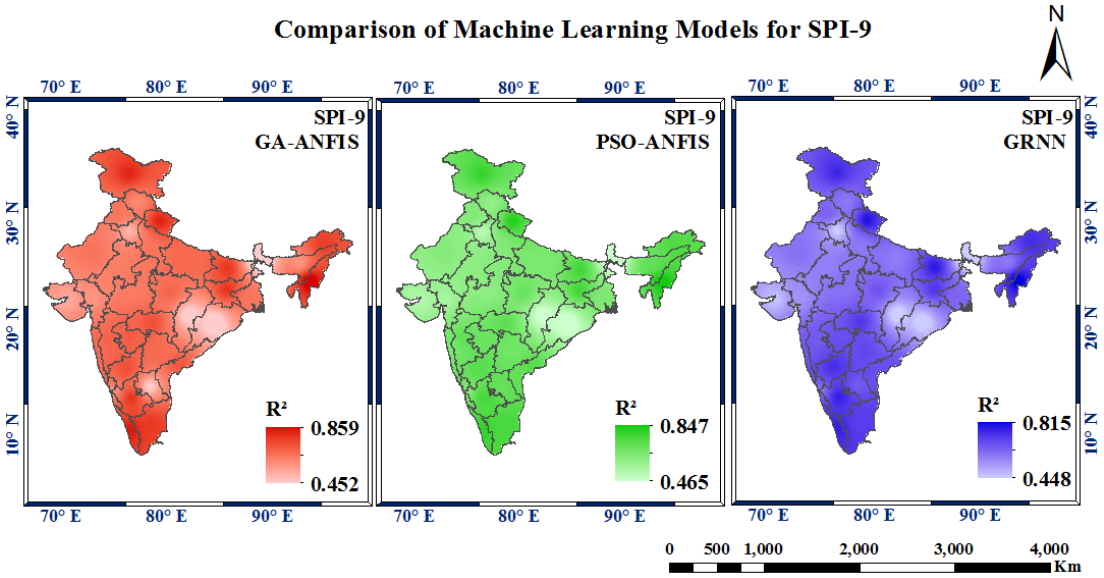

Figure 4.26 Spatial map representation for SPI-9 using GA-ANFIS, PSO-ANFIS and GRNN (R^2)

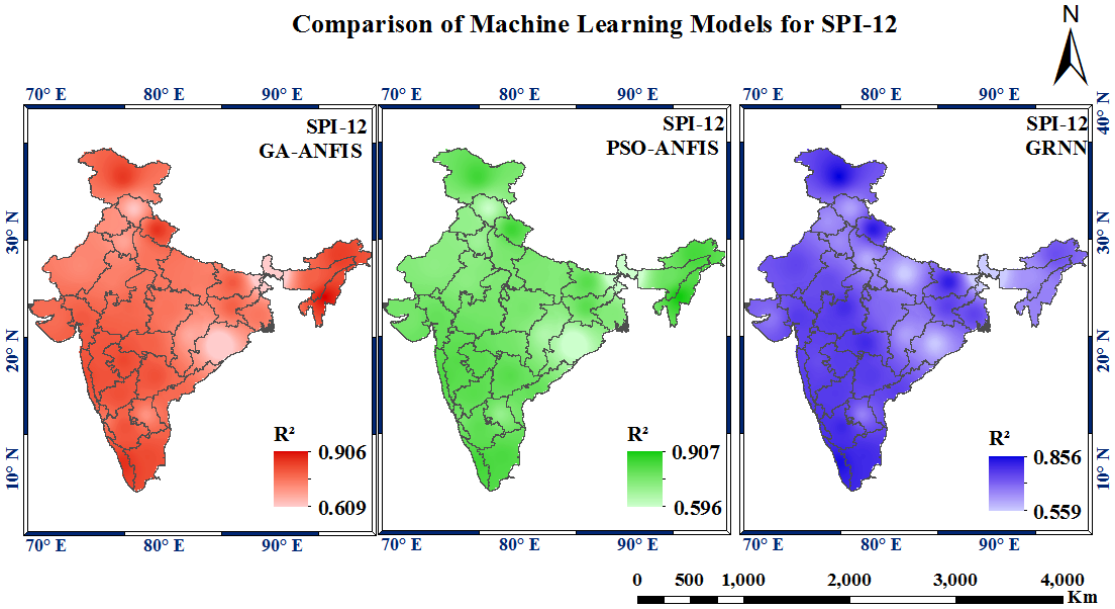

Figure 4.27 Spatial map representation for SPI-12 using GA-ANFIS, PSO-ANFIS and GRNN (R^2)

4.3 COMPARISON OF DROUGHT INDICES

The two drought indices, EDI and SPI with 9-month and 12-month timescales exhibits the capacity to detect from extreme drought (SPI< −2.0, EDI< −2.0) to extreme wet conditions (SPI > +2.0, EDI > +2). From the timeseries plot of the observed and predicted drought indices, it helps in understanding the level of severity of a dry and wet event. Through timeseries plots depicting the observed and predicted drought indices, the study offers valuable insights into the severity of both dry and wet events. Each drought index exhibits a distinct range of values that defines the severity of a drought event. By computing the EDI, SPI-9, and SPI-12, the study accurately identifies and distinguishes drought events across thirty-four meteorological subdivisions. As part of the analysis, droughts are categorized into different classes, such as moderate, severe, and extreme, based on the observed values of the respective indices. The ability to assess drought severity using EDI and SPI-9, SPI-12 provides critical information for understanding the impacts of climatic variability on water resources, agriculture, and ecosystems. Moreover, the comparative analysis of these indices enables researchers and policymakers to quantify the magnitude of drought events and devise appropriate mitigation strategies accordingly.

4.3.1 Temporal patterns of drought conditions in the Central Northeast

The study investigates into the temporal patterns of drought events in the Central Northeast region through the analysis of essential drought indices: EDI, SPI-9 and SPI-12. To visualize these patterns, Figure 4.28, Figure 4.29, and Figure 4.30 present the timeseries plots for EDI, SPI-9, and SPI-12, respectively. Figure 4.28 illustrates the timeseries plot for the EDI in the Central Northeast region. An interesting observation emerges as all the meteorological subdivisions in this region experience nearly similar drought events throughout the study period. The EDI time series plot exhibits a uniform pattern for both dry and wet events, indicating consistent fluctuations in evaporative demand. Notably, the region did not encounter any extreme droughts during this period based on the EDI calculations. However, the plot reveals the occurrence of five severe drought conditions, particularly in subdivisions like Bihar, Orissa, and Uttarakhand.

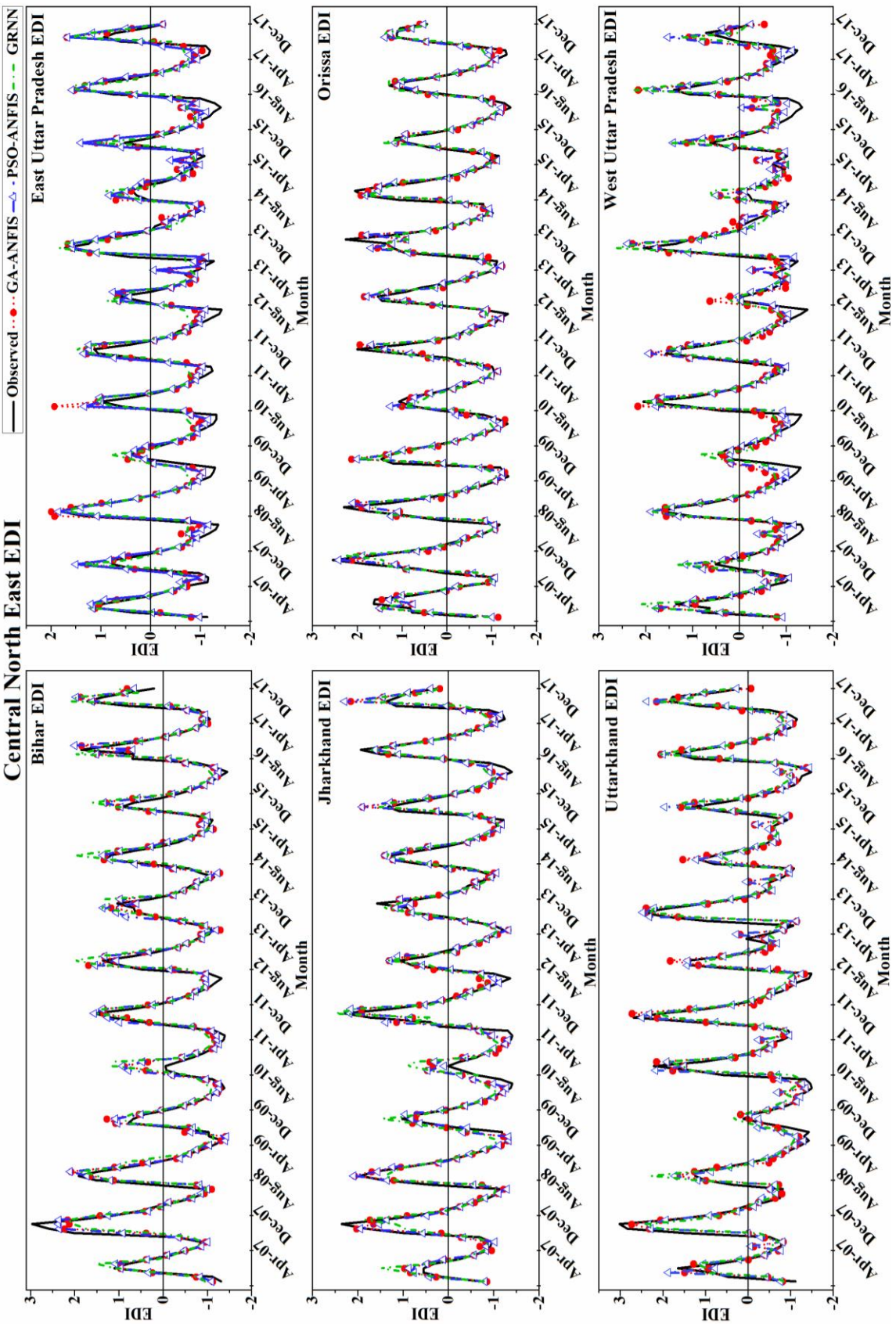

Figure 4.28 Timeseries plot of Central Northeast for EDI using GA-ANFIS, PSO-ANFIS and GRNN models

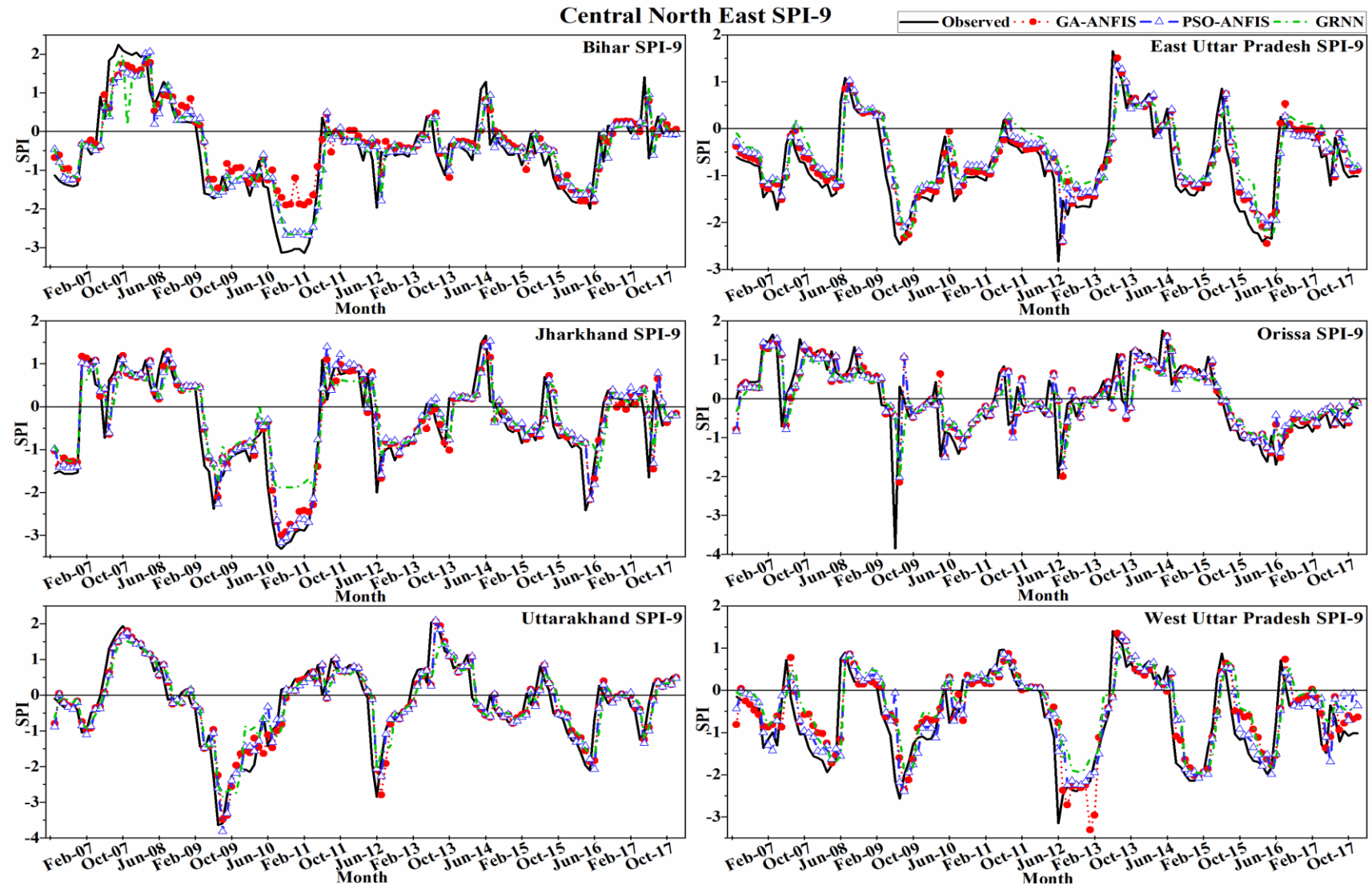

Figure 4.29 Timeseries plot of Central Northeast for SPI-9 using GA-ANFIS, PSO-ANFIS and GRNN models

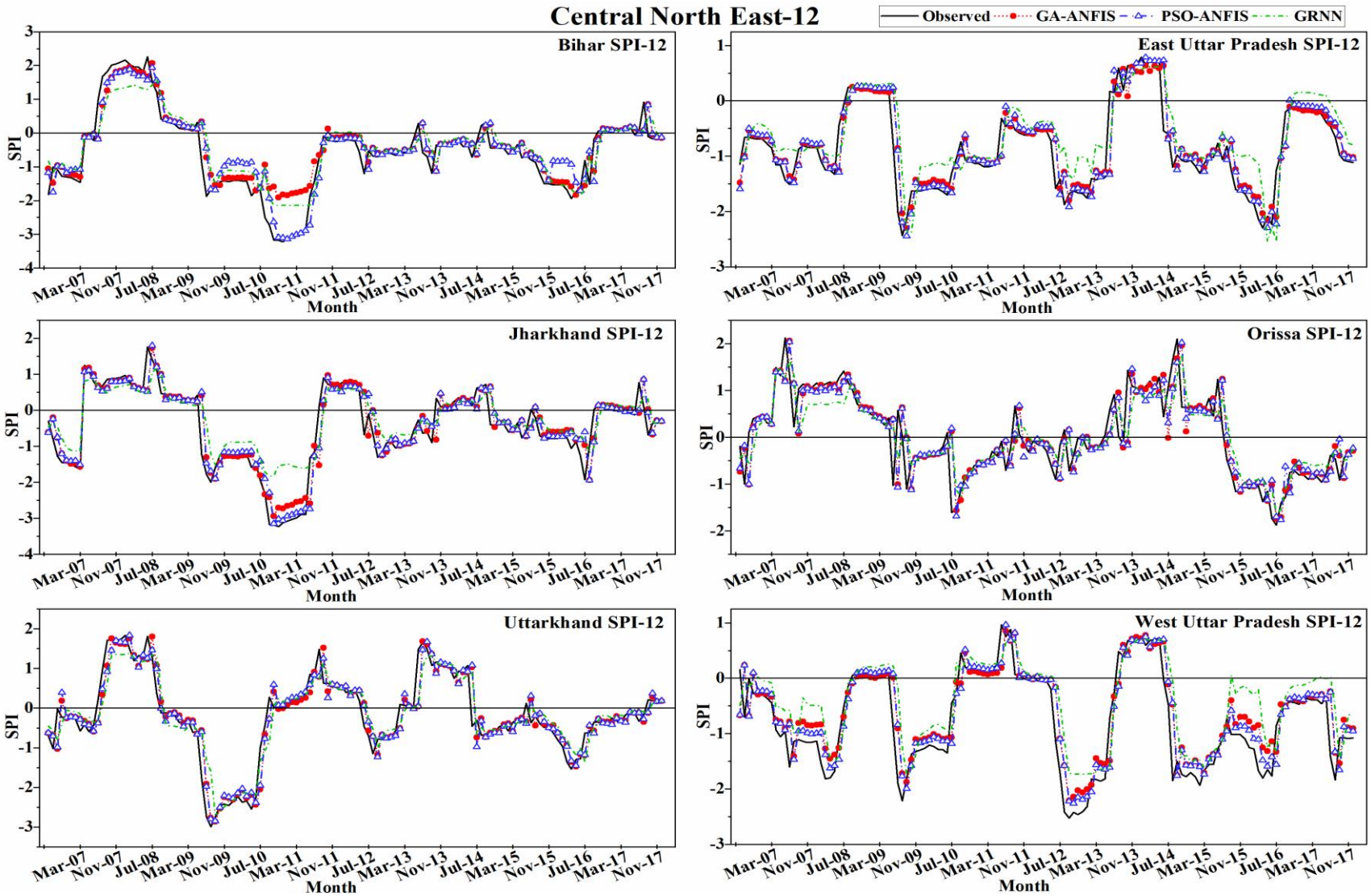

Figure 4.30 Timeseries plot of Central Northeast for SPI-12 using GA-ANFIS, PSO-ANFIS and GRNN models

Figure 4.29 presents the SPI-9 time series plot for the Central Northeast region. Unlike the EDI, the SPI-9 plot indicates that the region experienced extreme drought conditions in all six meteorological subdivisions during the study period. This index captures the severity and duration of dry and wet spells in the region, offering valuable insights into the extent of water stress. Figure 4.30 represents the SPI-12 timeseries plot, providing a comprehensive understanding of drought patterns with a longer timescale. The predictions made by GA-ANFIS, PSO-ANFIS and GRNN are also presented alongside the observed values. These models demonstrate their ability to capture the trends of EDI, SPI-9 and SPI-12 in most of the meteorological subdivisions, highlighting their effectiveness in predicting drought events.

Overall, the time series plots provide valuable insights on the temporal variability of drought events in the Central Northeast region, helping researchers and policymakers identify patterns and trends crucial for drought management strategies. The absence of extreme drought events based on the EDI highlights the region's resilience to severe water stress. In contrast, SPI-9 and SPI-12 provide valuable information about the duration and severity of droughts, aiding in assessing the impact on water resources and agriculture.

4.3.2 Temporal patterns of drought conditions in the North-East

In the North-East region, for EDI, it has been observed that no extreme drought has been experienced during the study period. This region also experienced severe and moderate dry conditions. For the SPI-9 and SPI-12, both the timescale exhibits an extreme, severe and moderate dry conditions occurring in the study area. The occurrence of dry conditions is not uniform but varies from year to year. Figure 4.31, Figure 4.32 and Figure 4.33 shows for EDI, SPI-9 and SPI-12 respectively showing the dry and wet conditions occurred during the study period. Figure 4.31 displays the EDI timeseries plot for the North-East region, indicating that no extreme drought events were experienced during the study period. However, the region witnessed occurrences of severe and moderate dry conditions. The plot illustrates the variability of evaporative demand, with fluctuations in dry and wet events throughout the study period.

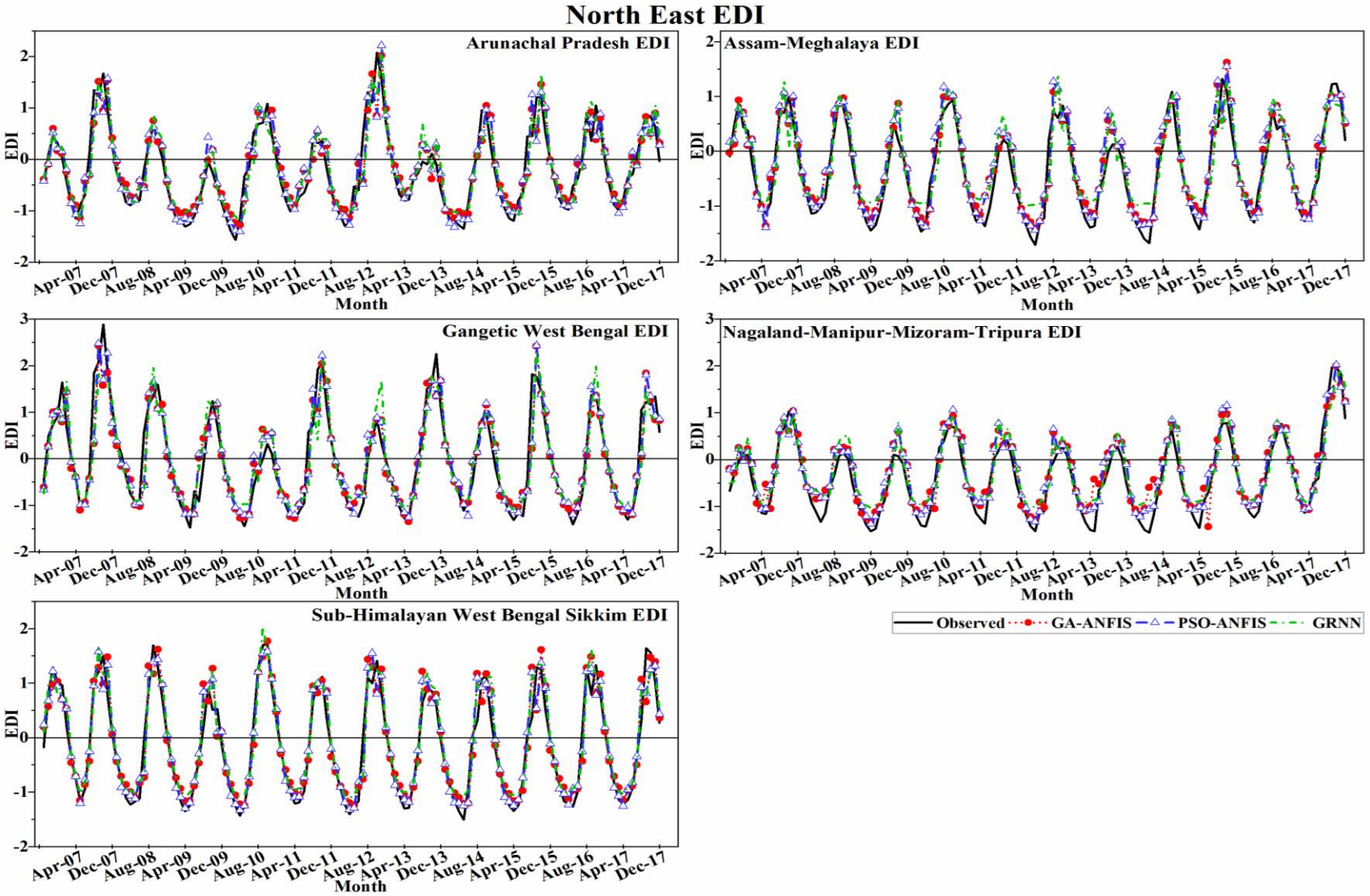

Figure 4.31 Timeseries plot of Northeast for EDI using GA-ANFIS, PSO-ANFIS and GRNN models

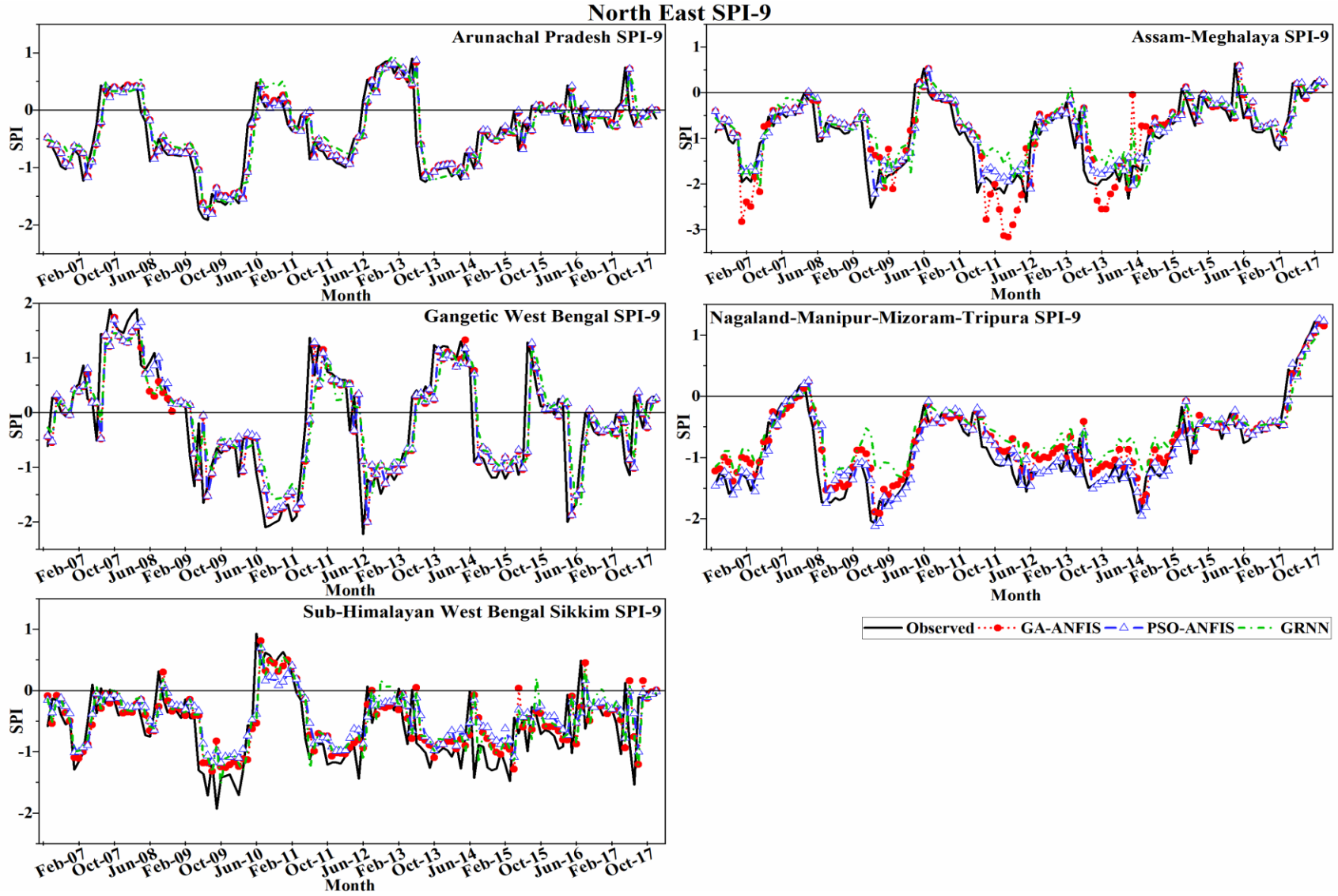

Figure 4.32 Timeseries plot of Northeast for SPI-9 using GA-ANFIS, PSO-ANFIS and GRNN models

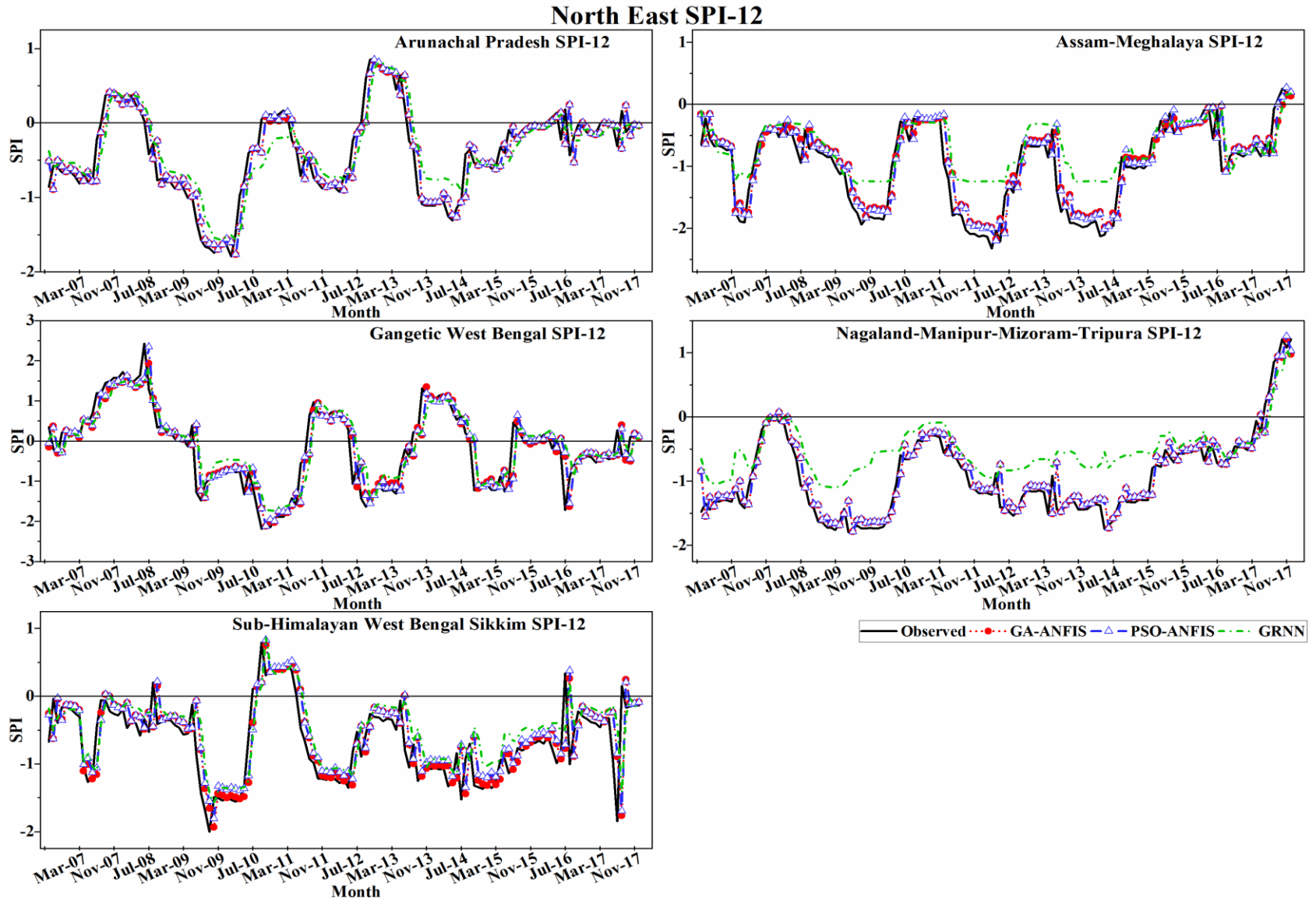

Figure 4.33 Timeseries plot of Northeast for SPI-12 using GA-ANFIS, PSO-ANFIS and GRNN models

For SPI-9 and SPI-12 (Figure 4.32 and Figure 4.33, respectively), the timeseries plots depict a broader range of drought conditions in the North-East region. Both timescales reveal the presence of extreme, severe, and moderate dry conditions during the study period. Notably, the occurrence of dry conditions is not uniform but varies from year to year, highlighting the region's susceptibility to interannual variability in precipitation. The time series plots offer valuable visual representations of drought dynamics, enabling researchers and stakeholders to better understand the temporal patterns of drought events in the North-East region.

4.3.3 Temporal patterns of drought conditions in the Northwest

The Northwest region, characterized by arid and semi-arid climates, is subjected to distinct hydroclimatic conditions that impact drought occurrences. The time series plots presented in Figure 4.34, Figure 4.35, and Figure 4.36 offer valuable insights into the nature and severity of dry conditions experienced in the region over the study period. The EDI time series plot (Figure 4.34) indicates that the Northwest region predominantly experiences dry conditions of a moderate nature. This is consistent with the arid and semi-arid nature of the region, where evaporative demand typically exceeds precipitation, resulting in prolonged dry spells.

In comparison, the SPI-9 and SPI-12 time series plots (Figure 4.35 and Figure 4.36, respectively) demonstrate a broader range of drought conditions experienced in the Northwest region. Both indices reveal the presence of extreme, severe, and moderate dry conditions. The SPI-9 and SPI-12 plots offer a comprehensive assessment of the duration and intensity of drought events, highlighting the region's vulnerability to prolonged dry spells over varying timescales. The contrasting results between EDI and SPI-9/SPI-12 underscore the importance of considering multiple drought indices in drought analysis. While EDI provides insights into evaporative demand and dryness patterns, SPI-9 and SPI-12 capture the combined influence of precipitation and evaporative demand, offering a more holistic view of drought severity.

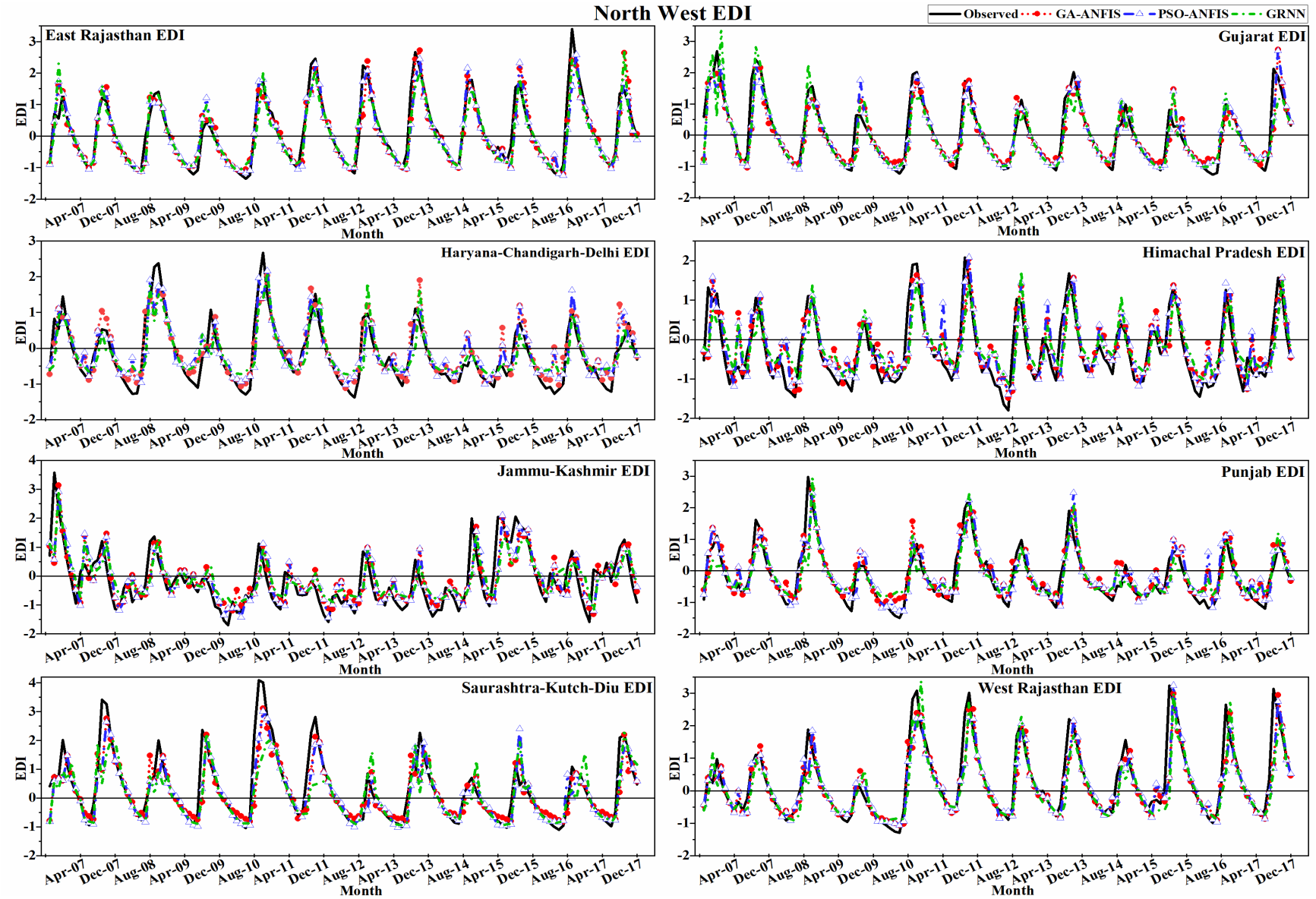

Figure 4.34 Timeseries plot of Northwest for EDI using GA-ANFIS, PSO-ANFIS and GRNN models

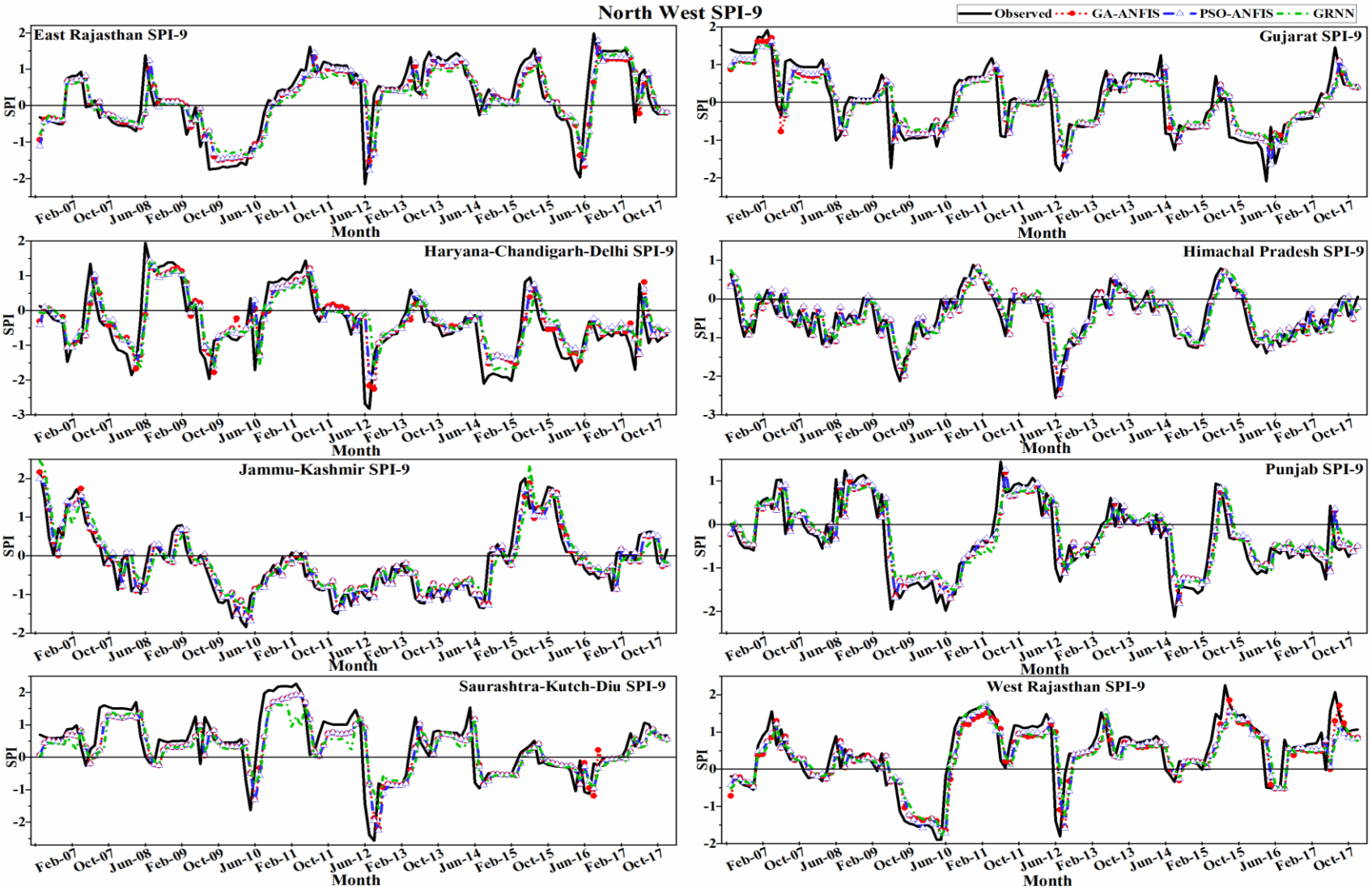

Figure 4.35 Timeseries plot of Northwest for SPI-9 using GA-ANFIS, PSO-ANFIS and GRNN models

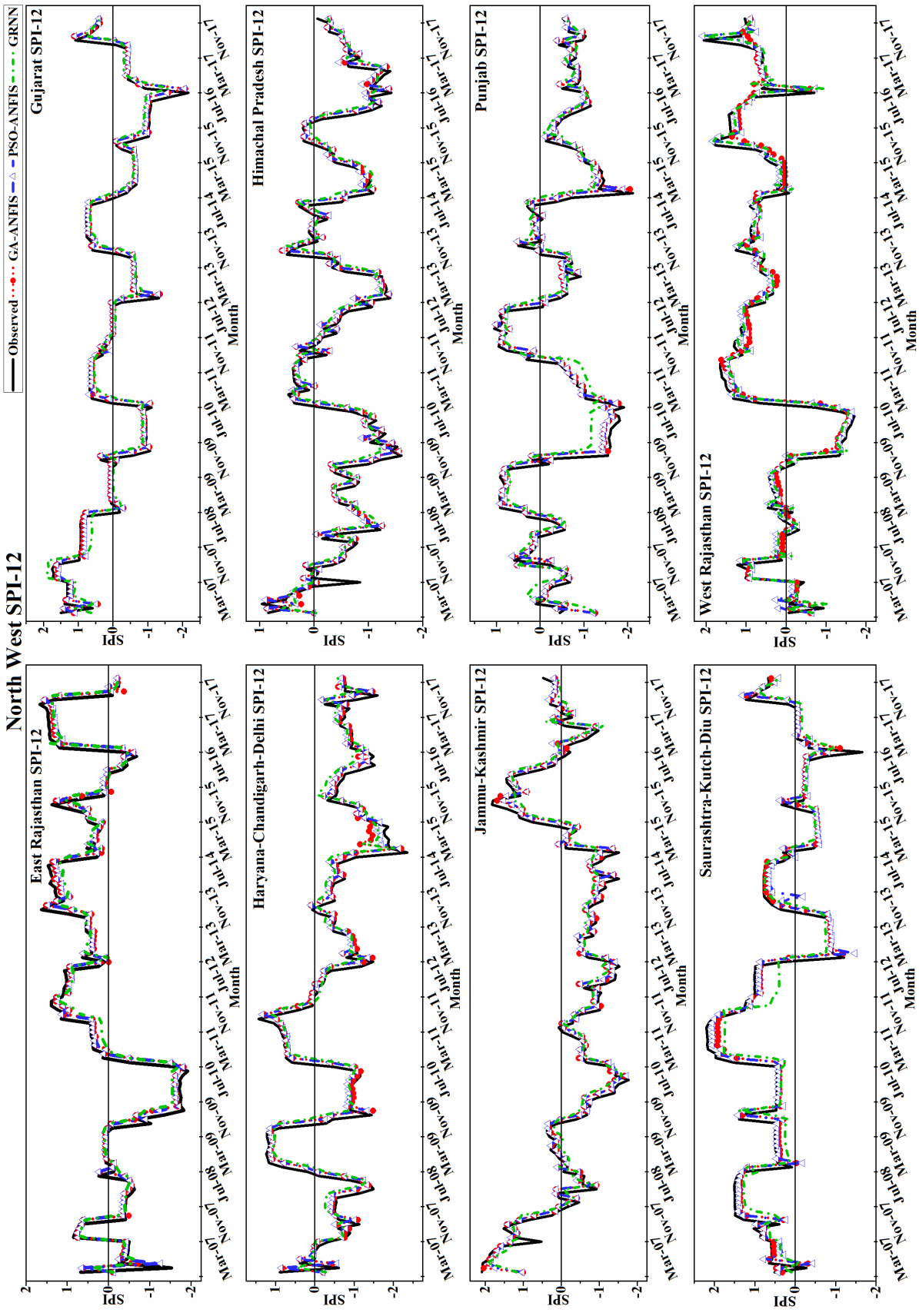

Figure 4.36 Timeseries plot of Northwest for SPI-12 using GA-ANFIS, PSO-ANFIS and GRNN models

4.3.4 Temporal patterns of drought conditions in the Peninsular

The Peninsular region comprises of six meteorological subdivisions. The time series plots in Figure 4.37, Figure 4.38, and Figure 4.39 provide graphical representations of the dry and wet conditions observed during the study period. The EDI time series plot (Figure 4.37) highlights the extreme dryness observed in the Tamil-Nadu-Pondicherry subdivision, emphasizing the region's susceptibility to prolonged periods of water scarcity and drought. The SPI-9 and SPI-12 time series plots (Figure 4.38 and Figure 4.39, respectively) further illustrate the prevalence of extreme, severe, and moderate dry conditions across the Peninsular region. The SPI-9 and SPI-12 indices integrate precipitation and evaporative demand, enabling a comprehensive assessment of drought severity over varying timescales. The analysis of these indices provides valuable insights into the duration and intensity of drought events, contributing to a better understanding of the region's water resource management challenges.

4.3.5 Temporal patterns of drought conditions in the West Central

The West Central region comprises nine meteorological subdivisions, each exhibiting distinct hydroclimatic characteristics. The time series plots in Figure 4.40, Figure 4.41, and Figure 4.42 provide graphical representations of the dry and wet conditions that occurred during the study period. The EDI time series plot (Figure 4.40) indicates that extreme dryness is not prevalent in any of the subdivisions within the West Central region. Instead, the region primarily experiences severe and moderate drought conditions, suggesting a dependence on local moisture availability. However, when considering the SPI-9 and SPI-12 time series plots (Figure 4.41 and Figure 4.42, respectively), it becomes evident that the entire West Central region experiences extreme dry conditions. The SPI indices integrate both precipitation and evaporative demand, offering a comprehensive view of drought severity over varying timescales. These plots highlight the occurrence of prolonged and intense drought events in the region, which can have significant implications for water resources, agriculture, and ecological systems.

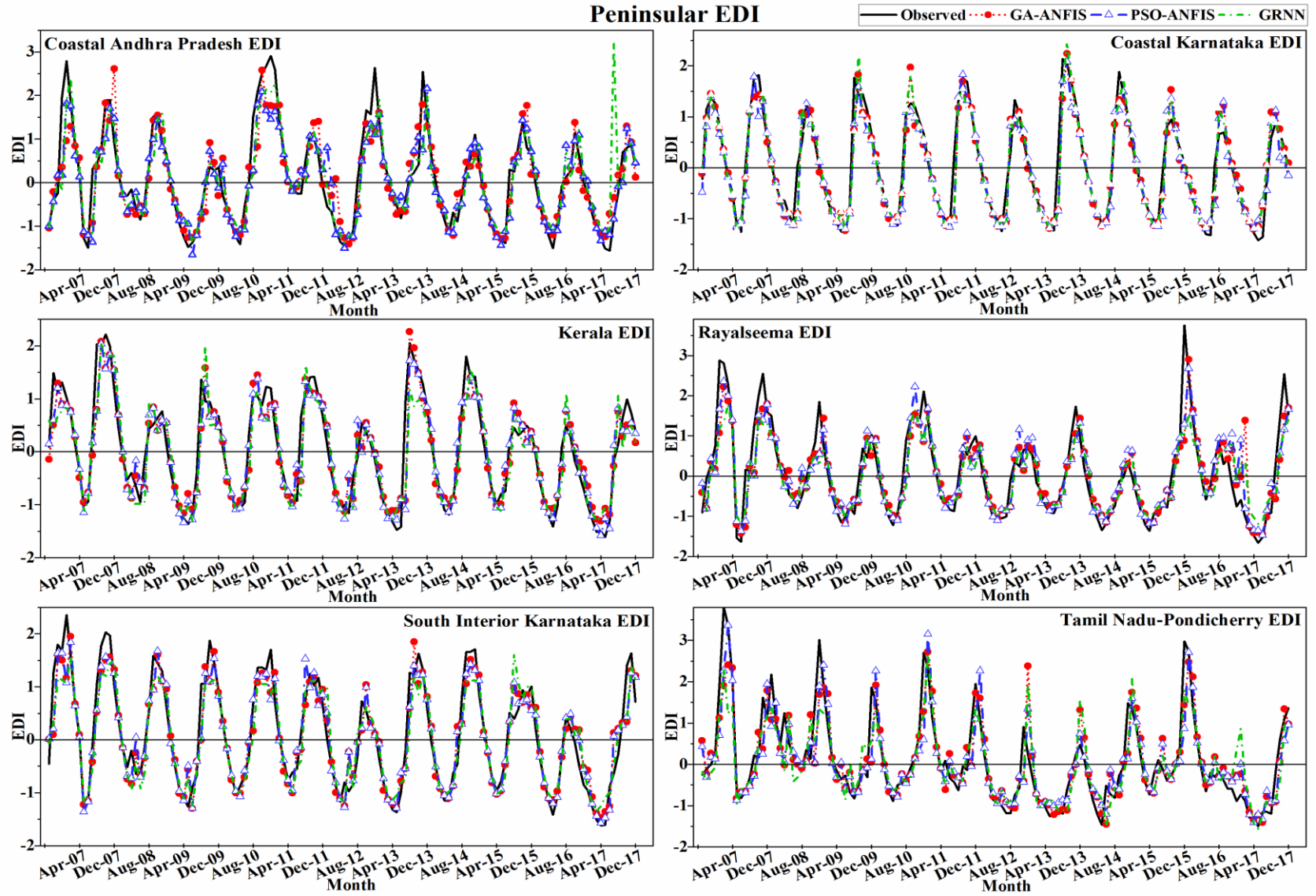

Figure 4.37 Timeseries plot of Peninsular for EDI using GA-ANFIS, PSO-ANFIS and GRNN models

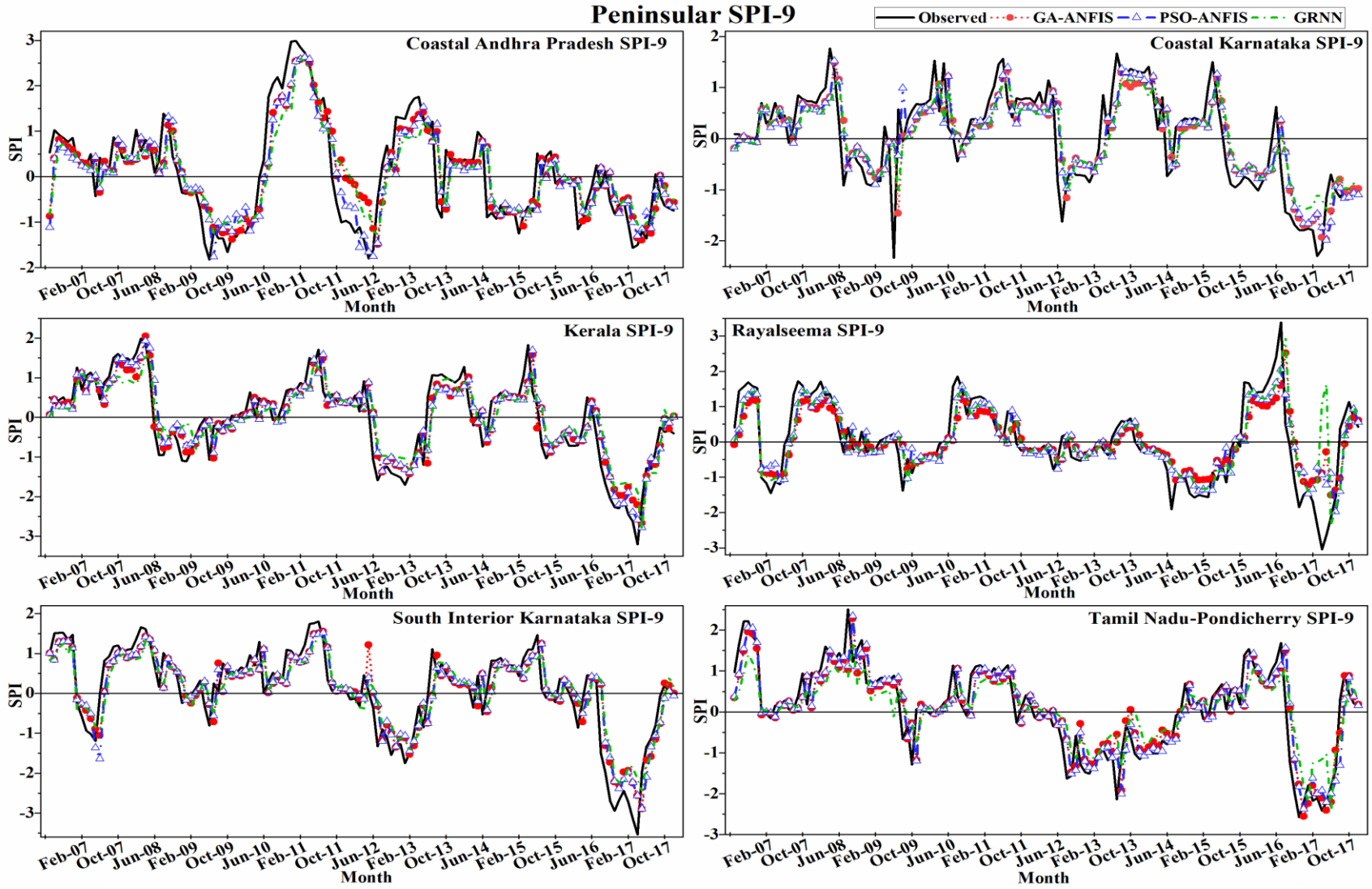

Figure 4.38 Timeseries plot of Northwest for SPI-9 using GA-ANFIS, PSO-ANFIS and GRNN models

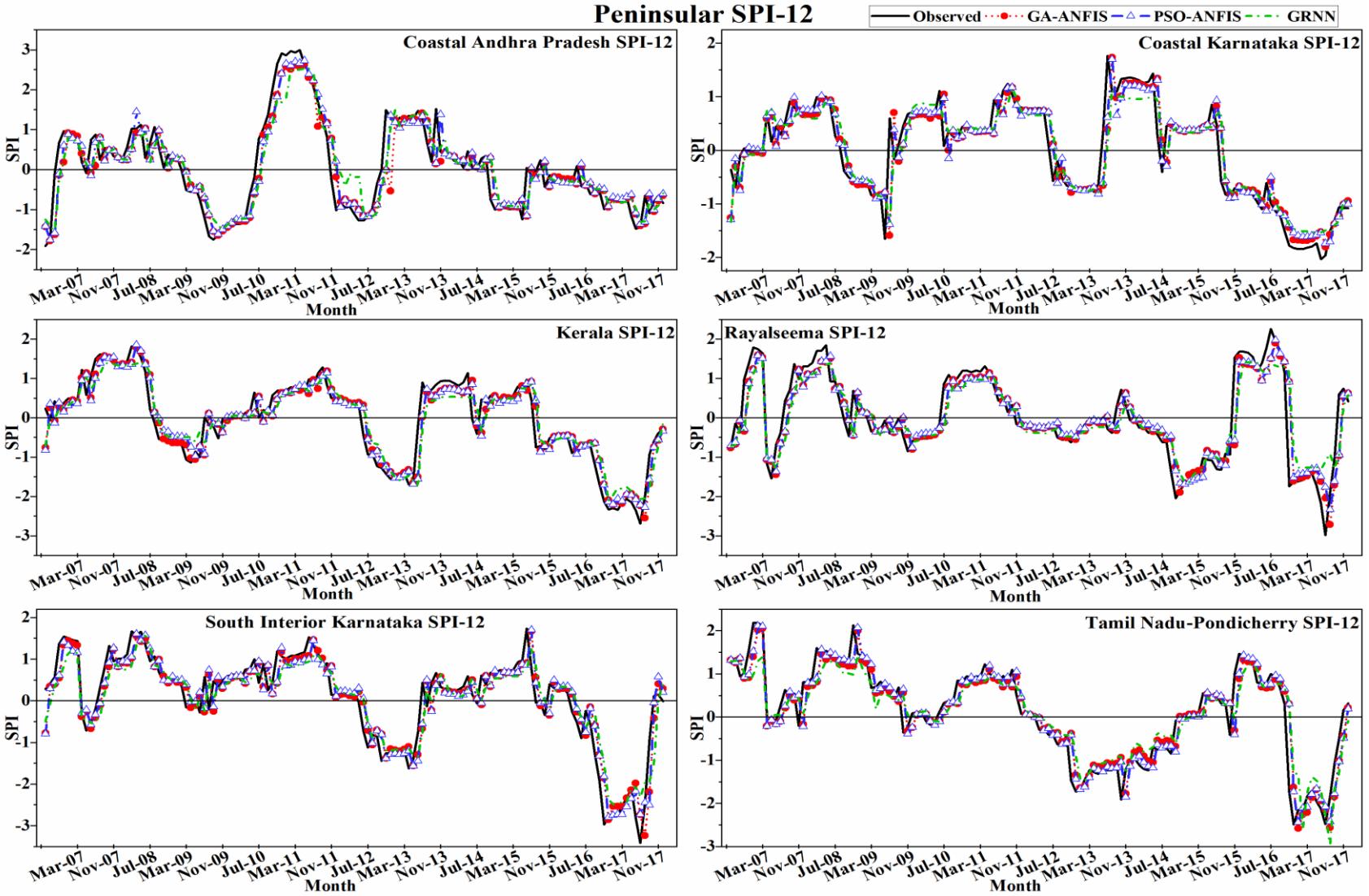

Figure 4.39 Timeseries plot of Northwest for SPI-12 using GA-ANFIS, PSO-ANFIS and GRNN models

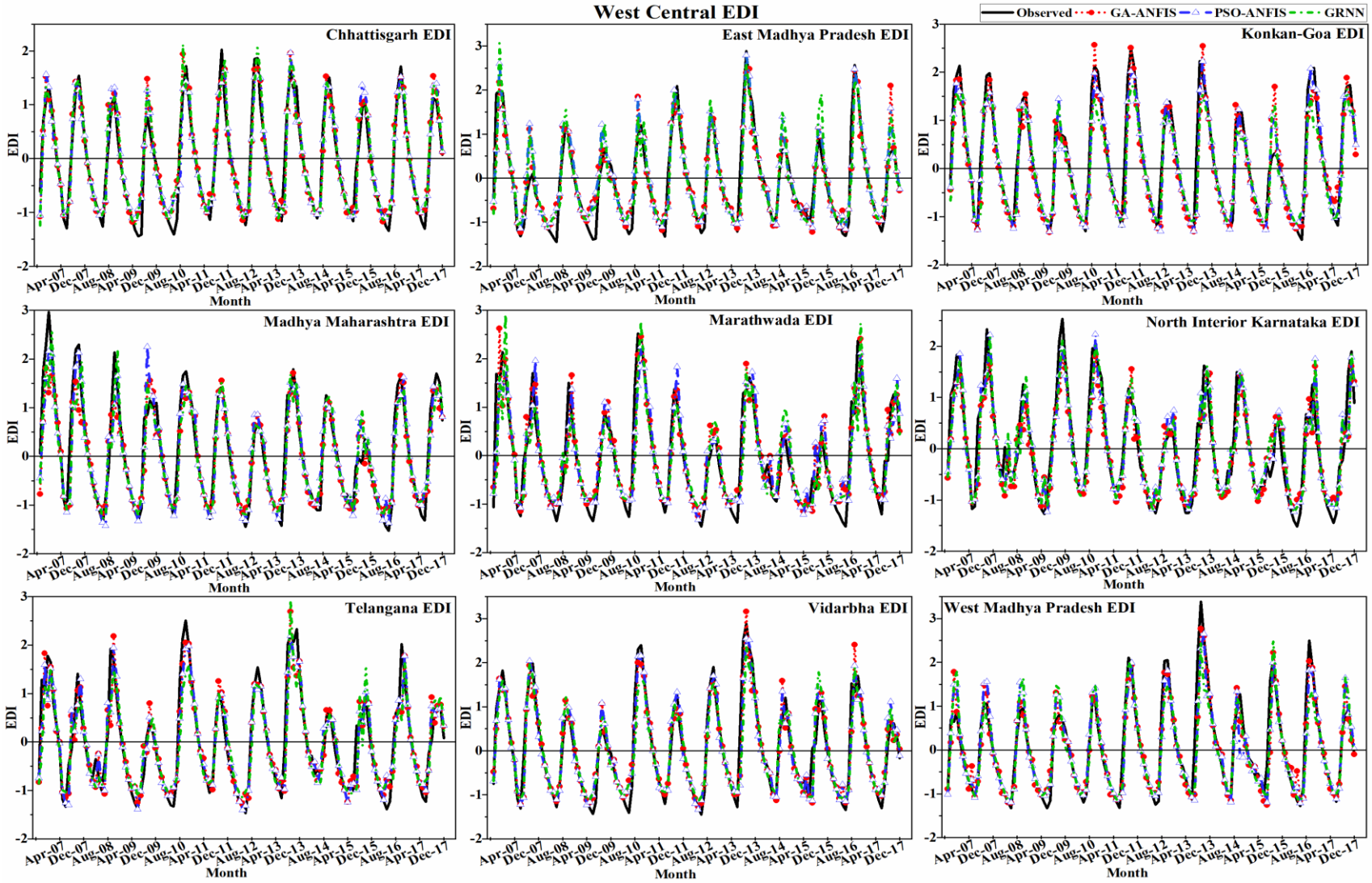

Figure 4.40 Timeseries plot of West Central for EDI using GA-ANFIS, PSO-ANFIS and GRNN models

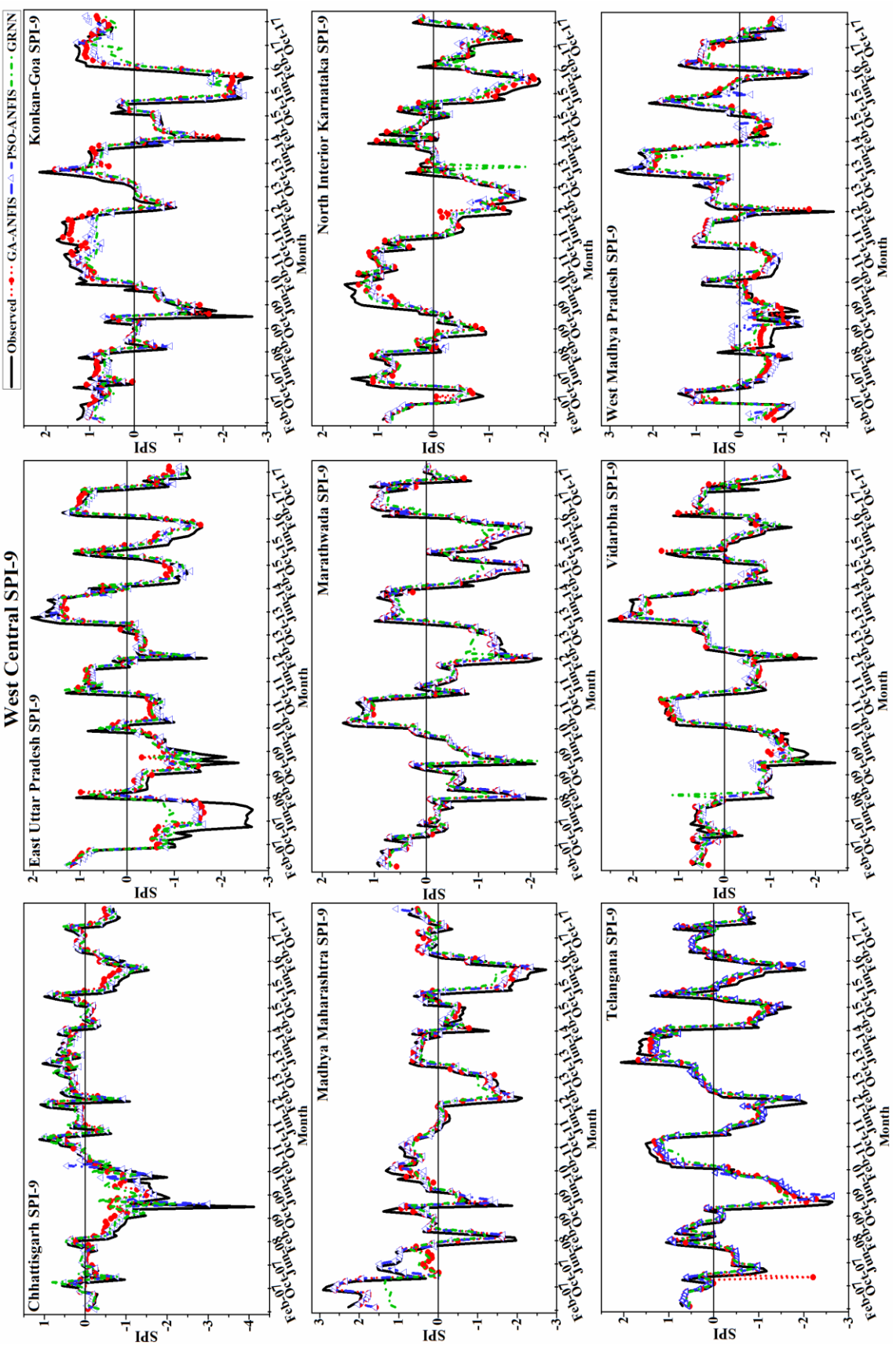

Figure 4.41 Timeseries plot of West Central for SPI-9 using GA-ANFIS, PSO-ANFIS and GRNN models

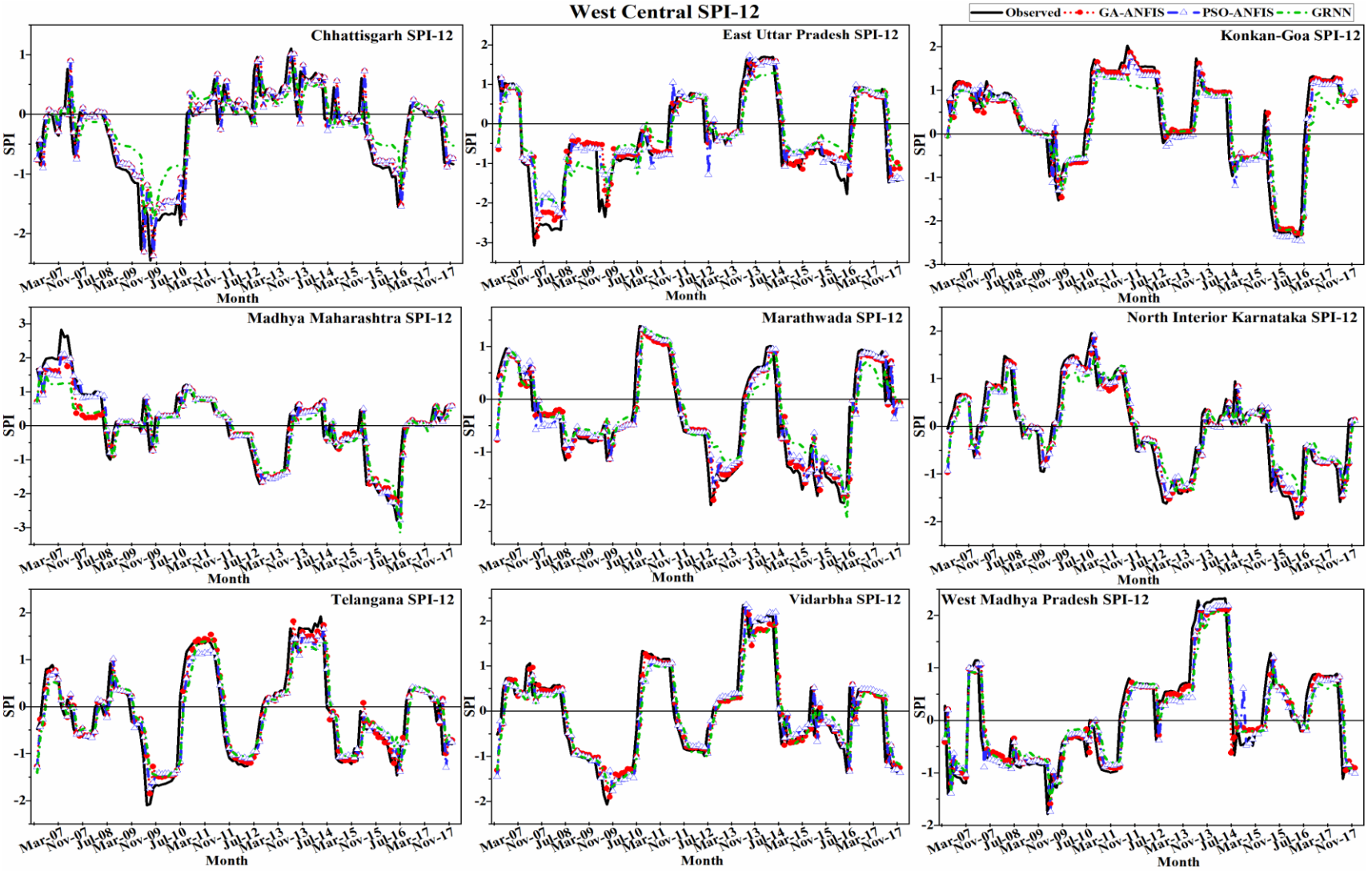

Figure 4.42 Timeseries plot of West Central for SPI-12 using GA-ANFIS, PSO-ANFIS and GRNN models

The temporal patterns of drought events in different regions of India has been investigated. The study uses different drought indices including EDI, SPI-9 and SPI-12 to analyse and visualise the patterns of dry and wet conditions over specific timescales. The overview covers thirty-four meteorological subdivisions. From timeseries plot it emphasizes the importance of considering multiple drought indices for a comprehensive drought analysis, as each index provides unique insights into different aspects of drought severity.

4.3.6 Regional drought across Jodhpur using station data: A case study

A case study has been taken up in the Jodhpur region which is situated in the western part of Rajasthan. Jodhpur exhibits a hot and arid climate and remains extremely hot and dry throughout the year.

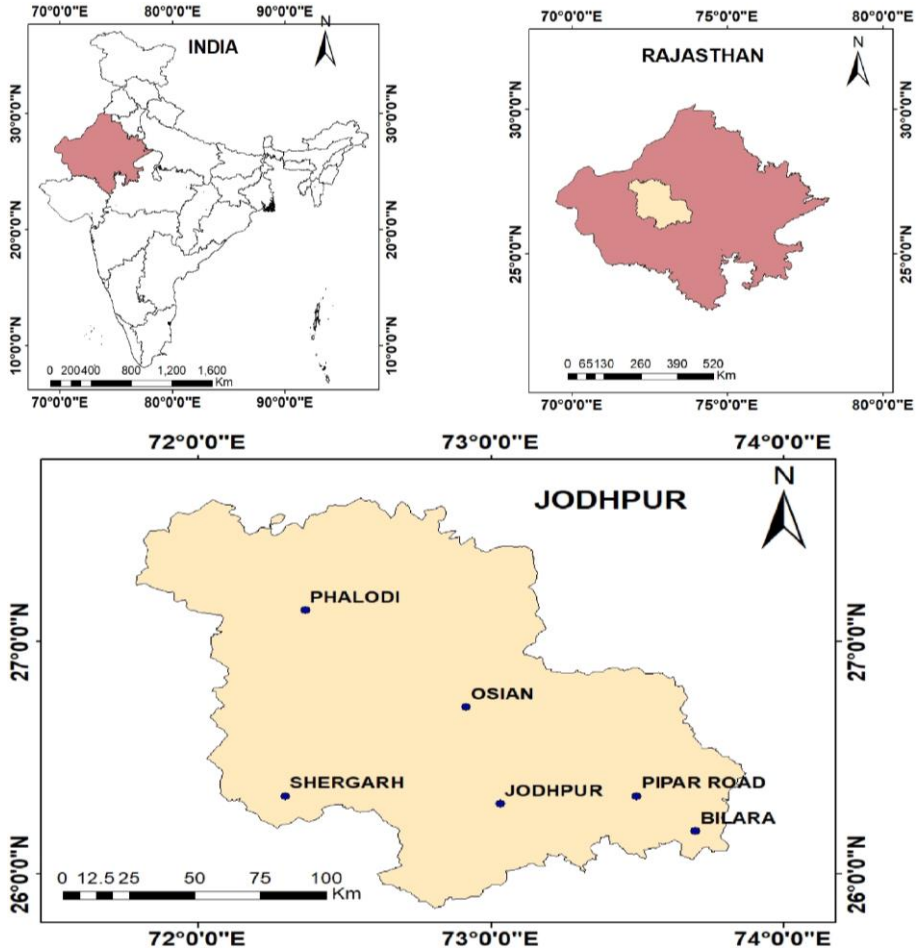

Figure 4.43 Rainfall station location of Jodhpur

A brief rainfall has been observed from late June to September and during the monsoon season, the temperature would slightly decrease. The average rainfall received during the study period is 350 mm. In this study, six rainfall stations located at different places in Jodhpur were considered for the analysis. The choice of Jodhpur as the case study site is justified by its unique climate conditions and water resource management challenges. Being a region with limited and erratic rainfall, it faces heightened vulnerability to drought and water scarcity. The case study conducted in the Jodhpur region contributes to the broader understanding of hydroclimatic patterns in arid regions and aid in formulating region-specific adaptation and mitigation strategies for climate change-induces challenges. Figure 4.43 represents the rainfall station location of Jodhpur for the study. Table 4.11 shows the statistical properties of the rainfall for the study area.

Table 4.11 Statistical properties of rainfall for the study

Station	Location	Max (mm)	Min (mm)	Mean (mm)	Standard deviation	Coefficient of variance
Jodhpur	26°18'N 73°19'47.99"E	376.86	0.00	30.36	59.02	1.94
Osian	26°43'1.19"N 72°55'1.2"E	296.12	0.00	27.88	51.70	1.85
Phalodi	27°75'8.79"N 72°22'1.2"E	282.43	0.00	19.70	39.02	1.98
Bilara	26°10'58.79"N 73°42'E	495.04	0.00	34.52	67.63	1.96
Shergarh	26°19'58.79"N 72°17'59.99"E	313.72	0.00	21.55	44.45	2.06
Pipar Road	26°19'58.79"N73° 30'E	705.32	0.00	34.48	70.14	2.03

EDI has been used in a limited studies and Rajasthan, one of the driest states in India has not been explored using soft computing techniques in areas with drought or climate extremes. Hence, the present study is aimed to predict regional drought across six stations within the Jodhpur district of Rajasthan state, India. The models based on ANFIS optimised by nature-based optimisers were applied for time-series prediction of monthly EDI. The Genetic algorithm (GA) and Particle swarm optimiser (PSO) were used to optimise the premise and resulting parameters of ANFIS. Both algorithms have

demonstrated their ability to search for optimal global solutions. A Generalised Regression Neural Network (GRNN) modelling was also adopted for comparative performance evaluation with ANFIS-based models.

The findings of this study suggest that GA-ANFIS, PSO-ANFIS and GRNN can be used as a means of forecasting the EDI (Azimi et al. 2022) in the arid region. Comparing the results overall, it reveals that the GA-ANFIS and PSO-ANFIS models perform better than the GRNN model in most of the rainfall stations in the study area. The findings from all the models show that, in all the stations, the correlation between observed and predicted values as in terms of R^2 increases considerably as the number of forecast input combinations increases. The Osian Road rainfall station depicts better results for 2- input model combinations for GA-ANFIS and PSO-ANFIS model, revealing a high degree of correlation for models. The Shergarh rainfall station using the GA-ANFIS model yields better results among all the six rainfall stations for 3 and 5- input model combinations, indicating a high degree of correlation for the models. In terms of R^2, NRMSE, NNSE and MAE, the prediction results have also revealed that employing the hybrid models, i.e., GA-ANFIS and PSO-ANFIS, is more effective at forecasting the EDI in all rainfall stations. The performance of R^2 values is presented in Table 4.12. An R^2 value between 0.7 and 0.9 indicates a high degree of correlation, a values between 0.5 and0.7 indicates a moderate degree of correlation and a value between 0.3 and 0.5 indicates a low degree of correlation (Belayneh and Adamowski 2013).

Table 4.12 Performance of R^2 of the models

Station	Statistics	GA-ANFIS			PSO-ANFIS			GRNN		
		2	**3**	**5**	**2**	**3**	**5**	**2**	**3**	**5**
Jodhpur	R^2	0.74	0.73	0.72	0.72	0.73	0.7	0.7	0.61	0.64
Osian		**0.75**	0.74	0.73	**0.75**	0.74	0.73	0.73	0.67	0.63
Phalodi		0.74	0.73	0.74	0.72	0.74	0.69	0.69	0.71	0.66
Bilara		0.62	0.66	0.66	0.64	0.68	0.66	0.66	0.55	0.57
Shergarh		0.74	**0.75**	**0.78**	0.73	0.74	0.76	0.76	0.7	0.63
Pipar Road		0.66	0.67	0.69	0.66	0.67	0.7	0.7	0.63	0.59

Overall, in this study, the hybrid models GA-ANFIS and PSO-ANFIS outperformed the standalone model like GRNN in forecasting drought. Hybrid models are developed by combining different machine learning models and proves to be better methods than standalone (Adnan et al., 2021). The GA and PSO are high level problem solving algorithms (Sörensen and Glover 2013) where it is combined with ANFIS to generate high quality solutions. Hence, several studies recommended using hybrid models that increase the forecast accuracy and hybrid models are becoming more popular in drought forecasting and other studies related to hydrology (Hajirahimi and Khashei, 2022).

Violin plots are also like box plots, but they are more informative than box plots. The violin plot is a single representation that combines the box plot and density trace (or smoothed histogram) in a synergistic way to reveal dataset (Hintze and Nelson 1998). The violin plots provide a better indication of the shape of the distribution by showing the existence of clusters in data. The tip of the violin plot at the top represents the maximum data value, the bottom tip represents the minimum data value and it shows the indication of how much data has been accumulated at each point.

Figures 4.44 to 4.46 show that violin plots for all six different rainfall stations were obtained for the different input combinations i.e., 2-, 3- and 5- input combinations In this study, the violin plot represents the observed data, GA-ANFIS, PSO-ANFIS and GRNN for 2, 3 and 5- input combinations. From the violin plot, one can visualise the distribution shape of the models and conclude which model has a better prediction accuracy w.r.t to the observed data. It depicts the performance of the models across various rainfall stations. Each violin plot includes information about the mean, median, maximum and minimum values offering a comprehensive view of the model's predictive behaviour. Patterns in the violin plots reveal how well the models capture the variability in observed data. By comparing the distribution shapes across different models, one can make qualitative assessment of the prediction accuracy. The model where the violin plots closely align the observed data indicate better prediction accuracy. The collection of violin plots serves as a comprehensive visual tool for model comparison and assessment.

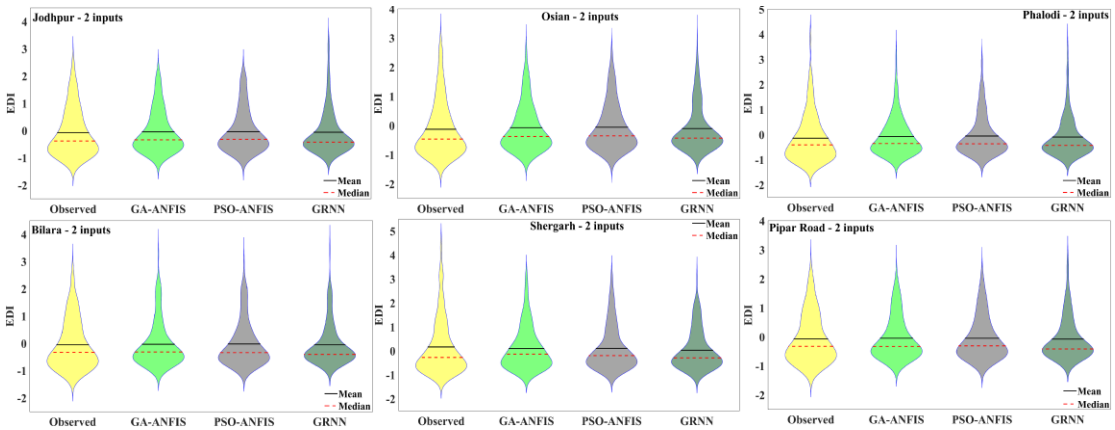

Figure 4.44 Violin plots for 2-input combinations

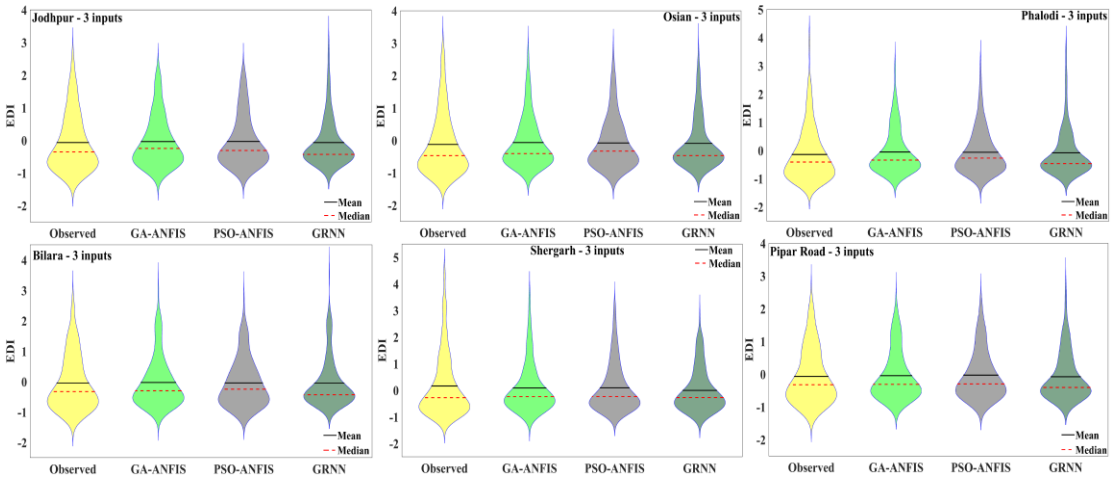

Figure 4.45 Violin plots for 3-input combinations

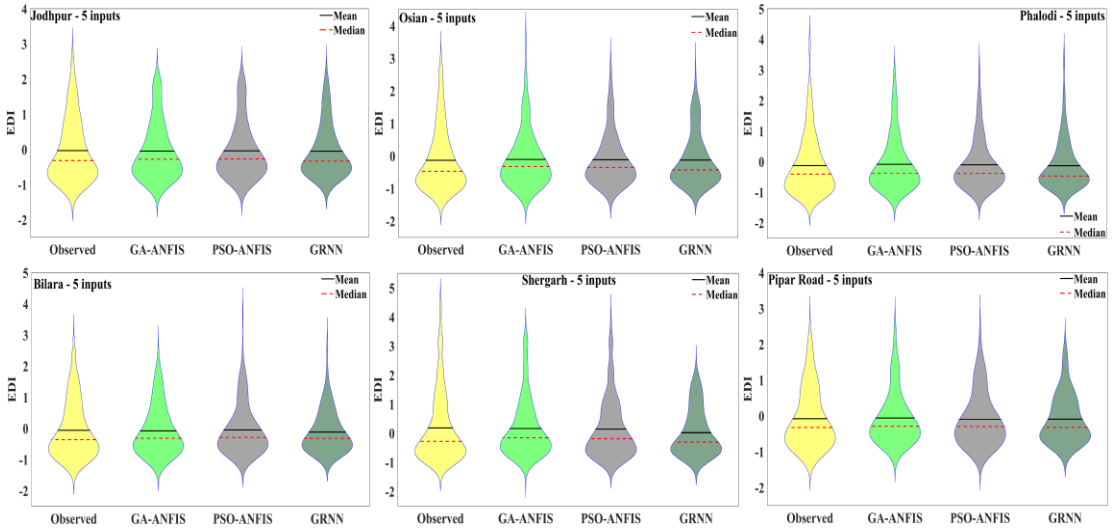

Figure 4.46 Violin plots for 5-input combinations

Jodhpur being an arid region the case for forecasting drought using the EDI is relevant. In this study, soft computing techniques like GA-ANFIS, PSO-ANFIS and GRNN have been developed to forecast the EDI drought index in Jodhpur, Rajasthan, India, for six rainfall stations. The outcomes of the monthly EDI evaluation were compared with different machine learning algorithms. The study compares the various models and finds that the GA-ANFIS and PSO-ANFIS models which are hybrid machine learning algorithms perform better than the GRNN model. Hybrid machine learning algorithms, such as GA-ANFIS and PSO-ANFIS has shown remarkable capabilities in producing accurate drought predictions. The application of these algorithms to the rainfall station data in the Jodhpur region of western Rajasthan has yielded highly reliable results in predicting meteorological drought indices. Likewise, the rainfall stations data for the Jodhpur region with the meteorological subdivision rainfall data of western Rajasthan depicts a similar result. The obtained results using the station data of Jodhpur and the western Rajasthan meteorological subdivision rainfall data holds good for both. Also, it is observed that, there is not much deviation in the rainfall dataset for both station data and meteorological subdivision data. Hence, it is reliable to use the meteorological subdivision rainfall data in predicting the meteorological drought indices in other regions with similar climatic conditions.

4.3.7 Effectiveness of Drought Indices in detecting historical droughts

The study investigates into the computation and analysis of crucial drought indices, namely EDI, SPI-9 and SPI-2. The data utilized for this investigation spans an extensive 60-year period, from 1958 to 2017, encompassing diverse climatic conditions and capturing the intricacies of drought patterns over the years. India has experienced several major drought events during the study period, with 14 notable droughts occurring in the years 1965, 1966, 1968, 1972, 1974, 1979, 1982, 1986, 1987, 2002, 2004, 2009, 2014, and 2015 (Mishra et al. 2019). To comprehensively understand and compare the results obtained from the adopted drought indices, the study focused on two significant drought years, 2002 and 2009, and their correlation with the EDI, SPI-

9, and SPI-12. The drought year for 2004, 2014 and 2015 have also been considered for the analysis and the figures are appended w.r.t Figures A.1.1 to A.1.9

To visually represent and verify the spatial distribution and severity of drought occurrences, spatial distribution maps were prepared for the EDI, SPI-9, and SPI-12 indices. These maps serve as valuable tools to comprehend the geographical extent and intensity of drought events in the study area. The incorporation of spatial distribution maps aids in identifying regions that are particularly vulnerable to droughts, facilitating informed decision-making for drought mitigation and resource allocation. To gain insights into the drought dynamics during the entire study period, maps for the remaining drought years have been included in the report's appendices. This comprehensive approach ensures a holistic evaluation of drought occurrences over the 60-year duration, enabling researchers and policymakers to identify recurrent drought-prone regions and formulate targeted strategies for drought management and adaptation. By focusing on significant drought years and adopting multiple drought indices, the study enhances our understanding of drought patterns and their implications for various regions.

4.3.7.1 Drought year 2002

The drought in India in the year 2002 has a significant event that affected several regions of the country. It was one of the severe drought India experienced in recent time and has a significant impact on agriculture, water availability and overall economy. The complexity of this drought event suggests that both natural climatic factors and human activities may have played pivotal roles in its occurrence, making it a crucial case study for understanding and managing droughts. From Figure 4.47, the analysis using EDI revealed that during May and June, the majority of the regions in India experienced moderate dry conditions, with a few exceptions such as Uttarakhand, Jammu-Kashmir, Arunachal Pradesh, and Assam-Meghalaya. However, in the following months, the conditions shifted towards near-normal, indicating a relatively stable situation with neither severe drought nor excessive wetness in most areas. This temporal pattern is

essential for understanding the dynamics of drought events and devising appropriate drought management strategies.

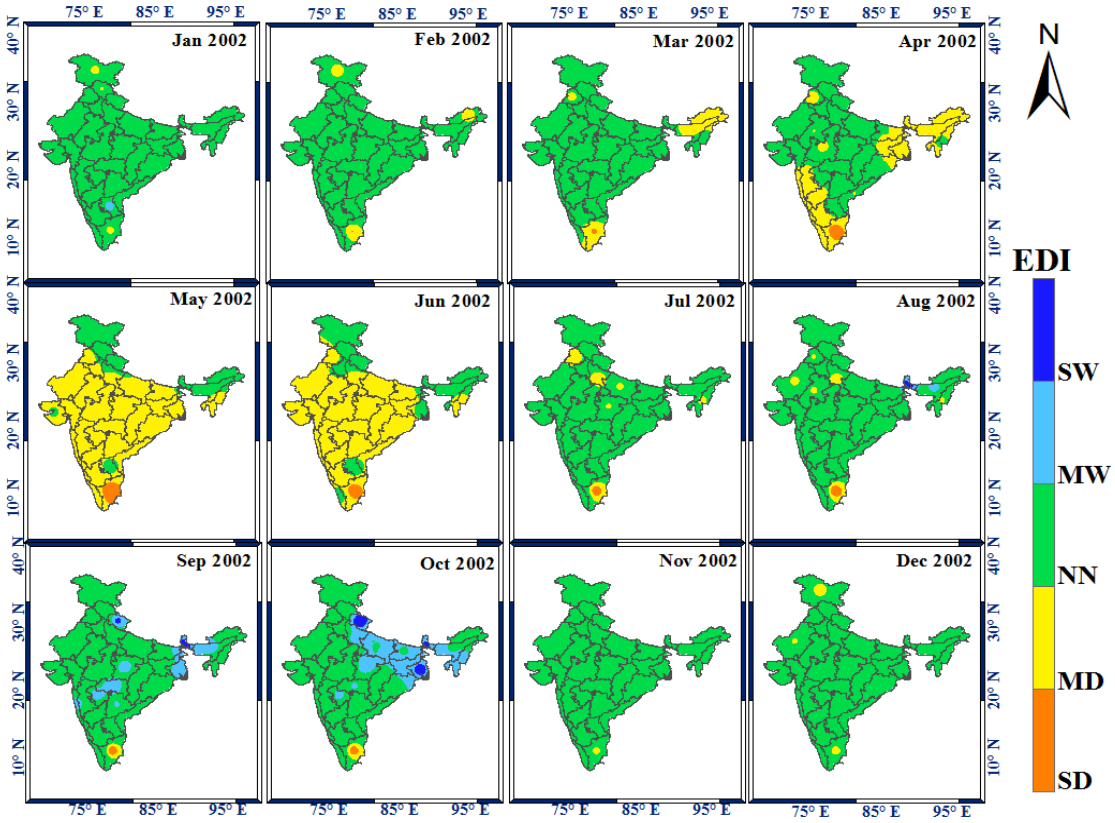

Figure 4.47 Spatial Distribution maps for drought year 2002 using EDI

Moving on to SPI-9 as depicted in Figure 4.48, the spatial distribution map for the drought year 2002 showed that the most severe drought conditions occurred from July to December, encompassing the monsoon, post-monsoon, and winter seasons. During this period, the homogenous regions of Central Northeast, Northwest, certain parts of Peninsular, and the West Central regions experienced a range of drought conditions, varying from extreme drought to moderate drought. Although drought conditions were observed in other months as well, they were less widespread. Notably, Tamil Nadu-Pondicherry experienced an extreme drought condition throughout the year, emphasizing the region's vulnerability to prolonged dry spells.

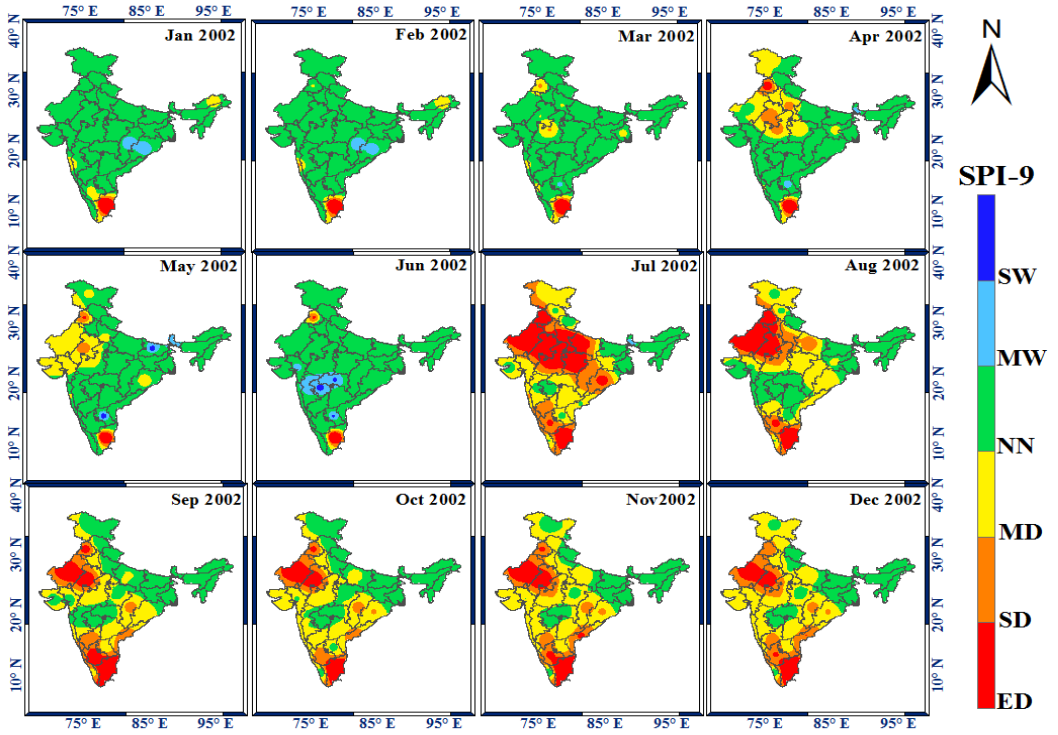

Figure 4.48 Spatial Distribution maps for drought year 2002 using SPI-9

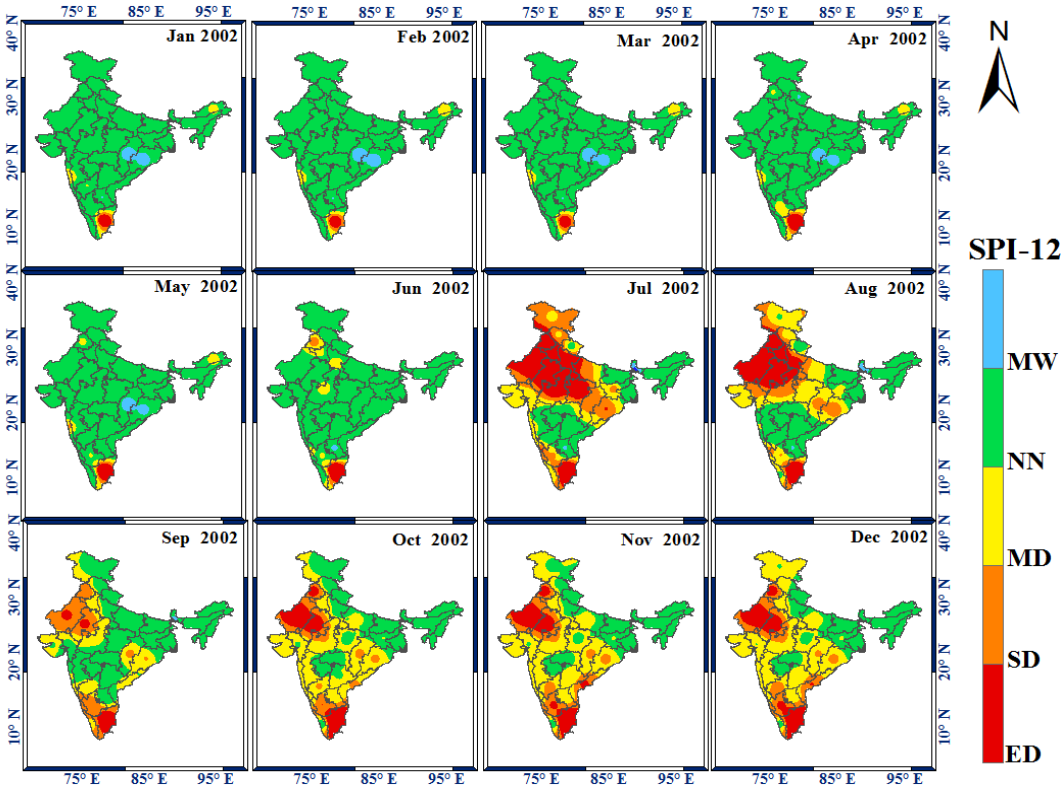

Figure 4.49 Spatial Distribution maps for drought year 2002 using SPI-12

The analysis for SPI-12 mirrored the findings for SPI-9, where drought conditions were most prominent from July to December, affecting the same regions. The SPI-12 results have been presented with Figure 4.49 which indicated that dry conditions persisted during this period, aligning with the SPI-9 results. In Tamil Nadu-Pondicherry, the extreme drought condition prevailed consistently throughout the year, as evidenced by both SPI-9 and SPI-12.

Overall, it has been observed that SPI-9 and SPI-12 shows a good representation for the drought in India during 2002. The key factors contributing to the drought during 2002 could primarily be a combination of natural and human factors. Inadequate monsoon rainfall during the monsoon season also triggers drought in the region. Furthermore, human-induced factors such as deforestation, land degradation, and improper land use practices also contributed to the severity of the drought. These activities disrupt local weather patterns, decrease the land's capacity to retain moisture, and increase soil erosion, intensifying the effects of the drought. The human impact on the environment can amplify the vulnerability of specific regions to drought events. It is important to emphasize that droughts are complex phenomena influenced by various interrelated factors. The specific combination of natural and human-induced factors contributing to drought can vary significantly from one region to another within India. Each region's unique climate, geographical features, and human activities can play a distinct role in shaping drought conditions.

4.3.7.2 Drought year 2009

The year 2009 was another significant period of drought in India. Several meteorological subdivisions across the country faced severe drought conditions during this year. The drought in 2009 had a detrimental effect on agriculture, water resources and livelihoods. By utilizing the Effective Drought Index (EDI), this study effectively captured the severity of the 2009 drought and its temporal distribution across the study area. The analysis of the EDI revealed that from the month of April until July, significant parts of the region experienced moderate dry conditions, as graphically illustrated in Figure 4.50. During this period, the deficiency of rainfall and the

consequent reduction in soil moisture had a substantial impact on the agricultural sector, impeding crop growth and negatively affecting yields. Additionally, the scarcity of water resources during this critical time further exacerbated the plight of both rural and urban populations, posing challenges to daily life and economic activities.

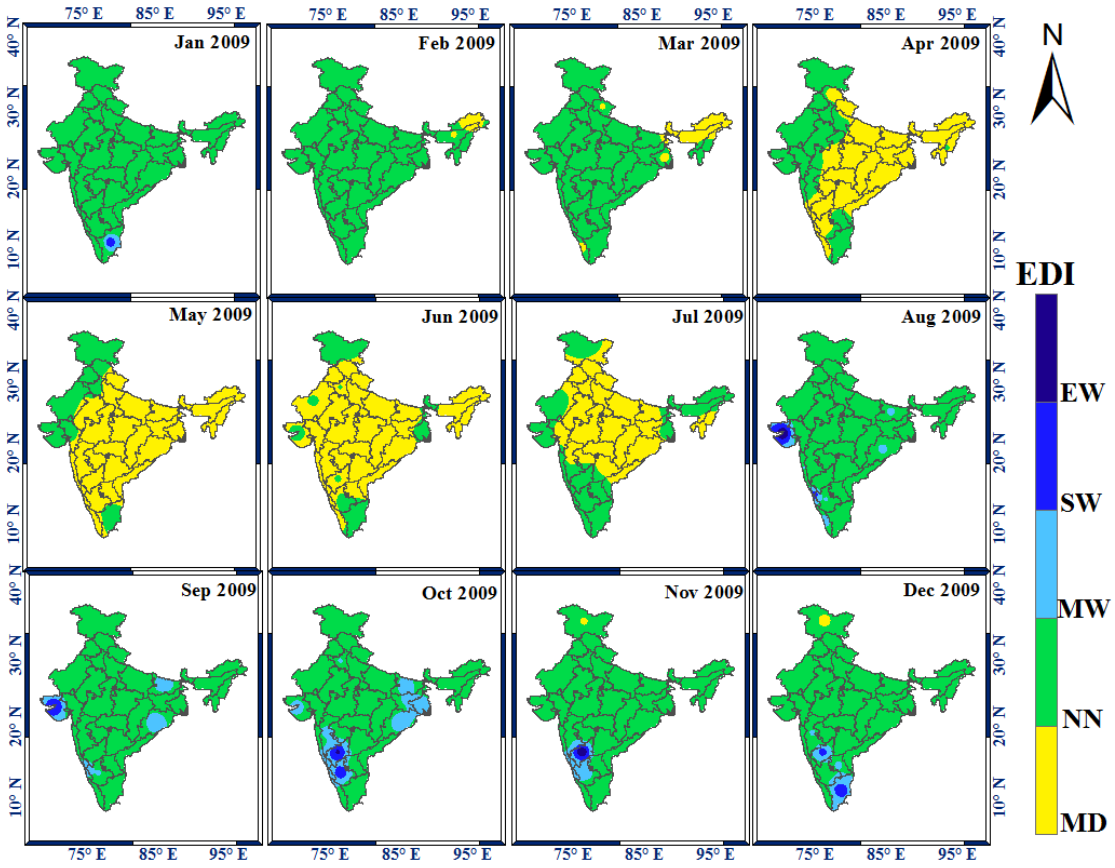

Figure 4.50 Spatial Distribution maps for drought year 2009 using EDI

The analysis of SPI-9 for the year 2009 revealed compelling insights into the spatiotemporal patterns of drought conditions. From the month of May until December, the study area experienced varying degrees of drought severity, ranging from moderate to extreme conditions. During the month of May, a noteworthy aspect of the analysis was that the entire study area faced moderate to extreme dry conditions. Specifically, certain regions, such as the North-East, encountered severe to extreme drought, while other meteorological subdivisions displayed moderate to extreme drought conditions. These findings demonstrate the pervasive nature of the drought's impact across the

region, affecting diverse climatic zones. From Figure 4.51 the month of June, July, and August, became evident that Central Northeast, Northwest, and some parts of the West Central regions experienced extreme drought conditions. During this period, the deficiency of rainfall and prolonged dry spells significantly impacted agricultural activities, water resources, and overall livelihoods.

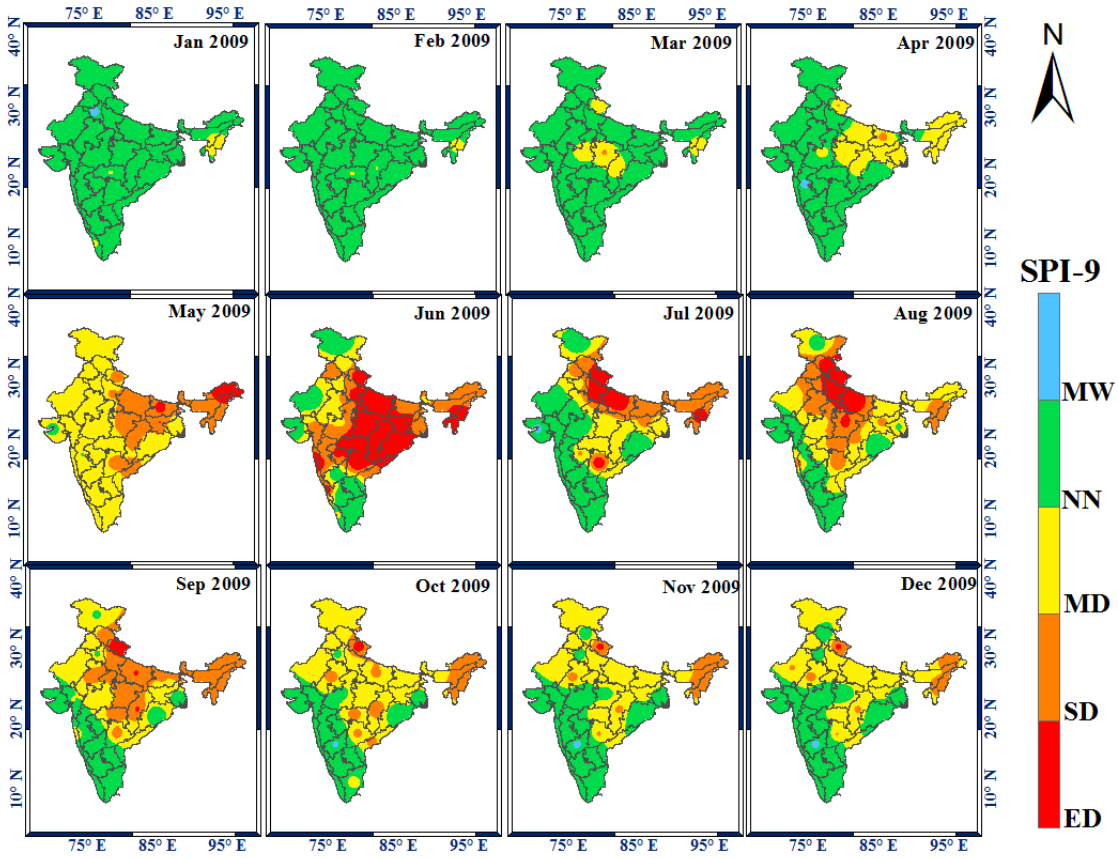

Figure 4.51 Spatial Distribution maps for drought year 2009 using SPI-9

The assessment of the SPI-12 for the year 2009 provided valuable insights into the drought conditions prevailing across the study area. The analysis revealed that the drought patterns identified by SPI-12 which is presented in Figure 4.52 were similar to those observed by SPI-9 during the same year, highlighting the consistency and reliability of both indices in capturing drought severity.

The SPI-12 analysis indicated that the drought conditions during 2009 persisted from June to December, indicating a prolonged period of water scarcity and its adverse

impacts on various sectors such as agriculture, water resources, and overall socio-economic well-being. This extended duration of drought highlighted the importance of long-term drought monitoring and preparedness to address the sustained challenges posed by water scarcity. It is noteworthy that, despite the similarity in the timing of drought occurrence between SPI-9 and SPI-12, the severity of drought conditions as depicted by SPI-12 was relatively less compared to SPI-9. This observation suggests that SPI-12, with its longer timescale, tends to smooth out short-term fluctuations in precipitation and emphasizes the overall long-term drought trend. As a result, SPI-12 might exhibit fewer instances of extreme drought severity compared to SPI-9, which primarily focuses on short-term drought impacts.

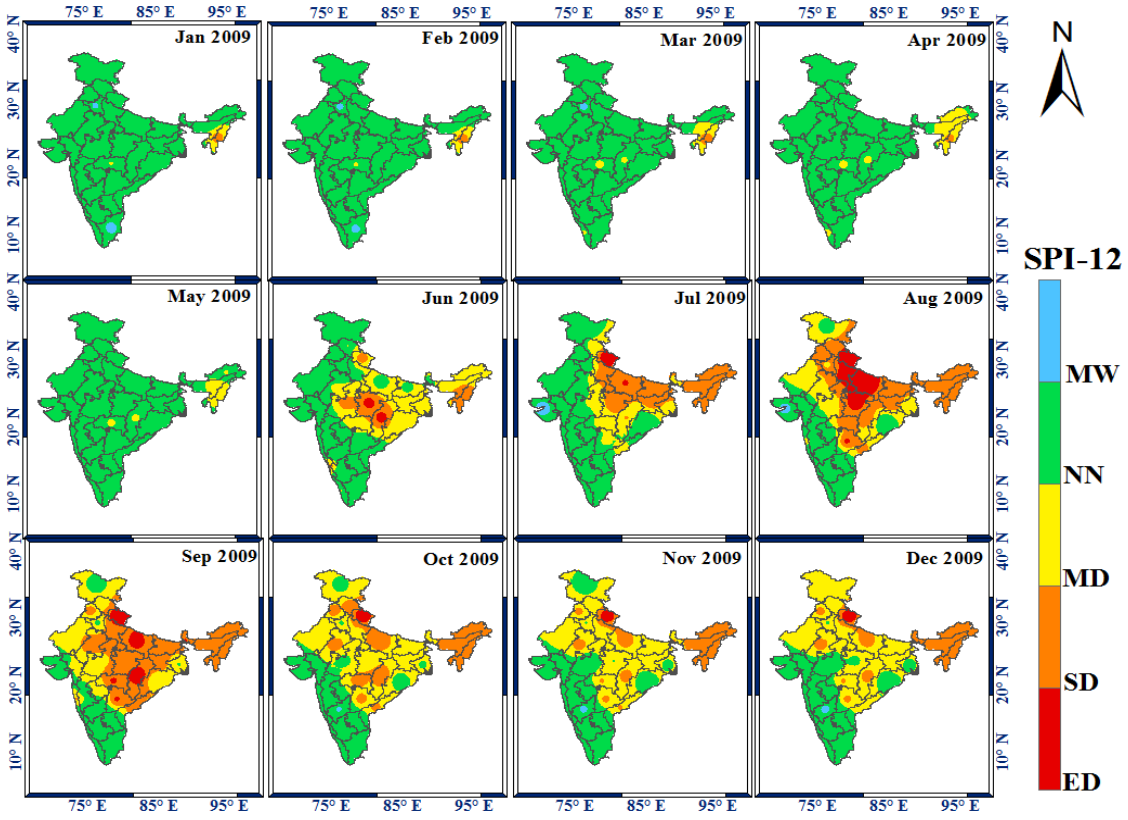

Figure 4.52 Spatial Distribution maps for drought year 2009 using SPI-12

Overall, the findings from the results reveals that, SPI-9 and SPI-12 are more effective than EDI in detecting the historical droughts. One of the key factors contributing to drought conditions is inadequate monsoon rainfall. The deficit or insufficient rainfall

during the monsoon season has been identified as a significant cause of drought in India. The study findings confirm this observation, as the analysis of SPI-9 and SPI-12 clearly revealed periods of water scarcity and drought in regions experiencing below-average monsoon precipitation. These findings underscore the importance of monitoring and understanding monsoon variability and its impact on drought conditions to facilitate proactive drought preparedness and water resource management. The year 2009 stands out as an illustrative example, wherein the uneven distribution of rainfall in various parts of the study region played a pivotal role in exacerbating the drought conditions. This irregular rainfall pattern led to the over-exploitation of groundwater resources due to excessive farming practices and inadequate water management, intensifying the severity of the drought. The results from SPI-9 and SPI-12 for the year 2009 highlighted the region's vulnerability to such fluctuations in rainfall, stressing the need for sustainable water management practices to mitigate the impacts of drought.

CHAPTER 5

SUMMARY AND CONCLUSIONS

5.1 BACKGROUND

This chapter presents the conclusions drawn based on the research insights gained from the study findings. Rainfall is one of the key factors for climatic parameters causing an impact on the environment. Drought, a prolonged and complex phenomenon, poses challenges in predicting its occurrence, magnitude, and intensity. India is a place with diverse climatic conditions spread all over from snow-cap-filled mountains to dry arid lands making this study a very challenging one. The research involved a comprehensive analysis of rainfall and meteorological drought indices for thirty-four meteorological subdivisions in India, using a 60-year dataset spanning from 1958 to 2017. The spatial variability of rainfall across the study area resulted in wide variations from region to region, further adding to the intricacies of the investigation. To ascertain trends in rainfall and meteorological drought indices, EDI, SPI-9 and SPI-12, the Mann-Kendall test was applied for annual, monthly, winter, pre-monsoon, monsoon, and post-monsoon periods across the thirty-four meteorological subdivisions. The research findings underscore the significance of understanding rainfall patterns and their impact on drought conditions, especially in a country as diverse as India. The study reveals valuable insights into the temporal and spatial variations of rainfall, highlighting the need for region-specific drought assessment and preparedness strategies. The application of machine learning algorithms for predicting meteorological drought indices has been carried out highlighting their suitability for drought prediction in diverse climatic conditions. The study also emphasized the significance of historical drought analysis, enabling a deeper understanding of past drought occurrences and their contributing factors.

5.2 Trend analysis of rainfall and meteorological drought indices

The findings from the Mann-Kendall test for trend analysis indicate noteworthy patterns in the rainfall behaviour across various timescales in the study area. Over the study

period, a substantial proportion of meteorological subdivisions exhibited a declining trend. The declining trends in annual, monthly, pre-monsoon, monsoon, post-monsoon, and winter rainfall highlight a concerning change in the precipitation patterns over the years. Such changes in rainfall trends have significant implications for the wetness and dryness conditions experienced in the region, as indicated by the numerical representation of drought indices, namely EDI and SPI. Notably, it was observed that during the non-monsoon period, a substantial portion of the study area experienced dry conditions. This emphasizes the critical role of seasonal rainfall in maintaining water availability and mitigating drought impacts. The declining rainfall trends could be attributed to climate change, characterized by rising temperatures and changes in seasonal precipitation patterns.

The numerical representation of drought indices highlights the sensitivity of wetness and dryness conditions to the observed changes in rainfall. As such, understanding the rainfall trends and their correlation with drought conditions is of utmost importance in developing effective mitigation strategies to address the impacts of drought. Given the diverse climatic conditions in the study region, the identification of declining rainfall trends and increasing dryness demands urgent attention from policymakers and water resource managers. Proactive measures are essential to build climate resilience, secure water resources, and devise adaptive strategies to cope with drought challenges.

Overall, the trends in rainfall and their effects on drought conditions call for a comprehensive approach towards climate monitoring and adaptive water management. By recognizing the implications of changing rainfall patterns, stakeholders can collaboratively work towards sustainable solutions to combat drought and secure the well-being of the region's inhabitants and ecosystems.

5.3 Prediction of meteorological drought indices using machine learning algorithms

The abilities of the machine learning algorithms to predict the meteorological drought indices, EDI, SPI-9 and SPI-12 has been investigated. The study has been carried out

for 60 years (1958-2017). Based on the performance of the machine learning algorithms, it has been found that the hybrid models, GA-ANFIS and PSO-ANFIS models were found to provide better results as compared with the GRNN model. Despite having diverse climatic characteristics in the study area, this study's findings revealed a significant effect on the prediction accuracy of the meteorological drought indices using machine learning techniques.

An interesting aspect discovered in the study was the influence of the timescale of the SPI on the prediction accuracy of the machine learning algorithms. As the timescale of the SPI increased, a noticeable enhancement in the prediction accuracy was observed, indicating the relevance and effectiveness of machine learning techniques in capturing long-term drought patterns. To comprehensively evaluate the models performance, several evaluation metrics, including R^2, NSE, and RRMSE, were employed for all three indices, EDI, SPI-9, and SPI-12. The outcomes consistently demonstrated the superiority of GA-ANFIS and PSO-ANFIS over the GRNN model, with significant improvements in R^2, NSE, and RRMSE values in most regions.

In addition to the model comparisons, the research emphasized the pivotal role of rainfall in predicting meteorological drought indices. It is evident that accurate and timely precipitation data greatly influences the efficacy of drought prediction. This emphasizes the importance of understanding rainfall patterns and trends in devising effective mitigation strategies and planning for regions susceptible to drought conditions. With the identification of robust and accurate machine learning models for predicting the drought indices, this study may be beneficial in understanding drought behaviour and identifying drought-prone locations and preparing mitigation strategies to overcome the impacts of droughts.

5.4 Detecting Historical Droughts: Assessing the Efficacy of Drought Indices

The core of effectively detecting and comprehensively assessing historical drought events lies in the understanding and management of past drought occurrences. For this purpose, the meteorological drought indices, namely EDI, SPI-9, and SPI-12, are diligently computed and compared with the identified drought years within the study

period. This detailed evaluation of appropriate drought indices provides valuable insights into the characteristics, patterns, and impacts of historical drought events. Analysing and comparison of the meteorological drought indices EDI, SPI-9, and SPI-12, it becomes evident that SPI-9 and SPI-12 serve as reliable indicators for identifying previous drought events. These indices exhibit a robust ability to represent and evaluate drought conditions with precision, making them invaluable tools for drought detection and assessment.

The significance of detecting historical droughts and analysing the efficacy of drought indices extends beyond broad research. Such endeavours hold profound implications for better comprehending past drought events, effectively preparing for future droughts, and advancing the development of sustainable water management practices and policies. By collecting knowledge from historical drought data, decision-makers can formulate informed strategies to mitigate the impacts of drought, enhance water resource management, and ensure long-term resilience in the face of changing climate patterns.

Overall, the integration of historical drought analysis and the evaluation of drought indices contribute significantly to the advancement of drought research, resource planning, and environmental conservation. This study serves as a vital bridge towards a more informed and proactive approach to drought management and sustainable water usage, ultimately benefitting communities, ecosystems, and economies impacted by drought conditions.

5.5 FUTURE SCOPE

The future scope of research in the domain of drought indices and machine learning holds promising avenues for exploration and enhancement. Further research may be carried out for drought indices using the same machine learning models and for the same indices to explore and evaluate other machine learning models. The exploration of diverse algorithms holds the potential to unlock novel perspectives, offering opportunities to elevate the precision and dependability of drought predictions. Moreover, the scope of this work can be extended to encompass the forecasting of

future drought events not only the current study area but also in diverse regions. This broader geographical exploration can contribute to a more comprehensive understanding of drought patterns and trends across varied landscapes.

Furthermore, the future scope extends beyond the current study offering opportunities for advancement in predictive modelling, global applicability, climate change integration and a more nuanced understanding of drought. These avenues of exploration collectively contribute to the ongoing efforts in effective drought management and sustainable water resource planning.

5.6 LIMITATION OF THE STUDY

While the study contributes significantly to the understanding of drought patterns and the effectiveness of machine learning models in predicting meteorological drought indices, there are several limitations on the study. Since the study is confined to the Indian region specifically the thirty-four meteorological subdivisions, the findings may not be directly applicable to other geographical locations. Limitations in data quality, gaps or inaccuracies may influence the precision of the analysis. The study does not explicitly incorporate climate change variables which could significantly impact drought patterns. However, the specific investigation of drought termination dynamics is not extensively explored, providing potential for further research.

APPENDICES

APPENDIX-1

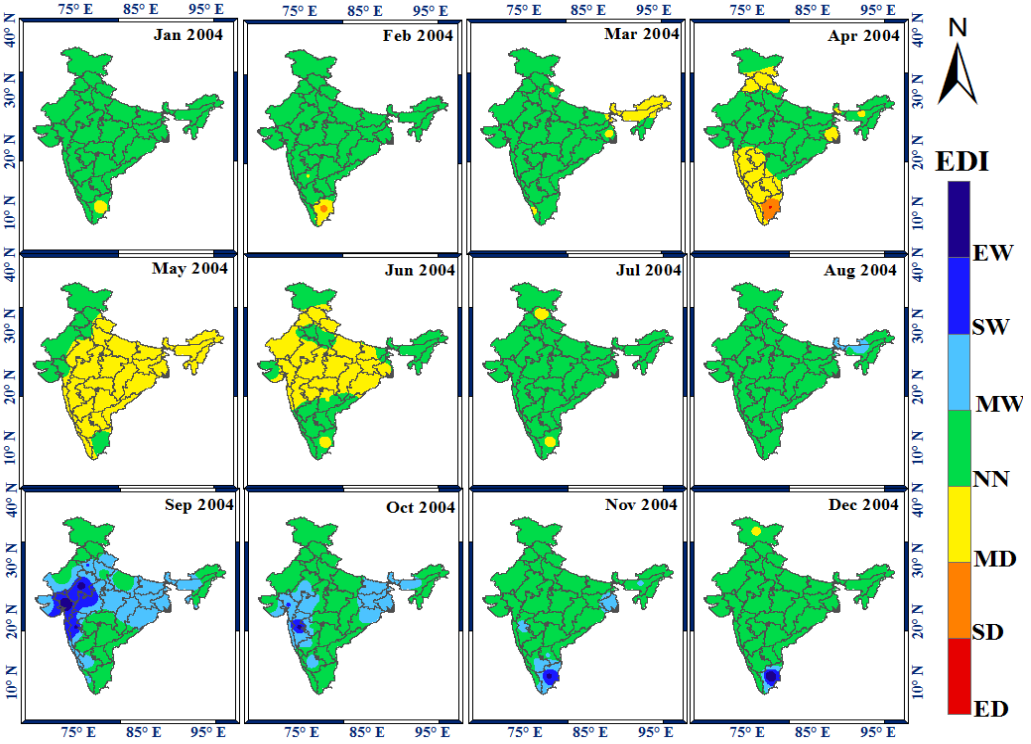

Figure A.1.1 Spatial Distribution maps for drought year 2004 using EDI

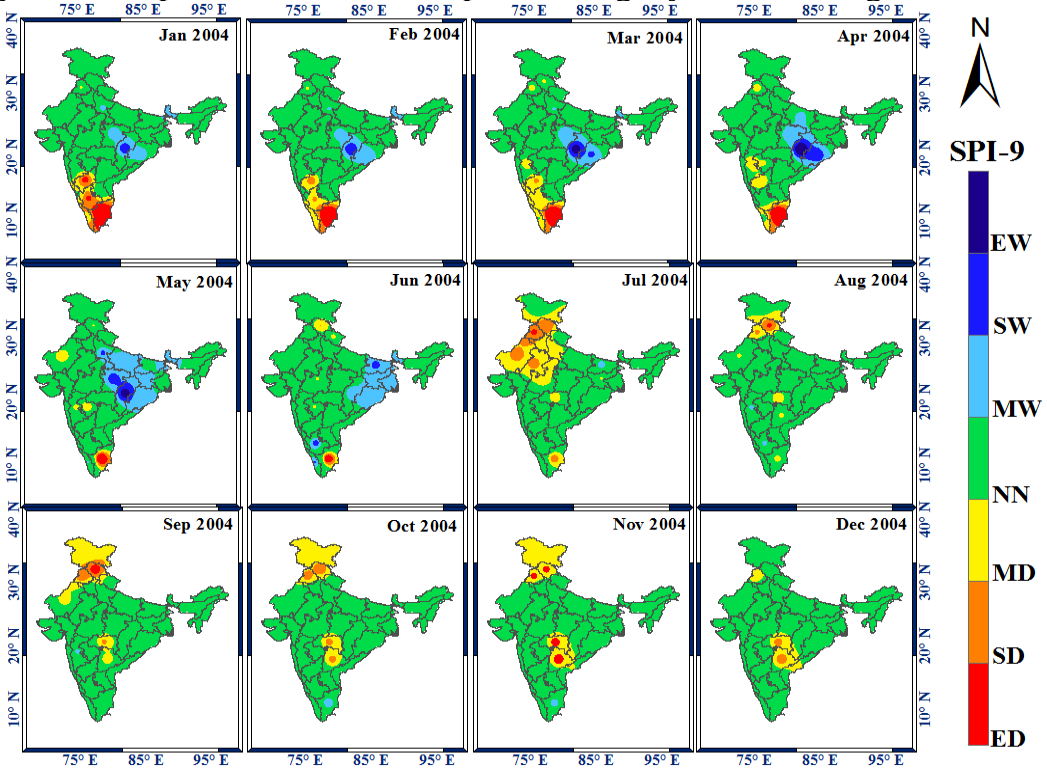

Figure A.1.2 Spatial Distribution maps for drought year 2004 using SPI-9

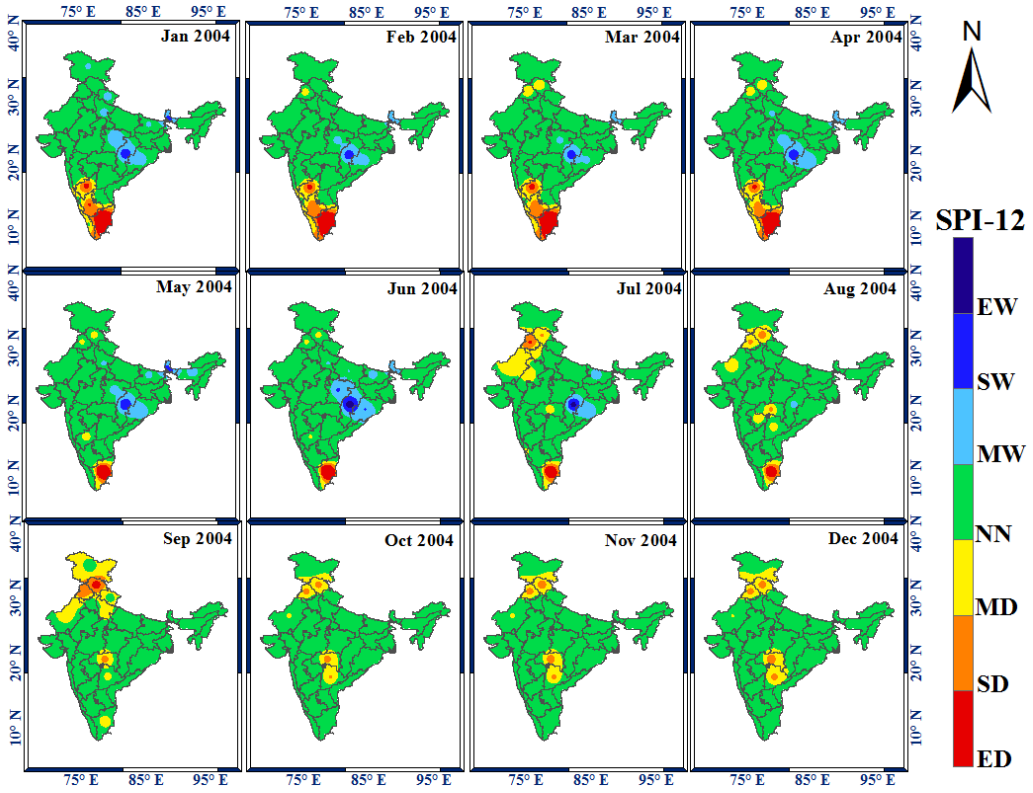

Figure A.1.3 Spatial Distribution maps for drought year 2004 using SPI-12

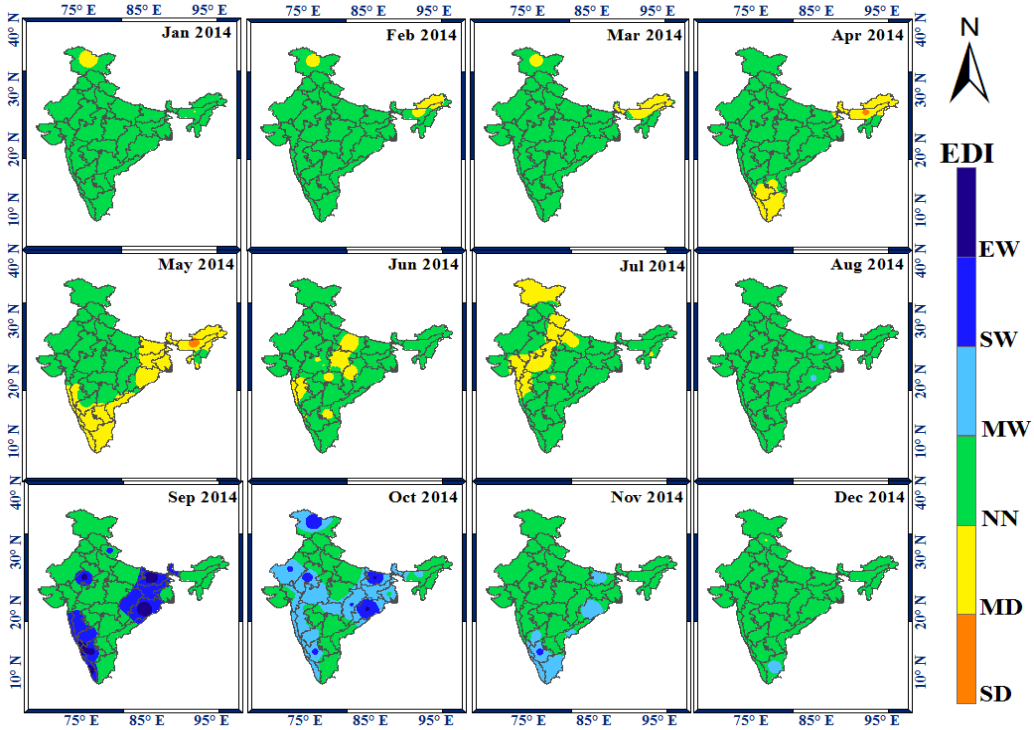

Figure A.1.4 Spatial Distribution maps for drought year 2014 using EDI

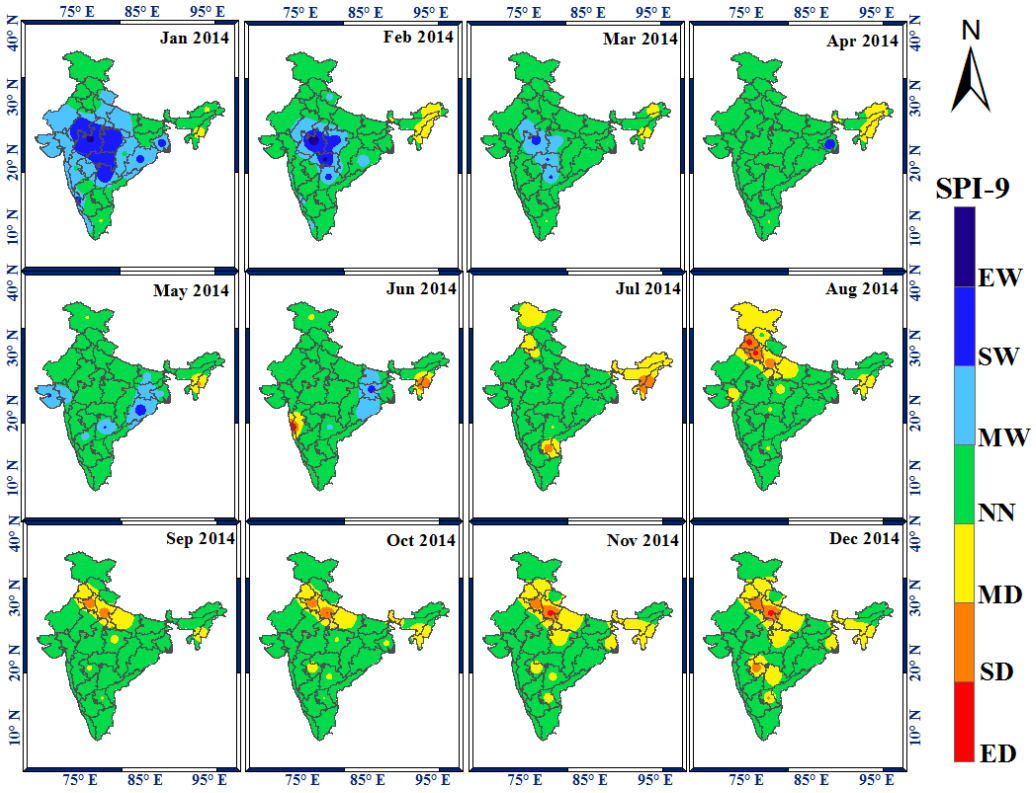

Figure A.1.5 Spatial Distribution maps for drought year 2014 using SPI-9

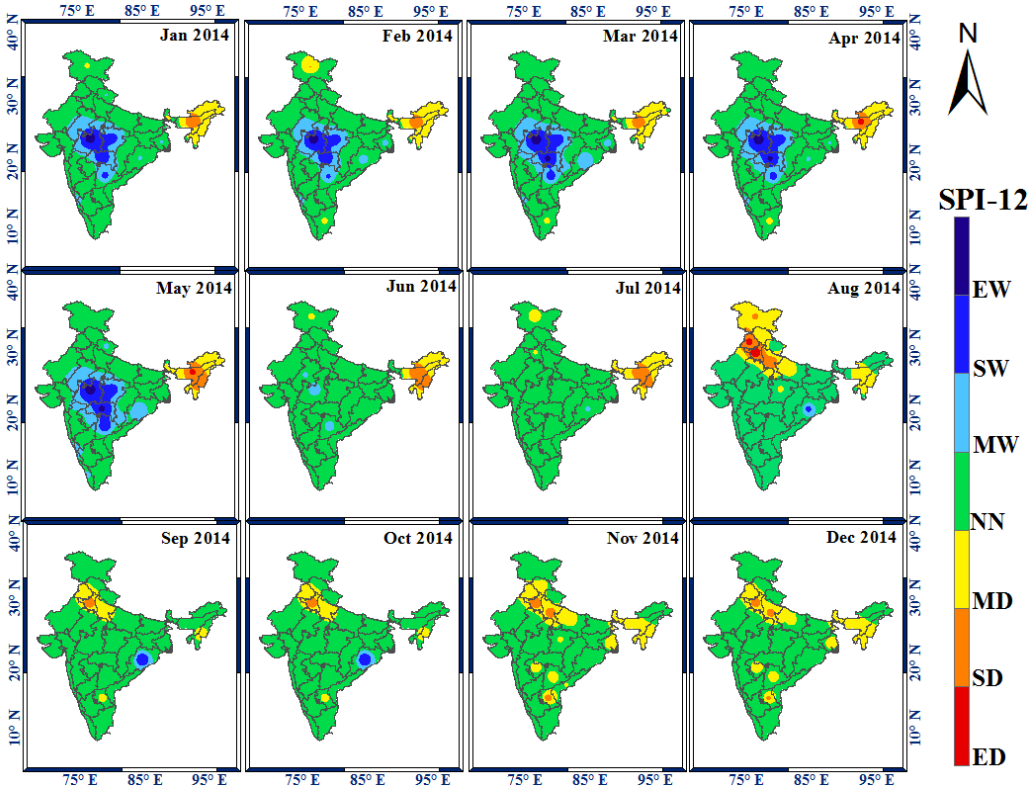

Figure A.1.6 Spatial Distribution maps for drought year 2014 using SPI-12

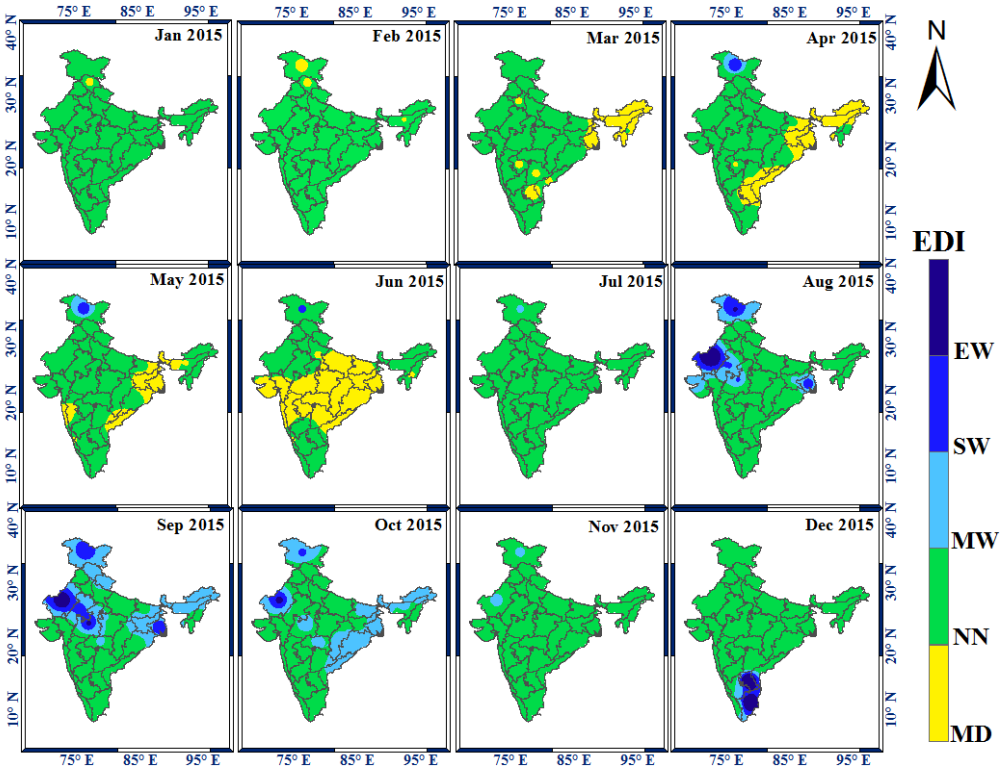

Figure A.1.7 Spatial Distribution maps for drought year 2015 using EDI

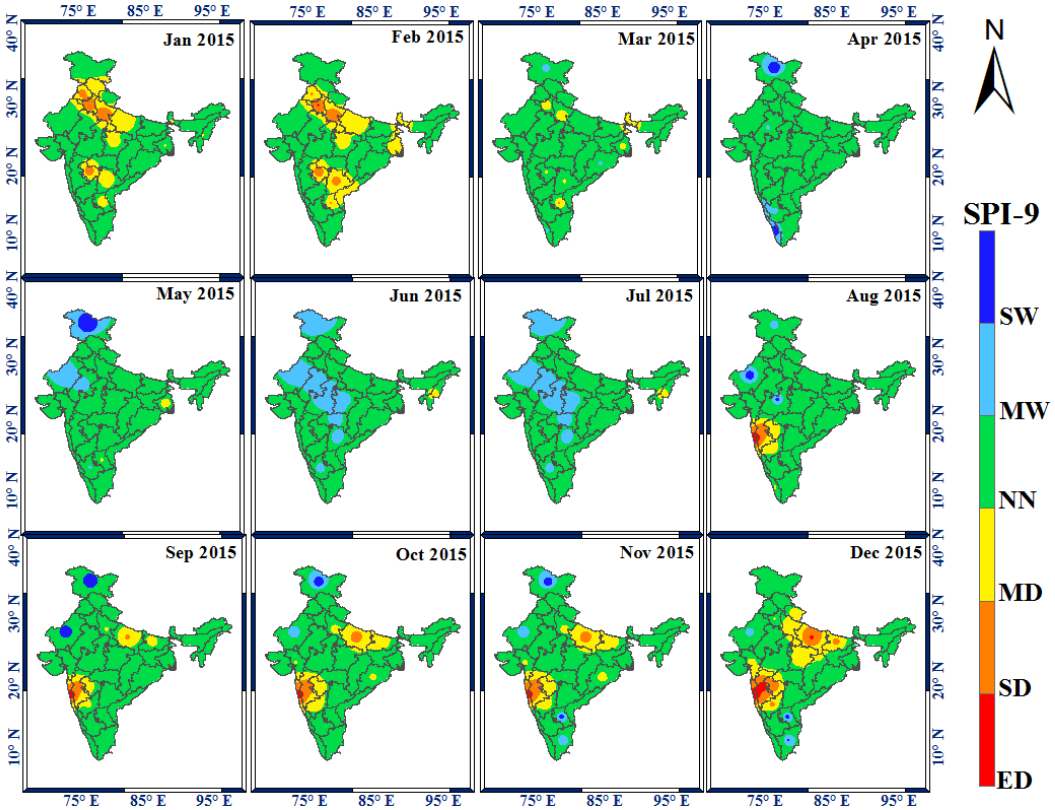

Figure A.1.8 Spatial Distribution maps for drought year 2015 using SPI-9

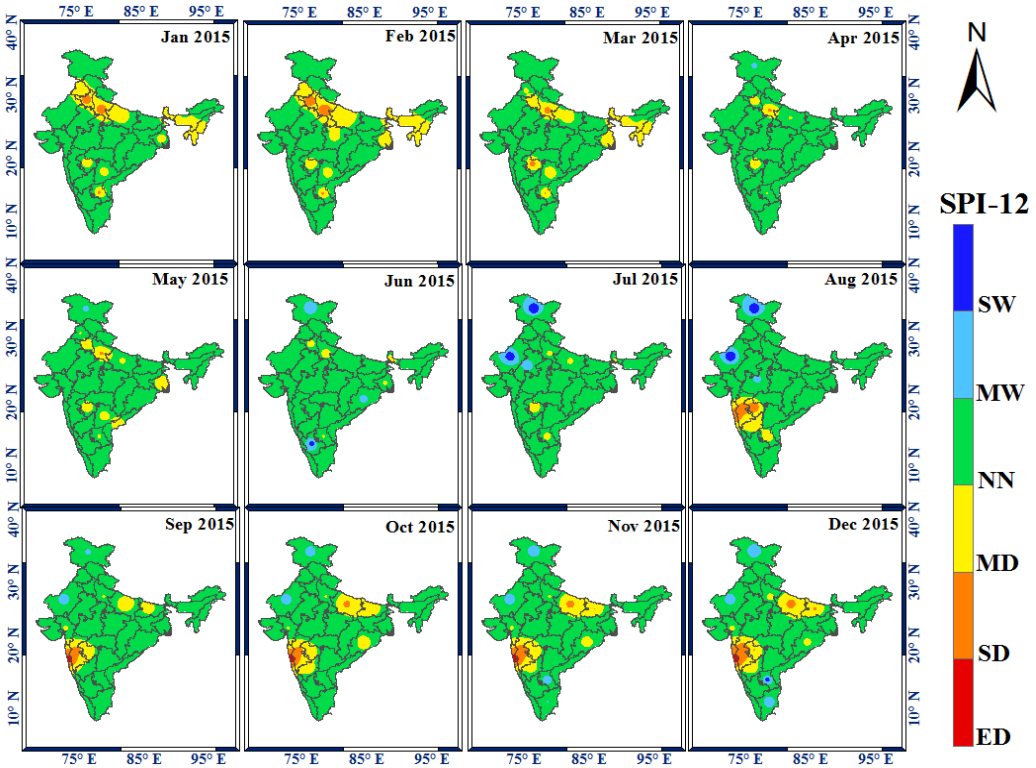

Figure A.1.9 Spatial Distribution maps for drought year 2015 using SPI-12

REFERENCES

Achite, M., Jehanzaib, M., Elshaboury, N., and Kim, T. W. (2022). "Evaluation of Machine Learning Techniques for Hydrological Drought Modeling: A Case Study of the Wadi Ouahrane Basin in Algeria." *Water (Switzerland)*, 14(3).

Achour, K., Meddi, M., Zeroual, A., Bouabdelli, S., Maccioni, P., and Moramarco, T. (2020). "Spatio-temporal analysis and forecasting of drought in the plains of northwestern Algeria using the standardized precipitation index." *J. Earth Syst. Sci.*, 129(1).

Adnan, R. M., Mostafa, R. R., Islam, A. R. M. T., Gorgij, A. D., Kuriqi, A., and Kisi, O. (2021). "Improving drought modeling using hybrid random vector functional link methods." *Water (Switzerland)*, 13(23), 1–22.

Agana, N. A., and Homaifar, A. (2018). "EMD-based predictive deep belief network for time series prediction: An application to drought forecasting." *Hydrology*, 5(1).

Aghelpour, P., Bahrami-Pichaghchi, H., and Kisi, O. (2020). "Comparison of three different bio-inspired algorithms to improve ability of neuro fuzzy approach in prediction of agricultural drought, based on three different indexes." *Comput. Electron. Agric.*, 170(January), 105279.

Ahmadalipour, A., Moradkhani, H., and Demirel, M. C. (2017). "A comparative assessment of projected meteorological and hydrological droughts: Elucidating the role of temperature." *J. Hydrol.*, 553, 785–797.

Ahmed, M. K., Alam, M. S., Yousuf, A. H. M., & Islam, M. M. (2017). A long-term trend in precipitation of different spatial regions of Bangladesh and its teleconnections with El Niño/Southern Oscillation and Indian Ocean Dipole. *Theoretical and Applied Climatology*, *129*, 473-486.

Alawsi, M. A., Zubaidi, S. L., Al-Bdairi, N. S. S., Al-Ansari, N., and Hashim, K. (2022). "Drought Forecasting: A Review and Assessment of the Hybrid Techniques and Data Pre-Processing." *Hydrology*, 9(7), 1–23.

AlHakeem, D., Mandal, P., Haque, A. U., Yona, A., Senjyu, T., & Tseng, T. L. (2015, July). A new strategy to quantify uncertainties of wavelet-GRNN-PSO based solar PV

power forecasts using bootstrap confidence intervals. In *2015 IEEE power & energy society general meeting* (pp. 1-5). IEEE.

Ali, M., Deo, R. C., Downs, N. J., and Maraseni, T. (2018). "Multi-stage committee based extreme learning machine model incorporating the influence of climate parameters and seasonality on drought forecasting." *Comput. Electron. Agric.*, 152(April), 149–165.

Amrit, K., Pandey, R. P., and Mishra, S. K. (2018). "Characteristics of meteorological droughts in northwestern India." *Nat. Hazards*, 94(2), 561–582.

Azimi, S. M. E., Sadatinejad, S. J., Malekian, A., and Jahangir, M. H. (2022). "Application of artificial intelligence hybrid models for meteorological drought prediction." *Nat. Hazards*, (0123456789).

Baniya, B., Tang, Q., Xu, X., Haile, G. G., and Chhipi-Shrestha, G. (2019). "Spatial and temporal variation of drought based on satellite derived vegetation condition index in Nepal from 1982–2015." *Sensors (Switzerland)*, 19(2), 430.

Barua, S., Ng, A. W. M., and Perera, B. J. C. (2012). "Artificial Neural Network–Based Drought Forecasting Using a Nonlinear Aggregated Drought Index." *J. Hydrol. Eng.*, 17(12), 1408–1413.

Belayneh, A., and Adamowski, J. (2013). "Drought forecasting using new machine learning methods." *J. Water L. Dev.*, 18(9), 3–12.

Belayneh, A., Adamowski, J., and Khalil, B. (2016). "Short-term SPI drought forecasting in the Awash River Basin in Ethiopia using wavelet transforms and machine learning methods." *Sustain. Water Resour. Manag.*, 2(1), 87–101.

Belayneh, A., Adamowski, J., Khalil, B., and Ozga-Zielinski, B. (2014). "Long-term SPI drought forecasting in the Awash River Basin in Ethiopia using wavelet neural networks and wavelet support vector regression models." *J. Hydrol.*, 508, 418–429.

Byakatonda, J., Parida, B. P., Moalafhi, D. B., and Kenabatho, P. K. (2018). "Analysis of long term drought severity characteristics and trends across semiarid Botswana using two drought indices." *Atmos. Res.*, 213(July), 492–508.

Byun, H.-R., and Wilhite, D. A. (1999). "Objective Quantification of Drought Severity and Duration." (1980), 2747–2756.

Caviedes, C. N. (2001), El Niño in History: Storming Through the Ages (1st ed.), *University Press of Florida* (published 18 September 2001), *ISBN 978-0-8130-2099-0*

Chanapathi, T., Thatikonda, S., and Raghavan, S. (2018). "Analysis of rainfall extremes and water yield of Krishna river basin under future climate scenarios." *J. Hydrol. Reg. Stud.*, 19(June), 287–306.

Cheng, Q., Gao, L., Zhong, F., Zuo, X., and Ma, M. (2020). "Spatiotemporal variations of drought in the Yunnan-Guizhou Plateau, southwest China, during 1960–2013 and their association with large-scale circulations and historical records." *Ecol. Indic.*, 112(November 2019), 106041.

Chouhan, T. S. (1992), Desertification in the World and Its Control, Scientific Publishers, *ISBN 978-81-7233-043-9*

Citakoglu, H., and Coşkun, Ö. (2022). "Comparison of hybrid machine learning methods for the prediction of short-term meteorological droughts of Sakarya Meteorological Station in Turkey." *Environ. Sci. Pollut. Res.*, 29(50), 75487–75511.

D.E.Goldberg, and Holland, J. H. (1989). "Enhancement of xylanase production by sol-gel immobilization of Aspergillus awamori K-1." *Genet. Algorithms Mach. Learn.*

Datta, P., and Das, S. (2019). "Analysis of long-term precipitation changes in West Bengal, India: An approach to detect monotonic trends influenced by autocorrelations." *Dyn. Atmos. Ocean.*, 88(May).

Deng, S., Chen, T., Yang, N., Qu, L., Li, M., and Chen, D. (2018). "Spatial and temporal distribution of rainfall and drought characteristics across the Pearl River basin." *Sci. Total Environ.*, 619–620, 28–41.

Deo, R. C., Tiwari, M. K., Adamowski, J. F., and Quilty, J. M. (2017). "Forecasting effective drought index using a wavelet extreme learning machine (W-ELM) model." *Stoch. Environ. Res. Risk Assess.*, 31(5), 1211–1240.

Docheshmeh Gorgij, A., Alizamir, M., Kisi, O., and Elshafie, A. (2022). "Drought modelling by standard precipitation index (SPI) in a semi-arid climate using deep learning method: long short-term memory." *Neural Comput. Appl.*, 34(3), 2425–2442.

Ebrahimpour, M., Rahimi, J., Nikkhah, A., and Bazrafshan, J. (2015). "Monitoring

agricultural drought using the standardized effective precipitation index." *J. Irrig. Drain. Eng.*, 141(1), 1–9.

Eberhart, R., & Kennedy, J. (1995, November). Particle swarm optimization. In *Proceedings of the IEEE international conference on neural networks* (Vol. 4, pp. 1942-1948).

Elbeltagi, A., Pande, C. B., Kumar, M., Tolche, A. D., Singh, S. K., Kumar, A., and Vishwakarma, D. K. (2023). "Prediction of meteorological drought and standardized precipitation index based on the random forest (RF), random tree (RT), and Gaussian process regression (GPR) models." *Environ. Sci. Pollut. Res.*, (0123456789).

Farooq, O. (2002), *"India's Heat Wave Tragedy"*, *BBC News* (published 17 May 2002), *archived* from the original on 10 January 2014, *retrieved 1 October 2011*

Feng, P., Wang, B., Liu, D. L., and Yu, Q. (2019). "Machine learning-based integration of remotely-sensed drought factors can improve the estimation of agricultural drought in South-Eastern Australia." *Agric. Syst.*, 173(March), 303–316.

Ganguli, P., and Reddy, M. J. (2014). "Ensemble prediction of regional droughts using climate inputs and the SVM – copula approach." *Hydrol. Process.*, 28(19), 4989–5009.

Gebremeskel Haile, G., Tang, Q., Leng, G., Jia, G., Wang, J., Cai, D., Sun, S., Baniya, B., and Zhang, Q. (2019). "Long-term spatiotemporal variation of drought patterns over the Greater Horn of Africa." *Sci. Total Environ.*, 704, 135299.

Ghosh, K. G. (2018). "Analysis of Rainfall Trends and its Spatial Patterns During the Last Century over the Gangetic West Bengal, Eastern India." *J. Geovisualization Spat. Anal.*, 2(2).

Guntu, R. K., Rathinasamy, M., Agarwal, A., and Sivakumar, B. (2020). "Spatiotemporal variability of Indian rainfall using multiscale entropy." *J. Hydrol.*, 587, 124916.

Haied, N., Foufou, A., Chaab, S., Azlaoui, M., Khadri, S., Benzahia, K., and Benzahia, I. (2017). "Drought assessment and monitoring using meteorological indices in a semi-arid region." *Energy Procedia*, 119, 518–529.

Hajirahimi, Z., and Khashei, M. (2022). *Hybridization of hybrid structures for time series forecasting: a review*. *Artif. Intell. Rev.*, Springer Netherlands.

Hassan, A. G., Fullen, M. A., and Oloke, D. (2019). “Problems of drought and its management in Yobe State, Nigeria.” *Weather Clim. Extrem.*, 23(April 2018).

Hintze, J. L., and Nelson, R. D. (1998). “Violin plots: A box plot-density trace synergism.” *Am. Stat.*, 52(2), 181–184.

Healy, M., *South Asia: Monsoons*, Harper College, archived from *the original* on 29 September 2011, *retrieved 1 October 2011*.

Huang, G., Zhu, Q., and Siew, C. (2006). “Extreme Learning Machine : A New Learning Scheme of Feedforward Neural Networks.” 70, 25–29.

Huang, Y. F., Ang, J. T., Tiong, Y. J., Mirzaei, M., and Amin, M. Z. M. (2016). “Drought Forecasting using SPI and EDI under RCP-8.5 Climate Change Scenarios for Langat River Basin, Malaysia.” *Procedia Eng.*, 154, 710–717.

Jana, C., Alam, N. M., Mandal, D., Shamim, M., and Kaushal, R. (2017). “Spatio-temporal rainfall trends in the twentieth century for Bundelkhand region, India.” *J. Water Clim. Chang.*, 8(3), 441–455.

Jang, J. R. (1993). “ANFIS : Adap tive-Ne twork-Based Fuzzy Inference System.” 23(3).

Kalisa, W., Zhang, J., Igbawua, T., Ujoh, F., Ebohon, O. J., Namugize, J. N., and Yao, F. (2020). “Spatio-temporal analysis of drought and return periods over the East African region using Standardized Precipitation Index from 1920 to 2016.” *Agric. Water Manag.*, 237(January), 106195.

Karamouz, M., Rasouli, K., and Nazif, S. (2009). “Development of a hybrid Index for drought prediction: Case study.” *J. Hydrol. Eng.*, 14(6), 617–627.

Karamouz, M., Torabi, S., and Araghinejad, S. (2004). “Analysis of Hydrologic and Agricultural Droughts in Central Part of Iran.” *J. Hydrol. Eng.*, 9(5), 402–414.

Kennedy, J., and Eberhart, R. (1995). “Particle Swarm Optimization.” *IEEE Trans. Neural Networks*, 1942–1948.

Khan, N., Sachindra, D. A., Shahid, S., Ahmed, K., Shiru, M. S., and Nawaz, N. (2020). “Prediction of droughts over Pakistan using machine learning algorithms.” *Adv. Water Resour.*, 139(August 2019), 103562.

Kisi, O., Docheshmeh Gorgij, A., Zounemat-Kermani, M., Mahdavi-Meymand, A., and

Kim, S. (2019). “Drought forecasting using novel heuristic methods in a semi-arid environment.” *J. Hydrol.*, 578(August), 124053.

Kimmel, T. M. (2000), *Weather and Climate: Koppen Climate Classification Flow Chart*, University of Texas at Austin, archived from *the original* on 15 January 2016, *retrieved 8 April 2007*

Li, F., Li, H., Lu, W., Zhang, G., and Kim, J. C. (2019). “Meteorological drought monitoring in Northeastern China using multiple indices.” *Water (Switzerland)*, 11(1), 1–17.

Li, Q., He, P., He, Y., Han, X., Zeng, T., Lu, G., and Wang, H. (2020). “Investigation to the relation between meteorological drought and hydrological drought in the upper Shaying River Basin using wavelet analysis.” *Atmos. Res.*, 234, 104743.

Liu, X., Xu, X., Yu, M., and Lu, J. (2016). “Hydrological Drought Forecasting and Assessment Based on the Standardized Stream Index in the Southwest China.” *Procedia Eng.*, 154, 733–737.

Malik, A., and Kumar, A. (2020). “Meteorological drought prediction using heuristic approaches based on effective drought index: a case study in Uttarakhand.” *Arab. J. Geosci.*, 13(6).

Malik, S., Pal, S. C., Sattar, A., Singh, S. K., Das, B., Chakrabortty, R., and Mohammad, P. (2020). “Trend of extreme rainfall events using suitable Global Circulation Model to combat the water logging condition in Kolkata Metropolitan Area.” *Urban Clim.*, 32(January).

Mallya, G., Mishra, V., Niyogi, D., Tripathi, S., and Govindaraju, R. S. (2015). “Trends and variability of droughts over the Indian monsoon region.” *Weather Clim. Extrem.*, 12(2014), 43–68.

Marumbwa, F. M., Cho, M. A., and Chirwa, P. W. (2019). “Analysis of spatio-temporal rainfall trends across southern African biomes between 1981 and 2016.” *Phys. Chem. Earth*, 114(April), 102808.

Mathew, M. M. M., K, S., Mathew, M. M. M., Arulbalaji, P., and Padmalal, D. (2021). “Spatiotemporal variability of rainfall and its effect on hydrological regime in a tropical monsoon-dominated domain of Western Ghats, India.” *J. Hydrol. Reg. Stud.*, 36(July

2020), 100861.

Mckee, T. B., Doesken, N. J., and Kleist, J. (1993). "The relationship of drought frequency and duration to time scales." *Eight Conf. Appl. Climatol.*, 179–183.

Mehrabi, M., Sharifpur, M., and Meyer, J. P. (2012). "Application of the FCM-based neuro-fuzzy inference system and genetic algorithm-polynomial neural network approaches to modelling the thermal conductivity of alumina-water nanofluids." *Int. Commun. Heat Mass Transf.*, 39(7), 971–977.

Michalewicz, Z. (1996). "Evolutionary algorithms for constrained parameter optimization problems." *Evol. Comput.*, 4(1), 1–32.

Mishra, A. K., and Desai, V. R. (2006). "Drought forecasting using feed-forward recursive neural network." *Ecol. Modell.*, 198(1–2), 127–138.

Mishra, A. K., Desai, V. R., and Singh, V. P. (2007). "Drought Forecasting Using a Hybrid Stochastic and Neural Network Model." *J. Hydrol. Eng.*, 12(6), 626–638.

Mishra, V., Tiwari, A. D., Aadhar, S., Shah, R., Xiao, M., Pai, D. S., and Lettenmaier, D. (2019). "Drought and Famine in India, 1870–2016." *Geophys. Res. Lett.*, 46(4), 2075–2083.

Mokhtar, A., Jalali, M., He, H., Al-Ansari, N., Elbeltagi, A., Alsafadi, K., Abdo H.G., Sammen S.Sh., Gyasi-Agyei Y., & Rodrigo-Comino, J. (2021). Estimation of SPEI meteorological drought using machine learning algorithms. *IEEE Access*, *9*, 65503-65523.

Mokhtarzad, M., Eskandari, F., Jamshidi Vanjani, N., and Arabasadi, A. (2017). "Drought forecasting by ANN, ANFIS, and SVM and comparison of the models." *Environ. Earth Sci.*, 76(21), 1–10.

Mondol, M. A. H., Ara, I., and Das, S. C. (2017). "Meteorological Drought Index Mapping in Bangladesh Using Standardized Precipitation Index during 1981-2010." *Adv. Meteorol.*, 2017.

Mouatadid, S., Raj, N., Deo, R. C., and Adamowski, J. F. (2018). "Input selection and data-driven model performance optimization to predict the Standardized Precipitation and Evaporation Index in a drought-prone region." *Atmos. Res.*, 212, 130–149.

Mukherjee, S., Aadhar, S., Stone, D., and Mishra, V. (2018). "Increase in extreme

precipitation events under anthropogenic warming in India." *Weather Clim. Extrem.*, 20(March), 45–53.

Musonda, B., Jing, Y., Iyakaremye, V., and Ojara, M. (2020). "Analysis of long-term variations of drought characteristics using standardized precipitation index over Zambia." *Atmosphere (Basel).*, 11(12), 1–20.

Nabipour, N., Dehghani, M., Mosavi, A., and Shamshirband, S. (2020). "Short-Term Hydrological Drought Forecasting Based on Different Nature-Inspired Optimization Algorithms Hybridized with Artificial Neural Networks." *IEEE Access*, 8, 15210–15222.

Omran, M., Engelbrecht, A. P., and Salman, A. (2005). "Particle swarm optimization method for image clustering." *Int. J. Pattern Recognit. Artif. Intell.*, 19(3), 297–321.

Panda, A., and Sahu, N. (2019). "Trend analysis of seasonal rainfall and temperature pattern in Kalahandi, Bolangir and Koraput districts of Odisha, India." *Atmos. Sci. Lett.*, 20(10), 1–10.

Pandey, V., Srivastava, P. K., Singh, S. K., Petropoulos, G. P., and Mall, R. K. (2021). "Drought identification and trend analysis using long-term chirps satellite precipitation product in bundelkhand, india." *Sustain.*, 13(3), 1–20.

Prodhan, F. A., Zhang, J., Hasan, S. S., Pangali Sharma, T. P., and Mohana, H. P. (2022). "A review of machine learning methods for drought hazard monitoring and forecasting: Current research trends, challenges, and future research directions." *Environ. Model. Softw.*, 149(9), 105327.

Reihanifar, M., Danandeh Mehr, A., Tur, R., Ahmed, A. T., Abualigah, L., & Dąbrowska, D. (2023). A new multi-objective genetic programming model for meteorological drought forecasting. *Water*, *15*(20), 3602.

Rhee, J., and Im, J. (2017). "Meteorological drought forecasting for ungauged areas based on machine learning: Using long-range climate forecast and remote sensing data." *Agric. For. Meteorol.*, 237–238, 105–122.

Rozos, E., Dimitriadis, P., and Bellos, V. (2022). "Machine learning in assessing the performance of hydrological models." *Hydrology*, 9(1), 1–17.

Rustum, R., Adeloye, A., and Mwale, F. (2017). "Spatial and temporal Trend Analysis

of Long Term rainfall records in data-poor catchments with missing data, a case study of Lower Shire floodplain in Malawi for the Period 1953–2010." *Hydrol. Earth Syst. Sci. Discuss.*, (November), 1–30.

Saini, A., Sahu, N., Kumar, P., Nayak, S., Duan, W., Avtar, R., and Behera, S. (2020). "Advanced rainfall trend analysis of 117 years over west coast plain and hill agro-climatic region of India." *Atmosphere (Basel).*, 11(11), 1–25.

Sanikhani, H., Kisi, O., Mirabbasi, R., and Meshram, S. G. (2018). "Trend analysis of rainfall pattern over the Central India during 1901–2010." *Arab. J. Geosci.*, 11(15).

Shahi, N. K., Rai, S., Verma, S., and Bhatla, S. (2023). "RD_Assessment of future changes in high-impact precipitation events.pdf."

Shen, R., Huang, A., Li, B., and Guo, J. (2019). "Construction of a drought monitoring model using deep learning based on multi-source remote sensing data." *Int. J. Appl. Earth Obs. Geoinf.*, 79(219), 48–57.

Shi, J., Cui, L., and Tian, Z. (2020). "Spatial and temporal distribution and trend in flood and drought disasters in East China." *Environ. Res.*, 185(March), 109406.

Shiru, M. S., Shahid, S., Chung, E. S., and Alias, N. (2019). "Changing characteristics of meteorological droughts in Nigeria during 1901–2010." *Atmos. Res.*, 223(March), 60–73.

Singh, G., Panda, R. K., and Nair, A. (2020). "Regional scale trend and variability of rainfall pattern over agro-climatic zones in the mid-Mahanadi river basin of eastern India." *J. Hydro-Environment Res.*, 29(October), 5–19.

Song, Y., & Ren, Y. (2005, October). A Predictive model of nonlinear system based on generalized regression neural network. In 2005 International Conference on Neural Networks and Brain (Vol. 3, pp. 2009-2012). IEEE.

Sörensen, K., and Glover, F. W. (2013). "Metaheuristics." Encycl. Oper. Res. Manag. Sci., 1, 960–970.

Specht, D. F. (1991). "A General Regression Neural Network." IEEE Trans. Neural Networks, 2(6), 568–576.

Spinoni, J., Vogt, J. V., Naumann, G., Barbosa, P., and Dosio, A. (2018). "Will drought events become more frequent and severe in Europe?" *Int. J. Climatol.*, 38(4), 1718–

1736.

Svoboda, M., and Fuchs, B. (2017). *Handbook of Drought Indicators and Indices**.

Tan, R., and Perkowski, M. (2015). "Wavelet-Coupled Machine Learning Methods for Drought Forecast Utilizing Hybrid Meteorological and Remotely-Sensed Data." *2015 Int. Conf. Data Min.*, 50–56.

Tesfamariam, B. G., Gessesse, B., and Melgani, F. (2019). "Characterizing the spatiotemporal distribution of meteorological drought as a response to climate variability: The case of rift valley lakes basin of Ethiopia." *Weather Clim. Extrem.*, 26(October), 100237.

Thomas, J., and Prasannakumar, V. (2016). "Temporal analysis of rainfall (1871-2012) and drought characteristics over a tropical monsoon-dominated State (Kerala) of India." *J. Hydrol.*, 534, 266–280.

Tian, M., Wang, P., and Khan, J. (2016). "Drought forecasting with vegetation temperature condition index using arima models in the guanzhong plain." *Remote Sens.*, 8(9), 690.

Tirivarombo, S., Osupile, D., and Eliasson, P. (2018). "Drought monitoring and analysis: Standardised Precipitation Evapotranspiration Index (SPEI) and Standardised Precipitation Index (SPI)." *Phys. Chem. Earth*, 106, 1–10.

Vicente-Serrano, S. M., Peña-Angulo, D., Beguería, S., Domínguez-Castro, F., Tomás-Burguera, M., Noguera, I., Gimeno-Sotelo, L., and Kenawy, A. El. (2022). "Global drought trends and future projections." *Philos. Trans. R. Soc. A Math. Phys. Eng. Sci.*, 380(2238).

Vicente-Serrano, S. M., Schrier, G. Van der, Beguería, S., Azorin-Molina, C., and Lopez-Moreno, J. I. (2015). "Contribution of precipitation and reference evapotranspiration to drought indices under different climates." *J. Hydrol.*, 526, 42–54.

Wambua, B., M. Mutua, B., and M. Raude, J. (2014). "Performance of Standardized Precipitation Index (SPI) and Effective Drought Index (EDI) in Drought forecasting u..." *Int. J. Eng. Res. Technol.*, 3(11), 547–556.

Wang, L., Yu, H., Yang, M., Yang, R., Gao, R., and Wang, Y. (2019). "A drought index: The standardized precipitation evapotranspiration runoff index." *J. Hydrol.*,

571(February), 651–668.

Xu, L., Chen, N., Zhang, X., and Chen, Z. (2018). “An evaluation of statistical, NMME and hybrid models for drought prediction in China.” *J. Hydrol.*, 566(January), 235–249.

Yacoub, E., and Tayfur, G. (2020). “Spatial and temporal of variation of meteorological drought and precipitation trend analysis over whole Mauritania.” *J. African Earth Sci.*, 163.

Yaduvanshi, A., Zaroug, M., Bendapudi, R., and New, M. (2019). “Impacts of 1.5°c and 2°c global warming on regional rainfall and temperature change across india.” *Environ. Res. Commun.*, 1(12), 0–14.

Yao, S., Guo, D., and Yang, G. (2012). “Three-dimensional aerodynamic optimization design of high-speed train nose based on GA-GRNN.” *Sci. China Technol. Sci.*, 55(11), 3118–3130.

Yibin, S., and Ying, R. (2005). “A predictive model of nonlinear system based on generalized regression neural network.” *Proc. 2005 Int. Conf. Neural Networks Brain Proceedings, ICNNB’05*, 3, 2009–2012.

Zamani, R., Mirabbasi, R., Nazeri, M., Meshram, S. G., and Ahmadi, F. (2018). “Spatio-temporal analysis of daily, seasonal and annual precipitation concentration in Jharkhand state, India.” *Stoch. Environ. Res. Risk Assess.*, 32(4), 1085–1097.

Zhang, R., Chen, Z. Y., Xu, L. J., and Ou, C. Q. (2019). “Meteorological drought forecasting based on a statistical model with machine learning techniques in Shaanxi province, China.” *Sci. Total Environ.*, 665, 338–346.

Zhang, Y., Li, W., Chen, Q., Pu, X., and Xiang, L. (2017). “Multi-models for SPI drought forecasting in the north of Haihe River Basin, China.” *Stoch. Environ. Res. Risk Assess.*, 31(10), 2471–2481.

Zhong, R., Chen, X., Lai, C., Wang, Z., Lian, Y., Yu, H., and Wu, X. (2019). “Drought monitoring utility of satellite-based precipitation products across mainland China.” *J. Hydrol.*, 568(November 2018), 343–359.

Zou, L., Xia, J., Ning, L., She, D., and Zhan, C. (2018). “Identification of hydrological drought in Eastern China using a time-dependent drought index.” *Water (Switzerland)*, 10(3), 1–19.

Zounemat-Kermani, M., & Teshnehlab, M. (2008). Using adaptive neuro-fuzzy inference system for hydrological time series prediction. *Applied soft computing*, *8*(2), 928-936.

PUBLICATIONS

JOURNAL PAPERS

1. **Kikon, Ayilobeni**, and B. M. Dodamani. "Trend Analysis of Rainfall and Meteorological Drought Indices over India during 1958–2017." *Water Conservation Science and Engineering* 8, no. 1 (2023): 41. https://doi.org/10.1007/s41101-023-00215-x
2. **Kikon, Ayilobeni**., Dodamani B M., (2023), "ANFIS based Soft Computing Models for Forecasting Effective Drought Index over an Arid Region of India." *Journal of AQUA – Water Infrastructure, Ecosystems and Society production and system.* https://doi.org/10.2166/aqua.2023.204
3. **Kikon, Ayilobeni**., Deka, P.C. (2021), "Artificial intelligence application in drought assessment, monitoring and forecasting: a review." *Stochastic Environment Research and Risk Assessment* (2021). https://doi.org/10.1007/s00477-021-02129-3
4. **Kikon, Ayilobeni**., Deka P.C**.** (2022), "Forecasting of Meteorological Drought Using Machine Learning Algorithm". In: Rao C.M., Patra K.C., Jhajharia D., Kumari S. (eds) Advanced Modelling and Innovations in Water Resources Engineering. Lecture Notes in Civil Engineering, vol 176. Springer, Singapore. https://doi.org/10.1007/978-981-16-4629-4_4

CONFERENCE PROCEEDINGS

1. **Kikon Ayilobeni**, Dodamani B. M., "Meteorological Drought Index Forecasting based on Machine Learning Techniques in the Homogenous Region of North East India", ***27th HYDRO 2022- International Conference on Hydraulics, Water Resources, and Coastal Engineering***, at PEC, Chandigarh, India during 22th-24th December 2022.
2. **Kikon, Ayilobeni** and Dodamani B M., "A Deep Leaning Approach for prediction of meteorological drought over the region of Nagaland," *12th International Workshop on Statistical Hydrology (STAHY-2022),* 17th-20th September 2022,

University of Cagliari, Chia, Sardinia, Italy. (Received Young Scientist Travel Grant Award from DST-SERB, GOI).

3. **Kikon, Ayilobeni** and Deka, P.C., "Trend Analysis of meteorological drought for Peninsular India region," *25th HYDRO 2020- International Conference on Hydraulics, Water Resources, and Coastal Engineering*, at NIT, Rourkela, India during 26th-28th March 2021. (**Received Best paper award**).
4. **Kikon, Ayilobeni** and Deka, P.C., "Forecasting of Meteorological Drought using Machine Learning Algorithm." National Conference on *"Advanced Modelling and Innovations in Water Resources Engineering", (AMIWRE-2021*), at NIT, Jamshedpur, India during 20-21 February 2021.
5. **Kikon, Ayilobeni** and Deka, P.C., "Application of Optimized Machine Learning Technique in Drought forecasting using SPI," *Drought and Water Scarcity: addressing current and future challenges, 20-21st March 2019,* **OXFORD UNIVERSITY**, UK.
6. **Kikon, Ayilobeni** and Deka, P.C., "Spatial Interpolation of Rainfall data with ArcGIS approach," *8th International Engineering Symposium (IES)-2019*, March 13-15, 2019, **Kumamoto University**, Japan.

RESUME

NAME	**:**	**AYILOBENI KIKON**
Date of Birth	:	14th October
Mobile	:	+91 8277418544
Email	:	ayilobeni@gmail.com
Permanent Address	:	HOUSE NO. 18, ORIENTAL COLONY, NEAR DIMAPUR GOVERNMENT COLLEGE, DIMAPUR, NAGALAND - 797112
Qualifications	:	B.E. (Civil Engineering), M.Tech (Water Resources Engineering & Management)
Publications	:	International journals - 3 Book Chapter - 1 International conferences - 6